CENTER FOR DRUG EVALUATION AND RESEARCH

APPLICATION NUMBER:

204677Orig1s000

PHARMACOLOGY REVIEW(S)

Tertiary Pharmacology Review

By: Paul C. Brown, Ph.D., ODE Associate Director for Pharmacology and Toxicology, OND IO
NDA: 204677
Submission date: 12/21/2012
Drug: florbetaben
Sponsor: Piramal Imaging SA
Indication: detection of β-amyloid in the brain

Reviewing Division: Division of Medical Imaging Products

Background Comments:
The pharmacology/toxicology reviewer and team leader in the Division of Medical Imaging Products reviewed the nonclinical information for florbetaben and found it adequate to support approval from a pharmacology/toxicology perspective for the indication listed above.

Carcinogenicity studies have not been conducted with florbetaben. This is acceptable because the product is an imaging agent that is used acutely.

Conclusions:
I concur with the Division pharmacology/toxicology recommendation that this NDA can be approved. Calling florbetaben a “Radioactive Diagnostic Agent for Positron Emission Tomography” for its Established Pharmacologic Class is consistent with other drugs in the class. I have provided additional comments on labeling separately.

Reference ID: 3468094

This is a representation of an electronic record that was signed electronically and this page is the manifestation of the electronic signature.

/s/

PAUL C BROWN
03/10/2014

DEPARTMENT OF HEALTH AND HUMAN SERVICES

PUBLIC HEALTH SERVICE

FOOD AND DRUG ADMINISTRATION

CENTER FOR DRUG EVALUATION AND RESEARCH

PHARMACOLOGY/TOXICOLOGY NDA/BLA REVIEW AND EVALUATION

Application number:	204677
Supporting document/s:	
Applicant's letter date:	December 21, 2012
CDER stamp date:	December 21, 2012
Product:	Florbetaben
Indication:	Florbetaben is proposed for the detection of β-amyloid in the brain, thereby assisting in the differential or confirmatory diagnosis in adult patients who are being evaluated for Alzheimer's disease and other causes of cognitive decline.
Applicant:	Piramal Imaging SA
Review Division:	Medical Imaging Products
Reviewer:	Sunny Awe, Ph.D.
Supervisor/Team Leader:	Adebayo Laniyonu, Ph.D.
Division Director:	Libero Marzella, M.D.
Project Manager:	Sharon Thomas

Template Version: September 1, 2010

Reference ID: 3361527

Disclaimer

Except as specifically identified, all data and information discussed below and necessary for approval of NDA 204677 are owned by Piramal Imaging SA or are data for which Piramal Imaging SA has obtained a written right of reference.

Any information or data necessary for approval of [NDA 204677 that [name of applicant] does not own or have a written right to reference constitutes one of the following: (1) published literature, or (2) a prior FDA finding of safety or effectiveness for a listed drug, as reflected in the drug's approved labeling. Any data or information described or referenced below from reviews or publicly available summaries of a previously approved application is for descriptive purposes only and is not relied upon for approval of NDA 204677.

Reference ID: 3361527

TABLE OF CONTENTS

1 EXECUTIVE SUMMARY 14

1.1 INTRODUCTION 14

1.2 BRIEF DISCUSSION OF NONCLINICAL FINDINGS 14

PHARMACOKINETICS 15

TOXICOLOGY 16

REPEAT-DOSE TOXICITY STUDIES: REPEAT-DOSE TOXICITY STUDIES WERE CONDUCTED IN RATS AND DOGS. 17

1.3 RECOMMENDATIONS 18

13.1 CARCINOGENESIS, MUTAGENESIS, IMPAIRMENT OF FERTILITY 18

13.2 ANIMAL TOXICOLOGY AND/OR PHARMACOLOGY 19

8.1 PREGNANCY 19

PREGNANCY CATEGORY C. 20

8.3 NURSING MOTHERS 20

2 DRUG INFORMATION 21

2.1 DRUG 21

2.2 RELEVANT INDS, NDAS, BLAS AND DMFS 21

2.3 DRUG FORMULATION 22

2.4 COMMENTS ON NOVEL EXCIPIENTS 22

2.5 COMMENTS ON IMPURITIES/DEGRADANTS OF CONCERN 23

2.6 PROPOSED CLINICAL POPULATION AND DOSING REGIMEN 23

2.7 REGULATORY BACKGROUND 23

3 STUDIES SUBMITTED 23

3.1 STUDIES REVIEWED 23

Reference ID: 3361527

3.2 STUDIES NOT REVIEWED 27

3.3 PREVIOUS REVIEWS REFERENCED 27

4 PHARMACOLOGY 27

4.1 PRIMARY PHARMACOLOGY 28

4.2 SECONDARY PHARMACOLOGY 57

4.3 SAFETY PHARMACOLOGY 59

5 PHARMACOKINETICS/ADME/TOXICOKINETICS 95

5.1 PK/ADME 95

5.2 TOXICOKINETICS 103

6 GENERAL TOXICOLOGY 172

6.1 SINGLE-DOSE TOXICITY 172

6.2 REPEAT-DOSE TOXICITY 192

7 GENETIC TOXICOLOGY 202

7.2 OTHER GENETIC TOXICITY STUDIES 214

8 CARCINOGENICITY 230

9 REPRODUCTIVE AND DEVELOPMENTAL TOXICOLOGY 230

10 SPECIAL TOXICOLOGY STUDIES 231

11 INTEGRATED SUMMARY AND SAFETY EVALUATION 240

REPEAT-DOSE TOXICITY: REPEAT-DOSE TOXICITY STUDIES WERE CONDUCTED IN RATS AND DOGS. 242

12 APPENDIX/ATTACHMENTS 245

Reference ID: 3361527

Table of Tables

Table 1: Composition of Florbetaben solution for injection 22

Table 2: Composition of the BAY 94-9172 formulations 29

Table 3: AD pathology represented in neurodegenerative disease TMA 55

Table 4: Neurodegenerative disease TMAs qualitatively and quantitatively capture the characteristic inclusion pathology 56

Table 5: Proposed guidelines for neurodegenerative disease TMA 57

Table 6: Effect of ZK 6057184 on urine volume, urinary excretion of electrolytes and Na+/K+ ratio after a single injection (i.v.) in conscious male rats 69

Table 7: Effect of ZK 6057184 on serum creatinine concentration, creatinine excretion, creatinine clearance and serum urea concentration after a single injection (i.v.) in conscious male rats 69

Table 8: Effect of ZK 6057184 on total protein excretion, NAG excretion, osmolality in serum and urine and on osmolar clearance after a single injection (i.v.) in conscious male rats 70

Table 9: Effect of ZK 6057184 after single intravenous administration (t-10 min) on the latency of rats on the accelerating rotarod (from 4 to 33 rpm over 240 sec) 74

Table 10: Experimental design of the Cardiovascular Safety Pharmacology Study in Conscious Beagle Dogs. 78

Table 11: Representative data on the blood pressure, respiratory rate, temperature and ECG obtained at pre-dose and 240 minutes post-dose during the Cardiovascular Safety Pharmacology Study in Conscious Beagle Dogs as provided by the sponsor 79

Table 12: Summary ECG data obtained following administration of PEGN3.HCl (68.4X MHD) during the Cardiovascular Safety Pharmacology Study in Conscious Beagle Dogs as provided by the sponsor 80

Table 13: Effect of ZK 6057184 on cardiac output and stroke volume at various time intervals 91

Table 14: Pharmacokinetic Parameters of [^{19}F]AV1/ZK in the male rat (disposition kinetics after i.v. (intravenous) administration of 0.5 mg/kg (50 % PEG400 solution) n = 3 98

Table 15: Blood concentration of ZK6013443 after single i.v. administration in rats 99

Table 16: Total blood radioactivity time profile after single i.v. administration of ZK 6013443 in rats 101

Table 17: Treatment Schedule employed for the study 104

Reference ID: 3361527

Table 18: Mean plasma concentrations [µg/L] of ZK 6016468 after intravenous bolus administration of ZK 6057184 using the test formulation in toxicity studies..... 106

Table 19: Pharmacokinetic parameters of ZK 6016468 after intravenous bolus administration of ZK 6057184 using the test formulation in toxicity studies..... 107

Table 20: Mean plasma concentrations (µ/L) of ZK 6016468 after intravenous bolus administration of ZK 6057184 using the clinical reference formulation 107

Table 21: Pharmacokinetic parameters of ZK 6016468 after intravenous bolus administration of ZK 6057184 using the clinical reference formulation..... 108

Table 22: Treatment Schedule employed for the study as provided by the sponsor 110

Table 23: Mean plasma concentrations [µg/L] and pharmacokinetic parameters of ZK 6016468 on Day 1 and Day 25. Geometric means and S.D., n = 6 to n = 10..... 112

Table 24: Biodistribution and excretion of ZK 6013443 after single i.v. administration in male NMRI mice (values are given in mean ± S.D.; n=3) 117

Table 25: Summary of Organ Dosimetry to an Average Adult Patient (70 kg) from an Intravenous Dose of 18F- FAβ extrapolated from Mouse. Mouse normal data sampled at time points 2, 5, 15, 30, 60, 120 and 240 mins 119

Table 26: Cumulative estimates for Human provided by the sponsor based on the mouse data and metabolic and organ scaling 120

Table 27: Biodistribution after i.v. injection of BAY 949172 + ZK 6057184 formulation A..... 124

Table 28: Biodistribution after i.v. injection of BAY 94-9172 and ZK 6057184 formulation B 125

Table 29: Stability of ZK6013443 after incubation in human plasma detected by HPLC 130

Table 30: Metabolites of ZK 6013443 in plasma and urine after i.v. administration in male NMRI mice detected by HPLC..... 130

Table 31: Metabolites of ZK 6013443 in plasma after i.v. injection in male NMRI mice detected by HPLC (gamma-detector)..... 133

Table 32: Total radioactivity expressed as %ID/g (d.c.) in mouse blood and brain at 30 min after injection of [^{18}F]BAY 949172 136

Table 33: Extraction efficiency for brain and plasma samples at 30 min after extraction with acetonitrile and centrifugation 136

Reference ID: 3361527

Table 34: Results of metabolite analysis in mouse plasma and brain by ion exchange chromatography after intravenous administration of [^{18}F]BAY 94-9172 to mice 30 min post application (mean values of three animals) 138

Table 35: Definition of metabolite fractions by HPLC peak(s) and confirmed co-elution with reference substances 142

Table 36: ZK 6016468: Summary of incubations with liver microsomes of different species with NADPH. 145

Table 37: ZK 6016468: Summary of incubations with hepatocytes of man and rat (suspension) #4) 146

Table 38: [^{14}C]BAY 94-9172: Formation of metabolites in mouse liver microsomes (NMRI, male) 149

Table 39: [^{14}C]BAY 94-9172: Metabolic pattern in pooled plasma samples 0.083 to 6 h following intravenous administration of 1 mg/kg b.w. [^{14}C]BAY 94-9172 to male mice (NMRI) established with RP chromatography 150

Table 40: [^{14}C]BAY 94-9172: Plasma concentrations [µg-eq/L] and pharmacokinetic parameters of BAY 94-9172 after intravenous administration of 1 mg/kg b.w. [^{14}C]BAY 94-9172 to male mice (NMRI) 151

Table 41: [^{14}C]BAY 94-9172: Metabolic pattern in pooled brain extracts 0.083 to 6 h following intravenous administration of 1 mg/kg b.w. [^{14}C]BAY 94-9172 to male mice (NMRI) established with RP chromatography 153

Table 42: [^{14}C]BAY 94-9172: Metabolic pattern in pooled brain extracts 0.083 to 6 h following intravenous administration of 1 mg/kg b.w. [^{14}C]BAY 94-9172 to male mice (NMRI) established with ion exchange chromatography 153

Table 43: [^{14}C]BAY 94-9172: Brain concentrations [µg-eq/L] and pharmacokinetic parameters of BAY 94-9172 after intravenous administration of 1 mg/kg b.w. [^{14}C]BAY 94-9172 to male mice (NMRI) 154

Table 44: Incubation conditions employed by the sponsor for the study 156

Table 45: BAY 94-9172: Inhibitory effects of ZK 6057184 on formation of metabolites from standard probes mediated by cytochrome P450 isoforms (duplicate incubations, mean value) using pooled human liver microsomes 157

Table 46: CYP isoform-selective activities of pooled human liver microsomes MP004 161

Table 47: BAY 94-9172: Formation of metabolites in human liver microsomes 162

Reference ID: 3361527

Table 48: BAY 94-9172: Determination of kinetic parameters of M-1 formation applying human liver microsomes 164

Table 49: BAY 94-9172: Influence of different CYP isoform-selective inhibitors on M-1 formation from [^{14}C]BAY 94-9172 (1 µM) catalyzed by human liver microsomes (0.05 mg protein/mL) ... 166

Table 50: BAY 94-9172: Influence of different CYP isoform-selective inhibitors on M-1 and polar metabolite formation from [^{14}C]BAY 94-9172 (0.5 µM) catalyzed by human liver microsomes (0.12 mg protein/mL) 166

Table 51: PET measurements with [^{18}F]BAY 949172 and [^{18}F]BAY 6 168

Table 52: Quantitative parameters evaluated in the comparison between [^{18}F]BAY 949172 and [^{18}F]BAY 6 171

Table 53: Animal allocation for the study 173

Table 54: Animal allocation employed during the study 183

Table 55: Animal allocation for the study 188

Table 56: Chromosomal aberrations (% aberrant cells excluding gaps) in cultured human Lymphocytes 206

Table 57: Summary data on assay involving pulse treatment (3 hours) without and with S9 mix (mean values of two independent cultures) 212

Table 58: Summary data on assay involving continuous treatment (24 hours) without S9 mix; Pulse treatment (3 hours) with S9 mix (mean values of two independent cultures) 213

Table 59: Summary data of the chromosomal aberration study with (b) (4) (b) (4) (b) (4) (b) (4) 227

Table 60: Summary data on local findings of a local tolerance test in rabbits after a single intravenous application-Day 3 Necropsy 233

Table 61: Summary data on local findings of a local tolerance test in rabbits after a single intravenous application-Day 8 Necropsy 234

Table 62: Summary data on local findings of a local tolerance test in rabbits after a single paravenous application-Day 3 Necropsy 234

Table 63: Summary data on local findings of a local tolerance test in rabbits after a single paravenous application-Day 8 Necropsy 235

Table 64: Summary of toxicity studies conducted on Florbetaben 244

Reference ID: 3361527

Table of Figures

Figure 1: [^{19}F]Florbetaben (blue fluorescence) and [3H]Florbetaben (black silver grains) bind to cored (first row), non-cored (second row) beta-amyloid deposits as confirmed with Bielschowsky silver stain.31

Figure 2: [^{19}F]Florbetaben (middle row, blue fluorescence) and anti-beta-amyloid antibody 1E8 (left row, dark red staining) were subsequently bound/immunohistochemically stained on cortical brain sections from AD patients to detect beta-amyloid deposits. 32

Figure 3: Graph presenting % concordance of [^{19}F] Florbetaben fluorescence with 1E8 anti-beta amyloid immunoreactivity 33

Figure 4 : [^{3}H]-ZK 6016468 binding to different pathologies 35

Figure 5: Florbetaben binds to beta-amyloid plaques, but not to Tau lesions or α-synuclein Lewy bodies as analyzed by high resolution emulsion autoradiography using [^{3}H]-Florbetaben combined with subsequent immunohistochemistry for different pathological lesions. 36

Figure 6: Example of brain tissue sections from AD patients incubated with the non-radioactive drug substance ZK6016468. 38

Figure 7: Example of a brain tissue section from a FTD patient incubated with the non-radioactive drug substance ZK 6016468. 39

Figure 8: Case 200010004 Cerebellum. 40

Figure 9: Case 200020006 Cerebellum. 40

Figure 10: Case 200040012 Cerebellum. 41

Figure 11: ^{3}H-Florbetaben (5nM) competitive binding against increasing concentration of Florbetaben or BTA-1 (10^{-13}M-10^{-6}M) on one AD frontal cortical autopsy brain tissue. 44

Figure 12: ^{3}H-Florbetaben binding (5 nM) on frontal, parietal, temporal cortex, hippocampus, caudate nucleus and cerebellum from AD compared with CTRL; frontal cortex (FC), temporal cortex (TC), parietal cortex (PC), hippocampus (Hip), caudate nucleus (Cau) and cerebellum (CB); *p<0.05, **p<0.01, ***p<0.001, Mann-Whitney test. 44

Figure 13: A, B) Representative saturation binding and scatcbard plots of ^{3}HFlorbetaben (0.01 - 200nM) on one AD frontal cortical autopsy tissue. C, D) ^{3}H-Florbetaben (0.01 -40 nM) saturation binding on frontal cortical autopsy brain tissue of AD (n=3) and CTRL (n=3) 45

Figure 14: ^{3}H-Florbetaben binding (5 nM) on homogenates from frontal, parietal, temporal cortex, hippocampus from EOAD compared with LOAD and CTRL. **p<0.01, ***p<0.001, EOAD *vs* CTRL;

Reference ID: 3361527

ttp<0.01, LOAD *vs* CTRL; Kruskal-Wallis with Dunns *post lloc-test.* EOAD, early onset AD, LOAD, late onset AD. 46

Figure 15: ^{3}H-Florbetaben binding (5 nM) in homogenates from frontal, parietal, temporal cortex and hippocampus autopsy brain tissue from AD ApoE ε4 carrier with AD ApoE ε4 non-carrier and CTRL. *p<0.05, **p<0.01, ***p<0.001, AD ApoE ε4 carrier vs CTRL, ^p<0.05, ^^p<0.01, AD ApoE ε4 non-carrier vs CTRL (ApoE ε4 non-carrier); Kruskal-Wallis with Dunn's *post hoc-test* 47

Figure 16: Case S04/185 putaminal fundus region 49

Figure 17: Case S05/121 piriform cortex. 49

Figure 18: Case 06/025 insular gyrus. 50

Figure 19: Case S06/056 subcallosal area 50

Figure 20: Case S05/121 Cerebellum. 51

Figure 21: Case 03/711 temporal cortex. 51

Figure 22: Case 04/042 frontal cortex. 52

Figure 23: Case 03/213. Frontal cortex of an AD diseased patient. 52

Figure 24: Case 04/171. Frontal cortex of a Dementia with Lewy Body patient (DLB). 53

Figure 25: Effects of ZK 6057184 on HERG-mediated potassium current 60

Figure 26: Effects of three consecutive intravenous infusions over 10 minutes each of vehicle and ZK 6057184 on mean arterial blood pressure (MAP) in anesthetized dogs 85

Figure 27: Effects of three consecutive intravenous infusions over 10 minutes each of vehicle and ZK 6057184 on systolic arterial blood pressure (SAP) in anesthetized dogs 85

Figure 28: Effects of three consecutive intravenous infusions over 10 minutes each of vehicle and ZK 6057184 on diastolic arterial blood pressure (DAP) in anesthetized dogs 86

Figure 29: Effects of three consecutive intravenous infusions over 10 minutes each of vehicle and ZK 6057184 on left ventricular end-diastolic pressure (LVEDP) in anesthetized dogs 86

Figure 30: Effects of three consecutive intravenous infusions over 10 minutes each of vehicle and ZK 6057184 on central venous pressure (CVP) in anesthetized dogs 87

Figure 31: Effects of three consecutive intravenous infusions over 10 minutes each of vehicle and ZK 6057184 on mean pulmonary artery pressure (PAPm) in anesthetized dogs 87

Reference ID: 3361527

Figure 32: Effects of three consecutive intravenous infusions over 10 minutes each of vehicle and ZK 6057184 on heart rate (HR) in anesthetized dogs (data are presented as means) 88

Figure 33: Effects of three consecutive intravenous infusions over 10 minutes each of vehicle and ZK 6057184 on max. rate of rise of left ventricular pressure (dp/dt max) in anesthetized dogs 89

Figure 34: Effects of three consecutive intravenous infusions over 10 minutes each of vehicle and ZK 6057184 on cardiac output (CO) in anesthetized dogs 89

Figure 35: Effects of three consecutive intravenous infusions over 10 minutes each of vehicle and ZK 6057184 on stroke volume (SV) in anesthetized dogs 90

Figure 36: Effects of three consecutive intravenous infusions over 10 minutes each of vehicle and ZK 6057184 on total peripheral resistance (TPR) in anesthetized dogs 90

Figure 37: Figure 44: Effects of three consecutive intravenous infusions over 10 minutes each of vehicle and ZK 6057184 on pulmonary vascular resistance (PVR) in anesthetized dogs 91

Figure 38: Effects of three consecutive intravenous infusions over 10 minutes each of vehicle and ZK 6057184 on the ECG time interval RR (RR) in anesthetized dogs 92

Figure 39: Effects of three consecutive intravenous infusions over 10 minutes each of vehicle and ZK 6057184 on the ECG time interval PR (PR) in anesthetized dogs 92

Figure 40: Effects of three consecutive intravenous infusions over 10 minutes each of vehicle and ZK 6057184 on the ECG time interval QRS (QRS) in anesthetized dogs 93

Figure 41: Effects of three consecutive intravenous infusions over 10 minutes each of vehicle and ZK 6057184 on the ECG time interval QT (QT) in anesthetized dogs 93

Figure 42: Effects of three consecutive intravenous infusions over 10 minutes each of vehicle and ZK 6057184 on the corrected ECG time interval QT (QTc) in anesthetized dogs 94

Figure 43: Serum concentration-time profile of [19F]AV1/ZK after i.v. bolus injection of 0.5 mg/kg in 50 % PEG 400 solution (blue lines; animals 4, 5 and 6) in the male rat 97

Figure 44: Blood concentration profile of ZK6013443 (in % ID) after single i.v. administration in rats (n=4. individual animals are shown); Square: Blood concentration profile of ZK6013443 (in % ID) of the first 20 min post i.v. administration in rat 100

Figure 45: Total blood radioactivity time profile (in % ID) after single i.v. administration of ZK 6013443 in rats (n=3; individual animals are shown) 102

Figure 46: Plasma concentrations [µg/L] *vs.* time curve of ZK 6016468 after intravenous bolus administration of ZK 6057184 to male and female rats 0.01 109

Reference ID: 3361527

Figure 47: Plasma concentrations [µg/L] *vs.* time curve of ZK 6016468 after intravenous bolus administration of ZK 6057184 to male and female Beagle dogs [BAY 94-9172/T0078654] on Day 1. (Geometric means of n = 6 to n = 10.) 114

Figure 48: Plasma concentrations [µg/L] *vs.* time curve of ZK 6016468 after intravenous bolus administration of ZK 6057184 to male and female Beagle dogs [BAY 94-9172/T0078654] on Day 25. (Geometric means of n = 6 to n = 10.) 114

Figure 49: Activity-time profile in brain and blood obtained after i.v. administration of Bay 949172+ZK6057184 formulated in two different formulations (values are given in mean ± S.D.; n=3).. 125

Figure 50: Analytical HPLC-chromatogram (gamma-detector): Liver microsomes and cofactors were incubated with ZK6013443 for 30 min at 37°C and afterwards ZK6013443 and metabolites were extracted and analyzed by HPLC. 128

Figure 51: HPLC-chromatogram of ZK 6013443 taken after 120min incubation in human plasma and PBS 130

Figure 52: HPLC-chromatogram of ZK 6013443 of plasma and urine 131

Figure 53: HPLC-chromatogram of NH2-AV-1 131

Figure 54: Analytical HPLC-chromatogram (gamma-detector) of extracted plasma 5 min p.i. of ZK6013443/ZK6016468) 133

Figure 55: HPLC chromatogram 134

Figure 56: Chromatogram of reference compounds [1-14C]fluoroacetic acid, [1-^{14}C]fluoroethanol, [^{18}F]fluoride with ion exchange chromatography and online radioactivity detection 137

Figure 57: Metabolite pattern in mouse plasma after intravenous administration of [^{18}F]BAY 94-9172 with ion exchange chromatography and online radioactivity detection 138

Figure 58: Metabolite pattern in mouse brain after intravenous administration of [^{18}F]BAY 94-9172 with ion exchange chromatography and online radioactivity detection 140

Figure 59: Metabolite pattern in mouse plasma after intravenous administration of [^{18}F]BAY 94-9172 (animal 1, 30 min) spiked with reference compounds [1-14C]fluoroacetic acid, [1-^{14}C]fluoroethanol, [^{18}F]fluoride with ion exchange chromatography and online radioactivity detection 141

Figure 60: Proposed major metabolic pathways of [^{18}F]BAY 94-9172 in mice 141

Figure 61: Graphical depiction of percentages of metabolite fractions in plasma over time 143

Figure 62: Graphical depiction of percentages of metabolite fractions in brain over time 144

Reference ID: 3361527

Figure 63: [^{14}C]BAY 94-9172: Metabolite profiles following incubation of [^{14}C]BAY 94-9172 (10 µM, top and 2 µM, bottom) with 0.5 mg liver microsomal protein/mL 150

Figure 64: [^{14}C]BAY 94-9172: Plasma concentration *vs*. time curves of total radioactivity, BAY 94-9172 and metabolites after intravenous administration of 1.0 mg/kg b.w. to mice (NMRI) [study No. I 4939-5/A] 152

Figure 65: [^{14}C]BAY 94-9172: Plasma concentration *vs*. time curves of total radioactivity, BAY 94-9172 and metabolites after intravenous administration of 1.0 mg/kg b.w. to mice (NMRI) [study No. I 4939-5/A] 154

Figure 66: Schematic BAY 94-9172: Metabolic pathways in mouse *in vivo* 155

Figure 67: BAY 94-9172: Effect on inhibition on phenacetin *O*-deethylation, amodiaquine *N*-deethylation, diclofenac 4'-hydroxylation and dextromethorphan *O*-demethylation by ZK 6057184 in human liver microsomes *in vitro* 159

Figure 68: BAY 94-9172: Effect on inhibition on midazolam 1'-hydroxylation and testosterone 6ß-hydroxylation by ZK 6057184 in human liver microsomes *in vitro* 160

Figure 69: BAY 94-9172: Metabolite formation by screening a panel of human recombinant CYP isoforms ([redacted] (b) (4) at a concentration of 0.5 µM [^{14}C]BAY 94-9172 164

Figure 70: BAY 94-9172: Michaelis Menten plot of incubation of [^{14}C]florbetaben with human liver microsomes (formation of M-1, experiment GCM 2079 G) 165

Figure 71: BAY 94-9172: Eadie-Hofstee plot of incubation of [^{14}C]florbetaben with human liver microsomes (formation of M-1, experiment GCM 2079 G) 165

Figure 72: A-C: PET images of [^{18}F]BAY 949172 and [^{18}F]BAY-6 in Monkey 3 at different time intervals after the injection. 170

Figure 73: Time activity curves for the whole brain uptake (A) and the regional uptake (B) in thalamus, cortex and cerebellum of [^{18}F]BAY 949172 and [^{18}F]BAY-6 in Monkeys 1 and 3 171

Reference ID: 3361527

1 Executive Summary

1.1 Introduction

Florbetaben, (4-[(E)-2-(4-{2-[2-(2-[18F]fluoroethoxy)ethoxy]ethoxy}phenyl)vinyl]-N-methylaniline) is a polyethyleneglycol stilbene derivative labeled with fluoride-18 (^{18}F) for Positron Emission Tomography (PET). It is proposed for detection of Aβ plaques in brains, thereby assisting in the differential or confirmatory diagnosis in adult patients who are being evaluated for Alzheimer's disease (AD) or other causes of cognitive decline.

1.2 Brief Discussion of Nonclinical Findings

Pharmacology

Primary Pharmacodynamics: *In vitro* affinity studies on Florbetaben were conducted using a competition assay with synthetic Aβ fibrils or human AD homogenate and (b) (4) as ligand. Florbetaben demonstrates reasonable inhibition of ZK 6006755 binding to synthetic Aβ fibrils (IC_{50}=146±34 nM) and to human AD brain homogenate (IC50=24±5.4nM). Autoradiography study indicates that Florbetaben binds to Aβ amyloid plaque like structures in the grey matter in post mortem human AD brain tissue sections and the data correlated with the immunohistochemistry data from anti-amyloid antibody obtained in the same brain tissue sections. Tritium-labeled [^{3}H] Florbetaben bound to homogenates of the frontal cortex, temporal cortex, parietal cortex, hippocampus and caudate of AD patients in comparison to age matched controls and no influence on ^{3}H-Florbetaben binding to AD brain homogenates was demonstrated on the ApoE ε4 status of the AD patients. Florbetaben demonstrates no binding to amyloid precursor protein (APP) immunoreactive structures as well as to tau-positive pathologies and alpha-synuclein positive lesions in cortical brain tissue sections of Fronto-temporal Dementia (FTD) and Lewy Body Disease patients, respectively.

Secondary Pharmacodynamics: Selectivity of ^{3}H-Florbetaben was evaluated using radioligand binding assay to assess possible binding of the product to up to 79 various receptors, transporter and binding sites. The data indicates that following Florbetaben administration at the proposed dose, Florbetaben concentration in the body will be too low to cause any interaction at any of the evaluated receptors, transporter and binding sites.

Safety Pharmacology: *In vitro* cardiovascular safety study conducted demonstrated that Florbetaben (up to 1250X expected human unbound plasma level of estimated human dose) did not affect the HERG K^{+} current in stably transfected Chinese Hamster Ovary (CHO) cells. Cardiovascular safety study conducted in conscious telemetered dogs showed no Florbetaben-related effects on the ECG parameters, rhythm, or blood pressure. Another dog study on effect of consecutive injection of Florbetaben (up to 3449X MHD) in beagle anesthetized dogs

Reference ID: 3361527

demonstrated no effect on the evaluated cardiohemodynamic and ECG parameters. The parameters include blood pressure, stroke volume, heart rate, mPAR, blood pressure, cardiac output, ECG time intervals (RR, PR, QRS, QT and QTc) among others.

A study evaluating the effect of Florbetaben (up to 1395X MHD) on renal function was conducted in conscious male rats. The study demonstrates no change in renal excretion rates of fluids, creatinine, osmolar clearance as well as sodium and potassium. Behavioral studies were conducted in conscious rats to investigate neurotropic effects of Florbetaben on behavior, temperature, motor coordination and other CNS functions. The data demonstrated no effect on behavior, temperature, motor coordination or CNS in animals treated with Florbetaben (117X-1395X MHD). Respiratory study conducted using whole body plethysmography system in conscious rats showed that Florbetaben up to 1395X MHD demonstrated no effect on the respiratory frequency, tidal volume or minute volume in the animals.

Pharmacokinetics

In vitro analysis using HPLC/UV or LC/MS/MS demonstrates that Florbetaben is bound to human plasma proteins (blood/plasma ratio of 0.44 in human) and stable in serum and moderately stable in liver microsomes. The *in vivo* data obtained from rats showed that Florbetaben is characterized by blood clearance of 6.7 L/h/kg, volume of distribution of 2.8 L/kg and distribution $t_{1/2}$ of 0.15 h. Blood kinetics study conducted in rats demonstrates that Florbetaben remained in the blood longer than 3 hours post injection. Blood radioactivity time profile of Florbetaben was evaluated and found that following a single intravenous injection in rats demonstrates an initial rapid distribution followed by a slight but constant increase in distribution over the 3 hours observation period, and a distribution $t_{1/2}$ of 2.7±1.0 min. Toxicokinetics data from dogs indicates no sex-related differences in exposure in the treated animals and no accumulation or induction in terms of $AUC_{(0-6)}$ or C_{max} following repeated dosing.

Biodistribution data from NMRI mice indicates initial brain uptake of radioactivity (4.77±0.15%ID/g at 2 min) and initial wash out of radioactivity from the brain (1.59 ± 0.13%ID/g at 30 min). However, slow clearance was observed in the brain Florbetaben was mostly excreted in the kidney and the feces and a total recovery of 98.46% was reported at 4 hour post injection. The dosimetry data demonstrated no potential radiation toxicity of radioactivity Stability and metabolite identification studies conducted in mice following an intravenous injection of [^{18}F]Florbetaben using HPLC and LC-MS/MS showed that Florbetaben is metabolized to [^{18}F]fluoroacetaldehyde (non-polar fraction) and [^{18}F]-fluoroacetic acid (polar fraction).

Characterization of the polar metabolites showed that similar metabolites in the plasma and brain samples of [^{18}F]Florbetaben. *In vitro* data on biotransformation of Florbetaben in liver microsomes and hepatocytes of rat, dog, mouse and human indicates that demethylation was the major pathway in human and rat hepatocytes while glucuronidation and acetylation as phase II reaction was observed as major pathways respectively in human and rat hepatocytes. However, oxidative cleavage of the fluoro ethylene glycol side chain was observed as major pathway only in rat hepatocytes.

The possibility of Florbetaben acting as a direct inhibitor of major human cytochrome P450 isoforms was investigated *in vitro* and it was shown that no direct-acting inhibitory potency of Florbetaben on biotransformation reactions catalyzed by CYP 1A2, 2C8, 2C9, and 2D6 (IC_{50} >2 µM). IC_{50} values of 1.6 µM and 1.4 µM were reported to the inhibition of CYP3A4 activity by midazolam and testosterone respectively. The data suggests that no clinically relevant drug-drug interactions would occur to Florbetaben via inhibition of the employed major human cytochrome P450 isoforms.

An *in vitro* CYP phenotyping study conducted to evaluate the CYP isoforms contributing to the oxidative metabolism of Florbetaben in the absence and presence of CYP isoform-selective inhibitors and incubations with recombinant human CYP demonstrated that [^{14}C]Florbetaben is a substrate of several CYP isoforms in human, however, no significant involvement of polymorphic enzymes CYP2C19 and 2D6 was observed. The data shows that the human CYP isoforms is not expected to significantly alter the metabolism of [^{14}C]Florbetaben since the plasma level of Florbetaben would be too low for any polymorphic CYPs or any significant alterations to occur even when single CYP inhibitors are co-administered to the patients.

The PET evaluation of [^{18}F]Florbetaben and a closely related PET tracer, [^{18}F]BAY 1008472, . [^{18}F]BAY 1008472 demonstrates faster uptake, a lower nonspecific binding and faster wash-out than [^{18}F]Florbetaben in rhesus monkey.

Toxicology

<u>Single-dose toxicity studies:</u> Acute and expanded single-dose toxicity studies were conducted in rats and rabbits.

There were no mortalities in any control or in rats intravenously administered Florbetaben at 50, 100 and 400 µg/kg (116X, 233X and 930X MHD). No serious treatment-related alterations in the functional and histopathological parameters assessed were reported in the animals. However, 100 µg/kg and 400 µg/kg (233X and 930X MHD) caused mild transient alterations in erythrocytic parameters in male rats, serum phosphorus in female rats and troponin I in males and female rats on Day 3. Based on this result, NOAEL of 116X MHD was established in this study. This study was repeated at two dose levels (50 and 100 µg/kg -116X and 233X MHD) and the animals were observed over two days and sacrificed on the third day. No mortality, clinical signs of toxicity, changes in clinical chemistry or any effect on gross necropsy or histopathological parameters was reported in the study. The NOAEL of 100 µg/kg (233X MHD) was determined in the study.

In rabbits, an expanded single-dose toxicity study with 14 days recovery period was conducted on the rabbits administered 4.9, 24.4 and 48.8 µg/kg (0, 11.4X, 56.7X and 113.5X MHD). No serious treatment-related alterations in the functional and histopathological parameters assessed were reported in this study. However, there were mild transient alterations in serum liver transaminase enzymes (ALT and AST) at 48.8 µg/kg in one male rabbit on Day 3. The NOAEL as determined by the endpoint assessed in this study was 48.8 µg/kg (113.5X MHD). In another expanded single-dose toxicity study, higher doses (25 and 250 µg/kg (58.1X and 581X MHD) of Florbetaben were administered to the rabbits and the animals were also observed for

14 days. There was no mortality or any serious treatment-related alterations in the functional and histopathological parameters. There were elevated troponin levels on Day 15 in both treated and control groups. There were also elevated AST and ALT values in one animal administered 581X MHD on Day 3. NOAEL obtained from the study was 250 µg/kg (581X MHD).

Repeat-dose toxicity studies: Repeat-dose toxicity studies were conducted in rats and dogs.

Repeated administration of Florbetaben (45, 175 and 700 µg/kg - 105X, 407X and 1628X MHD) to rats over a period of 4 weeks followed by a recovery period of 4 weeks caused no serious treatment-related alterations in the functional and histopathological parameters assessed in the study. There was however reports of alteration in respiratory parameters in the first two weeks of treatment at 175 and 700 µg/kg (407X and 1628X MHD) treated groups. NOAEL of 45 µg/kg (105X MHD) was determined in this study. Necropsy data indicates a number of microscopic findings in the 407X and 1628X MHD and vehicle-treated groups. The findings include tubular vacuolation in the kidney, hypertrophy in the urinary bladder with vacuoles in urinary epithelia, presence of foamy macrophages in the lung, small intestine and lymph nodes and chronic inflammation at the injection site. These findings were attributed to the 20% w/v hydropropyl-beta-cyclodextrin vehicle.

Florbetaben (12.5, 50 and 200 µg/kg (29X, 116X and 465X MHD) was repeatedly administered to dogs over 4 weeks followed by a recovery period of 4 weeks. No mortality or serious clinical signs were reported in the animals. One of the dogs administered 465X MHD demonstrated spontaneous hyperactivity, spasms and coughing on Day 9. During weeks 1, 3 and 4, partial AV block was observed in one dog and bimodal waves was reported in another dog in the group administered 465X MHD. No microscopic or macroscopic effects were reported in this study except lesions found at the injection site in the treated and control animals. However, the animals showed full recovery by the 4-week-treatment recovery period. NOAEL of 50 µg/kg (116X MHD) was determined in this study.

Genetic Toxicity: Mutagenic potential of Florbetaben was evaluated in the bacterial reverse mutation (Ames) test. Florbetaben (up to 5.0 mg/plate) did not induce point mutations in all five strains of *Salmonella typhimurium* and one strain of *Escherichia coli* tested in the absence and presence of a metabolic activation system. No induction of chromosomal aberrations in human peripheral lymphocytes *in vitro* in the presence or absence of metabolic activation was demonstrated by Florbetaben. Similar chromosomal aberration tests in human peripheral lymphocytes were also conducted on the mix of Florbetaben impurities ([redacted] (b) (4) [redacted] (b) (4) [redacted] (b) (4) [redacted] (b) (4) and found negative. However, the mix demonstrated a weak mutagenic potential in the bacterial reverse mutation test with *Salmonella typhimurium* strains TA100, TA1535 and TA1538. An impurity ([redacted] (b) (4) contained in the clinical batch of Florbetaben were evaluated for mutagenic potential and was negative in the bacterial reverse mutation test when tested up to (5.0 mg/plate) in the absence and presence of metabolic activation. [redacted] (b) (4) (2.5-50 µg/mL) was negative in forward cell mutation assay at the

thymidine kinase locus (TK +/-) in mouse lymphoma L1517Y cells with and without activation during a treatment time of 3 hours (pulse treatment) and 24 hours (continuous treatment)

Carcinogenicity: No studies were conducted. However, waiver from conducting the studies was sought and obtained.

Reproductive and developmental toxicity studies: No studies were conducted. However, waiver from conducting the studies was sought with justifications and the request was approved.

Local tolerance: Florbetaben was tested for injection site reaction effect in rabbits after a single injection (0.5 mL) into the uncongested marginal vein of the ear and a single paravenous application(1 mL) into the hind leg of rabbits. The study suggests no severe or irreversible effects following a single injection of the test article and the vehicle Local tolerance effect of Florbetaben was evaluated in dogs intravenously infused a single dose (5 µg/mL) in the uncongested vena cephalica antebrachii in the left fore leg and 0.9 % (w/v) NaCl-solution in the right foreleg (control). No compound-related effect at the injections sites was demonstrated in this study.

1.3 Recommendations

1.3.1 Approvability

Based on the adequacy of nonclinical studies data provided to support microdose proposed dosage of Florbetaben in the intended indication, the approval of the NDA is recommended from nonclinical perspective.

1.3.2 Additional Non Clinical Recommendations

None

1.3.3 Labeling

The following label recommendations reflect the findings from nonclinical studies or the absence of nonclinical data. Sections are organized with the Sponsor's proposed Neuroceq™ language first (with a single line strike-through where text was deleted) followed by DMIP P/T recommended statements for the Neuroceq ™ label (underlined text).,

13 NONCLINICAL TOXICOLOGY

13.1 Carcinogenesis, Mutagenesis, Impairment of Fertility

Sponsor: (b) (4)

(b) (4)

Animal studies have not been performed to evaluate the carcinogenic potential of Neuroceq™.

Neuroceq™ did not demonstrate mutagenic potential in an *in vitro* bacterial mutation assays (Ames test) using five strains of *Salmonella typhimurium* and one strain of *Escherichia coli* in an *in vitro* chromosomal aberration assay using human peripheral lymphocytes in the absence and presence of a metabolic activation.

No study on impairment of male or female fertility and reproductive performance was conducted in animals.

(b) (4)

Additional nonclinical recommendations for label sections that contain references to nonclinical studies are listed below.

Use in Specific Populations

8.1 Pregnancy

Pregnancy Category C

Sponsor: (b) (4)

(b) (4)

(b) (4)

Pregnancy Category C.

Risk Summary

There are no adequate and well controlled studies of Neuroceq™ in pregnant women. It is not known whether Florbetaben can cause fetal harm when administered to a pregnant woman or can affect reproductive capacity.

All radiopharmaceuticals, including Florbetaben, have the potential to cause fetal harm. The likelihood of fetal harm depends on the stage of fetal development and the magnitude of the radiopharmaceutical dose. Assess pregnancy status before administering Neuroceq™ to a female of child bearing potential. Neuroceq™ should be administered to a pregnant woman only if clearly needed.

Human Data

It is not known if Neuroceq™ crosses the human placenta.

Animal Data

Animal reproduction studies have not been conducted with Neuroceq™.

8.3 Nursing Mothers

Sponsor: H (b) (4)

It is not known whether Neuroceq™ is excreted in human milk. Because many drugs are excreted into human milk and because of the potential for radiation exposure to nursing infants from Neuroceq™, use alternate infant nutrition sources (e.g. stored breast milk or infant

formula) for 24 hours (>10 half-lives of radioactive decay for F 18 isotope) after administration of the drug or avoid use of the drug, taking into account the importance of the drug to the mother.

2 Drug Information

2.1 Drug

CAS Registry Number (Optional)- 902143-01-5

Generic Name- 4-[(*E*)-2-(4-{2-[2-(2-[18F]fluoroethoxy)ethoxy]ethoxy}phenyl)vinyl]-*N*-methylaniline

Code Name - ^{18}F-AV-1, BAY 94-9172, [^{18}F]AV1, [F-18]PEGN3, [F-18]Faβ, ZK060133443, ZK 6057184

Chemical Name- 4-[(*E*)-2-(4-{2-[2-(2-[18F]fluoroethoxy)ethoxy]ethoxy}phenyl)vinyl]-*N*-methylaniline

Molecular Formula/Molecular Weight- $C_{21}H_{26}FNO_3$/358.45

Structure or Biochemical Description- The chemical structure of Florbetaben is shown below:

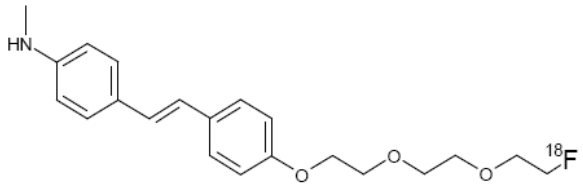

The nonclinical studies were carried out with a non-radioactive 19F-Florbetaben.

Pharmacologic Class- Radioactive Diagnostic Agent

2.2 Relevant INDs, NDAs, BLAs and DMFs

IND 78688

Reference ID: 3361527

2.3 Drug Formulation

The composition of Florbetaben solution for injection per mL and the function of each component is shown below:

Table 1: Composition of Florbetaben solution for injection

Composition	Function	Weight [mg]	Volume [mL)
Total Drug substance ^{18}F-Florbetaben (b) (4) (b) (4)	(b) (4)	≤0.003	
Excipients Ascorbic acid		4.4	
Ethanol (b) (4)		118	
Macrogol 400 (syn.: Polyethylene glycol 400)		200	
Sodium ascorbate		28.8	
(b) (4) water for injections		677.5	
Filling amount		1028.7	1.0 (b) (4))

2.4 Comments on Novel Excipients

No novel excipient was used in the manufacture of this product.

2.5 Comments on Impurities/Degradants of Concern

2.6 Proposed Clinical Population and Dosing Regimen

Adult patients who are being evaluated for Alzheimer's disease (AD) and other cognitive decline will be administered 300 MBq (8.1 mCi) contained in up to 10 mL solution for injection.

2.7 Regulatory Background

Florbetaben, a derivative of polyethyleneglycol stilbene labeled with fluoride-18 (^{18}F) developed as an intravenous injection for PET imaging is proposed for detection of Aβ plaques in brains, thereby assisting in the differential or confirmatory diagnosis in adult patients who are being evaluated for Alzheimer's disease (AD) or other causes of cognitive decline. Bayer HealthCare Pharmaceuticals Inc. submitted an initial Investigational New Drug (IND) application (78868) on Florbetaben to FDA on June 18, 2008. However, Bayer HealthCare Pharmaceuticals Inc. transferred the application to Piramal Imaging SA. Pursuant to 505(b) of the Federal Food, Drug, and Cosmetic Act and 21 CFR §314.1, the new sponsor submitted NDA 204-677 for Florbetaben (BAY 94-9172) Solution for Injection to the Agency on December 21, 2012.

3 Studies Submitted

3.1 Studies Reviewed

1) Determination of IC_{50} using A β1-42 fibrils
2) Determination of IC_{50} using human AD brain homogenate
3) *In vitro* characterization of biological activity of ZK6057184 ((b) (4) in comparison to ZK6087228 ((b) (4)
4) Autoradiographical analysis of binding of [^{18}F]-BAY 94-9172 to brain sections from Alzheimer's disease patients using two different formulations.
5) Binding characteristics of Florbetaben to different beta-amyloid plaque types.
6) Characterization of binding of [^{3}H]-ZK6016468 to beta-amyloid, tau and alpha synuclein pathology using high-resolution photo emulsion autoradiography
7) Characterization of ZK6016468 binding to beta-amyloid and tau-pathology using fluorescence microscopy
8) Florbetaben does not bind to amyloid precursor protein
9) Characterization of amyloid in regional post-mortem brain at different stages of AD-Part 1

10) Characterization of ^{3}H-Florbetaben binding on AD and CTRL autopsy brain tissue

11) Binding characterization of Florbetaben to beta-amyloid plaques /Part II

12) Neurodegenerative disease tissue microarray (TMA): Characterization of binding of AV-1 to different types of neurodegenerative pathologies

13) (b) (4) Pharmacology Data Report on Compound AID-1, (b) (4) (b) (4)

14) Effects of ZK 6057184 (BAY 94-9172) on HERG-mediated potassium current recorded from stably transfected CHO cells

15) Single intravenous dose safety study of PEGN3.HCL in Spraque-Dawley rats with CNS Safety Pharmacology Functional Observational Battery (FOB) and 14 days recovery

16) Effects of ZK 6057184 (BAY949172) on renal function of conscious male rats after a single intravenous injection

17) Effects of ZK 6057184 on the body temperature and the behavior of male and female rats after single intravenous injection.

18) Effect of ZK 6057184 on motor coordination of rats after single intravenous administration.

19) Effects of ZK 6057184 on pulmonary function of conscious unrestrained rats after single intravenous administration.

20) Cardiovascular Safety Pharmacology Study of a Single Intravenous Dose of PEGN3.HCl in Conscious Beagles.

21) Effects of three consecutive intravenous infusions of ZK 6057184 on cardiohemodynamics and ECG in anesthetized Beagle dogs.

22) Pharmacokinetics of [^{19}F]AV1/ZK

23) Blood kinetics of ZK 6013443 after single intravenous administration in rats.

24) Total blood radioactivity time profile after single intravenous administration of ZK6013443 in rats.

25) ZK 6057184 (ref. BAY 94-9172) Systemic toxicity study in rats after single intravenous injection of different formulations including toxicokinetics.

26) ZK 6057184 Toxicokinetic evaluation for repeated-dose toxicity study in male and female dogs with daily intravenous injection over a period of 4 weeks followed by a recovery period of 4 weeks.

27) Biodistribution of ZK 6013443 after single intravenous administration in mice

28) ^{18}F-FAβ NMRI Mouse model data. Dosimetry Report.

29) Influence of formulation of Bay 949172 (ZK6013443) added ZK6057184 on biodistribution in mice after single intravenous administration

30) Metabolic stability of ZK6013443 after incubation with human and mouse liver microsomes

31) Stability of ZK6013443 after incubation in human plasma and detection of metabolites of ZK6013443 in plasma and urine after single intravenous administration in mice

32) Identification of metabolites in plasma after intravenous administration of ZK6013443 in mice

33) Investigation of the polar metabolite fraction of [^{18}F] BAY 94-9172 in mice

34) Detection of metabolites in plasma and brain after intravenous administration of [18F]BAY 94-9172 to mice

35) *In Vitro* Metabolic Profiling and Species Comparison in Liver Microsomes and Hepatocytes.

36) [^{14}C]BAY 94-9172: Biotransformation in Mice.

37) Study A56318: Determination of the Inhibitory Potency of BAY 94-9172 Towards Human CYP Isoforms *in Vitro*

38) Study A56319: BAY 94-9172: Identification of Human CYP Isoforms Involved in the *In Vitro* Metabolism of [^{14}C]BAY 94-9172

39) Study A49560: Positron emission tomographic evaluation of compound [^{18}F]BAY 1008472 and [^{18}F]BAY 949172 in rhesus monkey.

Reference ID: 3361527

40) Study A35105: Acute intravenous toxicity study of polythyleneglycol (PEG)-stilbene in the rat.

41) Study A35107: Acute intravenous toxicity study of polythyleneglycol (PEG)-stilbene in the rat.

42) Study A35109: Single intravenous dose toxicity study of PEGN3.HCL in New Zealand White rabbits followed by 14 days recovery.

43) Study A35106: Acute intravenous toxicity study of Polyethyleneglycol (PEG)-stilbene in the rabbit.

44) Study A141484: ZK 6057184- Repeated-dose toxicity study in male and female rats with daily intravenous injection over a period of 4 weeks followed by a recovery period of 4 weeks.

45) Study A42190: ZK 6057184- Repeated-dose toxicity study in male and female dogs with daily intravenous injection over a period of 4 weeks followed by a recovery period of 4 weeks.

46) Study TOXT8078599: Evaluation of ZK 6057184 (ref. BAY 94-9172) in a bacterial reverse mutation study using Salmonella typhimurium (Ames-Test) and Escherichia coli.

47) Study TOXT7078598: Evaluation of the clastogenic potential of ZK 6057184 (ref. BAY 94-9172) in human peripheral blood lymphocytes.

48) Study EXTT9078888: Chromosome aberration test in human lymphocytes in vitro with (b) (4) (b) (4) (b) (4) (b) (4) – Impurities of ZK 6013443 (ref. BAY 94-9172)

49) Study TOXT2078629: Mix of (b) (4) (b) (4) (b) (4) and (b) (4) (Impurities of BAY 94-9172) - Systemic toxicity study in male and female rats with daily intravenous injection over a period of 2 weeks.

50) Evaluation of (b) (4) (b) (4) (b) (4) and (b) (4) potential impurities of ZK 6013443 (ref. BAY 94-9172) in a bacterial reverse mutation study using *Salmonella typhimurium* (Ames-Test) and *Escherichia coli*

51) Study TOXT9082216: Local tolerance test in rabbits after single intravenous administration in the uncongested ear vein and after single paravenous administration at the hind leg.

52) Study TOXT4078630: ZK 6057184 (ref.: (b) (4) Local tolerance test in the dog (M+F) after single infusion into the uncongested vena cephalica antebrachii.

53) Study TXST20070304: Local tolerance test of ZK 6057184 (ref.: (b) (4)) in the rabbit (M+F) after single intravenous administration into the uncongested vein of the ear and with single paravenous administration.

54) Study TOXT6081476: Evaluation of (b) (4) in a bacterial reverse mutation study using Salmonella typhimurium (Ames-Test)

55) Study TOXT0081083: Evaluation of (b) (4) in a bacterial reverse mutation study using *Salmonella typhimurium* (Ames-Test)

56) Study TOXT3081059: Forward cell mutation assay with (b) (4) at the thymidine kinase locus (TK+/-) in mouse lymphoma L5178Y cells

3.2 Studies Not Reviewed

1) BAY 94-9172 (ZK 6016468): Stable Labeling Synthesis of [^{13}C, $^{2}H_3$]ZK 6016468
2) Radiosynthesis of [^{14}C]ZK 6016468
3) ZK 6057184 (ref. BAY 94-9172, ZK 6013443) Dose range finding study in dogs (M+F) with intravenous administration of a single injection per dose in the dose escalation phase and daily i.v. administration over ca. 1 week in the confirmatory phase.

3.3 Previous Reviews Referenced

IND 78868

4 Pharmacology

Florbetaben is a [^{18}F] labeled polyethyleneglycol stilbene derivative proposed for PET imaging of Aβ amyloid plaques in brains of AD patients. The F-18 isotope has a half-life of 110 minutes. Florbetaben demonstrated a binding affinity to synthetic $A\beta_{1-42}$ fibrils and to post mortem human AD brain homogenate at nanomolar level (inhibition of I-125 IMPY binding: IC_{50}= 24nM ± 5.4 nM). ^{3}H-florbetaben more significantly bound to homogenates of the frontal cortex, temporal cortex, parietal cortex, hippocampus and caudate of AD patients in comparison to age matched controls. The ApoE ε4 status of the AD patients demonstrated no influence on ^{3}H-florbetaben binding to AD brain homogenates. Autoradiography data showed that Florbetaben binds to Aβ amyloid plaque like structures in the grey matter in post mortem human AD brain tissue sections. This correlated with the immunohistochemical demonstration of an anti-amyloid antibody in the same brain tissue sections. Florbetaben does not bind to tau-positive pathologies and alpha-synuclein positive lesions in cortical brain tissue sections of Fronto-temporal Dementia (FTD) and Lewy Body Disease patients, respectively. In addition, Florbetaben/^{3}H-florbetaben does not bind to amyloid precursor protein (APP) immunoreactive structures indicating that Florbetaben specifically binds to beta-amyloid deposits.

4.1 Primary Pharmacology

The sponsor conducted the following studies to establish the primary pharmacodynamics of Florbetaben:

***In vitro* characterization of biological activity of ZK 6016468**

In this study, the affinity of ZK 6016468 was determined using a competition assay with synthetic Aβ fibrils or human AD homogenate and I-125 labeled ZK6006755 as ligand. ZK6016468 employed during this study is the non-radioactive derivative of ZK6013443, F-18 labeled amyloid β (Aβ) peptide binding compound. The study involved

Determination of IC50 using A β1-42 fibrils and

Determination of IC50 using human AD brain homogenate

(a) Determination of IC50 using Aβ1-42 fibrils- This competition assay was conducted on I-125labeled IMPY, ZK 6006755, and ZK 6016488 tracers using synthetic Aβ1-42 fibrils in 96-well plates. The results of the competition assay shown that the inhibition of ZK6006755 binding to Aβ1-42 fibrils by ZK 6016468 gave IC_{50} [nM] range of 96-151 and mean IC_{50}±SD [nM] of 146±34. Thus, ZK 6016468 demonstrates reasonable inhibition of ZK 6006755 binding to synthetic Aβ fibrils with IC_{50} of 146±34 nM.

(b) Determination of IC50 using human AD brain homogenate-

The competition assay was conducted between ZK 6006755 and ZK 6016468 using brain homogenate obtained from two AD patients and the brain homogenate from an age-matched healthy as control. The result of the assay indicates that ZK 6016468 shows a high inhibition of ZK 6006755 binding to human AD brain homogenate (IC50=24±5.4nM)

***In vitro* characterization of biological activity of ZK 6057184 ((b) (4) in comparison to ZK 6087228 ((b) (4)**

The sponsor conducted competition assay on (b) (4) (b) (4)-ZK6087228 and (b) (4)-ZK 6057184) and I-125 labeled ZK 6006755 as tracer using brain homogenate obtained from one AD patients in a 96-well plates.

The result of the assay shows that both (b) (4) demonstrate the same affinity to human AD brain homogenate with IC50 values ranging from 31.7-42.6 (mean; 38.2±4.0 nM) and 35.5-43-6 nM (mean; 38.5±4.4 nM) for (b) (4)-ZK 6057184 and (b) (4)-ZK 6087228 respectively. This data indicates that both (b) (4) of BAY 949172 are biologically active in relation to imaging.

Autoradiographical analysis of binding of [18F]-BAY 94-9172 to brain sections from Alzheimer's disease patients using two different formulations.

The study evaluated the impact of two different formulations (A and B).

Table 2: Composition of the BAY 94-9172 formulations

	A:	B: New Formulation
Ethanol (b) (4)	(b) (4)	
PEG 400		
Ascorbic acid		
Sodium ascorbate		
(b) (4)		
Water		
pH		

(b) (4)

beta-amyloid binding properties of the tracer *in vitro*. (b) (4) The focus of this study is therefore to compare autoradiography on serial brain sections using two different vehicles.

Frozen brain sections of AD patients and healthy control (HC) were incubated with [^{18}F]-BAY 94-9172 using two different dilutions (1:500 and 1:50) of the A and B formulation. The brain sections were washed with buffer solution or alternatively with 40% ethanol and radioactive signals in plaque bearing grey matter regions were quantified using a phosphoimager device (Fuji BAS5000). The images were taken on a BX61 microscope (Olympus, Germany) using Cell P software (Olympus Soft Imaging Solutions). Analysis software (Aida Image Analyzer v.4.15)

was used for quantification of radioactive signals for each patient by measuring the signal intensity in 3 similar "regions of interest" (ROI, 1.6-1.7mm^2) in plaque bearing grey matter regions of each patient´s section. The mean values and standard deviations were calculated based on the intensities found in each ROI.

Results: The images of AD brain sections incubated with the 1:50 and 1:500 dilutions of the two formulations of Florbetaben showed specific plaque like structures in grey matter regions of the brain. The study demonstrated absence of comparable signals in sections of healthy controls. It was found that visual inspection did not reveal any obvious differences between the different treatments. Thus suggesting that despite the differences in the excipients of the current and the new formulations, no difference in the imaging pattern of beta-amyloids in the AD patients is envisaged.

The quantification of the Florbetaben signal in the grey matter region in both the AD and HC subjects was also conducted. The mean signal intensity values of four AD patients measured with the help of a phosphoimager device in three similar regions for each patient were obtained for the two formulations. No significant changes were found do not significantly differ between the signal intensities of the different Florbetaben formulations. Furthermore, the quantification of beta-amyloid plaque related signal strength and unspecific background in HC also did not reveal any significant differences between the formulations at the dilutions applied. This suggests that the variations in signal intensity among different AD cases probably reflect individual differences in the plaque load which might be unrelated to the different formulations employed during the study.

This study suggests that the modifications introduced into the current formulation to produce the planned "commercial" new formulation seem not to significantly change the beta-amyloid binding specificity of Florbetaben *in vitro*.

Binding characteristics of Florbetaben to different beta-amyloid plaque types

This study was conducted to determine the binding pattern of Florbetaben to different species of beta-amyloid depositions in AD brain. The amyloid depositions evaluated are core and non-coreplaques as well as the vascular depositions in different cortical regions of post-mortem human Alzheimer diseased brains. Paraffin embedded tissue from frontal and temporal cortices of 14 and 17 post-mortem cases, respectively, with AD were employed in this study. The focus of this study was to determine the concordance of Florbetaben binding with classical immunohistochemical detection of beta-amyloid depositions immunohistochemistry on the same section after Florbetaben binding. The sponsor conducted Florbetaben binding study and fluorescence microphotographs on the brain slices. This was followed by immunohistochemical detection of beta amyloid deposits using IE8 antibody (Tammer at al, 2002). A routine

Reference ID: 3361527

Bielschowsky staining was performed on an adjacent section to the section used for [^{19}F]Florbetaben binding to compare Florbetaben binding pattern with this classical beta-amyloid detection method. Microphotographs were taken using an Olympus BX61 microscope. As shown in the data, the overviews were placed side by side and the beta amyloid immunoreactive plaques compared with the Florbetaben positive ones. The concordance was expressed in % of 1E8 immunoreactivity and the data showed that [^{19}F]Florbetaben binds to non-cored, cored and vascular beta-amyloid deposits in the brain areas investigated (Figure 1). However, the sponsor did not consider cored and non-cored plaques separately. It was found that the binding is consistent with the pathological observations following the use of Bielschowsky reagent (Figure 1).

Amyloid deposition

Bielschowsky [^{19}F]Florbetaben [^{3}H]Florbetaben

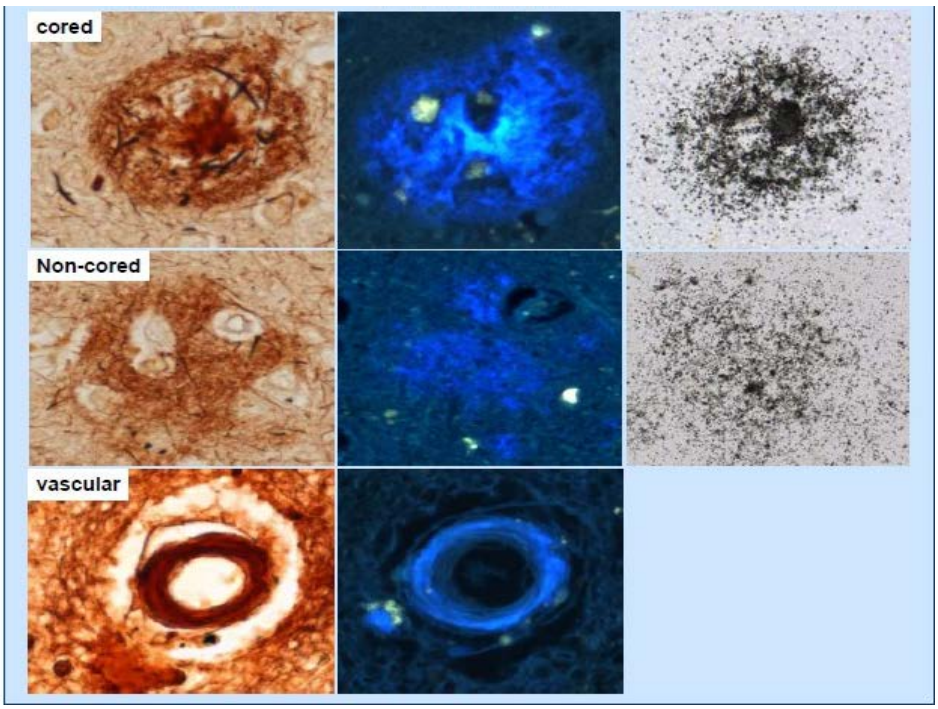

Figure 1: [^{19}F]Florbetaben (blue fluorescence) and [3H]Florbetaben (black silver grains) bind to cored (first row), non-cored (second row) beta-amyloid deposits as confirmed with Bielschowsky silver stain.

In addition, [^{19}F]Florbetaben (blue fluorescence) is also shown to bind to vascular beta-amyloid deposits (lower row) as confirmed by Bielschowsky silver stain. It was also reported that the pathological observation matched with the immunohistochemical staining using the 1E8 anti-beta-amyloid antibody shown below.

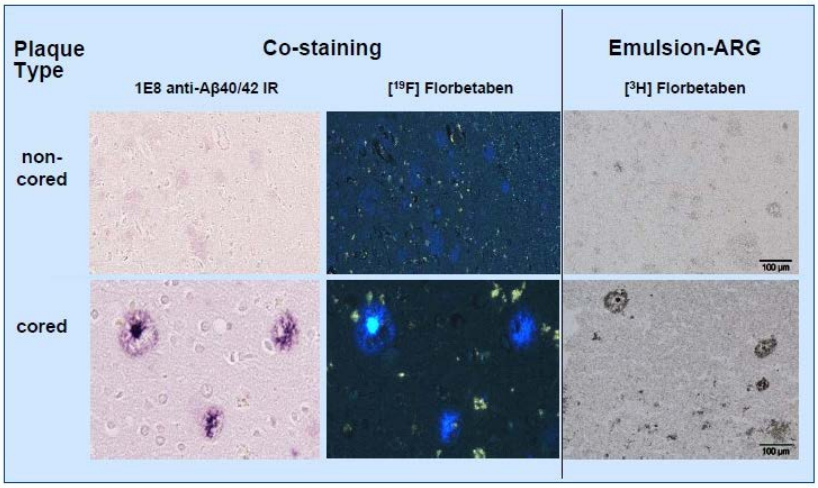

Figure 2: [^{19}F]Florbetaben (middle row, blue fluorescence) and anti-beta-amyloid antibody 1E8 (left row, dark red staining) were subsequently bound/immunohistochemically stained on cortical brain sections from AD patients to detect beta-amyloid deposits.

[^{19}F]Florbetaben fluorescence matched very well with 1E8 immunoreactivity (IR). The right row demonstrates [^{3}H]Florbetaben binding and autoradiographical detection with emulsion. Note the silver grain signals (black) resemble cored and non-cored beta amyloid deposits comparable to those seen in 1E8 immunohistochemistry and [^{19}F]Florbetaben binding, respectively.

During quantitative analysis, 14 frontal cortices and 17 temporal cortices were investigated out of which 11 frontal cortices and 16 temporal cortices were evaluable (Figure 3).Manual comparison of the immunohistochemical profiles with the profiles seen by [^{19}F]Florbetaben binding revealed a 94.41±5.83% concordance with immunohistochemistry in the frontal cortices and a 92.73±8.95% concordance in the temporal cortices. This indicates no significant difference between the concordance of the immunohistochemistry of the regions.

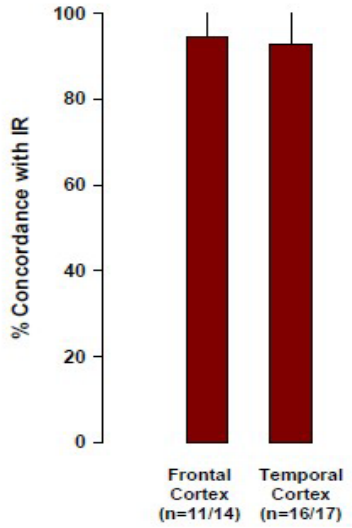

Figure 3: Graph presenting % concordance of [^{19}F] Florbetaben fluorescence with 1E8 anti-beta amyloid immunoreactivity

Reviewer's Comment: Agree with the result of this study which showed that [^{19}F/^{3}H] Florbetaben detected cored and non-cored beta amyloid plaque deposits as well as vascular depositions. However, the sponsor did not separately evaluate the cored and non-cored plaques in the different cortical regions of post-mortem human Alzheimer diseased brains evaluated during the study. As a result, added utility of the data in terms of revealing any variation in the intensity of Florbetaben binding to either the cored- or non-cored plaques is lacking.

Characterization of binding of [^{3}H]-ZK6016468 to beta-amyloid, tau and alpha synuclein pathology using high-resolution photo emulsion autoradiography

This study is necessitated by literature evidence (Rowe et al, 2008) showing that [^{18}F]-Florbetaben-PET retention matched the reported post-mortem distribution of beta amyloid plaques. Thus, the nature of Florbetaben binding to other pathological misfolded proteins needs further specification to assess its selectivity for beta-amyloid plaques over other proteins forming beta-pleated sheet structures. The proteins could be alpha-synuclein or tau, which form the basis of Lewy bodies and neurofibrillary tangles, respectively. Therefore, the selectivity of [^{3}H]-ZK 6016468 for beta-amyloid plaques in human post mortem brain tissue utilizing high-resolution photo emulsion autoradiography was assessed by the sponsor.

During this study, high-resolution emulsion autoradiography combined with subsequent immunohistochemistry was employed on the same brain sections to characterize [^{3}H]-ZK

6016468 binding to different pathologies. Frozen and paraffin tissue sections of AD patients, DLB (Dementia with Lewy Bodies) patients and HC (healthy control) were incubated with [^{3}H]-ZK 6016468. Paraffin sections were deparaffinized using routine histological methods before performing binding studies and immunohistochemistry. Emulsion autoradiography was performed on the sections by incubating them with 10 Bq/µL [^{3}H]-Florbetaben diluted in 25 mM HEPES buffer for one hour at room temperature in a humidified chamber. Following washing of the sections with HEPES buffer or 40% ethanol and dipping in distilled water for 10 seconds, the sections were fixed with formaldehyde. The sections were then immunostained with antibodies to beta-amyloid, tau or alpha synuclein. The slides were dipped into Kodak NTB photo emulsion (b) (4) exposed for 17 days in the dark and finally developed and fixed using Phenisol and Hypam solutions (b) (4) The pictures were taken on BX61 microscope (b) (4) using Cell P software ((b) (4)

The data showing [^{3}H]-ZK 6016468 binding as indicated by blackening of photo emulsion in form of silver grains was provided.(Figure 3) and (Figure 4) show plaque like structures that were co-immunostained with the beta-amyloid specific antibody (1E8) in the AD tissue (paraffin and frozen sections). No accumulation of silver grains above background levels was found in the tau neurofibrillary tangles and PHF-tau positive neurites. Tau pathology was detected with the AT8 antibody, which detects phosphorylated PHF-tau protein. In DLB sections, the presence of Lewy bodies and Lewy neurites could specifically be identified by immunostaining with LB509 antibody. However, all LB509 positive structures did not show an accumulation of silver grains above normal levels (Figure 3).

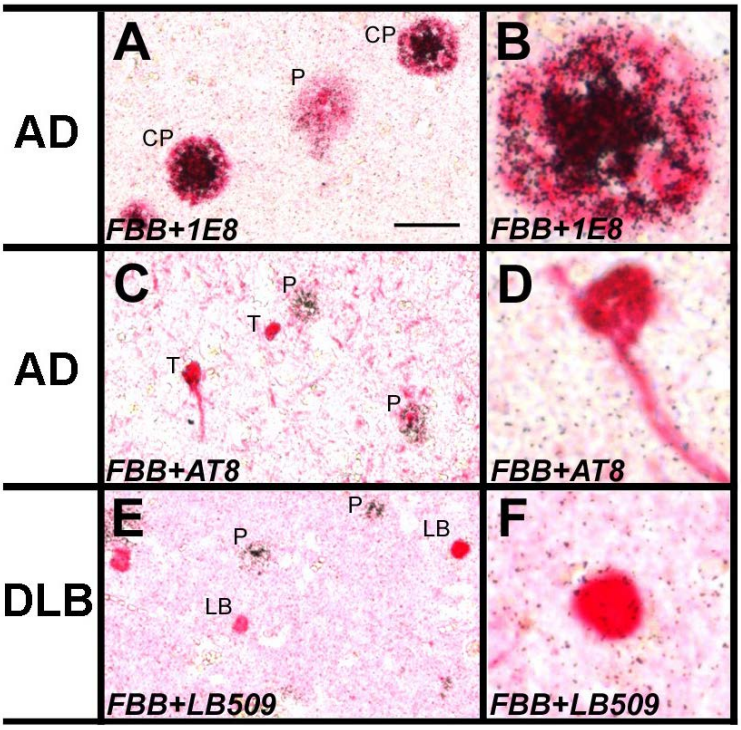

Figure 4 : [^{3}H]-ZK 6016468 binding to different pathologies

[^{3}H]-ZK 6016468 specifically binds to beta-amyloid plaques, but not to PHF-Tau or α-Synuclein pathology as analyzed by high resolution emulsion autoradiography using [^{3}H]-Florbetaben combined with subsequent immunohistochemistry for different pathologies. A. [^{3}H]-ZK 6016468 (FBB, silver grains) binding to beta-amyloid plaques on paraffin embedded cortical Alzheimer's disease (AD) tissue sections co-localized with anti-beta amyloid immunohistochemistry (1E8, red) in cored and non-cored plaques. B. Magnification of a cored plaque. C. FBB emulsion autoradiography combined with anti-PHF-tau immunohistochemistry (AT8, red). Note that no clusters of silver grains were found on AT8 immunoreactive NFTs. D. Magnification of a NFT. E. FBB emulsion autoradiography on Dementia with Lewy Body brain tissue sections combined with anti-Synuclein immunohistochemistry (LB509, red). There is no clustering of silver grains on Lewy bodies and Lewy neurites. F.Magnification of an alpha synuclein LB. Scale bar: 50 µM (applies for A, C and E). LB: Lewy body; CP: cored plaque; P: plaque; T: neurofibrillary tangle.

There were increased densities of silver grains, reminiscent of the plaque-like signals observed in AD tissue in the same sections beta-amyloid plaques, whose presence was confirmed by 1E8 staining (Figure 5). The sponsor reported that no pathology specific signals above background for [^{3}H]-ZK 6016468 and for the antibody stains on brain sections from healthy controls. This demonstrates high specificity of the applied reagents.

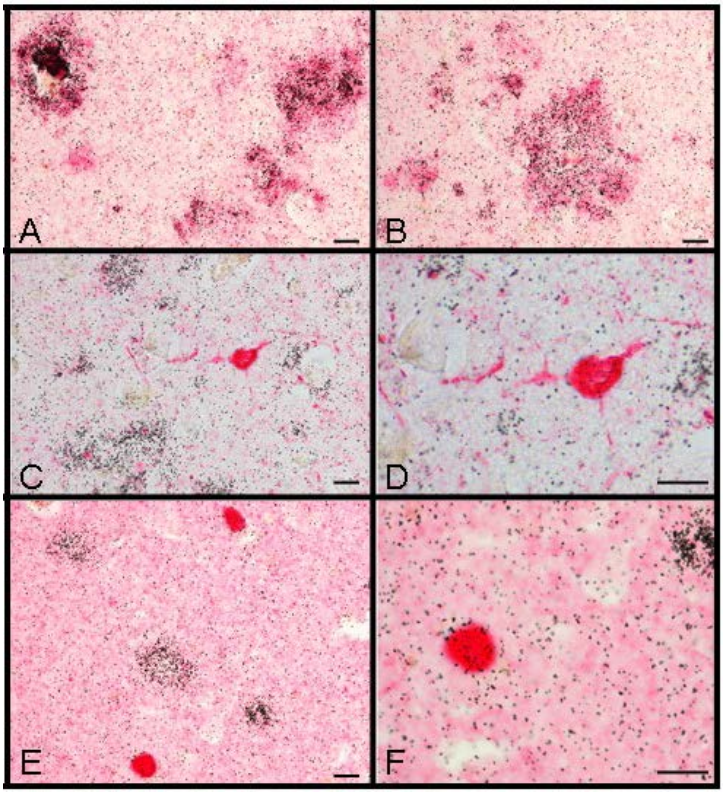

Figure 5: Florbetaben binds to beta-amyloid plaques, but not to Tau lesions or α-synuclein Lewy bodies as analyzed by high resolution emulsion autoradiography using [^{3}H]-Florbetaben combined with subsequent immunohistochemistry for different pathological lesions

In A-D images of frontal cortices of an AD patient and in E and F of a DLB patient are shown. A and B. [^{3}H]-Florbetaben binding (silver grains, black) to beta-amyloid plaques on paraffin embedded cortical Alzheimer's disease (AD) tissue sections co-localized with anti-beta-amyloid immunohistochemistry (1E8, red) C. [^{3}H]-Florbetaben emulsion autoradiography combined with anti-tau-immunohistochemistry (AT8, red). Note that no clusters of silver grains were found on AT8 immunoreactive NFTs or on the neuropil threads. Clustering of silver grains, was only observed as beta-amyloid plaque like structures D. Magnification of a NFT in C. E. [3H]-Florbetaben emulsion autoradiography on Dementia with Lewy Body Disease brain tissue sections combined with anti-α-synuclein-immunohistochemistry (red). There is no clustering of silver grains on Lewy bodies whereas clusters of silver grains, resembling beta-amyloid plaque like structures was observed. F. Magnification of α-synuclein Lewy Body in E. Scale bar: 15 μM.

This study indicates that [^{3}H]-ZK 6016468 specifically binds to beta-amyloid pathology and not to alpha synuclein containing Lewy bodies or tau neurofibrillary tangles.

Reviewer's Comment: Agrees with the results obtained from this study which indicates that Florbetaben-PET retention within the cortical grey matter regions of AD patients is attributable to the binding of [^{18}F]-Florbetaben to beta amyloid plaques. The immunohistochemistry and autoradiography techniques employed to characterize the binding of binding of [^{18}F]-Florbetaben to beta amyloid plaques add value to the credibility of the data obtained from this study.

Characterization of ZK 6016468 binding to beta-amyloid and tau-pathology using fluorescence microscopy

Available evidence indicates that pathological hallmarks of AD are beta-amyloid plaques and neurofibrillar tangles (NFT). NFT consists of Paired Helical Filaments (PHF) which are composed of hyperphosphorylated tau. In an attempt to characterize the selectivity of ZK 6016468 to beta-amyloid plaques over PHF, the sponsor analyzed the *in situ* binding of ZK 6016468 to tissue sections from patients with AD, patients with Frontotemporal Dementia (FTD) and healthy controls (HC) using fluorescence microscopy and the autofluorescence of [^{19}F]-Florbetaben.

Frozen tissue sections from the frontal lobe of 5 AD patients, 6 FTD patients and 4 age-matched HC were incubated with 10 µM ZK6016468 for 1 hour at room temperature. The sections were stained with the AT8 antibody generated in mouse which recognizes human PHF-Tau deposits. A Cy2-labelled secondary anti-mouse antibody was used for the detection of the primary antibody to visualize the underlying tau-pathology. The sections were then microscopically evaluated using the Olympus BX61 microscope and the standard UV filter block (excitation filter 360 - 370nm, emission filter 420nm) for detection of the auto-fluorescence of ZK6016468 upon binding to beta-amyloid plaques and the Cy2 filter block (excitation filter 470 - 490 nm, emission filter 510 - 550nm) for detection of the immunostaining.

The result of this study shows that the fluorescence microscopy of ZK6016468 visualized plaque like structures on AD brain tissue sections (6). The sponsor reported that no signals were visible on control sections from age matched controls or brain slices from patients with frontotemporal dementia (FTD) as shown in Figure 7, although PHF-Tau deposits could be detected by immunohistochemistry on the same FTD tissue sections. Furthermore, no co-staining of PHF-Tau with ZK 6016468 and the anti-human-PHF-Tau antibody was detected on AD brain tissue sections. This indicates that ZK 6016468 does not bind to PHF-Tau in human AD and FTD brain tissue sections demonstrating its specificity for beta-amyloid.

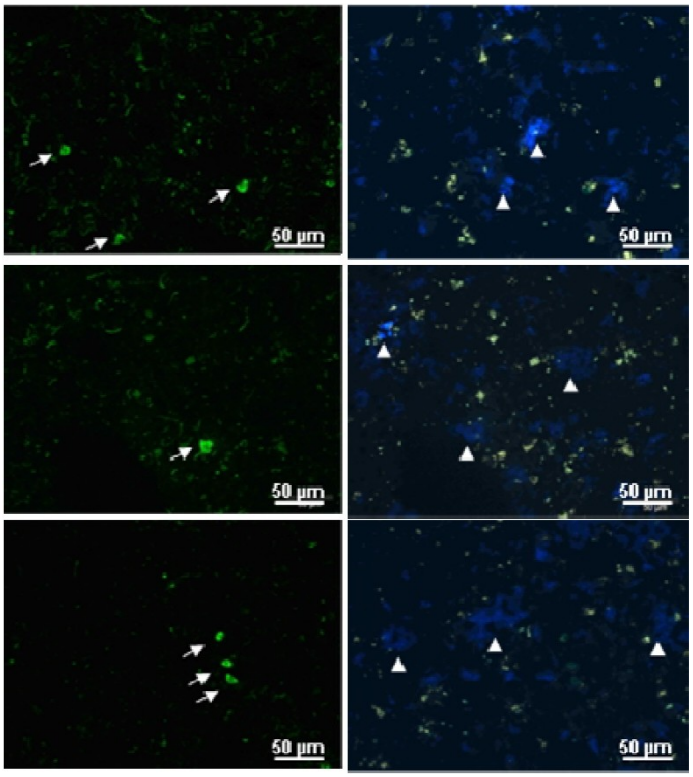

(A) ATS **(B) ZK6016468**

Figure 6: Example of brain tissue sections from AD patients incubated with the non-radioactive drug substance ZK6016468.

Images of AD brain tissue sections of three representative samples are shown. (B) Microscopic autofluorescence images of the non-radioactive drug substance ZK 6016468 using UV excitation show that ZK 6016468 binds to plaque like structures (blue autofluorescence; white arrow heads). (A) The same microscopic frames as in (A) are shown demonstrating immunoreactive signals depicting PHF-Tau depositions on the same sections as in B (green fluorescence, white arrows).

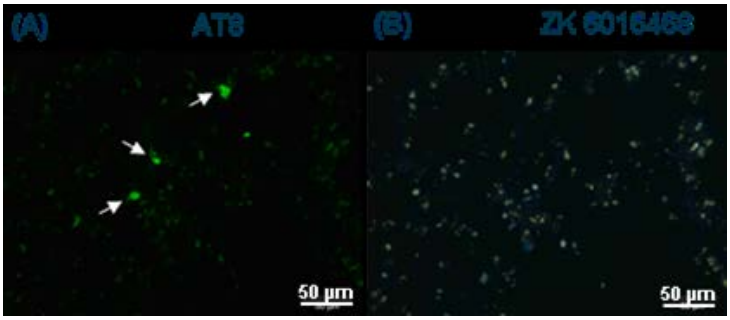

Figure 7: Example of a brain tissue section from a FTD patient incubated with the non-radioactive drug substance ZK 6016468.

Image of a FTD brain tissue section is shown. (B) Microscopic autofluorescence images of the non-radioactive drug substance ZK 6016468 using UV excitation show that ZK 6016468 does not bind to PHF-Tau like structures. (A) The same microscopic frames as in (B) are shown demonstrating immunoreactive signals depicting PHF-Tau depositions on the same sections as in B (green fluorescence, white arrows).

This study demonstrates that [^{19}F]-Florbetaben specifically binds to beta-amyloid pathology, and not to PHF-tau deposits in AD and FTD brain tissue section under the tested conditions.

Reviewer's Comment: Agrees with the data obtained from this study. The data shows that [^{19}F]-Florbetaben binds specifically to beta amyloid and not to any other protein deposits in the AD and FTD brain tissue sections. The data corroborates the data obtained from the characterization of [^{19}F]-Florbetaben to beta amyloid, tau and alpha synuclein pathology study reviewed above in establishing that the radioactive drug substance [^{18}F]-Florbetaben binds specifically to beta amyloid plaques.

<u>Florbetaben does not bind to amyloid precursor protein</u>

This study was conducted to determine if Florbetaben binds to amyloid precursor protein (APP). The study was performed on paraffin embedded human brain sections from cerebellar pieces of three Alzheimer diseased post-mortem brains (clinical Phase III study no. 14595). The brains were sliced (6-8 µm) and mounted and deparaffinized in graded alcohols before employed for subsequent investigations. Both [^{19}F]-Florbetaben at 10 µM concentration of and [^{3}H]-Florbetaben at 1.88 ng/µL (200µL/section) were used for binding studies while the detection of [^{19}F]-Florbetaben fluorescence involved the use of microscope (Olympus, BX61) equipped with UV filters. The [^{3}H]-Florbetaben binding studies were performed with emulsion autoradiography. The binding patterns were detected microscopically by searching for silver grain clusters. Furthermore, microphotographs were taken from a Bielschowsky stain, 6E10 and APP immunohistochemistry on subsequent sections (repetition of the Standard of Truth (SoT) staining. The sponsor compared the binding pattern of Florbetaben (fluorescence and emulsion

autoradiography) to the pattern detected using the immunohistochemical and histological methods.

The data obtained from this study demonstrated no resemblance in APP immunoreactivity patterns in the ischemic area observed neither with ^{19}F-florbetaben fluorescence nor with ^{3}H-florbetaben using emulsion autoradiography binding patterns as shown in Figure 8 to Figure 10 below.

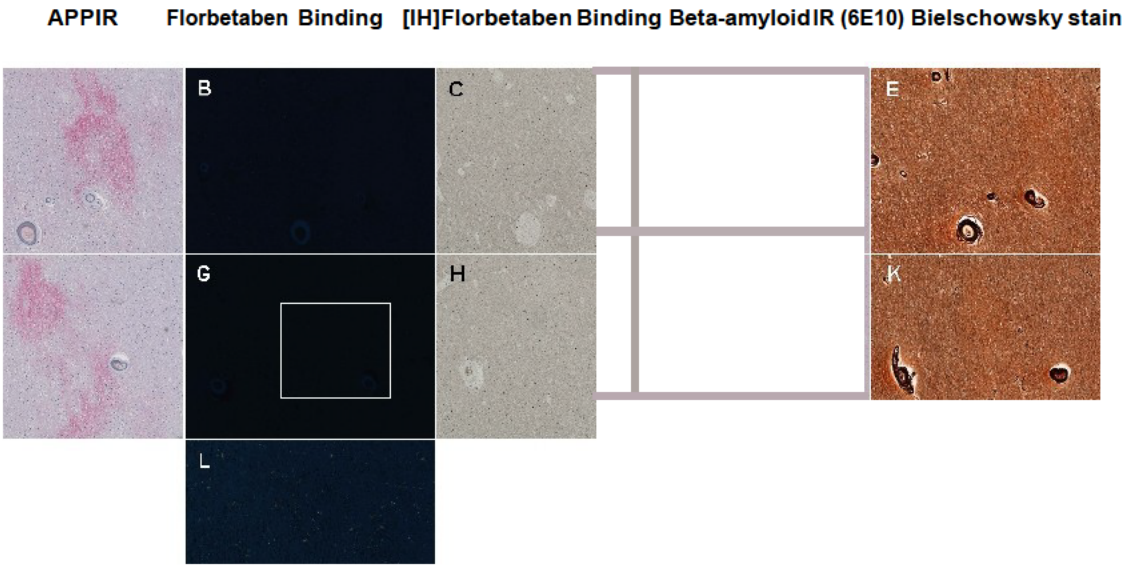

Figure 8: Case 200010004 Cerebellum.

White matter infarct with APP IR (A-E and F-L) Fotographs of the same affected areas in subsequent sections. (A, F) APP IR as detected using the antibody MAB348 [redacted] (b) (4). (B, G) UV detection of Florbetaben binding (10 µM). (C, H) 3H-florbetaben emulsion autoradiography (11.7 Bq/ µL=1.88 fg/ µL); (D, I) beta-amyloid IR as detected using the antibody 6E10 ([redacted] (b) (4) (E, K) Bielschowsky silver stain. (L) is a higher magnification of the square in (G). IR=Immunoreactivity; Bar:200 µm

Figure 9: Case 200020006 Cerebellum.

Small white matter infarct with APP IR (A-E) Fotographs of the same affected area in subsequent sections. (A) APP IR as detected using the antibody MAB348 ((b) (4) (B) UV detection of Florbetaben binding (10 µM). (C) 3H-florbetaben emulsion autoradiography (11.7 Bq/ µL=1.88 fg/ µL); (D) beta-amyloid IR as detected using the antibody 6E10 ((b) (4) (E) Bielschowsky silver stain. IR=Immunoreactivity; Bar: 200 µm

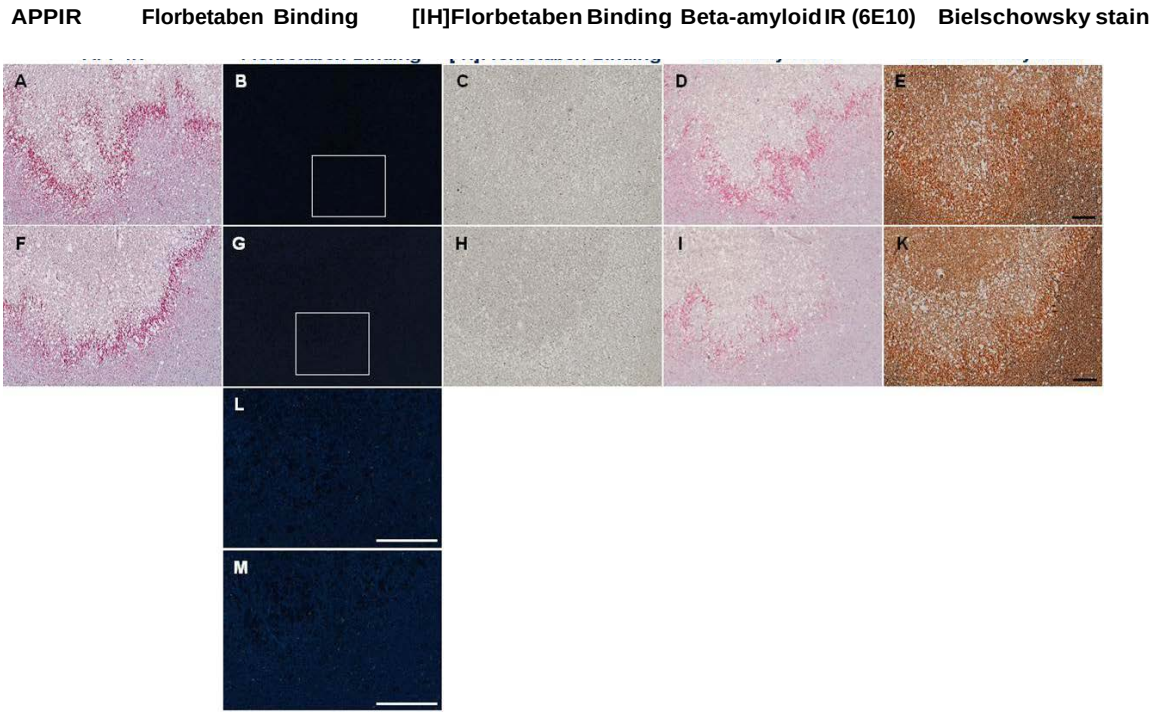

Figure 10: Case 200040012 Cerebellum.

Large white matter infarct with APP IR. (A-E and F-K) Fotographs of the same affected areas in subsequent sections. (A, F) APP IR as detected using the antibody MAB348 (b) (4) . (B, G) UV detection of Florbetaben binding (10 µM). (C, H) 3H-florbetaben emulsion autoradiography (11.7 Bq/ µL=1.88 fg/ µL). (D, I) beta-amyloid IR as detected using the antibody 6E10 ((b) (4) (E, K) Bielschowsky silver stain. (L, M) Higher magnification of the square in B and G, respectively. IR= Immunoreactivity; Bar: 200 µm

The data also shows positive immunoresponse seen with the 6E10 antibody only partially match with the immunopositivity of the APP antibody. The sponsor attributed this finding to additional reactivity of the 6E10 antibody with beta-amyloid precursor forms as described by the provider.

Reviewer's Comment: Agrees with the result of this study which indicates that Florbetaben does not bind to amyloid precursor protein (APP). The positive immunoresponse seen with the 6E10 antibody seems to reflect APP positivity. Thus, the immunopositivity is probably because of antibodies cross reactivity with beta-amyloid precursor forms.

Characterization of amyloid in regional post-mortem brain at different stages of AD-Part 1

This study was employed to characterize regional distribution of brain amyloid in AD autopsy brains. The Autopsy brain tissues used for the study were obtained from 14 AD cases (mean age 69.7±2.4years), each with a clinical diagnosis confirmed by pathological examination (NlNCDS-ADRDA and CERAD criteria), and 12 controls (mean age 76.6±*32* years) collected at the [redacted] (b) (4). The sponsor defines eight of the AD cases that clinically diagnosed as AD earlier than 65 years of age were defined as early-onset AD (EOAD) (mean age 63.5 ± 2.0 years), and six cases (mean age 78. 0 ± 2.0 years) diagnosed as AD older than 65 years of age were defined with late-onset AD (LOAD). Fresh frozen brain tissues harvested from the frontal, parietal, temporal cortex, hippocampus, caudate nucleus and cerebellum from 14 AD and 12 control subjects were homogenized in sucrose containing protease inhibitors (10 µL/mL) and stored at -80°C. The protein concentration was then determined using DC protein assay ([redacted] (b) (4)

The following assays were then conducted on [^{3}H]-Florbetaben.

(a) Single Concentration Measurement- This involves performing binding assay on 50 µL homogenates (100 µg tissue), incubated in PBS + 0.1% BSA, pH 7.4 (137 mM NaCI, 3 mM KCl, 10 mM sodium phosphate, 0.1% BSA; pH 7.4) containing 5 nM ^{3}H-Florbetaben for 3 hours at room temperature in a 500 µL mixture. Any nonspecific binding was determined in the presence of 0.75 µM unlabeled Florbetaben (Bayer Pharma AG, Germany). Single concentration ^{3}H-Florbetaben (5 nM) binding assays were performed on six brain regions (frontal, parietal, temporal cortex, hippocampus, caudate nucleus and cerebellum) isolated from 12 AD and I 2 control autopsy brain tissues.

(b) Saturation binding assays- The assays were conducted using 50 µL homogenates (100 µg tissue) from frontal cortex, hippocampus from 3 AD cases and 3 control subjects by incubation with ^{3}H-Florbetaben. Any non-specific binding was also determined in the presence of 0.75 µM unlabeled Florbetaben.

(c) Competitive binding assays- Fresh frozen postmortem tissues (gray matter) from the frontal cortex; temporal cortex, obtained from AD and control subjects were homogenized in sucrose containing protease inhibitors (10 µL/mL sucrose) and stored at -80°C.The competitive binding assays on ^{3}H-Florbetaben were then performed on 50 µL homogenates (100 µg tissue) from one AD frontal cortical tissue by incubation with 5 nM ^{3}H-Florbetaben in the presence of 10^{-13}-$5x10^{-4}$ M unlabeled Florbetaben and 2-(4'-Methylarninophenyl) benzothiazole (BTA-1) from [redacted] (b) (4), respectively.

ApoE genotyping – This DNA extraction for ApoE genotyping was performed on the brain tissue obtained from the thalamic region of each subject. This was followed by the amplification of

exon 4 of the ApoE gene using the INNO-LiP A ApoE Amp kit [redacted] (b) (4) to prepare a mastermix according to manufacturer's protocol. TaqPol enzyme and distilled H_20 were added to the mastermix, which was distributed to the extracted samples and the DNA template was amplified by PCR. The amplification of exon 4 of the ApoE gene in sufficient amounts was verified by separating the newly synthesized products using gel electrophoresis. An agarose gel was cast, samples loaded in the wells and run by electrophoresis for 2 hours. The gel was analyzed under UV -light; a band at 299 bp indicated presence of exon 4 of the ApoE gene. The determination of each individual ApoE genotype was performed using INNO-LiPA ApoE kit [redacted] (b) (4)

Data obtained from the binding assays were analyzed using GraphPad Prism software 5.0 (GraphPad Software, Inc., La Jolla, CA, USA). The comparison between AD and control group were analyzed by nonparametric Mann-Whitney test while multiple comparison analysis was done using one way ANOVA. The dissociation constant K_d, B_{max}, BP (binding potential, B_{max} K_d) as well as K_i were determined. The sponsor performed correlation analyses using non-parametric Spearman's rank order correlation.

Results:

Characterization of ^{3}H-Florbetaben binding on AD and CTRL autopsy brain tissue

The *in vitro* data shows competitive ^{3}H-Florbetaben binding with increasing concentration of Florbetaben or BTA-1 and binding affinity of 11.6 nM and 20 nM for Florbetaben and BTA-1 respectively on fibrillar amyloid on AD frontal cortical autopsy brain as shown in Figure 11.

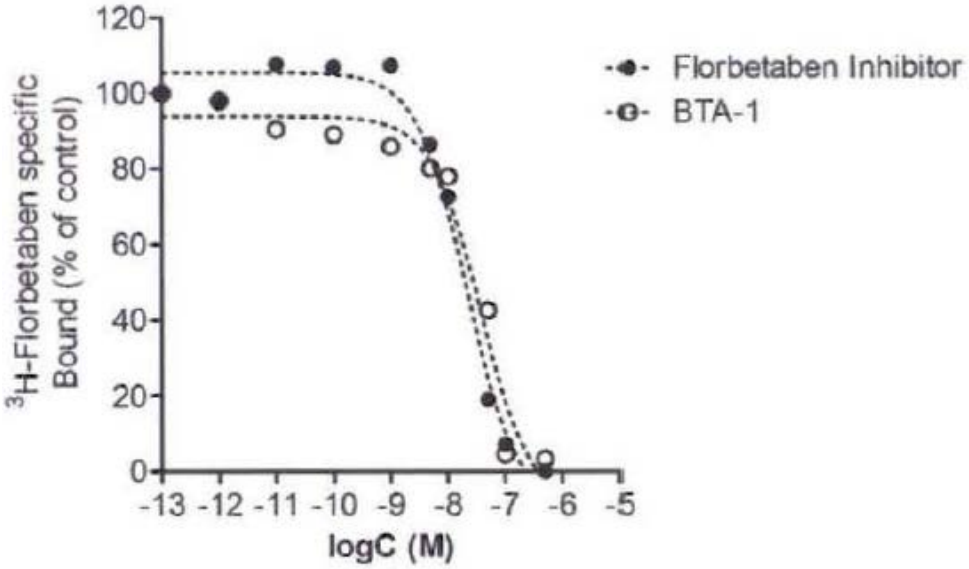

Figure 11: ^{3}H-Florbetaben (5nM) competitive binding against increasing concentration of Florbetaben or BTA-1 (10^{-13}M-10^{-6}M) on one AD frontal cortical autopsy brain tissue.

As a follow up on the K_i values determined from ^{3}H-Florbetaben competitive binding curve, the sponsor employed 5 nM ^{3}H-Florbetaben in the measurement of ^{3}H-Florbetaben binding on six brain regions of AD (n = 12) and CTRL (n = 12) autopsy brain tissue (frontal, parietal, temporal cortex, hippocampus, caudate nucleus and cerebellum). As shown in Figure 12, higher ^{3}H-Florbetaben binding was reported in the frontal, parietal, temporal cortex, caudate nucleus and hippocampus in AD compared with CTRL, but not in the cerebellum.

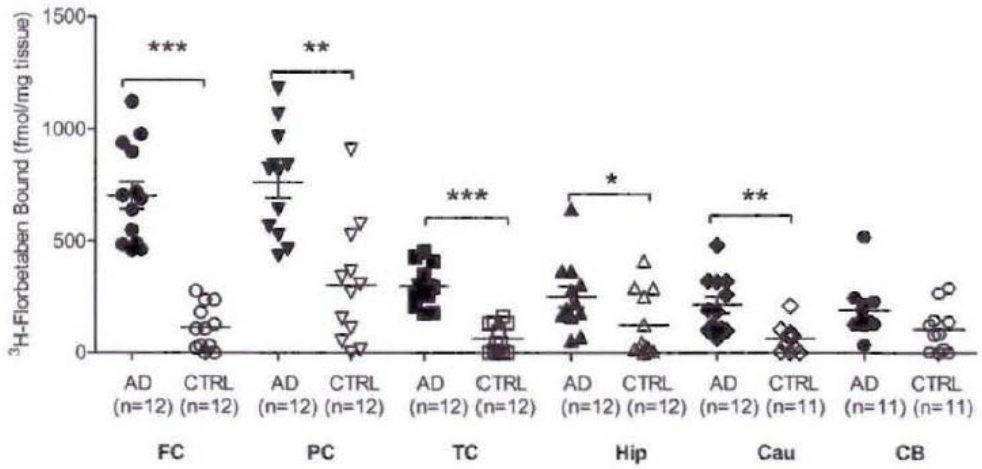

Figure 12: ^{3}H-Florbetaben binding (5 nM) on frontal, parietal, temporal cortex, hippocampus, caudate nucleus and cerebellum from AD compared with CTRL; frontal cortex (FC), temporal

cortex (TC), parietal cortex (PC), hippocampus (Hip), caudate nucleus (Cau) and cerebellum (CB); *p<0.05, **p<0.01, ***p<0.001, Mann-Whitney test.

The *in vitro* ^{3}H-Florbetaben (0.01-200 nM) saturation binding data indicates two binding sites in the AD frontal cortex. These are (1) high affinity site (K_d = 16 nM, B_{max} = 2431 fmol/mg tissue) and (2) a low affinity site (K_d = 135 nM, B_{max} = 12180 fmol/mg tissue) (Figure 13A, B). The sponsor focused subsequent saturation assays on the high affinity binding site. In an additional study, 0.01 – 40 nM ^{3}H-Florbetaben were used to perform an *in vitro* saturation ^{3}H-Florbetaben binding assays on frontal cortical autopsy brain tissue from AD and CTRL (Figure 13C, D).

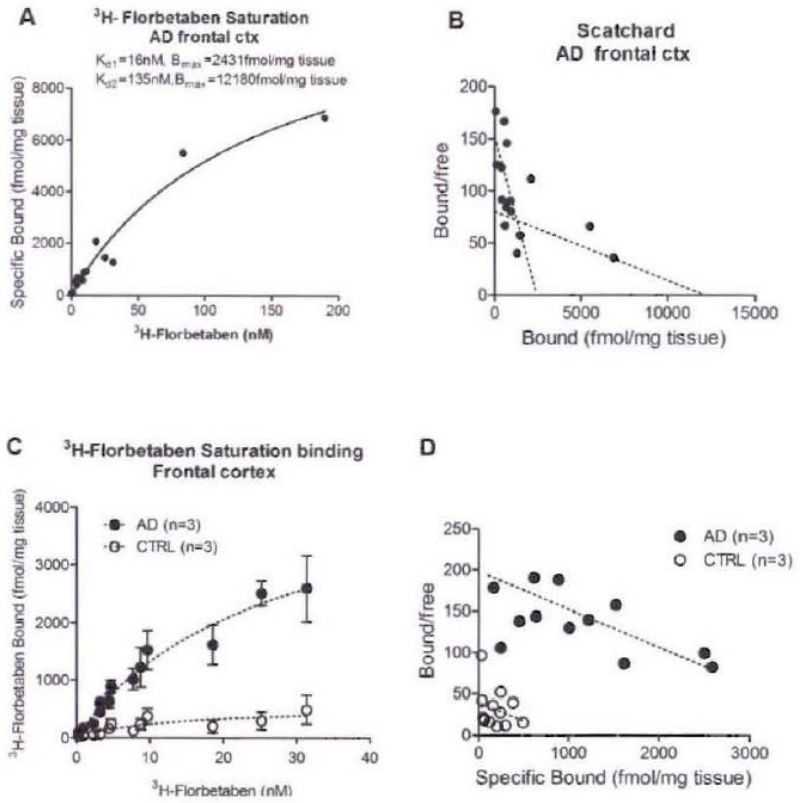

Figure 13: A, B) Representative saturation binding and scatcbard plots of ^{3}HFlorbetaben (0.01 - 200nM) on one AD frontal cortical autopsy tissue. C, D) ^{3}H-Florbetaben (0.01 -40 nM) saturation binding on frontal cortical autopsy brain tissue of AD (n=3) and CTRL (n=3)

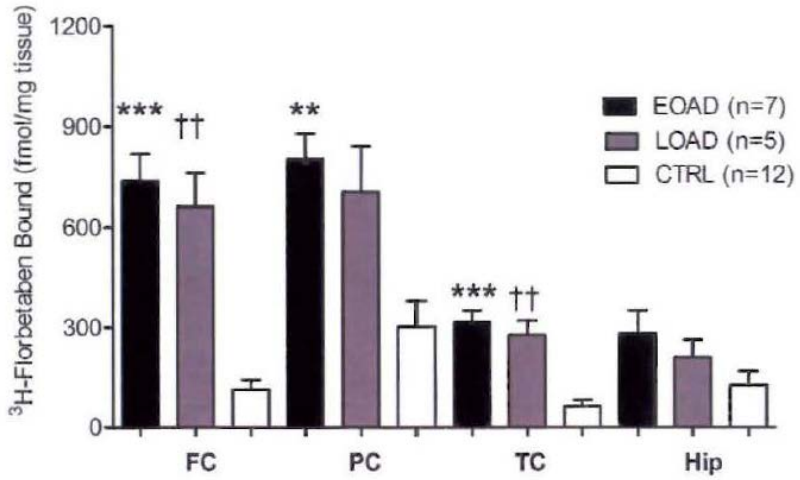

Figure 14: ^{3}H-Florbetaben binding (5 nM) on homogenates from frontal, parietal, temporal cortex, hippocampus from EOAD compared with LOAD and CTRL. **p<0.01, ***p<0.001, EOAD *vs* CTRL; ttp<0.01, LOAD *vs* CTRL; Kruskal-Wallis with Dunns *post lloc-test.* EOAD, early onset AD, LOAD, late onset AD.

The data obtained from the studies on comparison between ^{3}H-Florbetaben binding of EOAD, LOAD and CTRL indicates no significant binding between EOAD and LOAD unlike CTRL as shown in Figure 14.

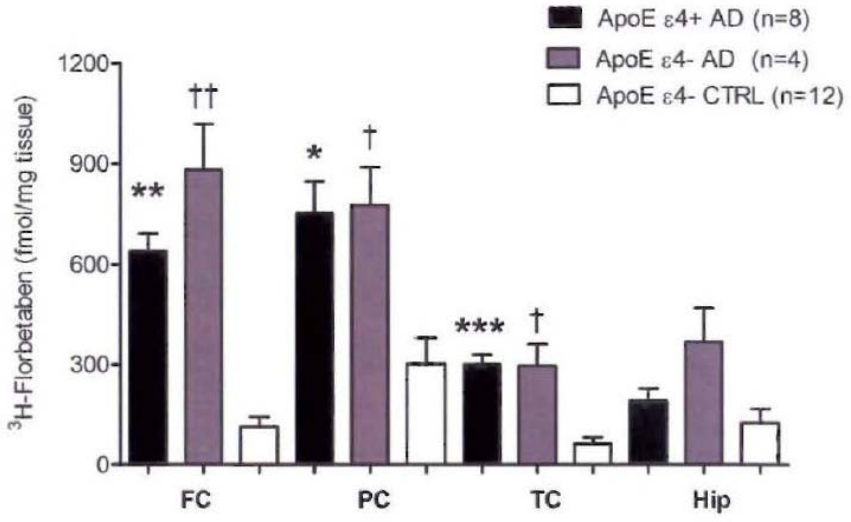

Figure 15: ^{3}H-Florbetaben binding (5 nM) in homogenates from frontal, parietal, temporal cortex and hippocampus autopsy brain tissue from AD ApoE ε4 carrier with AD ApoE ε4 non-carrier and CTRL. *p<0.05, **p<0.01, ***p<0.001, AD ApoE ε4 carrier vs CTRL, ^p<0.05, ^^p<0.01, AD ApoE ε4 non-carrier vs CTRL (ApoE ε4 non-carrier); Kruskal-Wallis with Dunn's *post hoc-test*

No significant difference in ^{3}H-Florbetaben binding between AD ApoE ε4 carrier (n=8) and AD ApoE ε4 non-carrier (n=4) was found in the frontal, parietal, temporal cortex, hippocampus, caudate nucleus, and cerebellum assessed during the comparison study (Figure 15). Higher ^{3}H-Florbetaben binding was observed on frontal, parietal, temporal cortex of AD ApoE ε4 carrier (n=8) and AD ApoE ε4 non-carrier (n=4) compared with CTRL (n=12).

Reviewer's Comment: This reviewer agrees with the data obtained in this study which indicates that saturation binding experiments revealed two ^{3}H-Florbetaben binding sites in the frontal cortex of AD patients; high and low affinity sites. The ranking order of ^{3}H-Florbetaben binding found in cortical regions of AD patients is frontal cortex > parietal cortex > temporal cortex. However, when compared to healthy controls frontal cortex and temporal cortex had a higher significance level (p<0.001), as compared to the parietal cortex (p<0.001I). The study shows that for the high affinity binding site the maximum number of binding sites (B_{max}) and the binding potential (BP) in frontal cortex samples of AD patients and were significantly increased in comparison to control subjects. However, no significant differences between ApoE ε4 carriers and ApoE ε4 non-carriers in any of the four regions (frontal, parietal, temporal cortex and hippocampus) were found in the investigated samples.

<u>Binding characterization of Florbetaben to beta-amyloid plaques /Part II</u>

In this study, the binding pattern of Florbetaben to different species of beta-amyloid depositions, i.e. cored and non-cored plaques as well as vascular depositions in different regions of post-

mortem human Alzheimer diseased brains was determined. The investigation was conducted using compound fluorescence and emulsion autoradiography (^{3}H-Florbetaben) for microscopic visualization.

^{19}F-Florbetaben binding studies- Binding studies of ^{19}F-Florbetaben was performed using the standard protocol. The brain sections were deparaffinized, rinsed in desalted water and washed three times (5 min in TBS (100 mM Tris, 154 mM NaCl, pH 7.5). Thereafter, the unspecific binding sites were blocked with TBS plus (TBS + 0.1% Triton X-100, 3% donkey serum, pH 7.5) for 60 min at room temperature (RT). A solution (1 mM) of ^{19}F-Florbetaben in ethanol was diluted in TBS and the slides were incubated with this solution for 1 hour at room temperature (RT) in a dark humidified chamber. The slides were washed four times 5 min in TBS, and analyzed using the UV filter of a Fluorescence microscope (Olympus, BX61, UV filter cube with an excitation filter BP360-370, dichromatic filter DM400 and emission filter BA420).The photographs of areas of interest were taken. The coverlips were then removed and the sections immunostained with the antibody 6E10 ((b) (4) using horseradish peroxidase as detection system. After rinsing the slides three times in TBS a routine procedure using the ABC Elite kit (Vectastain PK-6100; Vector Lab Inc.) for 15 min followed by the Vector ViP kit (SK-4600; Vector Lab Inc.) was employed for detection. The sections were then microscopically evaluated. The beta amyloid detected by immunohistochemistry appeared dark red. Overview photographs were taken from the same areas as used before for demonstration of ^{19}F-Florbetaben binding for better comparison.

^{3}F-Florbetaben binding studies- This study involved emulsion autoradiography conducted with ^{3}F-Florbetaben to illustrate the binding patterns of ^{3}F-Florbetaben. Deparaffinized sections were dipped 200 µL solution/ slide containing 10 Bq/ µL ^{3}H-Florbetaben in 25 mM HEPES buffer pH 7.5 (b) (4) containing 0.1% BSA ((b) (4)) for 1 hour at RT in a humidified chamber. The slides were then rinsed four times 2 min in 25 mM HEPES buffer containing 0.1% BSA pH 7.5, dipped in distilled water and dried. The sponsor further processed slide 4 (Caudate Putamen and Cerebellum) for immunohistochemistry using the 13E9 antibody recognizing beta-amyloid 1-40 (b) (4). In addition, the 1E8 antibody was used for immunohistochemistry following ^{3}H-Florbetaben ARG's on cases 03/213 and 03/711 for recognizing beta-amyloid 1-42. Immunohistochemistry was performed according to the protocol described above with the exception that alkaline phosphatase was used as detection enzyme instead of horseradish peroxidase. The slides were air dried and dipped in solubilized NTB emulsion (b) (4), dried and put into a black plastic box at 4°C for exposition for 21 days. The slides were then taken out and developed according to manufacturer's protocol using developing solution for 4 min ((b) (4) Slide 13 was immunohistochemically stained with the beta-amyloid 6E10 antibody ((b) (4)) using as the protocol described above. Microphotographs were then taken in an Olympus BX61 microscope.

The results of the study showed that ^{19}F-florbetaben and ^{3}H-florbetaben bound to non-cored, cored and vascular beta-amyloid deposits in the brain areas investigated. There was consistency in the binding with the pathological observations reported in Bielschowsky silver stain and immunohistochemistry using the 6E10 (Figure 16, Figure 17, Figure 18, Figure 19, Figure 20, Figure 21 and Figure 22 shown below) and 1E8 anti-beta-amyloid 1-42 antibodies (Figure 23 and Figure 24), respectively. The study demonstrated a partial overlap with the beta-amyloid 1-40 antibody 13E9 probably because beta-amyloid 1-40 immunoreactivity is mainly found in vascular depositions and some plaque forms. However, an uneven immunoreactivity was found in the 6E10 immunohistochemistry on the temporal and frontal cortex probes. This expression underestimated the real pathology of the beta amyloid deposits based on the

comparison of the patterns from immunohistochemistry with the Bielschowsky stain. The sponsor attributed the observation to oxidation of relevant epitopes and/or to the stability of the antibody 6E10 itself.

Reviewer's Comment: Agrees with the data obtained from this study which shows that the binding pattern of ^{19}F-Florbetaben/^{3}H-Florbetaben to cored and non-cored matched with beta-amyloid immunoreactivity and beta-amyloid detected by Bielschowsky stain. The study also detected vascular and parenchymal beta-amyloid depositions in the cerebellum.

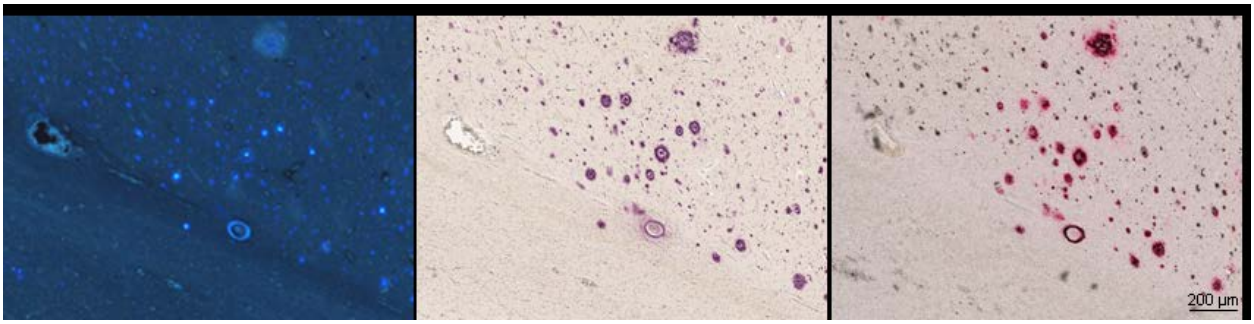

Figure 16: Case S04/185 putaminal fundus region

.
The fluorescence signals from bound Florbetaben (left panel) match with 6E10 anti-beta-amyloid 1-42 immunoreactivity subsequently stained on the same section (middle panel). The pattern of silver grain clusters demonstrating 3H-florbetaben binding matches partially, as expected, with 13E9 anti-beta-amyloid 1-40 immunoreactivity (right panel) and with the 6E10 anti-beta amyloid 1-42 immunoreactivity pattern seen in the middle panel. Note that the section of the right panel is 6 µm apart from the others.

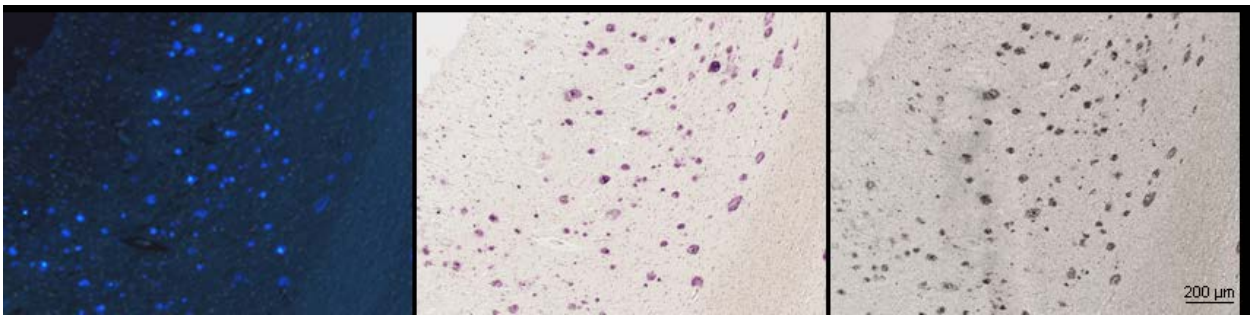

Figure 17: Case S05/121 piriform cortex.

The fluorescence signals from bound Florbetaben (left panel) match with 6E10 anti-beta-amyloid 1-42 immunoreactivity subsequently stained on the same section (middle panel). The pattern of silver grain clusters demonstrating ^{3}H-florbetaben binding (right panel) matches with the 6E10 anti-beta-amyloid 1-42 immunoreactivity pattern seen in the middle panel. Note that the section of the right panel is 12 µm apart from the others.

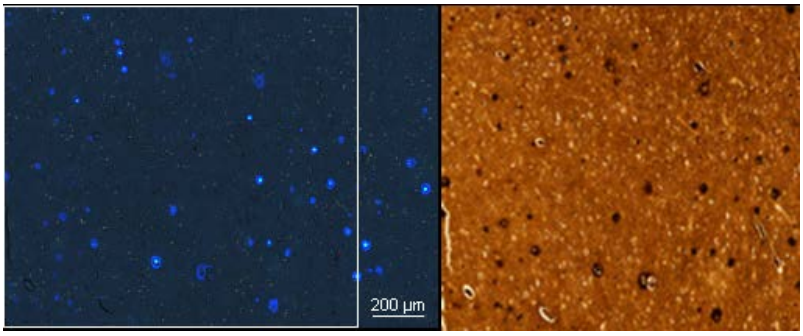

Figure 18: Case 06/025 insular gyrus.

Florbetaben binding fluorescence (left panel) matches the plaque pattern of the Bielschowsky stain (right panel). Both stains were performed on the same slide in a stepwise procedure. Florbetaben binding was done first, photographs taken and thereafter, the Bielschowsky stain was performed and photographs taken from the same region. The white frame depicts the region seen in the right panel.

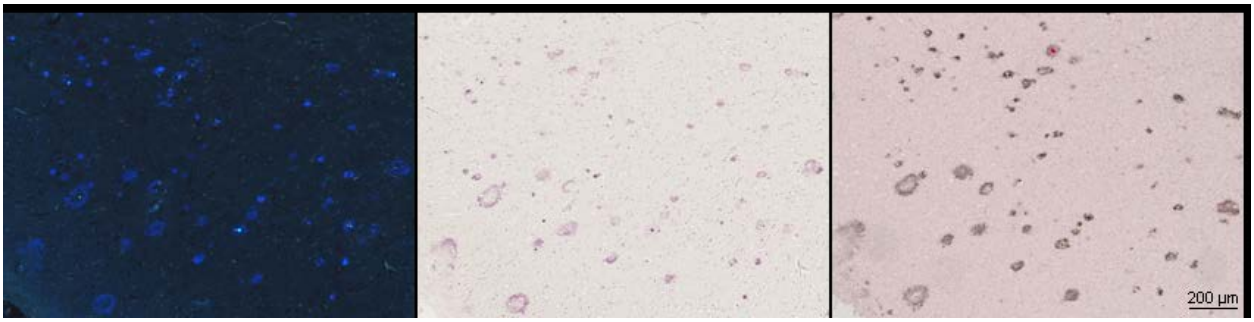

Figure 19: Case S06/056 subcallosal area

The fluorescence signals from bound Florbetaben (left panel) match with 6E10 anti-beta-amyloid 1-42 immunoreactivity subsequently stained on the same section (middle panel). The pattern of silver grain clusters demonstrating ^{3}H-florbetaben binding (right panel) matches with the 6E10 anti-beta-amyloid 1-42 immunoreactivity pattern seen in the middle panel. In the right panel no beta-amyloid 1-40 immunoreactivity could be detected. Note that the section of the right panel is 6 µm apart from the others.

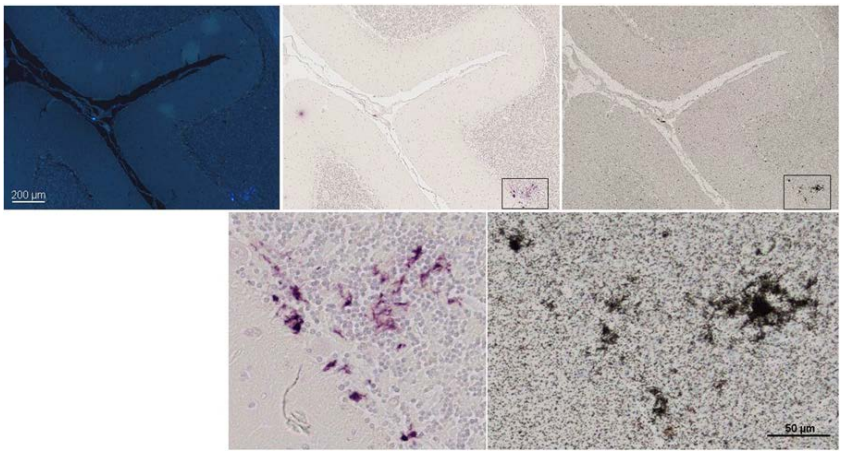

Figure 20: Case S05/121 Cerebellum.

The fluorescence signals from bound Florbetaben (left panel) match with 6E10 anti-beta-amyloid 1-42 immunoreactivity subsequently stained on the same section (middle panel). The pattern of silver grain clusters demonstrating ^{3}H-florbetaben binding (right panel) matches with the 6E10 anti-beta-amyloid 1-42 immunoreactivity pattern seen in the middle panel. Note that the section of the right panel is 12 µm apart from the others. The lower panels are a magnification of the area marked with a black box in the middle and upper left panels.

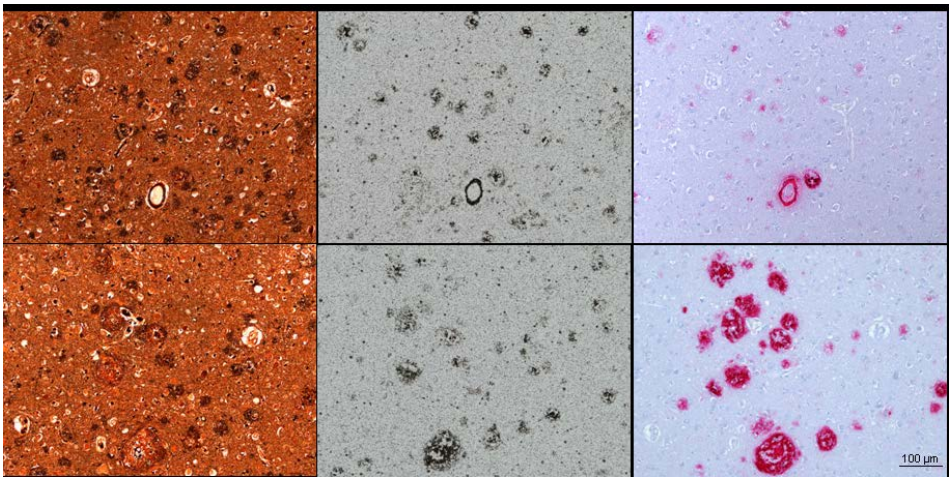

Figure 21: Case 03/711 temporal cortex.

The plaque pattern of the Bielschowsky stain (left panel) matches with silver grain clusters demonstrating ^{3}H-florbetaben binding (middle panel). The plaque and vascular pattern of silver grain clusters (middle panel) matches with the 6E10 anti-beta-amyloid 1-42 immunoreactivity pattern seen in the right panel. Note that the sections are 12 µm apart from each other.

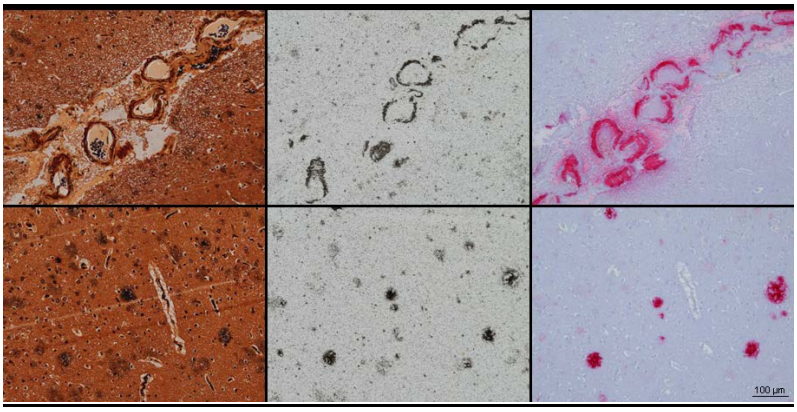

Figure 22: Case 04/042 frontal cortex.

The plaque pattern of the Bielschowsky stain (left panel) matches with silver grain clusters demonstrating 3H-florbetaben binding (middle panel). The plaque and vascular pattern of silver grain clusters (middle panel) matches with the 6E10 anti-beta-amyloid 1-42 immunoreactivity pattern seen in the right panel. Note that the sections are 12 µm apart from each other.

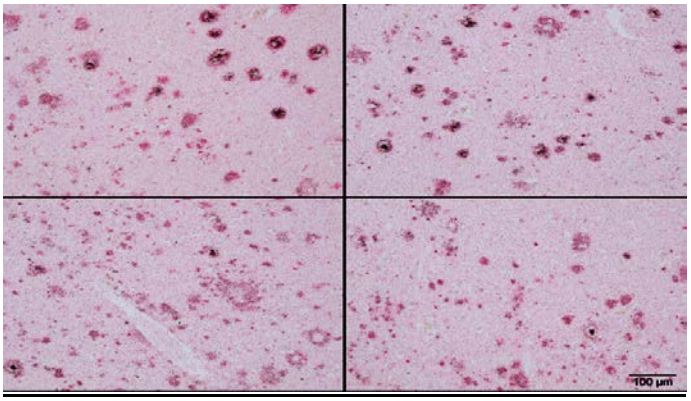

Figure 23: Case 03/213. Frontal cortex of an AD diseased patient.

^{3}H-florbetaben silver grain clusters overlay 1E8 beta-amyloid 1-42 immunoreactivity in the depositions seen.

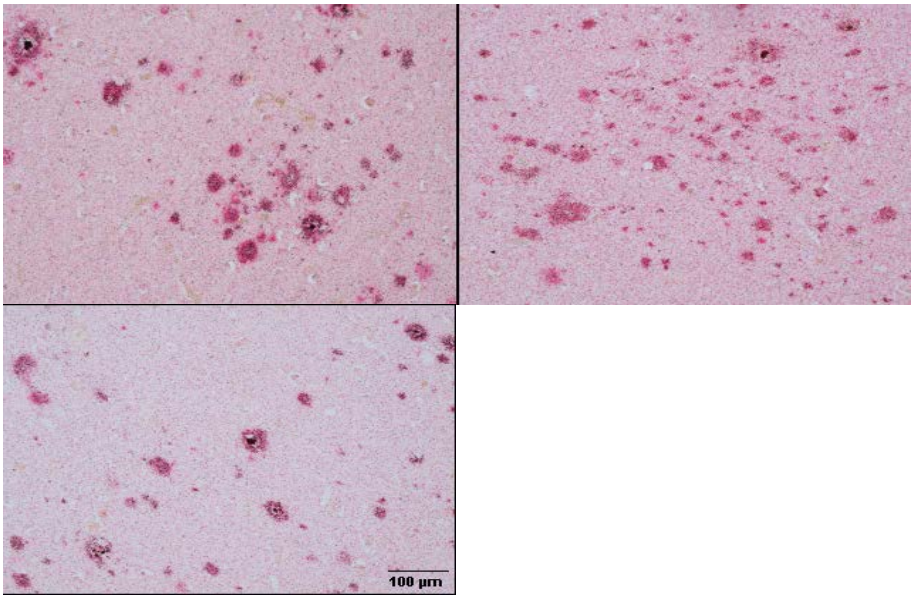

Figure 24: Case 04/171. Frontal cortex of a Dementia with Lewy Body patient (DLB).

^{3}H-florbetaben silver grain clusters overlay 1E8 beta-amyloid 1-42 immunoreactivity in the depositions seen.

Neurodegenerative disease tissue microarray (TMA): Characterization of binding of AV-1 to different types of neurodegenerative pathologies

Tissue microarray (TMA) was conducted on AD neurodegenerative disease to characterize the specificity of AV-1 (Florbetaben) in binding to amyloid beta plaque and not to other types of neurodegenerative pathology.

Brain tissues employed for this study were obtained from selected cases from series of neuropathology patients (1999-2003) at the (b) (4) After review by certified neuropathologists, consensus diagnoses were established according to published consensus criteria including AD, frontotemporal dementia, Lewy body disease, multiple system atrophy (MSA), corticobasal degeneration (CBD), and progressive supranuclear palsy (PSP). The brain tissues were fixed in 10% formalin, paraffin embedded, and cut into 6 µm thick sections. The sections were stained with hematoxylin/eosin, Thioflavin S, and Gallyas silver stains using standard protocols. The sections were rehydrated and endogenous peroxide blocked by incubation with methanol/hydrogen peroxide for immunohistochemical analysis. The sections were blocked with 2% fetal bovine serum in 50 mM Tris pH 7.4, 150 mM NaCl, and incubated with primary antibody overnight at 40°C. They were subsequently incubated with horseradish-peroxidase-conjugated anti-Ig antibodies (b) (4) followed by visualization with the avidin-biotin-peroxidase method with 3,3'-diaminobenzidine (Vectastain ABC kit, Vector Laboratories, Burlingame, CA). The monoclonal antibodies employed were 4G8 specific for amyloid (b) (4) PHFl specific for tau

phosphorylated at Ser396 and Ser404; Syn303 specific for a-synuclein; and 1510, specific for ubiquitin [redacted] (b) (4). The TMA was generated by using standard protocols during which de-identified tissue blocks were obtained and large tissue sections were stained with antibodies specific for Ab, tau, a-synuclein and ubiquitin. The regions with a high density of pathology were identified for core sampling. Using the marked slides as a guide, core biopsies (0.6 mm or 1 mm) were extracted from the donor blocks using a Beecher MTAI Manual Tissue Arrayer (Beecher Instruments, Inc., Sun Prairie, WI) and inserted into the recipient block at defined array coordinates. The TMA was then sectioned and stained as described above and the stained slides were digitized with the BLISS imaging system [redacted] (b) (4) The individual TMA cores were assessed for adequacy and only adequately sampled regions were scored for pathology by two neuropathologists using a semiquantitative scale for density of immunohistochemically labeled pathological inclusions in accordance with established neuropathological criteria. Ubiquitin immunohistochemistry was only scored in frontotemporal lobar degeneration with ubiquitin-positive inclusions (FTLD-U) because Ab, tau, and a-synuclein pathology are also detected with antibodies to ubiquitin.

Serial sections (6 µm thick) of paraffin embedded blocks were incubated with ^{3}H-Florbetaben ligand at tracer concentrations (at 0.05-0.2 nM) for one hour. The sections were washed and specific binding was assessed by emulsion radiography (previously described). The sponsor semi quantitatively scored the labeling of each core by radioligand as follows: 0 for no labeling, 1+ for weak labeling (difficult to distinguish from background) of rare lesions (2 or less lesions per core), 2+ for weak labeling of more frequent lesions (3 or more per core) or strong labeling (clearly distinguishable from background) of any lesions or 3+ for strong labeling of numerous (3 or more per core) lesions. The correlations between the scoring of the large tissue sections and the average TMA core score for a given region and pathology were assessed using (a) Kappa statistics to evaluate the dichotomized (qualitative) outcome measures (present versus absent) by region and lesion and (b) Spearman correlation coefficients to examine the semiquantitative outcome measures on the original 0 to 3 scale.

The sponsor assessed the adequacy of the TMA cores in sampling of the different brain regions on sections stained with hematoxylin and eosin and found that the targeted regions were correctly sampled in only 89.7% of 0.6mm tissue cores and there were difficulty to target structures of hippocampal formation in 50% to 82.1 % of 0.6 mm tissue cores. The technical problem was however resolved by generating an additional TMA paraffin block with 1.0 mm cores obtained from the hippocampal formation. Despite the effort, the CA2 region of the hippocampus was not re-sampled because of the small size. In totality, TMA consisted of 190 cores of 1.0 mm representing 6 distinct brain regions (4 to 6 cores per region) and the adequacy of tissue sampling improved to 94.7% with 1.0 mm cores including the hippocampal formation in which the dentate gyrus and CA1/subiculum were well-sampled in 87.5% and 91.2% respectively. Following the immunostaining of the TMA sections with a panel of antibodies, a variety of neurodegenerative disease lesions including senile plaques (Aba), neurofibrillary tangles and related tau pathology (PHF1 specific for phosphorylated tau protein), Lewy body and related a-synuclein pathology, and ubiquitin-positive inclusions were detected (Table 3 below as provided by the sponsor).

Table 3: AD pathology represented in neurodegenerative disease TMA

No.	Senile plaques				Tau				a-synuclein			
	Neocortex		Hippocampus		Neocortex		Hippocampus		Neocortex		Hippocampus	
	Section score	Average core score	Section score	Average core score	Section score	Average core score	Section score	Average core score	Section score	Average core score	Section score	Average core score
1	3	2.9	2	2.3	3	3.0	3	3.0	0	0	0	0
2	3	2.5	2	1.3	3	2.25	3	3.0	0	0	0	0
3	3	2.4	2	2.8	3	3.0	3	3.0	0	0	0	0
4	2	2.6	2	3.0	2	3.0	2	3.0	0	0	0	0
5	3	1.8	2	1.6	2	2.5	3	3.0	0	0	0	0
6	3	2.5	2	3.0	3	3.0	3	2.8	0	0	0	0

Data obtained from a quantitative assessment of the lesions using a semiquantitative scoring of the TMA cores performed in comparison to the large tissue sections is shown in Table 4 as provided by the sponsor.

In a large percentage of cases, the TMA quantitatively represented the extent of pathology in the large tissue sections (Average Spearman correlation coefficient 0.88 +/- 0.17, Wilcoxon signed rank test $p<0.0001$ for testing if the average Spearman correlation is different from 0). However, the pathology was not consistently represented in structures of the hippocampal formation as well as the cingulate gyrus (Ab and a-syn), basis pontis (tau), and entorhinal cortex (ubiquitin pathology in FTLD-U patients) ($p > 0.05$ for Spearman correlation). It was also observed that in the TMA generated with 1.0 mm cores including regions, the quantitative representation of the pathology increased in all instances except for detection of ubiquitin pathology in FTLD-U that was limited by the inclusion of only 3 brains in the TMA.

Table 4: Neurodegenerative disease TMAs qualitatively and quantitatively capture the characteristic inclusion pathology

Region	Protein	0.6 mm cores		0.6 mm and 1.0 mm cores combined	
		Kappa coefficient	Spearman coefficient (p-value)	Kappa coefficient	Spearman coefficient (p-value)
Neocortex	Tau	0.75	0.99 (<0.0001)	0.83	0.99 (<0.0001)
	Aβ	0.90	0.93 (<0.0001)	0.90	0.93 (<0.0001)
	αsyn	0.83	1.00 (<0.0001)	0.83	1.00 (<0.0001)
	Ubiquitin	1.00	NA[1]	1.00	NA
Subcortical white matter	Tau	0.84	1.00 (<0.0001)	0.84	ND[2]
	Aβ	1.00	NA	1.00	ND
	αsyn	0.81	1.00 (<0.0001)	0.81	ND
Cingulate gyrus	Tau	0.50	0.99 (<0.0001)	0.50	0.99 (<0.0001)
	Aβ	1.00	0.51 (0.19)	1.00	0.80 (0.017)
	αsyn	1.00	0.52 (0.18)	1.00	0.75 (0.032)
Entorhinal cortex	Tau	0.36	0.98 (<0.0001)	0.53	0.98 (<0.0001)
	Aβ	1.00	0.92 (<0.0001)	1.00	0.93 (<0.0001)
	αsyn	0.86	0.93 (<0.0001)	1.00	0.99 (<0.0001)
	Ubiquitin	1.00	0.87 (0.33)	1.00	0.87 (0.33)
Hippocampus, CA1/subiculum	Tau	1.00	0.74 (0.059)	1.00	0.88 (0.0081)
	Aβ	1.00	0.62 (0.13)	1.00	0.68 (0.096)
	αsyn	1.00	NA	1.00	NA
Hippocampus, dentate gyrus	Tau	1.00	1.00 (<0.0001)	0.72	0.90 (0.0063)
	Aβ	1.00	NA	1.00	NA
	αsyn	1.00	NA	1.00	NA
	Ubiquitin	1.00	1.00 (NA)	1.00	NA
Hippocampus, CA2	Tau	0	0.76 (0.0300)	0	ND
	Aβ	0.38	1.00 (<0.0001)	0.38	ND
	αsyn	0.33	0.52 (0.19)	0.33	ND
Basal ganglia	Tau	1.00	0.99 (<0.0001)	1.00	ND
	Aβ	0.64	NA	0.64	ND
	αsyn	1.00	1.00 (<0.0001)	1.00	ND
Pons, basis pontis	Tau	1.00	0.76 (0.14)	1.00	1.00 (<0.0001)
	Aβ	1.00	NA	1.00	NA
	αsyn	1.00	NA	1.00	NA
Pons, tegmentum	Tau	0.36	0.96 (<0.0001)	0.36	0.96 (<0.0001)
	Aβ	0.33	NA	1.00	NA
	αsyn	1.00	0.92 (<0.0001)	1.00	0.91 (<0.0001)
Cerebellum, dentate nucleus & white matter	Tau	0.57	0.87 (0.026)	0.57	ND
	Aβ	1.00	NA	1.00	ND
	αsyn	1.00	1.00 (<0.0001)	1.00	ND

[1]NA refers to data without variation and thus the Spearman coefficient is not applicable.
[2]ND (Not Done) refers to brains regions in which 1.0 mm cores were not obtained.

Based on the data above, the sponsor proposed that the number of cores necessary to reproduce the density of pathology in the large tissue sections by computing 2 to 6 random cores were selected for each subject and brain region and the average value for each type of pathology. As shown in Sponsor's Table 5, the proportion of TMA cores that correctly matched the score of the large tissue section was above 80% with 2 tissue cores except for the following: tau pathology in the cingulate gyrus, Ab pathology in the CAI/subiculum of the hippocampal formation, and a-syn in the pontine tegmentum. The TMA employed in this study quantitatively and qualitatively demonstrates the pathology characteristic of a wide array of variety of neurodegenerative diseases.

Table 5: Proposed guidelines for neurodegenerative disease TMA

Region	*# of cores (core diameter, mm)*	*Number*	*Protein*	*Proportion match*[1]	*95% confidence interval*
Neocortex	2 (0.6)	29	Tau	0.97	0.82, 0.99
			Aβ	0.86	0.68, 0.96
			αsyn	1.00	0.88, 1.00
Subcortical white matter	2 (0.6)	12	Tau	1.00	0.74, 1.00
			Aβ	1.00	0.72, 1.00
			αsyn	1.00	0.74, 1.00
Cingulate gyrus	2 (1.0)	8	Tau	0.63	0.25, 0.92
			Aβ	0.88	0.47, 1.00
			αsyn	0.88	0.47, 1.00
Entorhinal cortex	2 (0.6; 1.0)[2]	14	Tau	1.00	0.77, 1.00
			Aβ	1.00	0.77, 1.00
			αsyn	0.93	0.66, 1.00
Hippocampus, CA1/subiculum	2 (1.0)	7	Tau	1.00	0.59, 1.00
			Aβ	0.71	0.29, 0.96
			αsyn	1.00	0.59, 1.00
Hippocampus, dentate gyrus	2 (1.0)	7	Tau	0.86	0.42, 1.00
			Aβ	1.00	0.59, 1.00
			αsyn	1.00	0.59, 1.00
Basal ganglia	2 (0.6)	16	Tau	0.94	0.71, 1.00
			Aβ	0.94	0.70, 1.00
			αsyn	1.00	0.81, 1.00
Pons, basis pontis	2 (1.0)	5	Tau	1.00	0.48, 1.00
			Aβ	1.00	0.48, 1.00
			αsyn	1.00	0.48, 1.00
Pons, tegmentum	2 (0.6)	14	Tau	0.93	0.66, 1.00
			Aβ	1.00	0.77, 1.00
			αsyn	0.79	0.49, 0.95
Cerebellum, dentate nucleus & white matter	2 (0.6)	6	Tau	0.83	0.36, 1.00
			Aβ	1.00	0.54, 1.00
			αsyn	1.00	0.54, 1.00

.

[1]The proportion of brains in which the difference between the score for the large tissue section and the
computed averages for the randomly selected TMA cores was less than or equal to 0.5.
[2]Lewy body pathology was assessed using the 1 mm tissue cores.

Reviewer's Comment: The utility of this data is in combination with the available data on binding of ^{3}H-Florbetaben to beta amyloid with strong correlation to both thioflavin and amyloid beta specific antibody staining. No significant labeling of tau positive pathologies including neurofibrillary tangles, Pick bodies, coiled bodies, and globose tangles was demonstrated. The product also did not show any labeling of asynuclein positive lesions, including Lewy bodies, Lewy neuritis, glial cytoplasmic inclusions as well as labeling of non-amyloid beta containing ubiquitin positive inclusions (MND-type inclusions). Thus, the data from this neurodegenerative disease TMA in this study indicates that of ^{3}H-Florbetaben probably specifically binds to amyloid beta-containing pathology and not to any other types of degenerative pathology on the TMA.

4.2 Secondary Pharmacology

The sponsor assessed the selectivity of ^{3}H-Florbetaben by evaluating possible binding of the product to other target receptors using radioligand binding assay.

Study title: (b) (4) Pharmacology Data Report on Compound AID-1, (b) (4) (b) (4)

Study no.: (b) (4) ((b) (4) 1049459)

Study report location: 4.2.1.3: Page 1 – 39

Conducting laboratory and location: (b) (4)

Date of study initiation: June 14, 2005

GLP compliance: No

QA statement: NA

Drug, lot #, and % purity: NA

The activity of ^{3}H-Florbetaben (AID-1) was evaluated using radioligand binding assay. Methods employed for the evaluation involves running reference standards obtained from literature references(s) as an integral part of each assay to ensure the validity of the assay. The IC_{50} values were determined by a non-linear, least squares regression analysis using Data Analysis Toolbox™ (b) (4) The inhibition constants (K_i) values were calculated using the equation of Cheng and Prusoff (Cheng, Y., Prusoff, W.H., Biochem. Pharmacol. 22:3099-3108, 1973) using the observed IC_{50} of the tested compound, the concentration of radioligand employed in the assay, and the historical values for the K_o of the ligand (obtained experimentally at (b) (4)). The Hill coefficient (n_H) which defines the slope of the competitive binding curve was calculated using Data Analysis Toolbox™ Hill coefficients. Hill coefficients that is significantly different than 1.0 would suggest that the binding displacement does not follow the laws of mass with a single binding site.

The data showing IC_{50}±SEM, K_i±SEM and nH values of 79 receptors and binding sites composed of various subtypes were provided. The receptor subtypes, transporters and binding sites include selective and non-selective adenosine-α and –β sub types, benzodiazepine, cannabinoid, dopamine, estrogen, GABA, gabapentin, glutamate (NMDA, kainite, non-selective), histamine (H_1-H_4) imidazoline (central and peripheral), muscarinic (M_1-M_5), opiate (δ, κ, μ) potassium channel HERG, progesterone, prostanoid TXA_2, serotonin $5HT_{1A-6}$. Sigma (non-selective and sigma σ_{1-2}), testosterone, adenosine transporter, choline transporter, dopamine transporter (DAT), GABA transporter, glycine transporter, monoamine transporter,

norepinephrine transporter and serotonin transporter (SERT). None of the IC_{50}±SEM, K_i±SEM and nH values met the significance criteria at the concentrations and/or doses employed during this study. Of all the evaluated receptors, transporters and binding sites, the highest IC_{50} values of 10 µM and dissociation constants of 0.2 nM and 0.13 nM were obtained to estrogen ERα and ERβ respectively at 10 µM concentrations. The significance of this study is that it is highly unlikely that Florbetaben would induce any pharmacology effect at these receptor sites, binding sites or affect the transporter mechanism at the intended human dose.

Reviewer's Comment: Agrees with the result of this study.

4.3 Safety Pharmacology

Effects of ZK 6057184 (BAY 94-9172) on HERG-mediated potassium current recorded from stably transfected CHO cells

Key study findings: In this study, the potential of ZK 6057184 having intrinsic effects on the HERG (human ether-à-go-go-related gene) K^+ current in stably transfected CHO (Chinese Hamster Ovary) cells was investigated. ZK 6057184 did not affect the HERG K^+ current at the employed concentrations of 0.01, 0.1 and 1 µmol/L (12.5X, 125X and 1250X expected human unbound plasma level of estimated human dose of this product),

The sponsor employed whole cell configuration of patch-clamp technique for this study. The CHO cells, which stably express the HERG gene generated by a pcDNA3-KCNH2-FLAG expression vector maintained in cell culture using MEM ALPHA Medium supplemented with 10% (v/v) heat inactivated fetal calf serum, 1% (v/v) penicillin/streptomycin/L-glutamine solution and 200 µg/mL geneticin G-418 at 37°C and 5% CO_2 was also employed. The HERG K^+ current in the CHO cells was activated at a frequency of 0.1 Hz and recorded at room temperature for 3 minutes followed by observation with a test or negative control article 3 minutes for each concentration. The currents were recorded for 5 minutes during wash out treated group to test for reversibility of the effect. DMSO was employed as a negative control and ZK 344354 (E-4031) at 1 µmol/L was used as a positive control during the study. The HERG K^+ tail current amplitudes were obtained and the percentages of the amplitude relative to the pre-treatment control amplitude was calculated and compared to the negative control and ZK 6057184 using Mann-Whitney Rank Sum Test.

Results of the study (Figure 25) indicates that a stable HERG-mediated K^+ current was observed during 1st to 3rd DMSO applications and the test article at employed concentrations of 0.01, 0.1 and 1 µmol/L did not affect HERG-mediated K^+ current.

Reference ID: 3361527

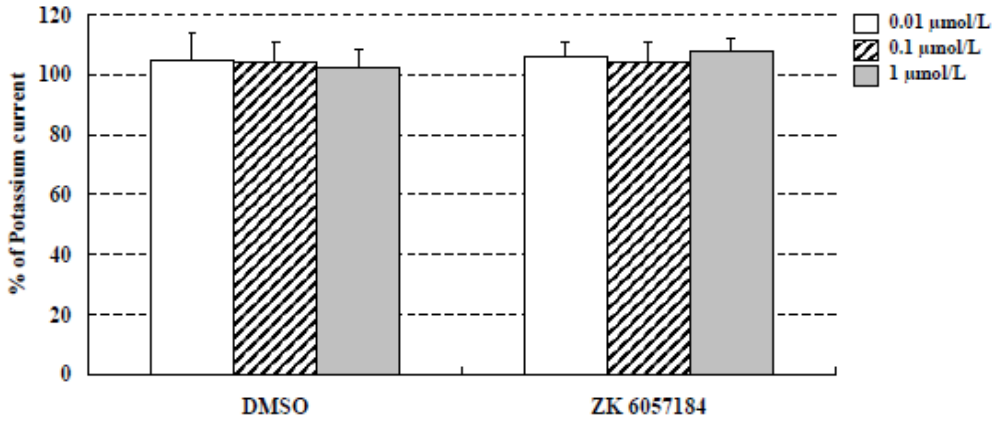

Each value represents the mean ± S.D. (n=5). Potassium current is expressed relative to pretreatment current = 100 %. ZK 6057184 was tested at 0.01, 0.1 and 1 µmol/L. 0.1 % DMSO are time-matching negative controls for each concentration group.

Figure 25: Effects of ZK 6057184 on HERG-mediated potassium current

However, the specific HERG channel blocker, E-4031 at 1 µmol/L, completely blocked the HERG K+ current by 96 % (n=5).

Reviewer's Comments: The reviewer agrees with the result of this study indicating that ZK 6057184 did not demonstrate any intrinsic effects on the HERG K^+ currents in stably transfected CHO cells at concentrations up to 1 µmol/L while the positive control, E-4031, induced up to 90% inhibition on the hERG cells.

Single intravenous dose safety study of PEGN3.HCL in Sprague-Dawley rats with CNS Safety Pharmacology Functional Observational Battery (FOB) and 14 days recovery

Key study findings: The safety profile and NOAEL were established in rats intravenously administered PEGN3.HCl followed by 14 days recovery. The CNS safety pharmacology FOB of PEGN3.HCl was also assessed after dosing on Day 1. No mortality or changes in clinical observations associated with PEGN3.HCl administration was reported during the study. However, there were reports of increased serum phosphorus in Day 3 females administered 100 µg/kg (233X MHD) which was not accompanied with any histological findings, thus, the etiology of this effect in the females could not be determined. The NOAEL in females is 50 µg/kg (117X MHD) while NOAEL from male rats is 100 µg/kg (233X MHD)

Study No.	M380-05
Study Report Location:	4.2.1.3 Pages 1-399.
Conducting laboratory Location:	(b) (4)

	(b) (4)
Date of study initiation:	November 3, 2005
GLP Compliance:	Yes
QA Statement:	Yes
Drug, lot #, and % purity:	PEGN3.HCl (PEGN3 hydrochloride), lot # K05-095; WZ-N99-86-22 and purity is stated to be 95.4%

Study Design:

The study was designed to determine the safety profile and establish NOAEL of PEGN3.HCl in male and female Sprague Dawley rats following a single intravenous administration of 5 male and 5 female rats. The main phase animals were sacrificed on Day 3 while the recovery phase animals were sacrificed on Day 15 after dosing as shown below.

Doses:	0, 10, 50, or 100 µg/kg (0, 23X, 117X and 233X MHD)
Frequency of dosing:	Single dose
Route of administration:	Intravenous Injection (MeODMT, FOB positive control, was given by intraperitoneal injection)
Dose volume:	4 mL/kg
Formulation/Vehicle:	PEGN3.HCl/20% 2-hydroxypropyl-β-cyclodextrin in saline
Species/Strain:	Sprague Dawley/Rats
Number/Sex/Group:	5/sex/group
Age:	8 Weeks (M) 8 Weeks (F)
Weight:	242-284g (M) 176-251g (F)
Satellite groups:	14 day Recovery group
Unique study design:	The rats were administered the test article and MeODMT on Day 1. Functional Observations on Day 1 approximately 15 minutes (range 15-23 minutes) after dosing. The blood samples were collected on Days 3 and 15 using EDTA as the anticoagulant before necropsies were performed on those days.

Observations and Results

Mortality

No mortality was reported in any of the animals. All the rats survived until the scheduled necropsy times.

Clinical Signs

No treatment-related clinical signs were observed.

Body Weights

No effect on body weight in treated animals in comparison to the control.

Feed Consumption

No effect on food intake reported in the animals throughout the study.

Reference ID: 3361527

Functional Observational battery

Home-cage observations- No changes were observed in the treated and negative control rats. However, the positive rats were found moving with flattened body posture.

Handling observations- No changes were observed in the treated and negative control rats.

Open field observations- No changes were observed in the treated and control rats. However, the females administered 117X MHD demonstrated reduction in rearing while the positive rats were found moving with flattened body posture. The sponsor described the observation in the female rats treated with the test article is not treatment-related. However, no data was provided to establish whether or not the behavioral effect was treatment related.

Reflexes and Physiological Measurements- No changes were observed in the treated and negative control rats. However, the positive male rats demonstrated less ability in righting reflex while the positive female rats showed 'more energetic response than normal' to the tail-pinch stimulus and both the male and female rats had lower body temperature.

Clinical pathology

Hematology- No changes were observed in the hematological parameters. However, increased mean corpuscular volume (MCV) and mean corpuscular hemoglobin (MCV) were reported in the male rats administered 233X MHD on day 3.

Clinical Chemistry- Clinical chemistry changes observed were:

1) Lower aspartate aminotransferase (AST) in 233X MHD- treated males in Day 3.
2) Decreased blood urea nitrogen (BUN) (177X and 233X MHD) and alanine aminotransferase (ALT) (233X MHD) and increased chloride (233X MHD) in males in Day 15.
3) Increased alkaline phosphatase (ALP) (23X MHD), increased sodium (23X and 233X MHD) and dose related increased phosphorous in all treated female groups in Day 3.
4) Decreased protein and albumin were also found in all treatment female groups on Day 15.

Gross Pathology

No treatment-related macroscopic findings were reported.

Organ Weights

No treatment-related organ weight change was reported. However, there were dose-related reductions in the absolute adrenal gland weight in the 117X and 233X MHD treated females which subsequently reflect in the adrenal -% body weight and -% brain weight.

Reference ID: 3361527

Histopathology

Adequate Battery –Yes

Peer Review –Yes

Histological Findings

Study	Repeat Dose Study			
Species	Rat			
Adrenals	x *			
Aorta	x			
Bone Marrow smear	x			
Bone (femur)	x			
Brain	x *			
Cecum	x			
Cervix	x			
Colon	x			
Duodenum	x			
Epididymis	x			
Esophagus	x			
Eye	x			
Fallopian tube	x *			
Gall bladder				
Gross lesions	x			
Harderian gland	x			

Heart	x *			
Ileum	x			
Injection site	x			
Jejunum	x			
Kidneys	x *			
Lachrymal gland	x			
Larynx				
Liver	x *			
Lungs	x			
Lymph nodes, cervical				
Lymph nodes mandibular	x			
Lymph nodes, mesenteric	x			
Mammary gland	x			
Nasal cavity				
Optic nerves	x			
Ovaries	x *			
Pancreas	x			
Parathyroid	x			
Peripheral nerve				
Pharynx				
Pituitary	x			
Prostate	x			

Rectum	X			
Salivary gland	x			
Sciatic nerve	x			
Seminal vesicles	x			
Skeletal muscle	x			
Skin	x			
Spinal cord	x			
Spleen	x *			
Sternum				
Stomach	x			
Testes	x *			
Thymus	x *			
Thyroid	x			
Tongue	x			
Trachea	x			
Urinary bladder	x			
Uterus	x			
Vagina	x			
Zymbal gland				

x, histopathology performed

* organ weight obtained

Reviewer's Comment: This reviewer agrees with the result of this study. There was no mortality or treatment-related serious adverse effects on clinical or cage side observations, body weights, body weight change, organ weight data, food consumption, FOB results, hematology parameters, clinical chemistry (repeated dose) gross necropsy findings or histopathology findings. However, Florbetaben caused mild increased MCV, chloride and MCH, lower AST,

BUN, and ALT in males while increased ALP, sodium, and phosphorous as well as decreased albumin and total protein were found in females. The sponsor claimed that the reductions in rearing reported in the females administered 117X MHD during the open-field observation assessment did not appear to be treatment-related. However, available evidence does not support the suggestion. This reviewer is of the opinion that the data has not shown any evidence of CNS effect because no similar positive result was found at other employed doses (23X and 233X MHD) in the females. This indicates that the effect is not dose related and the observation at 117X MHD seems to be an artifact. Furthermore, none of the other FOB parameters evaluated (including reflexes and physiological measurements) suggests any CNS-effects unlike the employed positive control which indicates the sensitivity of the testing system.

Effects of ZK 6057184 (BAY949172) on renal function of conscious male rats after a single intravenous injection

Key study findings: The study was conducted to evaluate ZK 6057184 for effect on the renal function in conscious rats following a single intravenous injection. The urine and blood samples collected from the rats were analyzed for renal function parameters. No change in the renal excretion rates of fluid and sodium and potassium as well as creatinine and osmolar clearances of treated- (0, 140X 349X and 1395X MHD) and control rats were demonstrated in this study. Thus, an intravenous injection of ZK 6057184 up to 1395X MHD does not affect the kidney function of male rats in this study.

Study No.	TOXT5078839
Study Report Location:	4.2.1.3 Pages 1-11.
Conducting laboratory Location:	(b) (4)
Date of study initiation:	July 18, 2008
GLP Compliance:	No
QA Statement:	No
Drug, lot #, and % purity:	ZK 6057184, lot # PB 07303977 and purity is stated to be 97.8%

Study Design:

Males rats employed for this study were randomized based on their body weight and divided into four groups of 10 rats each. The control group was administered the vehicle (20% 2-hydroxypropyl-β-cyclodextrin, 0.5% NaCl in water for injection) and the treated groups were

each administered 0.06, 0.15, or 0.6 mg/kg (0, 140X 349X,1395X MHD) of ZK 6057184. Tap water was orally administered at a volume of 20mL/kg to the rats immediately after the injection of the test article and the vehicle to the rats via the tail vein to stimulate diuresis in the animals. Urine c was collected from rats for 5 hours after which blood samples were collected by cardiac puncture under terminal O_2/N_2O anesthesia with 1.5 vol % isoflurane (initially 6 vol %). The serum was separated by centrifugation and both the urine and serum samples were stored at -20 °C for analysis. The urine volume, urinary excretion of electrolytes (Na^+, K^+), Na^+/K^+ ratio, serum urea concentration, creatinine concentration in serum and urine, creatinine excretion, creatinine clearance, N-acetyl-β-D-glucosaminidase (NAG) excretion, total protein excretion, osmolality in serum and urine, and osmolar clearance were determined. The concentrations of electrolytes, creatinine, urea, and NAG, were measured using an apparatus for combined electrolyte analyses and standard spectrophotometry (Advia 1650). Osmolality was measured with an osmometer (OM-6040) and the total urinary protein concentration measured with a semi-automated analyser for standardized reflectance photometric test-strip-evaluation (Miditron).

Doses:	0, 0.06, 0.15, or 0.6 mg/kg (0, 140X 349X,1395X MHD)
Frequency of dosing:	Single dose
Route of administration:	Intravenous Injection (ZK 6057184) and oral administration (water given as diuretic stimulus)
Dose volume:	5 mL/kg
Formulation/Vehicle:	ZK 6057184/20% 2-hydroxypropyl-β-cyclodextrin, 0.5% NaCl in water for injection
Species/Strain:	Wistar Crl:WI(Han) (b) (4)
Number/Sex/Group:	10 male rats/group
Weight:	175-197 g (M)
Satellite groups:	None

Results

The data obtained on the effect of ZK 6057184 on urine volume, urinary excretion of electrolytes and Na^+/K^+ ratio in conscious rats as shown in Table 6 indicates no significant change in any of the parameters in the treated and the control rats. It is noted that there is a reduction in Na+/K+ ratio with increasing doses of ZK 6057184 in the treated groups. This decrease could be as a result of reductions in Na^+ excretion with increasing ZK 6057184 doses while the K^+ excretion

remains statistically unchanged (Table 6). However, the reductions were not of high magnitude to cause any safety concern.

Table 6: Effect of ZK 6057184 on urine volume, urinary excretion of electrolytes and Na+/K+ ratio after a single injection (i.v.) in conscious male rats

Group	Treatment (dose, i.v. injection)	Urine volume (mL/100g b.w./5h)	Sodium Urinary excretion (µmol/100g b.w./5h)	Potassium Urinary excretion (µmol/100g b.w./5h)	Na+/K+ ratio
1	Vehicle[1] (5 mL/kg)	2.62±0.32	39.56±15.08	43.82±17.50	0.95±0.21
2	ZK 6057184 (0.06 mg/kg)	2.42±0.35	45.16±21.00	42.28±14.36	1.05±0.29
3	ZK 6057184 (0.15 mg/kg)	2.40±0.33	31.01±15.04	42.05±13.29	0.84±0.57
4	ZK 6057184 (0.6 mg/kg)	2.36±0.38	32.71±19.23	40.47±15.22	0.76±0.29

[1]Vehicle = 20% hydroxypropyl-beta-cyclodextrin with 0.5% NaCl in water for injections
Data are expressed as mean±S.D. (n = number of animals/group)

No changes were found in the serum creatinine concentration, creatinine excretion, creatinine clearance and serum urea concentration in ZK 6057184- and vehicle-treated conscious rats (Table 7). This indicates that it is very unlikely ZK 6057184 treatment up to 1395X MHD will affect any of the evaluated creatinine parameters.

Table 7: Effect of ZK 6057184 on serum creatinine concentration, creatinine excretion, creatinine clearance and serum urea concentration after a single injection (i.v.) in conscious male rats

Group	Treatment (dose, i.v. injection)	Serum creatinine concentration (µmol/L)	Creatinine excretion (µmol/100g b.w./5h)	Creatinine clearance (mL/min)	Serum urea concentration (mmol/L)
1	Vehicle[1] (5 mL/kg)	47.29±2.09	4.72±1.16	0.64±0.17	5.56±1.04
2	ZK 6057184 (0.06 mg/kg)	49.59±4.30	4.57±0.98	0.58±0.13	5.52±1.21
3	ZK 6057184 (0.15 mg/kg)	49.59±3.29	4.33±1.07	0.55±0.15	5.95±0.75
4	ZK 6057184 (0.6 mg/kg)	50.48±2.78	4.39±1.09	0.55±0.15	5.67±0.90

[1]Vehicle = 20% hydroxypropyl-beta-cyclodextrin with 0.5% NaCl in water for injections

Data are expressed as mean±S.D. (n = number of animals/group)

Similarly, ZK 6057184 did not affect the total protein excretion, NAG excretion, osmolality in serum and urine and on osmolar clearance in the treated conscious rats (Table 8).

Table 8: Effect of ZK 6057184 on total protein excretion, NAG excretion, osmolality in serum and urine and on osmolar clearance after a single injection (i.v.) in conscious male rats

Group	Treatment (dose, i.v. injection)	Total protein excretion (mg/100g b.w./5h)	NAG excretion (mU/100g b.w./5h)	Serum Osmolality (mOsm/kg H_20)	Urine Osmolality (mOsm/kg H_20)	Osmolar clearance (µL/min)
1	Vehicle[1] (5 mL/kg)	0.91±0.55	9.16±3.16	290±8	360±102	20.57±6.13
2	ZK 6057184 (0.06 mg/kg)	0.57±0.07[2]	9.74±3.91	293±18	377±76	19.89±5.93
3	ZK 6057184 (0.15 mg/kg)	0.71±0.37[3]	10.59±4.96	295±5	377±95	19.19±5.59
4	ZK 6057184 (0.6 mg/kg)	0.74±0.34[4]	9.43±3.51	290±5	364±101	18.74±6.09

[1]Vehicle = 20% hydroxypropyl-beta-cyclodextrin with 0.5% NaCl in water for injections
Data are expressed as mean±S.D. (n = number of animals/group)
[2]n=7
[3]n=8
[4]n=7

Reviewer's Comment: This reviewer agrees with the result of this study.

Effects of ZK 6057184 on the body temperature and the behavior of male and female rats after single intravenous injection

Key study findings: The study was conducted to investigate any neurotropic effects on behavior and body temperature in rats intravenously administered ZK 6057184 (140X - 1395X MHD). The effect of ZK 6057184 was evaluated in 62 behavioral and neurological symptoms and the rectal temperature was assessed. The study indicates that ZK 6057184 did not affect the behavior or the body temperature in all treated male and female rats.

Study No. TOXT3078792

Study Report Location: 4.2.1.3 Pages 1-17.

Conducting laboratory Location: (b) (4)

	(b) (4)
Date of study initiation:	July 18, 2008
GLP Compliance:	No
QA Statement:	No
Drug, lot #, and % purity:	ZK 6057184, lot# - Not available and purity is stated to be 96.8%

Study Design:

Male and female rats employed for this study were randomized based on their body weight and divided into four groups of 5 rats per sex each as shown below. The comprehensive observational assessment method as detailed by Irwin (Psychopharmacologia 13; 222-257; 1968) and Campbell and Richter (Acta Pharmacol. Toxicol 25: 345-363; 1967) was employed for this study. The control group was administered the vehicle (20% 2-hydroxypropyl-β-cyclodextrin, 0.5% NaCl in water for injection) and the treated groups were each administered 0.06, 0.15, or 0.6 mg/kg (0, 140X 349X or 1395X MHD) of ZK 6057184. After the treatments, systematic assessments of signs and symptoms were performed at 10 min, 4 h and 24 in the rats allocated to each treatment group using a symptom check list that addresses all the parameters that evaluated behavior. Any signs and symptoms that contrasted with the normal behavior were recorded under the number of the subject displaying them and the time of their occurrence.

The animal's behavior, autonomous-affective and neurologic responses to different environmental and situational stimuli were evaluated in a viewing arena (60 x 45 x 7 cm) and a plastic step (height: 5.5 cm; width: 18 cm) using a reflex bristle. A thermostatic copper plate (15 x 9 cm, 24 VDC, 48 W, 58°C) was used as a pain stimulus. The pupil size and the light-pupil response were determined using, an equiradiant ground glass light source (52 x 52 cm, 220 VAC, 60 W), a stereomicroscope (Leitz FP 1), and a focused microscopic lamp (Leitz) respectively. Motor incoordination was assessed using two parallel iron wires brazed at a distance of 4.5 cm and suspended horizontally at a height of .37 cm. Animals were categorized into motor incoordination grades I and II if animals pending with their forepaws from the lower wire did not grasp the upper wire within 5 sec and 20 sec, respectively. The rectal temperature was measured with a digital thermometer (type DM 852; ELLAB A/S; Denmark) via a thermocouple applicator (type PRA-22002-A; ELLAB A/S; Denmark) before and at 10 min, 4 h and 24 h after the treatments.

Doses:	0, 0.06, 0.15 or 0.6 mg/kg (0, 140X 349X or 1395X MHD)
Frequency of dosing:	Single dose
Route of administration:	Intravenous Injection
Dose volume:	5 mL/kg
Formulation/Vehicle:	ZK 6057184/20% 2-hydroxypropyl-β-cyclodextrin, 0.5% NaCl in water for injection
Species/Strain:	Wistar Crl:WI(Han) (b) (4)
Number/Sex/Group:	5/sex/group
Weight:	80-95 g (Males and females)
Satellite groups:	None

Results

The data showed that after an intravenous administration of a single dose of ZK 6057184 (0, 140X 349X,1395X MHD), no effects on the central nervous system and the autonomic nervous system were detected in female and male rats at time points 10 min, 4 h and 24h after injection. It was also observed that the body temperature of the animals remained unchanged after treatment.

Reviewer's Comment: This reviewer observed that young rats (weighing below 100g) were employed in the study. The sponsor did not provide any information about the reason why such immature rats were used for the study. Similarly, any possible effect the young age of the rats would have on the result of the study is not known. ZK 6057184 seems to be well tolerated in the treated animals at the employed doses.

Effect of ZK 6057184 on motor coordination of rats after single intravenous administration

Key study findings: The study was conducted to investigate the effect of intravenously administered ZK 6057184 (140X - 1395X MHD) on motor coordination of conscious rats. he data showed that ZK 6057184 had no effects on motor coordination in rats. The study probably suggests that ZK 6057184 causes no impairment of motor coordination in rats after single intravenous administration of doses up to 1395X MHD.

Reference ID: 3361527

Study No.	TOXT4078838
Study Report Location:	4.2.1.3 Pages 1-9.
Conducting laboratory Location:	[redacted] (b) (4)
Date of study initiation:	July 18, 2008
GLP Compliance:	No
QA Statement:	No
Drug, lot #, and % purity:	ZK 6057184, lot # - Not available and purity is stated to be 96.8%

Study Design:

Male rats employed for this study were divided into four groups of 12 rats per sex each as shown below. The animals were initially acclimatized to the rotarod for three consecutive days before the test date on the fourth day. A rotarod advanced system ([redacted] (b) (4) with 4 rod places for rats was employed for this study. The training phase conducted in 52 male rats consisted of three trials separated by at least 10 min intertribal intervals (ITI). Each rat was placed on the rotating rod set at a constant speed of 4 rpm and animals that fails to stay on the rod in 2 of 3 trials on the third training day was excluded from the study. Ten minutes after intravenous administration of the test article or vehicle for the control group on the fourth day, individual animals were placed on the rotating rod which accelerated continuously from 4 to 33 rpm over 240 s. The measurement was repeated after an ITI of at least 10 min and the latency to fall of the rod was recorded. Animals which did not fall off the rotarod within 240 sec were removed and recorded as 240 sec. The animals were then sacrificed.

Doses:	0, 0.06, 0.15 or 0.6 mg/kg (0, 140X 349X or1395X MHD)
Frequency of dosing:	Single dose
Route of administration:	Intravenous Injection
Dose volume:	5 mL/kg
Formulation/Vehicle:	ZK 6057184/20% 2-hydroxypropyl-β-cyclodextrin, 0.5% NaCl in water for injection
Species/Strain:	Wistar Crl:WI(Han) (b) (4)
Number/Sex/Group:	8 male rat/group
Weight:	91-114 g (Males and females)
Satellite groups:	None

Results

The data shows that ZK 6057184 (0, 140X 349X and 1395X MHD) caused no change in the latencies of rats on the accelerating rotarod as compared to the vehicle-treated group (Table 9).

Table 9: Effect of ZK 6057184 after single intravenous administration (t-10 min) on the latency of rats on the accelerating rotarod (from 4 to 33 rpm over 240 sec)

		Latency on rotarod (sec)		
Treatment	Dose (mg/kg)	Mean±S.D.	Median (25/75 percentile)	Minima/Maxima
Vehicle[1]	-	144.9±54.5	132 (109/175)	83/240
ZK 6057184	0.06	154.4±42.5	151 (118/179)	100/240
ZK 6057184	0.15	154.5±71.2	140 (102/222)	23.4/240
ZK 6057184	0.6	155.9±54.7	134 (114/208)	100/240

[1]Vehicle = 20% hydroxypropyl-beta-cyclodextrin with 0.5% NaCl in water for injections

(n = number of animals/group) S.D. = standard deviation

This indicates that ZK 6057184 at the employed doses demonstrated no effects on motor coordination in rats after single intravenous administration (10 min after administration). This study shows that it seems unlikely that ZK 6057184 would cause an impairment of motor coordination if administered at the clinical dose.

Reviewer's Comment: This reviewer agrees with the result of this study. However, this reviewer noted that juvenile rats were also employed in the study as in the previous study. The sponsor also conducted the study in the male rats rather than in both males and females. The use of juvenile rats and only male rats does not reflect the intended proposed population for this product. Overall, available data indicates that ZK 6057184 would probably not impair motor coordination when administered up to 1395X MHD.

Effects of ZK 6057184 on pulmonary function of conscious unrestrained rats after single intravenous administration

Key study findings: The potential effects of a single dose administration of ZK6057184 (140X - 1395X MHD) on respiratory function in conscious rats was investigated using whole body plethysmography system. The results indicates that ZK 6057184 did not cause any change in respiratory frequency, tidal volume or minute volume in the animals at any time point during the investigation.

Study No.	TOXT6079703
Study Report Location:	4.2.1.3 Pages 1-16.
Conducting laboratory Location:	(b) (4)
Date of study initiation:	November 19, 2008
GLP Compliance:	No
QA Statement:	No
Drug, lot #, and % purity:	ZK 6057184, lot# - Not available and purity is stated to be 96.8%

Study Design:

Reference ID: 3361527

Male and female rats were randomized based on their body weight into four groups of 6-8 rats per sex each. The control group was administered the vehicle (20% 2-hydroxypropyl-β-cyclodextrin, 0.5% NaCl in water for injection) and the treated groups were each intravenously administered 0.06, 0.15 or 0.6 mg/kg (0, 140X 349X or 1395X MHD) of ZK 6057184. The pulmonary functions of the animals was measured in the conscious unrestricted rats using whole body plethysmography (WSP) system and the data recorded with a computerized system (b) (4) The tidal volume, respiratory frequency and minute volume were measured or calculated before and 0.5, 1, 1.5, 3 and 5 hour(s) after treatment with the vehicle or ZK 6057184. The changes in the evaluated respiratory parameters before and after treatment were calculated and the values of the ZK 6057184-treated groups were compared with that obtained to the vehicle-treated group at corresponding time point.

Doses:	0, 0.06, 0.15 or 0.6 mg/kg (0, 140X 349X or 1395X MHD)
Frequency of dosing:	Single dose
Route of administration:	Intravenous Injection
Dose volume:	5 mL/kg
Formulation/Vehicle:	ZK 6057184/20% 2-hydroxypropyl-β-cyclodextrin, 0.5% NaCl in water for injection
Species/Strain:	Sprague Dawley Crl:CD, (b) (4)
Number/Sex/Group:	6-8 males/group
Age:	8-10 weeks
Weight:	297-384 g (Males and females)
Satellite groups:	None

Results

The data showed that ZK 6057184 (up to 1395X MHD) caused no major effects on respiratory frequency, tidal volumes and minute volume.

Reviewer's Comment: This reviewer opined that the period of observing the respiratory parameters employed by the sponsor in this study seems adequate. However, only male rats were employed in the study. The use of male rates does not reflect the intended population for the proposed indication of this product. The sponsor did not justify the use of male animals for this study. Overall, the data from this study suggests that ZK 6057184 up to 1395X MHD seems

not to induce any changes on the evaluated respiratory parameters when administered at the intended human dose.

Study title: **Cardiovascular Safety Pharmacology Study of a Single Intravenous Dose of PEGN3.HCl in Conscious Beagles.**

Key study findings: Potential cardiovascular effect and overtly cardiac toxicity of a single intravenous dose of PEGN3.HCl (0, 6.7X 34.2X and 68.4X MHD) was evaluated in conscious male and female Beagle dogs. No treatment-related effects were reported on the ECG parameters, rhythm, or blood pressure. The study suggests that PEGN3.HCl could be well tolerated at the employed doses and no potential cardiac adverse effect is expected at the clinical dose of PEGN3.HCl.

Study No.	M339-05
Study Report Location:	4.2.1.3 Pages 1-166.
Conducting laboratory Location:	Bayer Schering Pharma AG, Nonclinical Drug Safety, 13342 Berlin, Germany
Date of study initiation:	October 5, 2005
GLP Compliance:	Yes
QA Statement:	Yes
Drug, lot #, and % purity:	PEGN3.HCl, lot# C642918 and purity is stated to be 95.4%

Reference ID: 3361527

Study Design:

A total of 8 Beagle dogs were employed for this study. Single bolus injection of the vehicle or PEGN3.HCI was intravenously administered via the left saphenous vein and the clinical signs, ECG, heart rate, respiratory rate, blood pressure and body temperature of the dogs were evaluated within 24 hours post injection. The body temperature was measured using rectal probe while the ECG was evaluated for heart rate, rhythm and mean electrical axis. The study was designed as shown in Table 10.

Doses:	0, 2.9, 14.7 or 29.3 µg/kg (0, 6.7X 34.2X or 68.4X MHD)
Frequency of dosing:	Single dose
Route of administration:	Intravenous Injection
Dose volume:	0.5 mL/kg
Formulation/Vehicle:	PEGN3.HCl/20% 2-hydroxypropyl-β-cyclodextrin in saline
Species/Strain:	Canine/Beagle
Number/Sex/Group:	1-2/sex/group
Age:	11-12 weeks (males and female)
Weight:	7.5 – 12.5 kg (males and female)
Satellite groups:	None

Table 10: Experimental design of the Cardiovascular Safety Pharmacology Study in Conscious Beagle Dogs.

Group	Test Article	Dose Level*	Dose (µg/kg)	Dose Volume ((mL/kg)	Dosing Concentration	Number of Animals
1	PEGN3.HCl	6.7	2.9	0.5	5.9	2M/2F
2	PEGN3.HCl	34.2	14.9	0.5	29.4	1M/1F
3	PEGN3.HCl	68.4	29.3	0.5	58.6	1M/1F

*Anticipated maximum human dose (MHD) is 30 µg per 70 kg person as stated in the label for this product.
MHD based the dose multiple calculation on body weight

Reference ID: 3361527

Results:

Clinical signs: Clinical observation of the animals showed shivering in male dogs administered 34.2X MHD and female dogs administered 6.7X and 34.2X MHD. Struggling was also reported in the male at 34.2X MHD and female at 6.7X MHD while twitching was observed in the female dog administered 6.7X MHD. No clinical findings were reported in the control animal and the female dog treated with 68.4X MHD PEGN3.HCI in this study.

Body weights: No treatment related effect was reported on the body weight.

Body temperature: No treatment-related effect was reported.

Cardiovascular Evaluation: The data indicates that PEGN3.HCI treatment did not affect the ECG parameters, rhythm, or blood pressure. The sponsor provided pre-dose and post-dose data on the blood pressure, respiratory rate, temperature and ECG obtained at various time intervals within 24 hours after treatment. Representative data which includes pre-dose data and post-dose data obtained at 60 min and 240 min are shown in Table 11 below.

Table 11: Representative data on the blood pressure, respiratory rate, temperature and ECG obtained at pre-dose and 240 minutes post-dose during the Cardiovascular Safety Pharmacology Study in Conscious Beagle Dogs as provided by the sponsor

Reference ID: 3361527

Pre-Dose

ID/Sex of Dog	MHD	Average Systolic (mmHg)	Average Diastolic (mmHg)	Average MAP (mmHg)	RR (bpm)	Temp (°F)
1 -M	6.7	127.8	88.4	102.4	44	100.3
2 -M	6.7	121.6	72.2	91.2	25	101.9
3 -F	6.7	121.0	74.0	95.8	36	99.3
4 -F	6.7	130.8	94.0	108.8	36	99.4
5 -M	34.2	134.4	91.4	108.8	40	100.4
6 -F	34.2	141.4	72.4	104.0	32	98.6
7 -M	68.4	120.0	73.0	89.2	32	99.2
8 -F	68.4	126.2	68.4	94.4	28	100.2

240 Minutes Post-Dose

ID/Sex of Dog	MHD	Average Systolic (mmHg)	Average Diastolic (mmHg)	Average MAP (mmHg)	RR (bpm)	Temp (°F)
1 -M	6.7	141.6	89.8	112.4	24	98.5
2 -M	6.7	121.8	69.8	90.8	24	96.2
3 -F	6.7	128.6	86.0	103.6	24	96.1
4 -F	6.7	121.6	75.8	93.8	36	98.8
5 -M	34.2	133.2	78.0	104.2	20	98.1
6 -F	34.2	105.1	64.1	82.0	36	99.7
7 -M	68.4	104.8	55.6	77.0	40	99.2
8 -F	68.4	129.6	73.2	98.8	28	98.9

MAP – Mean Arterial Pressure

The ECG did not show any ST segment abnormalities, pronounced U waves, nor were T wave changes such as changes in polarity, increased amplitude, or flattening found. The summary of the ECG data obtained from the dog administered 68.4X MHD PEGN3.HCI is shown below.

Table 12: Summary ECG data obtained following administration of PEGN3.HCl (68.4X MHD) during the Cardiovascular Safety Pharmacology Study in Conscious Beagle Dogs as provided by the sponsor

Group 3 (29.3 µg/kg PEGN-3)

Study ID	P (msec)	QRS (msec)	QT (msec)	QTc (msec)[1]	MEA (deg)	HR (bpm)	Rhythm	Comments
7 pre-dose	36.4	44.8	200.0	224.2	-162	82	sa	significant right axis deviation
7- 2min	39.2	44.0	209.6	234.2	60	79	sa	--
7- 5 min	39.2	42.8	208.0	236.2	47	86	sa	--
7- 10 min	39.2	41.2	203.2	227.4	40	82	sa	--
7- 15 min	36.8	42.4	235.6	259.3	36	80	sa	trivial left axis deviation
7- 30 min	37.6	44.8	205.6	239.4	35	88	sa	trivial left axis deviation
7- 1 hr	38.4	44.0	202.0	226.3	22	81	sa	left axis deviation
7- 2 hr	34.4	41.6	222.4	241.7	62	75	sa	--
7- 4 hr	35.2	40.4	218.8	234.6	46	70	sa	--
7- 24 hr	40.0	40.0	228.0	252.7	58	77	sa	--
8 pre-dose	36.0	40.0	190.4	239.7	18	119	sr	left axis deviation
8- 2min	34.4	40.0	184.8	236.3	16	124	sr	left axis deviation
8- 5 min	36.0	40.0	177.6	228.5	25	127	sr	left axis deviation
8- 10 min	32.8	40.0	195.2	237.9	11	108	sr	left axis deviation
8- 15 min	34.4	40.0	196.8	243.7	9	112	sa	left axis deviation
8- 30 min	38.4	40.0	201.6	249.1	30	110	sa	trivial left axis deviation
8- 1hr	36.0	40.0	196.8	236.9	16	100	sa	left axis deviation
8- 2 hr	34.4	40.0	196.0	225.9	29	89	sa	left axis deviation
8- 4 hr	33.6	40.0	190.4	226.3	60	97	sa	--
8- 24 hr	35.2	40.0	187.2	224.7	51	102	sa	--
normal	<50	<60	150-250	193-265	40-100	70-160	sr/sa	

KEY: sr= sinus rhythm; sa= sinus arrhythmia; st= sinus tachycardia; sb= sinus bradycardia
[1]QTc: QT interval correction using Fredericia's Formula
MEA: mean electrical axis
HR: heart rate
significant left axis deviation -1 to -90 degrees
significant right axis deviation 160 to -90 degrees

Reviewer's Comment: This reviewer is of the opinion that this dog study was not well designed because inadequate number of dogs was used for the study. The sponsor employed test groups of one dog per sex to study the cardiovascular and overt toxicity of PEGN3.HCI. Thus, the result obtained from the study is inconclusive because of lack of any statistical analysis of the data. The clinical observation indicates that an additional study is required to assess the possible CNS effect of PEGN3.HCI as demonstrated by the data. Shivering, struggling and twitching reported in the animals could suggest potential CNS effect of PEGN3.HCI. It is noted that the sponsor stated that the effects did not appear to be dose-related and reported that similar effects were observed pre-treatment. However, the data indicates twitching, shivering and struggling before PEGN3.HCI administration, this could probably suggests that the dogs probably have underlying illness and should not have been used for the study. Apart from the safety signals shown by the clinical observations, no treatment-related effects were reported on the ECG parameters, rhythm, or blood pressure. The product seems well tolerated by the dogs.

Study title: **Effects of three consecutive intravenous infusions of ZK 6057184 on cardiohemodynamics and ECG in anesthetized Beagle dogs**

Key study findings: This study evaluated whether ZK 6057184 affects cardiohemodynamics and ECG in anesthetized dogs during and after intravenous administration of three consecutive

doses of ZK 6057184. ZK 6057184 (15, 40 and 150 µg/kg - 34.9X, 93X and 349X MHD) was injected every 30 minutes in ascending order via venous catheter in the left femoral vein. The study demonstrated that consecutive infusions of ZK 6057184 up to 349X MHD did not cause any treatment-related effect on the cardiohemodynamic and ECG parameters evaluated during the study in anesthetized Beagle dogs.

Study No.	TOXT7079704
Study Report Location:	4.2.1.3 Pages 1-53.
Conducting laboratory Location:	Bayer Schering Pharma AG, Nonclinical Drug Safety, 13342 Berlin, Germany
Date of study initiation:	December 11, 2008
GLP Compliance:	Yes
QA Statement:	Yes
Drug, lot #, and % purity:	ZK 6057184, lot # -Not provided and purity is stated to be 96.8%

Study Design:

Two groups of 6 Beagle dogs each were employed for this study. The dogs were anesthesized, intubated and ventilated. They were instrumented for cardiovascular parameters collections. One group of six dogs (3 females/3 males) was given ZK 6057184 in three ascending doses of 15, 40 and 150 µg/kg - 34.9X, 93X and 349X MHD) as three consecutive intravenous infusions (each infusion of 10 minutes) via a venous catheter in a volume of 0.075, 0.2 and 0.75 mL/kg. Another group, control animals (n=6) also received three consecutive intravenous infusions of 0.075, 0.2 and 0.75 mL/kg of the vehicle (60% PEG400 in water for injections). Left ventricular and aortic pressure were recorded via Millar Mikro-Tip catheter pressure transducer (via left common carotid artery), pulmonary arterial and central venous blood pressure via true size monitoring catheters connected to Statham pressure transducers (via left external jugular vein). Cardiac output was determined by a $PICCO_2$-System (Pulsion Medical Systems).

A standard lead II ECG and an additionally chest lead was installed and monitored via needle electrodes for determination of ECG intervals (RR, PR, QRS, QT and QTc) and visual inspection of the ECG waveforms for disturbances in rhythm and waveform morphology. Cardiohemodynamic and ECG parameters were continuously recorded up to 240 min after start of the first infusion. The data are expressed as mean±SD or % of pre-treatment. The changes of the hemodynamic data versus pre-treatment were calculated and compared with the vehicle group. One-way analysis of variance (ANOVA) was employed for data analysis. Arterial blood

Reference ID: 3361527

samples taken via the additional open lumen of the Millar catheter before dosing and at different time points (5, 10, 20, 30 min) and in addition after start of third infusion (60, 90, 120, 150, 180 min) post-injection were analyzed for blood pH, blood gases and concentrations of electrolytes (Na^+, K^+, Ca_2^+, Cl^-) and bicarbonate.

Doses:	15, 40 and 150 µg/kg (34.9X, 93X and 349X MHD)
Frequency of dosing:	Consecutive dosing (10 minutes each) in ascending order dose with 30 minutes interval.
Route of administration:	Intravenous Injection
Dose volumes:	0.075, 0.2 and 0.75 mL/kg respectively.
Formulation/Vehicle:	PEGN3.HCl/60% PEG400 in water for injections.
Species/Strain:	Canine/Beagle
Number/Sex/Group:	3/sex/group
Age:	12-15 months (males and female)
Weight:	9.7 – 17.8 kg (males and female)
Satellite groups:	None

Reference ID: 3361527

Results:

Cardiohemodynamic results: The data showing the cardiohemodynamic effects (in percent of pre-treatment values) during and after three consecutive intravenous infusions at 30 minutes intervals (over 10 minutes each) of vehicle and ZK 6057184 was provided. No statistically significant differences were found between the groups in all cardiohemodynamic parameters evaluated during the study as shown in Figures 33 to 44. However, changes in MAP were noted in the treated group for most of the observation period (Figure 30). Furthermore, gradual increases were also noted in both groups for mean pulmonary artery pressure (figure 6), max rate of rise of left ventricular pressure (over the whole recording period) (Figure 40) and for systemic arterial blood pressure (Figure 34), left ventricular end-diastolic pressure (Figure 36), central venous pressure (Figure 37), total peripheral resistance (Figure 43) and pulmonary vascular resistance (Figure 44) over the initial 90 min of treatment.

Reference ID: 3361527

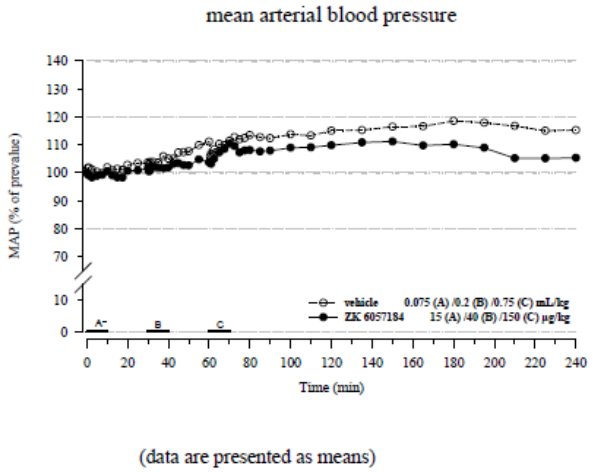

Figure 26: Effects of three consecutive intravenous infusions over 10 minutes each of vehicle and ZK 6057184 on mean arterial blood pressure (MAP) in anesthetized dogs

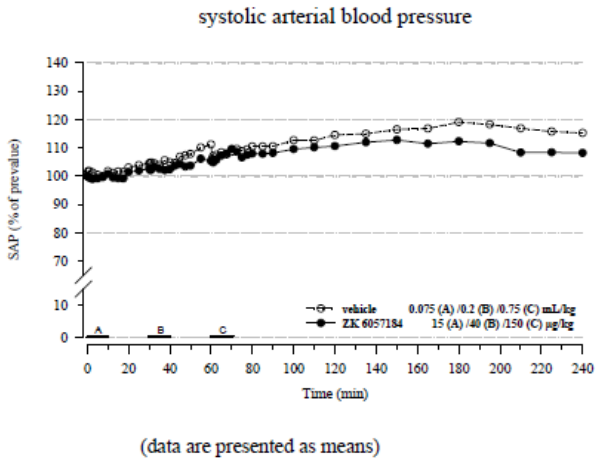

Figure 27: Effects of three consecutive intravenous infusions over 10 minutes each of vehicle and ZK 6057184 on systolic arterial blood pressure (SAP) in anesthetized dogs

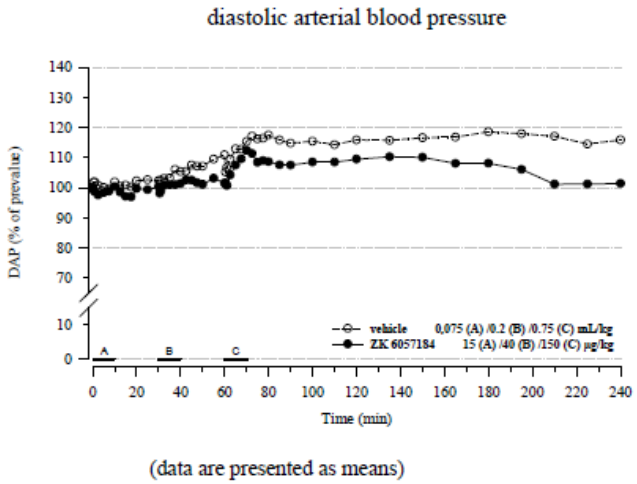

Figure 28: Effects of three consecutive intravenous infusions over 10 minutes each of vehicle and ZK 6057184 on diastolic arterial blood pressure (DAP) in anesthetized dogs

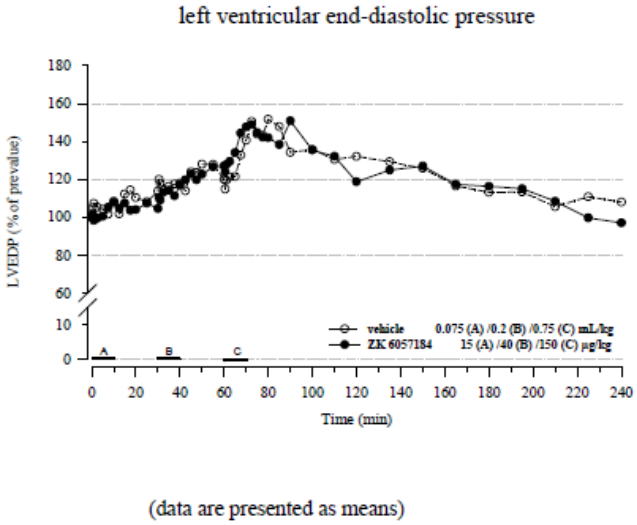

Figure 29: Effects of three consecutive intravenous infusions over 10 minutes each of vehicle and ZK 6057184 on left ventricular end-diastolic pressure (LVEDP) in anesthetized dogs

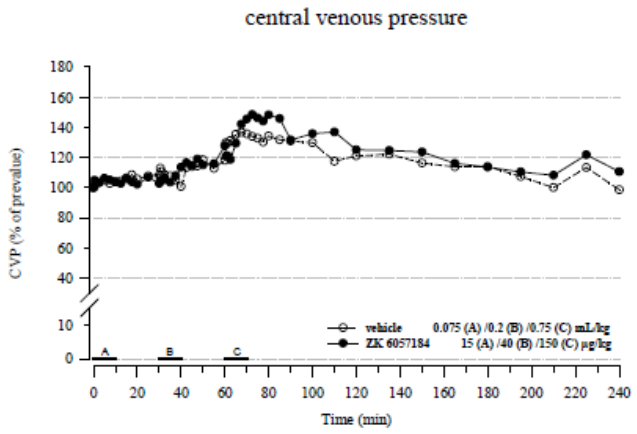

Figure 30: Effects of three consecutive intravenous infusions over 10 minutes each of vehicle and ZK 6057184 on central venous pressure (CVP) in anesthetized dogs

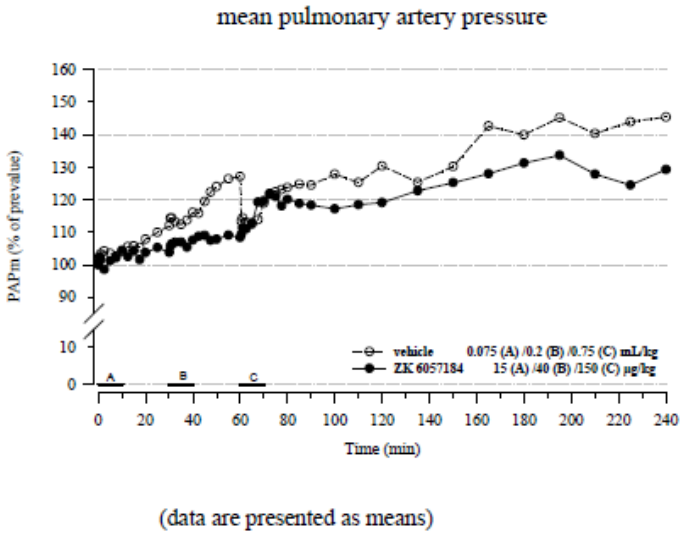

Figure 31: Effects of three consecutive intravenous infusions over 10 minutes each of vehicle and ZK 6057184 on mean pulmonary artery pressure (PAPm) in anesthetized dogs

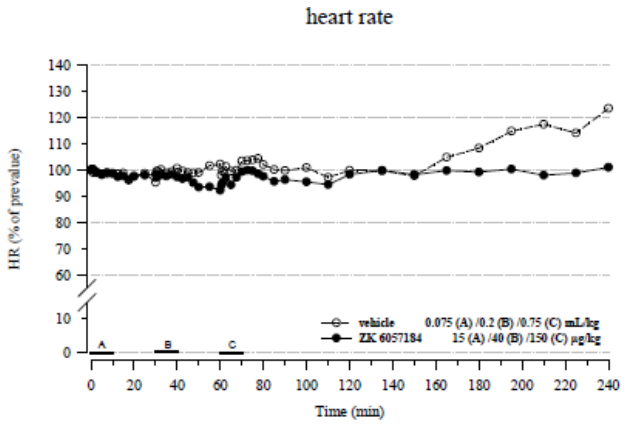

Figure 32: Effects of three consecutive intravenous infusions over 10 minutes each of vehicle and ZK 6057184 on heart rate (HR) in anesthetized dogs (data are presented as means)

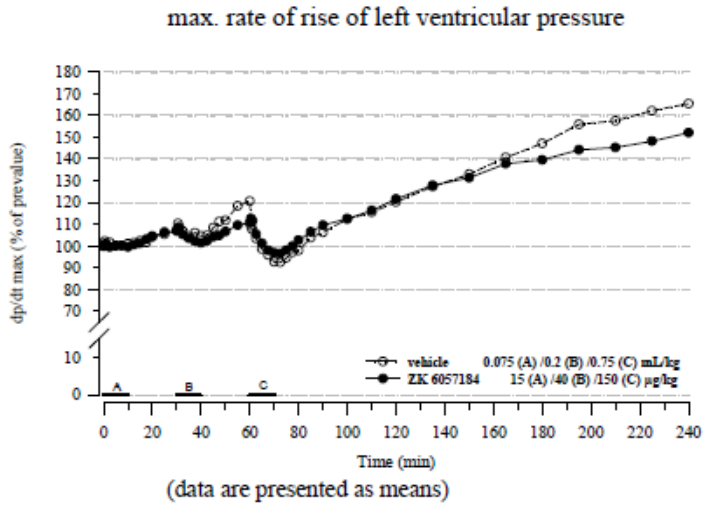

Figure 33: Effects of three consecutive intravenous infusions over 10 minutes each of vehicle and ZK 6057184 on max. rate of rise of left ventricular pressure (dp/dt max) in anesthetized dogs

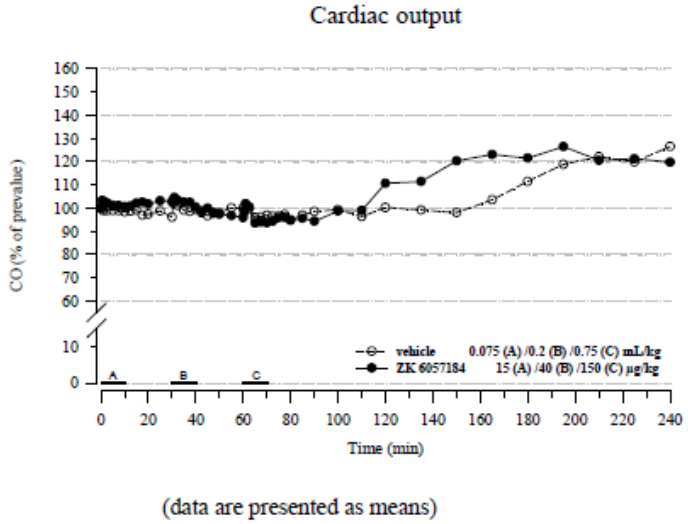

Figure 34: Effects of three consecutive intravenous infusions over 10 minutes each of vehicle and ZK 6057184 on cardiac output (CO) in anesthetized dogs

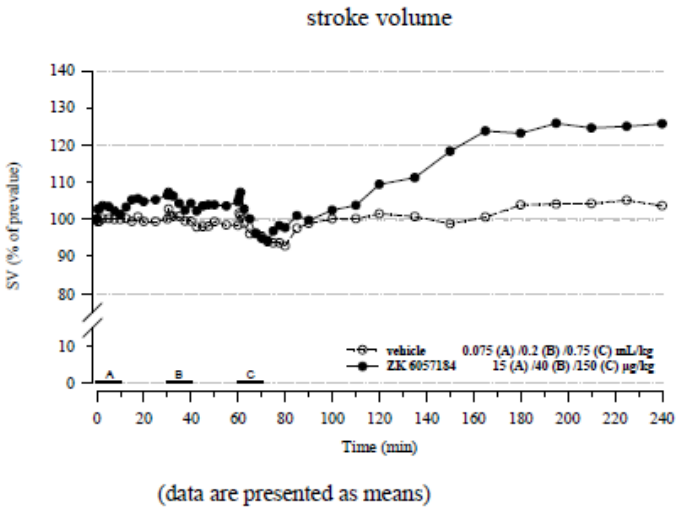

Figure 35: Effects of three consecutive intravenous infusions over 10 minutes each of vehicle and ZK 6057184 on stroke volume (SV) in anesthetized dogs

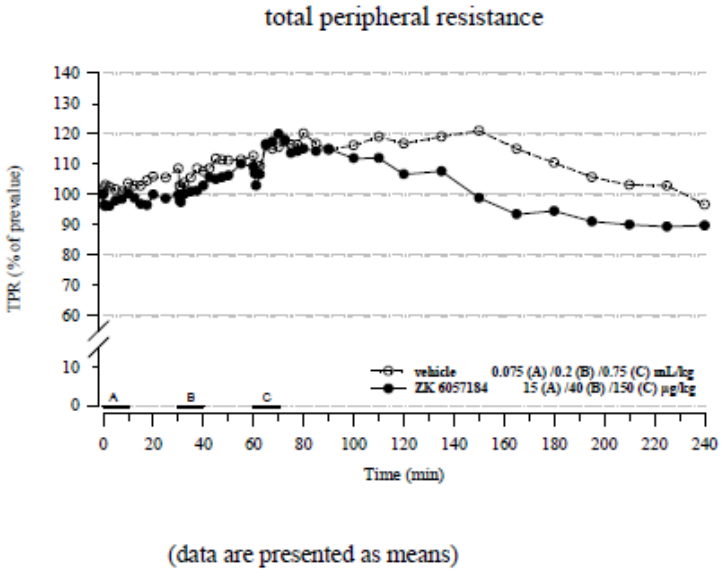

Figure 36: Effects of three consecutive intravenous infusions over 10 minutes each of vehicle and ZK 6057184 on total peripheral resistance (TPR) in anesthetized dogs

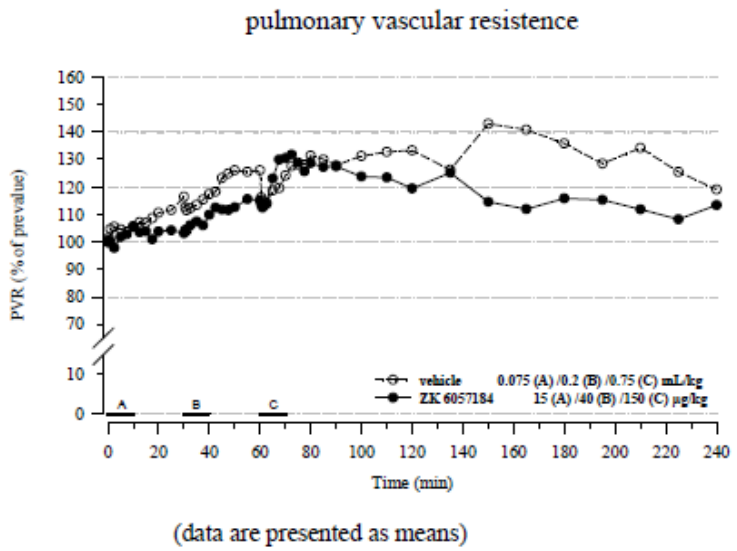

Figure 37: Figure 44: Effects of three consecutive intravenous infusions over 10 minutes each of vehicle and ZK 6057184 on pulmonary vascular resistance (PVR) in anesthetized dogs

The changes could be attributed to volume effect caused by consecutive infusions of the test article rather than any direct cardiohemodynamic effect of the test article itself. The data indicates that no statistically significant differences (ZK 6057184 versus vehicle) were found for cardiac output at 1 min and for stroke volume at 30 sec, 1 min, 30 min, 165 min, and 195 min as shown in the Table 13.

Table 13: Effect of ZK 6057184 on cardiac output and stroke volume at various time intervals

	Cardiac Output (L/min)		Stroke Volume (mL)	
Time [min]	Vehicle (0.075/0.2/ 0.75mL/kg)	ZK 6057184 (15/40/150 µg/kg)	Vehicle (0.075/0.2/ 0.75mL/kg)	ZK 6057184 (15/40/150 µg/kg)
Pre	2.22±0.42	2.08±0.47	21.5±4.9	20.4±4.4
1	2.19±0.36	2.15±0.53	21.3±4.6	21.0±4.7
30	2.12±0.32	2.17±0.69	21.5±4.9	21.8±5.1
165	2.29±0.58	2.63±1.15	21.3±4.2	25.5±7.1
195	2.62±0.96	2.71±1.29	22.0±4.0	26.0±7.5

Overall, consecutive infusions of 15, 40 and 150 µg/kg of ZK 6057184 at 30 minutes intervals in this study did not cause any apparent effects on cardiohemodynamics beyond the vehicle effects.

<u>Electrocardiography:</u> The data on ECG time interval during and after three consecutive intravenous infusions of vehicle and ZK 6057184 is presented in Figure 37, Figure 38, Figure 39, Figure 40, Figure 41 and Figure 42. The test article did not induce any apparent effects on the ECG time intervals (RR, PR, QRS, QT and QTc) beyond the vehicle effects as discussed

above. The vehicle effects were seen at the highest volume leading to transient increases in ECG time intervals (PR and QRS by 5 %, QT and QTc by 10 %).

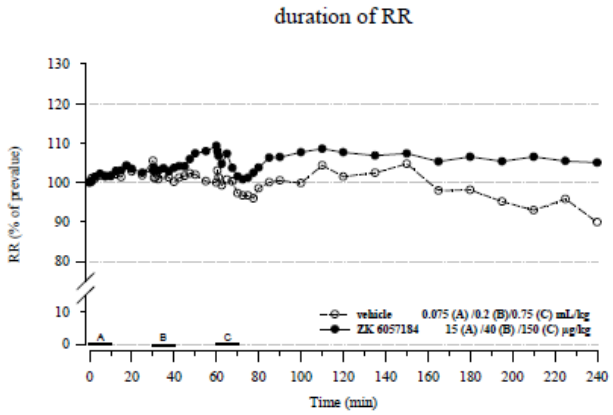

(data are presented as means)

Figure 38: Effects of three consecutive intravenous infusions over 10 minutes each of vehicle and ZK 6057184 on the ECG time interval RR (RR) in anesthetized dogs

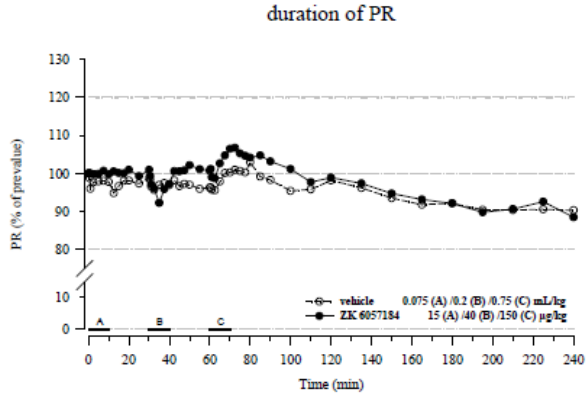

(data are presented as means)

Figure 39: Effects of three consecutive intravenous infusions over 10 minutes each of vehicle and ZK 6057184 on the ECG time interval PR (PR) in anesthetized dogs

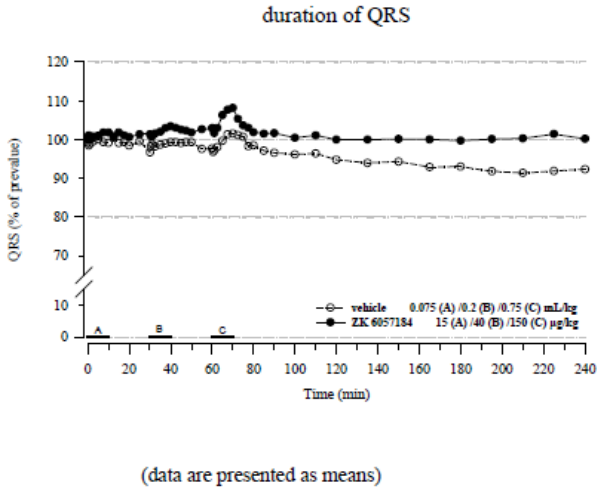

Figure 40: Effects of three consecutive intravenous infusions over 10 minutes each of vehicle and ZK 6057184 on the ECG time interval QRS (QRS) in anesthetized dogs

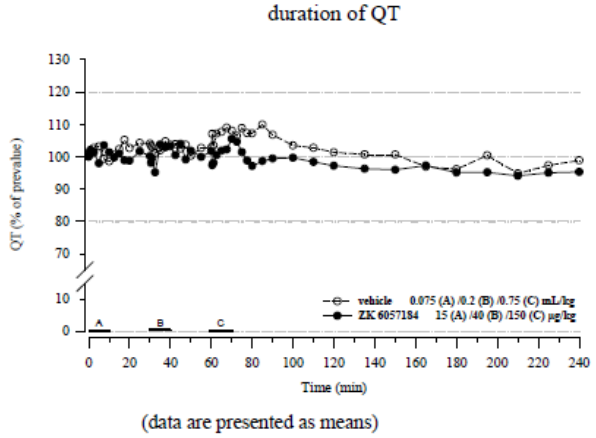

Figure 41: Effects of three consecutive intravenous infusions over 10 minutes each of vehicle and ZK 6057184 on the ECG time interval QT (QT) in anesthetized dogs

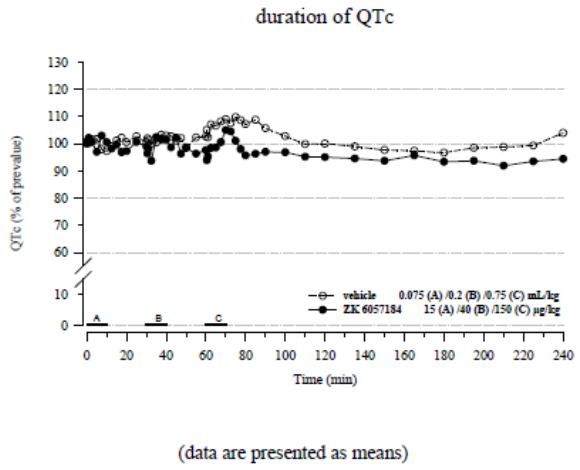

Figure 42: Effects of three consecutive intravenous infusions over 10 minutes each of vehicle and ZK 6057184 on the corrected ECG time interval QT (QTc) in anesthetized dogs

The data also shows that no ECG abnormalities occurred in the equilibration period and the ECG-waveform analysis indicates regular rhythm in all animals during and after the three consecutive administrations of ZK 6057184 or the vehicle. However, two ectopic atrial beats were seen at 120 min (60 min after administration of the highest dose) in a dog treated with ZK 6057184. This effect could be an incidental episode.

Blood parameters: No effects on serum electrolytes were observed in the animals and the blood pH and blood gases were within the physiological ranges of these parameters up to the highest employed 349X MHD dose.

Reviewer's Comment: Agrees with the results of this study. The study suggests that it is not expected that the evaluated cardiohemodynamic, ECG and blood parameters would be affected following the administration of ZK 6057184 at the proposed dose. However, this data does indicate that administration of repeated doses of ZK 6057184 within a short period of time could be problematic. Testing higher doses of ZK 6057184 could have provided added value to the data and actually revealed the effect of cardiohemodynamic and ECG parameters in overtly sensitive individuals even in cases of inadvertent administration of higher doses of the product. (b) (4) as a result of which the product could not be tested at higher doses. Furthermore, it is noted that 2-hour observation period employed in this study seems too short a time to adequately predict many of the evaluated parameters such as stroke volume, heart rate, mPAR, blood pressure more so that the changes in the treated animals in comparison with the control widens over time. Although this effect has been attributed to vehicle effect, however, since similar volume was administered to the control group, the "volume effect" theory might not be acceptable. No other explanation could presently be given as the cause of this effect.

5 Pharmacokinetics/ADME/Toxicokinetics

The sponsor conducted the following studies on the pharmacokinetics, absorption, distribution and metabolism of Florbetaben. The toxicokinetics study was conducted as part of the toxicity studies.

5.1 PK/ADME

Study title: Pharmacokinetics of [^{19}F]AV1/ZK

Key study findings: *In vitro* and *in vivo* characteristics of [^{19}F]AV1/ZK following a single intravenous administration to male Wistar rats was evaluated. protein binding, blood-plasma partitioning and stability of [^{19}F]AV1/ZK was performed using HPLC/UV or LC/MS/MS. The *in vivo* determination of the [^{19}F]AV1/ZK concentration in the serum was done using LC/MS/MS. The study demonstrates that [^{19}F]AV1/ZK was bound to human plasma proteins, with blood/plasma ratio of 0.44 in human and [^{19}F]AV1/ZK is stable in serum and found to be moderately stable in liver microsomes in all species tested. The *in vivo* data indicates that [^{19}F]AV1/ZK is characterized by blood clearance of 6.7 L/h/kg, volume of distribution of 2.8 L/kg and distribution $t_{1/2}$ of 0.15 h in this study.

Study Nos.	FP2005.4580, FP2005.4610, FP2005.4620, FP2005.4630, FP2006.3980
Study Report Location:	4.2.2.2. Pages 1-13.
Conducting laboratory Location:	Bayer Schering Pharma AG, Nonclinical Drug Safety, 13342 Berlin, Germany
Date of study initiation:	October 31, 2005
GLP Compliance:	No
QA Statement:	No
Drug, lot #, and % purity:	ZK 06016468, lot # and purity-Not provided.

Reference ID: 3361527

Study Design:

Plasma protein binding analysis- The fraction unbound (Fu) of [^{19}F]AV1/ZK in plasma was measured using a dialysis assay that separates unbound drug from total drug in equilibrium. The process involve spiking 150 µl of plasma with the test compound in 2 concentrations and dialyzed (7 h, 37°C) against PBS buffer using a 96-well Teflon dialysis apparatus (ht-dialysis) and a semi permeable membrane (regenerated cellulose, 12-14 kD). LC-MS/MS analysis was employed to measure the concentration of the test compound in the donor and receiver side and also for calculation of the unbound fraction.

In vitro blood plasma ratio analysis- The blood-plasma concentration ratio (B/P ratio) of the test compound was determined by adding [^{19}F]AV1/ZK in final concentrations of 0.3 and 3 µM to rat and human blood plasma The resulting blood and plasma samples were then incubated in duplicates at 37°C for 30 min and centrifuged at 3,000 rpm for 10 min to obtain plasma. The B/P ratios were calculated based on comparison of drug concentrations in control plasma versus plasma prepared from the treated blood samples.

In vitro serum stability determination- The stability of [^{19}F]AV1/ZK in serum liver microsomes from different species (mouse, rat and human) was determined. The test compound was incubated in the serum of the mouse, rat and human species at a concentration of 30 µM for 30 minutes. [^{19}F]AV1/ZK content was analyzed after precipitation with acetonitrile using LC/MS/MS. The stability of the test compound was quantified by comparing the remaining amount after 30 min with the amount of the 0 min-sample and is expressed in % of initial concentration.

Determination of *in vitro* metabolic stability in liver microsomes- The susceptibility of test compound regarding metabolic degradation via Phase 1 enzymes was investigated. Isolated microsomes of different species were incubated in the presence of cofactors (glucose-6-phosphate, $MgCl_2$, NADP, Glucose-6-Phosphate dehydrogenase) with the [^{19}F]AV1/ZK) at a concentration of 3 µM for 30 and 60 min time points. The analysis of [^{19}F]AV1/ZK content was performed after precipitation with methanol by HPLC/UV. The stability of the test compound was then quantified by comparing the remaining amount after 30 min and 60 min with the amount of the 0 min-sample. The stability is expressed in % of initial concentration [% recovery].

Determination of [^{19}F]AV1/ZK disposition kinetics in rat- Male rats (Han-Wistar; 200-250g; weight; n=3) employed for this study were catheterized in the right jugular veins with sterile cannula under isofluran anesthesia. The rats were intravenously injected a single 0.5 mg/kg dose of [^{19}F]AV1/ZK formulated in 50% PEG 400 in the tail vein and serial blood samples were collected via catheter at 0.083, 0.25, 0.5, 0.75, 1, 2, 4, 6, 8 and 24 hours post-dosing. Each sample was centrifuged at 2000 x g for 5 min to separate serum. The animals were sacrificed after sample collection. LC/MS/MS analysis of compound concentrations in serum was done after precipitation with acetonitrile (1:5, v/v) and the pharmacokinetic analysis was performed using WinNonLin software while the summary data were expressed as mean ± standard deviation (SD).

Results:

Plasma Protein Binding and Blood/Plasma Partitioning- The data on plasma protein binding in human at a concentration of [^{19}F]AV1/ZK (0.3 µM) following HT equilibrium dialysis indicates that [^{19}F]AV1/ZK was bound to plasma proteins, with a fraction unbound (Fu) of 1.6%. The B/P

ratio of 0.44 was also reported to [^{19}F]AV1/ZK in human in the concentration range of 0.3 – 3.0 µM during the study.

Serum Stability of [^{19}F] AV1/ZK in rat and human- Following the determination of the stability of [^{19}F]AV1/ZK in serum after 30 min incubation using single LC-MS analysis, up to 93 % recovery from rat serum and 88% recovery was reported from human serum.

Metabolic stability of [^{19}F]AV1/ZK in liver microsomes- The susceptibility of [^{19}F]AV1/ZK to degradation by phase-I oxidative metabolism was investigated using liver microsomes from different species and HPLC-UV analysis and [^{19}F]AV1/ZK was found to be moderately stable in the liver microsomes in the tested species. Within 30 minutes following an incubation with [^{19}F]AV1/ZK (3 µM), percent metabolic stability in liver microsomes of rat, mouse and human were 76%, 74% and 82% respectively. The data indicates similar susceptibility to cytochrome P450-mediated first-pass metabolism (Phase I) in rats, mouse, and humans. Furthermore, HPLC-UV revealed several putative metabolites, though the sponsor did not provide any data on these metabolites. However, a major metabolite of [^{19}F]AV1/ZK with a mass of 346, suspected to be the N-demethylated product of [^{19}F]AV1/ZK was detected by LC-MS/MS analysis.

Disposition Kinetics of [^{19}F]AV1/ZK in rats- The serum concentration-time profile of the animals injected 0.5 mg/kg [^{19}F]AV1/ZK in 50% PEG 400/0/9% NaCl is shown in sponsor's Figure 43.

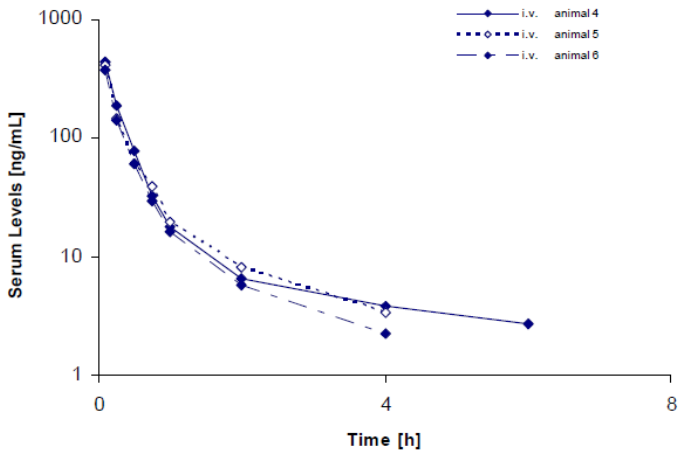

Figure 43: Serum concentration-time profile of [19F]AV1/ZK after i.v. bolus injection of 0.5 mg/kg in 50 % PEG 400 solution (blue lines; animals 4, 5 and 6) in the male rat

The summary of the pharmacokinetic parameters of [^{19}F]AV1/ZK following the measurement of serum levels in the intravenous kinetics using LC-MS/MS (Table 14).

Table 14: Pharmacokinetic Parameters of [^{19}F]AV1/ZK in the male rat (disposition kinetics after i.v. (intravenous) administration of 0.5 mg/kg (50 % PEG400 solution) n = 3

Parameter	(iv admin.)	Mean	SD
$T_{1/2}$ distribution (α)	[h]	**0.15**	0
$T_{1/2}$elimination (ß)	[h]	**1.1**	0.07
MRT	[h]	**0.6**	0.07
CL	[L/h/kg]	**3.1**	0.5
CL_b	[L/h/kg]	**6.7**	0.96
V_{dss}	[L/kg]	**2.8**	1.3
AUC $_{(0\rightarrow\infty)}$	[µg*h/L]	**163**	25

CL: Serum Clearance
Cl_b: Blood Clearance
V_{dss}: Distribution volume at steady state
AUC: Area under the c-t curve, for the measured time period given in brackets
MRT: Mean residence time

The data showed that [^{19}F]AV1/ZK could be rapidly distributed based on the distribution $t_{1/2}$ of 0.15 h, volume of distribution at steady state of approximately 2.8 L/kg and free distribution into tissue of >0.7 L/kg. A serum clearance of 3.1 L/h/kg and blood clearance of 6.7 L/h/kg was also reported indicating a relatively rapid elimination of [^{19}F]AV1/ZK from the rat blood.

Study Title: Blood kinetics of ZK 6013443 after single intravenous administration in rats.

Key study findings: The blood kinetics following a single intravenous injection of ZK 6013443 (using (b) (4) as precursor) to female Wistar rats was characterized in this study. The data suggests an initial fast clearance of radioactivity from the blood followed by a slight increase in radioactivity in the blood, which remained constant 5 min post injection over the 3 hours observation period. The radioactive metabolite generated following an intravenous administration of ZK 6013443 remained in the blood even after 3 hours observation period employed in this study.

Study No.	KM06032
Study Report Location:	4.2.2.2. Pages 1-13.
Conducting laboratory Location:	Bayer Schering Pharma AG, Nonclinical Drug Safety, 13342 Berlin, Germany
Date of study initiation:	February, 2006
GLP Compliance:	No

QA Statement: No

Drug, lot #, and % purity: ZK 6013443 ([redacted] (b) (4) precusor), lot # - Not provided and purity- 96%.

Study Design:

Animal treatment- The female Wistar rats (n=4) employed for this study were cannulated to insert a catheter for blood sample collection under anesthesia. The rats were clinically examined throughout the study. A bolus dose of 2.8-5.0 MBq/300 µL per rat of ZK 6013443 was intravenously injected via the tail vein and a volume of 400 µL blood was removed from each rat via catheter at 1, 3, 5, 15, 30, 60, 120, 180 min after injection. The blood samples were measured using Gamma-counter Automatic 1480 [redacted] (b) (4) using an energy window of 20 – 1800 keV and a measurement period of 30 seconds.

Results:
The data on the blood concentration kinetics following a single bolus intravenous injection of ZK 6013443 to the female rats is shown below:

Table 15: Blood concentration of ZK6013443 after single i.v. administration in rats

	%ID			
Time	1 Rat 1	2 Rat 2	3 Rat 4	4 Rat 5
0	0.01	0.00	0.00	0.01
1	3.01	6.45	7.77	13.36
3	2.89	3.45	3.91	5.58
5	2.25	2.86	3.46	4.31
15	2.78	3.80	3.60	5.08
30	2.96	4.51	4.05	5.67
60	3.75	4.53	4.90	6.01
120	4.80	5.04	4.84	6.53
180	4.92	4.53		5.56

The data demonstrates an initial rapid increase in the blood concentration in the rats within a minute after intravenously injecting the test compound. The blood level reduced between 1 to 5 minutes and then after 5 min post injection, the blood concentration slightly increased and remained constant over the investigated time period of 3 hours. This data is also shown in Figure 44 below:

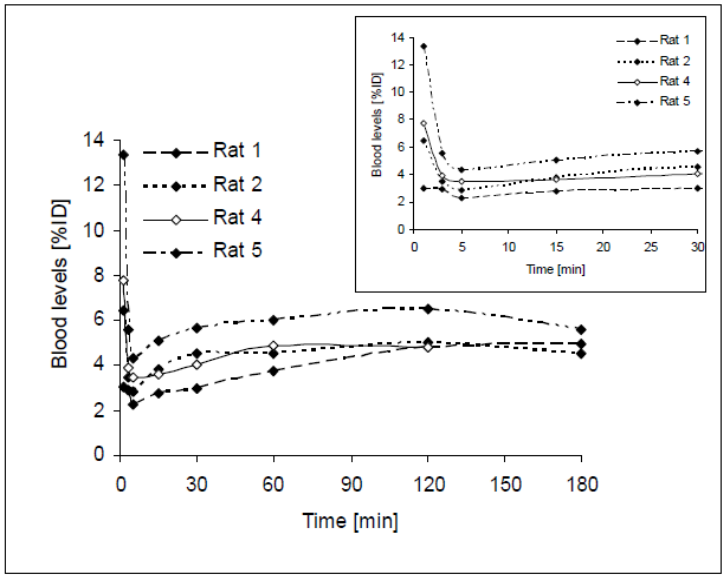

Figure 44: Blood concentration profile of ZK6013443 (in % ID) after single i.v. administration in rats (n=4. individual animals are shown); Square: Blood concentration profile of ZK6013443 (in % ID) of the first 20 min post i.v. administration in rat

The study suggests that ZK 6013443 is rapidly cleared from the body and it seems the radioactive metabolite formed following an intravenous injection of the test compound was not cleared from the blood stream but rather remained at constant level in the blood up to 3 hours post treatment.

Reviewer's Comment: Agrees with the result of this study. However, the 3 hour observation period seems too short for this study to provide additional and more conclusive information on the kinetics of ZK 6013443 following an intravenous injection to the rats. The sponsor should have further extended the observation period by another 3-6 hours to provide a better profile on the blood concentration of ZK 6013443.

Study Title: Total blood radioactivity time profile after single intravenous administration of ZK6013443 in rats.

Key study findings: This study evaluated the total blood radioactivity time profile following a single intravenous injection of ZK 6013443 (using (b) (4) as precursor) to male Wistar rats. The results obtained from the study demonstrated an initial rapid distribution of radioactivity followed by a slight but constant increase in distribution 5 min post injection over the 3 hours observation period. The study showed that the radioactive metabolite generated following an intravenous administration of ZK 6013443 remained in the blood even an hour after injection. A distribution $t_{1/2}$ of 2.7±1.0 min was obtained from this study.

Study No. KM06224

Study Report Location:	4.2.2.2. Pages 1-12.
Conducting laboratory Location:	Bayer Schering Pharma AG, Nonclinical Drug Safety, 13342 Berlin, Germany
Date of study initiation:	June 20, 2006
GLP Compliance:	No
QA Statement:	No
Drug, lot #, and % purity:	ZK 6013443 ([redacted] (b) (4) precursor), lot # - Not provided and purity- 96%.

Study Design:

Animal treatment- Male Wistar rats (n=3) employed for this study were cannulated to insert a catheter for blood sample collection under anesthesia. The rats were clinically examined throughout the study. A bolus dose of 3.3-5.9 MBq/300 µL per rat of ZK 6013443 was intravenously injected via the tail vein and a volume of 200 µL blood was removed from each rat via catheter at 1, 2, 3, 4, 5, 15, 30, 60 min post injection. The blood samples were measured using Gamma-counter Automatic 1480 [redacted] (b) (4) using an energy window of 20 – 1800 keV and a measurement period of 30 seconds.

Results:
The data on the total blood radioactivity obtained from the rats following a single bolus intravenous injection of ZK 6013443 is shown below:

Table 16: Total blood radioactivity time profile after single i.v. administration of ZK 6013443 in rats

Time	%ID		
	Rat 1	Rat 2	Rat 3
0	0.029	0.028	0.029
1	4.941	17.487	16.582
2	3.367	10.972	11.488
3	2.889	7.927	9.861
4	3.150	7.235	8.687
5	3.062	7.472	7.628
15	3.258	5.955	7.304
30	4.109	7.816	8.933
60	3.551	8.522	10.478

The data demonstrate an initial fast distribution of radioactivity in the rats within a minute after intravenously injecting the test compound. This is followed by a reduction in radioactivity distribution between 1 to 15 minutes and then 15 min post injection; there was a constant rise in the distribution of radioactivity over the investigated time period of 1 hour. This data is also shown in the Figure 45.

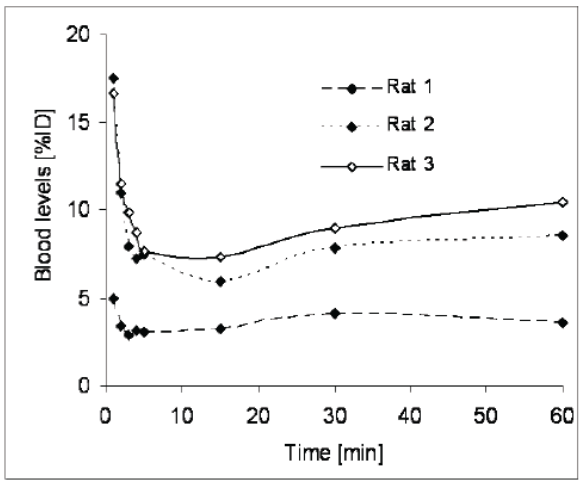

Figure 45: Total blood radioactivity time profile (in % ID) after single i.v. administration of ZK 6013443 in rats (n=3; individual animals are shown)

The study suggests that ZK 6013443 is rapidly distributed and a distribution $t_{1/2}$ was obtained from the study. The data also showed that the radioactive metabolite formed following an intravenous injection of the test compound was not cleared from the blood stream but rather remained at constant level in the blood up to 1 hours post treatment.

Reviewer's Comment: The result corroborates the study reviewed above on the kinetics of ZK 6013443 indicating rapid clearance from the blood. The present study equally lacked adequate period of observation that could have provided additional information on the distribution of ZK 6013443 following an intravenous injection to the rats. of ZK 6013443 in this study. It is noted that ZK 6013443 is rapidly distributed within a minute after injection.

5.2 Toxicokinetics

(If not included in toxicity studies)

Study title: **ZK 6057184 (ref. BAY 94-9172) Systemic toxicity study in rats after single intravenous injection of different formulations including toxicokinetics**

Key study findings: Toxicokinetics data after daily intravenous injection of ZK 6057184 (45, 175 and 700 µg/kg –volume 5mL/kg) of the preclinical test formulation ((b) (4) in Water for injection) to rats was obtained from three groups of 6 rats/sex/group while the control group was administered equivalent volume of the vehicle. The impact of the formulation on toxicokinetics was assessed by a single injection of 2.5 µg/kg ZK 6057184 (volume 0.5 mL/kg) of the preclinical formulation to a group of rats while 2.5 µg/kg ZK 6057184 (volume 0.5 mL/kg) of the clinical formulation (containing (b) (4) was also injected to three groups of rats. Evaluation of clinical profile and toxicokinetics of the animals showed that no mortality or clinical changes were reported in the animals and no sex-related differences in exposure were reported. A dose-dependent exposure with a C_{max} of 19.9 to 399 µg/L and $AUC_{(0-6)}$ of 7.45 to 159 µg/h/L with the (b) (4) based preclinical formulation was reported following a single intravenous injection of ZK 6057184 (45, 175 and 700 µg/kg. Data from the clinical formulation in comparison to the same 2.5 µg/kg dose of preclinical formulation showed that the exposure with the preclinical formulation was higher than with the clinical formulation (C_{max} of 0.559 µg/L compared to C_{max} of 0.943 µg/L). This indicates that the preclinical formulation is well suitable for toxicity studies and assessment of potential adverse effects resulting from injection of the PET tracer Florbetaben.

Study No.	TOXT5081051
Study Report Location:	4.2.2.2. Pages 1-184.
Conducting laboratory Location:	Bayer Schering Pharma AG, Nonclinical Drug Safety, 13342 Berlin, Germany

Date of study initiation:	October 28, 2009
GLP Compliance:	Yes
QA Statement:	Yes
Drug, lot #, and % purity:	ZK 6057184, lot # -Not provided and purity is stated to be 97.1%

Study Design: The treatment schedule employed for the study is shown in Table 17 as provided by the sponsor.

Table 17: Treatment Schedule employed for the study

Group	Number of animals/sex	Compounds	Dose [µg/kg]	Concentration [µg/mL]	Appl. volume [mL/kg]	Treatment [Date]
1	6M + 6F	Vehicle (Test Formulation)	0	0	5	28 Oct 09
2[a]	6M + 6F	ZK 6057184 (Reference Formulation)	2.5[a]	5[a]	0.5	28 Oct 09
7[a]	6M + 6F	ZK 6057184 (Reference Formulation)	2.5[a]	5[a]	0.5	09 Dec 09
8	6M + 6F	ZK 6057184 (Reference Formulation)	2.5	5	0.5	11 May 10
3	6M + 6F	ZK 6057184 (Test Formulation)	2.5	5	0.5	28 Oct 09
4	6M + 6F	ZK 6057184 (Test Formulation)	45	9	5	28 Oct 09
5	6M + 6F	ZK 6057184 (Test Formulation)	175	35	5	28 Oct 09
6	6M + 6F	ZK 6057184 (Test Formulation)	700	140	5	28 Oct 09

M = male F = female
a: The content of the reference formulations used for treatment of groups 2 and 7 were below the acceptable limit, so that a further group of animals (group 8) was treated with the reference formulation with a correct content of ZK 6057184 at formulation analysis.

The animals were monitored for mortality, clinical observations, body weight and body weight gain. Blood samples were collected from the rats at 5 and 15 min (or 0.0833 and 0.25 h), 1.5, 3, 6 and 24 h post injection of ZK 6057184 (b) (4) and the plasma concentrations of the (b) (4) ZK 6016468 (BAY 94-9172) were determined by a validated LC-MS/MS method in rats. The pharmacokinetic parameters were calculated from the geometric plasma concentrations by non-compartmental analysis using the KINCALC program. The animals were then sacrificed without necropsy.

Doses:	45, 175 and 700 µg/kg (105X, 407X and 1627X MHD)
Frequency of dosing:	Consecutive dosing (10 minutes each) in ascending order dose with 30 minutes interval.
Route of administration:	Intravenous Injection
Dose volumes:	0.5 or 5 mL/kg
Formulation/Vehicle:	Preclinical formulation- (b) (4) [redacted] Clinical formulation- (b) (4) [redacted]
Species/Strain:	Rat/Wistar
Number/Sex/Group:	6/sex/group
Age:	8 weeks (males and female)
Weight:	243-316 g (males) 171-201 g (female)
Satellite groups:	None
Deviation from study protocol: None that significantly affect study outcome	1)

Results:

Toxicokinetics: No sex-related differences in the plasma concentrations were reported in the animals.

The toxicokinetics profile of the preclinical formulation demonstrated C_{max} which slightly increased over the employed dose range while $AUC_{(0-6)}$ increased nearly dose-proportionally from 0.045 mg/kg to 0.7 mg/kg as shown in sponsor's Table 18 and Table 19. However, the plasma concentration decreased rapidly after the injection, to less than 2 % of the C_{max} at 3 h in the 0.7 mg/kg treated group and was below the LLOQ of 0.05 µg/L at 24 h.

Table 18: Mean plasma concentrations [µg/L] of ZK 6016468 after intravenous bolus administration of ZK 6057184 using the test formulation in toxicity studies

Reference ID: 3361527

Dose	0.0025 mg/kg		0.045 mg/kg		0.175 mg/kg		0.7 mg/kg	
Group	3		4		5		6	
Time [h]	Mean geom.	S.D. geom.	Mean geom.	S.D. geom.	Mean geom.	S.D. geom.	Mean geom.	S.D. geom.
0.0833	0.943	1.24	19.9	1.08	83.1	1.05	399	1.05
0.25	0.330	1.18	6.80	1.16	28.7	1.06	145	1.10
1.5	<0.0500	n.c.	0.385	1.12	2.01	1.19	8.98	1.19
3	n.c.	n.c.	0.139	1.14	0.603	1.24	3.29	1.28
6	n.c.	n.c.	<0.0500	n.c.	0.131*	1.15	0.627	1.36
24	<0.0500	n.c.	<0.0500	n.c.	<0.0500	n.c.	<0.0500	n.c.

*: n = 5 n.c.: not calculated

Table 19: Pharmacokinetic parameters of ZK 6016468 after intravenous bolus administration of ZK 6057184 using the test formulation in toxicity studies

Dose	[mg/kg]	0.0025	0.045	0.175	0.7
Group		3	4	5	6
AUC(0-6)	[µg·h/L]	n.c.	7.45#	32.9	159
$AUC(0\text{-}6)_{norm}$	[kg·h/L]	n.c.	0.183#	0.207	0.251
C_{max}	[µg/L]	0.943	19.9	83.1	399
$C_{max,norm}$	[kg/L]	0.416	0.487	0.523	0.628
t_{max}	[h]	0.0833	0.0833	0.0833	0.0833

#: AUC was extrapolated to 6 h n.c.: not calculated
Equivalent doses were used for the calculation of dose-normalized parameters of ZK 6016468 using a factor of 0.907

It was observed that the exposure after administration of 0.0025 mg/kg in form of the three PEG based clinical formulations was similar. The concentration at 5 min after administration of dose group 8 seemed to be slightly higher compared to groups 2 and 7. However, the concentration at 0.25 h was similar for the respective values of the other two dose-groups as shown Table 20 and Table 21.

Table 20: Mean plasma concentrations (µ/L) of ZK 6016468 after intravenous bolus administration of ZK 6057184 using the clinical reference formulation

Dose [mg/kg]	0.0025 mg/kg		0.0025 mg/kg		0.0025 mg/kg	
Group	2		7		8	
Time [h]	Mean geom.	S.D. geom.	Mean geom.	S.D. geom.	Mean geom.	S.D. geom.
0.0833	0.475	1.23	0.409	1.30	0.559	1.25
0.25	0.113	2.16	0.107	1.22	0.107	2.10
1.5	<0.0500	n.c.	<0.0500	n.c.	<0.0500	n.c.
3	<0.0500	n.c.	<0.0500	n.c.	<0.0500	n.c.
6	<0.0500	n.c.	n.c.*	n.c.	n.c.	n.c.
24	<0.0500	n.c.	<0.0500	n.c.	<0.0500	n.c.

* = n = 5

Table 21: Pharmacokinetic parameters of ZK 6016468 after intravenous bolus administration of ZK 6057184 using the clinical reference formulation

Dose	[mg/kg]	0.0025	0.0025	0.0025
Group		2	7	8
AUC(0-6)	[µg·h/L]	n.c.	n.c.	n.c.
$AUC(0\text{-}6)_{norm}$	[kg·h/L]	n.c.	n.c.	n.c.
C_{max}	[µg/L]	0.475	0.409	0.559
$C_{max,norm}$	[kg/L]	0.209	0.180	0.246
t_{max}	[h]	0.0833	0.0833	0.0833

Equivalent doses were used for the calculation of dose-normalized parameters of ZK 6016468 using a factor of 0.907

Exposure to preclinical and clinical formulations was compared and it was observed that the concentrations in the 3 groups treated with clinical formulation (groups 2, 7 and 8) did not reach the concentrations of the group treated with the same dose of ZK 6057184 in the (b) (4) based (preclinical) formulation (group 3) as shown in sponsor's Figure 46. It was found that the 5 and 15 min values of the respective dose were about 2- or 3-fold higher comparing with the clinical formulation. The sponsor suggests that the release of a compound from a (b) (4) formulation could be prolonged and subsequently results in a change of the volume of distribution. This probably leads to higher exposure with the (b) (4) formulation.

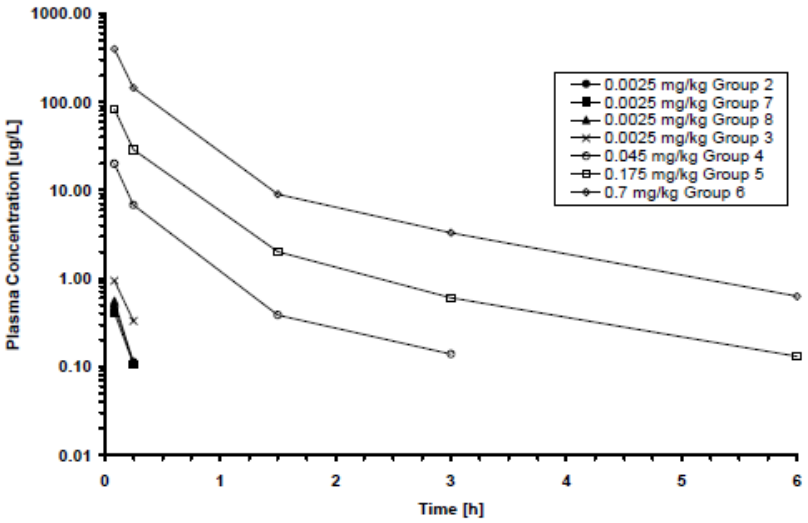

Figure 46: Plasma concentrations [µg/L] *vs.* time curve of ZK 6016468 after intravenous bolus administration of ZK 6057184 to male and female rats 0.01

Reviewer's Comment: This study was necessitated by an effort to allow higher concentrations and higher administration volume to achieve high multiples of the intended human dose. The sponsor used a different composition of the formulation for the repeated-dose toxicity study (preclinical formulation) than the composition of formulation used for the clinical drug product (clinical formulation). This reviewer agrees with the results of this study which attributed the prolonged exposure of the preclinical formulation to change in volume of distribution induced by (b) (4) in the preclinical formulation. The justification for the use of (b) (4) formulation for the preclinical studies is to enable high dose multiples be tested for toxicity and reveal overtly sensitivity to the product

Study title: **ZK 6057184 Toxicokinetic evaluation for repeated-dose toxicity study in male and female dogs with daily intravenous injection over a period of 4 weeks followed by a recovery period of 4 weeks.**

Key study findings: The toxicokinetics of ZK 6057184 (b) (4) following daily intravenous administration to dogs over a period of 4 weeks at doses of 0.0125, 0.05 and 0.2 mg/kg was investigated. No sex-related differences in exposure was observed in the treated animals and the repeated dosing of the animals did not cause any accumulation or induction in terms of $AUC_{(0-6)}$ or C_{max}. However, on Day 25, there was dose-related increase in C_{max} and $AUC_{(0-6)}$ from 2.52 µg/h/L at 0.0125 mg/kg to 44.2 µg/h/L at the highest employed dose of 0.2 mg/kg.

Study No.	TOXT0078654
Study Report Location:	4.2.2.2. Pages 1-87.

Conducting laboratory Location:	Bayer Schering Pharma AG, Nonclinical Drug Safety, 13342 Berlin, Germany
Date of study initiation:	March 13, 2008
GLP Compliance:	Yes
QA Statement:	Yes
Drug, lot #, and % purity:	ZK 6057184, lot # -Not provided and purity is stated to be 99.2%

Study Design: Please see table 27 for study design.

Table 22: Treatment Schedule employed for the study as provided by the sponsor

Group	No. of animals per group	Individual animal nos.	Compound	Concentration ZK 6057184 in µg/mL	Dose/day ZK 6057184 [µg/kg]	Administration volume [mL/kg]
1 (control)	3M / 3F + 2M* / 2F*	M: 201 – 205 F: 206 – 209, 230	vehicle	0	0	1.0
2 (low)	3M / 3F	M: 211 – 213 F: 214, 215, 231	ZK 6057184	12.5	12.5	1.0
3 (mid)	3M / 3F	M: 217– 219 F: 220 – 222	ZK 6057184	50	50	1.0
4 (high)	3M / 3F + 2M* / 2F*	M: 223 – 227 F: 210, 216, 228, 229, 232	ZK 6057184	200	200	1.0

M: male animals
F: female animals
*: recovery animals

Doses:	12.5, 50 and 200 µg/kg (29X, 116.3X and 465X MHD)
Frequency of dosing:	Once daily
Route of administration:	Intravenous Injection
Dose volumes:	1 mL/kg
Species/Strain:	Dog/Beagle
Number/Sex/Group:	Groups 1 and 4: 5/sex/group
	Groups 2 and 3: 3/sex/group
Age:	11-13 months (males and female)
Weight:	6-9.8 kg (males);
	7.2-8.9 kg (female)
Satellite groups:	Two recovery groups of 2 female and 2 males per group (ZK 6057184-treated and vehicle-treated control groups).
Deviation from study protocol:	No major deviation reported

Reference ID: 3361527

Blood samples were collected from all animals including recovery animals on Day 1/2 and on Day 25/26 at 2 and 15 minutes, 1.5, 3, 6 and 24 hours after injection. The plasma samples were stored at ≤-70°C and the plasma concentrations of ZK 6016468 were determined by LC-MS/MS. The treatment schedule employed for the study is shown in sponsor's Table 22.

Results:

Toxicokinetics: No sex-related differences in the plasma concentrations were reported in the animals.

Pharmacokinetic parameters: Data on mean plasma concentrations and mean pharmacokinetic parameters evaluated during the study is shown in Table 28. No plasma concentrations (above LLOQ) of the test compound were found in the samples from the control group while varying plasma concentrations of the compound were reported in the treated groups (Table 23).

Table 23: Mean plasma concentrations [µg/L] and pharmacokinetic parameters of ZK 6016468 on Day 1 and Day 25. Geometric means and S.D., n = 6 to n = 10

Reference ID: 3361527

		Day 1					
Dose	[mg/kg]	0.0125		0.05		0.2	
Time [h]		Mean geom.	S.D. geom.	Mean geom.	S.D. geom.	Mean geom.	S.D. geom.
0.0333		9.73	1.22	32.3	1.18	148	1.18
0.25		1.89	1.21	6.69	1.10	34.9	1.13
1.5		0.159	1.10	0.677	1.16	3.43	1.24
3		0.0703	1.20	0.270	1.40	1.34	1.21
6		<0.0500	n.c.	0.105	1.19	0.424	1.42
24		<0.0500	n.c.	<0.0500	n.c.	0.0801	2.05
$AUC(0\text{-}t_n)$	[µg·h/L]	2.45	1.13	9.27	1.05	49.1	1.13
$AUC(0\text{-}t_n)_{norm}$	[kg·h/L]	0.217	1.13	0.204	1.05	0.271	1.13
AUC(0-6)	[µg·h/L]	2.56#	1.12	9.27	1.05	45.4	1.11
$AUC(0\text{-}6)_{norm}$	[kg·h/L]	0.227#	1.12	0.204	1.05	0.251	1.11
C_{max}	[µg/L]	9.73	1.22	32.3	1.18	148	1.18
$C_{max,norm}$	[kg/L]	0.861	1.22	0.711	1.18	0.819	1.18
$C(24)/C_{max}$	[%]	n.c.	n.c.	n.c.	n.c.	0.0726	1.37
t_{max}	[h]	0.0333	1.00	0.0333	1.00	0.0333	1.00
		Day 25					
Dose	[mg/kg]	0.0125		0.05		0.2	
Time [h]		Mean geom.	S.D. geom.	Mean geom.	S.D. geom.	Mean geom.	S.D. geom.
0.0333		7.68	1.21	27.8	1.31	121	1.24
0.25		1.87	1.10	8.34	1.17	34.4	1.19
1.5		0.135	2.30	0.948	1.14	3.82	1.12
3		0.0820	1.09	0.388	1.21	1.70	1.14
6		n.c.	n.c.	0.126	1.13	0.710	1.40
24		<0.0500	n.c.	<0.0500	n.c.	0.0978	2.33
$AUC(0\text{-}t_n)$	[µg·h/L]	2.45	1.13	10.5	1.16	49.7	1.17
$AUC(0\text{-}t_n)_{norm}$	[kg·h/L]	0.216	1.13	0.231	1.16	0.275	1.17
AUC(0-6)	[µg·h/L]	2.52#	1.11	10.5	1.16	44.2	1.15
$AUC(0\text{-}6)_{norm}$	[kg·h/L]	0.223#	1.11	0.231	1.16	0.244	1.15
C_{max}	[µg/L]	7.68	1.21	27.8	1.31	121	1.24
$C_{max,norm}$	[kg/L]	0.680	1.21	0.613	1.31	0.667	1.24
$C(24)/C_{max}$	[%]	n.c.	n.c.	n.c.	n.c.	0.115	1.51
t_{max}	[h]	0.0333	1.00	0.0333	1.00	0.0333	1.00
$R_A C_{max}$	[%]	79.4	1.32	86.2	1.35	81.3	1.17
$R_A AUC(0\text{-}6)$	[%]	98.4	1.15	113	1.16	97.4	1.13

T0078654_ZK6016468.xls \ summary \ Nie \ 25 Aug 2009
= AUC was extrapolated to 6 h
Equivalent doses were used for the calculation of dose-normalized parameters of ZK 6016468 using a factor of 0.907.

C_{max} values obtained on Day 1 and Day 25 increased in a dose-dependent manner throughout the employed dose range during the study. Similarly, exposure of ZK 6016468 in terms of $AUC_{(0\text{-}6)}$ also increased dose-dependently as shown in sponsor's Figure 47 and Figure 48. it was reported that repeated administration of the test article did not cause any accumulation or induction in terms of $AUC_{(0\text{-}6)}$ or C_{max} during this study.

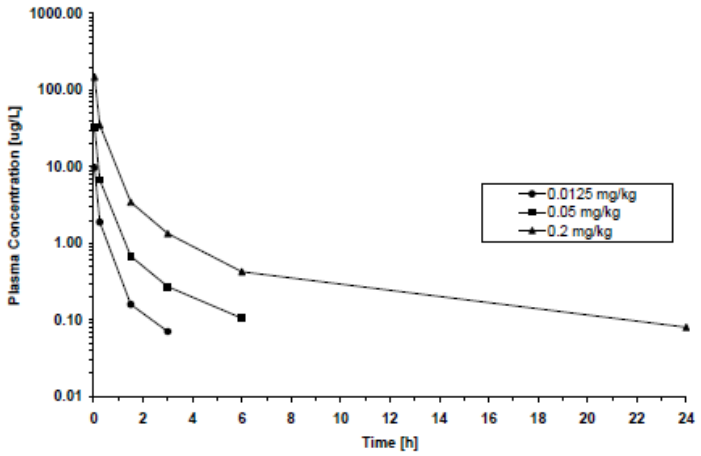

Figure 47: Plasma concentrations [µg/L] *vs.* time curve of ZK 6016468 after intravenous bolus administration of ZK 6057184 to male and female Beagle dogs [BAY 94-9172/T0078654] on Day 1. (Geometric means of n = 6 to n = 10.)

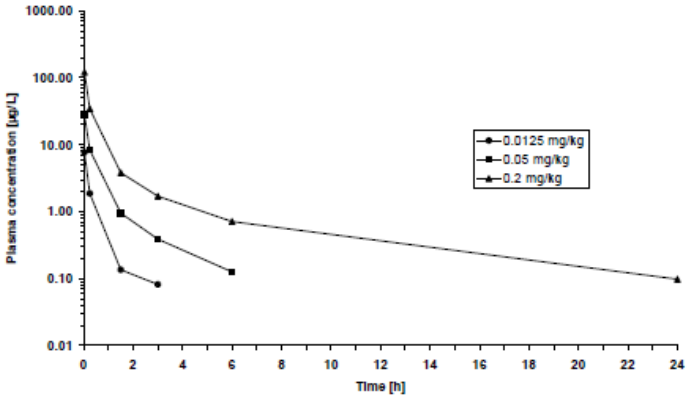

Figure 48: Plasma concentrations [µg/L] *vs.* time curve of ZK 6016468 after intravenous bolus administration of ZK 6057184 to male and female Beagle dogs [BAY 94-9172/T0078654] on Day 25. (Geometric means of n = 6 to n = 10.)

Reviewer's Comment: The data is similar to that obtained from the toxicokinetics study in rats reviewed above. However, the added value of this dog study is that the data is more relevant to the human situation and the exposure levels are measured as [redacted] (b) (4) ZK 6016468 rather than the [redacted] (b) (4) (ZK 6057184). The data on $AUC_{(0-6)}$ and C_{max} after repeat dosing suggests that no accumulation or induction in terms of $AUC_{(0-6)}$ or C_{max} is envisaged in overtly sensitive human subjects. This supports the safety of this compound in the clinics. This reviewer agrees with the results of this study.

Study title: **Biodistribution of ZK 6013443 after single intravenous administration in mice**

Key study findings: The biodistribution and excretion of ZK 6013443 (F-18 labeled) with emphasis on brain uptake and brain clearance was investigated following an intravenous injection of 112.6kBq or 102.2kBq of ZK 6013443 to male NMRI mice via tail vein. Urine and feces samples collected at different time points from the mice. The radioactivity of urine, feces as well as organs and tissues isolated from the animals were measured using the gamma counter and the data on %ID/g tissue and %ID/organ demonstrates high initial brain uptake of radioactivity (4.77 ± 0.15%ID/g at 2 min) and a fast initial wash out of radioactivity from the brain (1.59 ± 0.13%ID/g at 30 min). Slow clearance was also observed in the brain demonstrated by the presence of radioactivity in the brain at 4 hour post injection. However, the blood concentration remained virtually unchanged throughout the study. No accumulation was reported in any organ and tissue including the bones indicating that no radiation toxicity or defluorination is envisaged with this tracer. The data also demonstrate that ZK 6013443 was mostly excreted in the kidney and the feces and a total recovery of 98.46% was reported at 4 hour post injection.

Study No.	KM05279
Study Report Location:	4.2.2.2. Pages 1-20.
Conducting laboratory Location:	Bayer Schering Pharma AG, TRG DG, Molecular Imaging Research, 13342 Berlin, Germany
Date of study initiation:	October 2005
GLP Compliance:	No
QA Statement:	No
Drug, lot #, and % purity:	ZK 6057184, lot # and purity-Not provided

Study Design:

Reference ID: 3361527

Doses:	112.6kBq or 102.2kBq
Frequency of dosing:	Single bolus injection
Route of administration:	Intravenous Injection
Dose volumes:	100 µL
Formulation:	ZK 6023443
Species/Strain:	Mice/NMRI
Number/Sex/Group:	3 males/time point
Age:	11-13 months
Weight:	23.4-35.2 g (males);
Satellite groups:	None
Deviation from study protocol:	No major deviation reported

The NMRI mice were (n=3 per time point) intravenously injected 112.6kBq (in 100µL; all time points except 2 min) or 102.2kBq (in 100µL; 2min time point) of ZK 6013443 per animal via the tail vein at 2, 5, 15, 30, 60, 120, 240 min (time points). The urine and feces were collected from the mice at the indicated time points after which the animals were sacrificed under anesthesia and spleen, liver, kidney, lung, femur, heart, brain, fat, thyroid, muscle, skin, blood, tail, stomach

(without content), testicle, intestine (with content), pancreas, adrenals, and the remaining body (designated as carcass) were removed and measured for radioactivity using the gamma counter. The results of the biodistribution and excretion given as mean value ± standard deviation were reported as % of injected dose per gram of tissue (%ID/g) and % of injected dose per organ (%ID), respectively.

Results:

The data on the distribution and excretion after a single intravenous injection of ZK 6013443 to male NMRI mice is shown in Table 24. The data showed that ZK 6013443 demonstrated rapidinitial brain uptake (4.77 ± 0.15%ID/g at 2 min) and fast clearance from the brain (1.59 ± 0.13%ID/g at 30 min) in the mice. However, at 4h post injection, less than 1% of the injected radioactivity was still detected in the brain, suggesting a reduced clearance of the radioactivity at later time points. The blood concentration of radioactivity remained nearly constant over the investigated time period (between 1.86%ID/g and 1.28%ID/g). The biodistribution data showed that at 2 min time point, the skin had the lowest level of distribution (0.72%ID/g) while the lungs had the highest level (13.35%ID/g); however, at 4 hour time point the level in the lung was reduced to 1.26%ID/g. No accumulation of ZK 6013443 was found in any organ or tissue evaluated during this study. It was also reported that within 4 hour post administration about 30% of the injected dose was excreted mainly via the kidney (25.45%ID) and 5.48%ID was excreted via the feces (total recovery at 4h post infection. was 98.46%ID).

Table 24: Biodistribution and excretion of ZK 6013443 after single i.v. administration in male NMRI mice (values are given in mean ± S.D.; n=3)

[F-18] AV1	2 min		5 min		15 min		30 min		60 min		2 h		4 h	
	% ID/g	SD	% ID/g	SD	% ID/g	SD	% ID/g	SD	% ID/g	SD	% ID/g	SD	% ID/g	SD
Spleen	1.43	0.03	1.14	0.13	0.90	0.08	1.20	0.15	1.30	0.26	0.97	0.16	0.91	0.20
Liver	9.15	2.17	13.82	0.95	12.14	0.72	13.46	1.87	14.12	1.14	9.46	0.66	6.84	1.34
Kidney	6.01	0.22	3.99	0.37	3.66	0.44	4.84	0.74	4.46	0.68	3.76	0.31	2.23	0.22
Lung	13.35	5.18	2.73	0.15	1.90	0.02	2.11	0.33	2.06	0.17	1.60	0.29	1.26	0.23
Femur	1.56	0.38	1.01	0.41	0.85	0.10	1.11	0.35	1.60	0.31	2.29	0.31	4.64	0.58
Heart	3.28	0.20	1.90	0.21	1.62	0.08	1.59	0.21	1.87	0.26	1.38	0.23	1.13	0.22
Brain	4.77	0.15	2.57	0.13	1.68	0.13	1.59	0.13	1.49	0.15	1.08	0.19	0.95	0.13
Fat	1.02	0.54	1.95	0.78	2.25	0.31	6.26	0.23	4.65	0.19	1.88	0.66	1.21	0.15
Thyroid	2.71	0.74	1.59	0.40	1.48	0.33	1.23	0.98	1.55	0.11	1.12	0.10	1.55	0.14
Muscel	1.82	0.05	1.81	0.70	2.94	2.85	1.50	0.47	1.18	0.10	0.72	0.13	0.76	0.20
Skin	0.72	0.13	1.71	0.09	2.19	0.02	2.44	0.41	2.04	0.10	1.21	0.19	0.92	0.15
Blood	1.81	0.28	1.28	0.06	1.29	0.05	1.61	0.30	1.86	0.24	1.73	0.40	1.35	0.25
Tail	3.35	0.57	4.11	2.99	3.44	0.77	6.31	1.17	2.80	0.52	2.41	1.00	2.03	0.40
Stomach	2.85	0.69	2.71	0.54	2.55	0.41	5.13	0.56	3.60	1.91	3.14	0.21	2.42	1.09
Testicle	1.26	0.12	1.22	0.09	1.21	0.13	1.29	0.10	1.41	0.27	1.02	0.15	0.87	0.12
Intestine	1.78	0.22	3.83	0.55	5.71	0.81	10.22	0.56	16.40	3.00	14.40	2.79	13.52	2.08
Pancreas	2.90	0.17	2.33	0.15	1.44	0.14	2.94	0.39	2.67	0.18	0.82	0.17	1.05	0.26
Adrenales	3.80	0.77	4.72	2.67	4.20	0.78	4.69	0.31	2.91	0.12	1.47	0.41	2.11	0.36
[F-18] AV1	2 min		5 min		15 min		30 min		60 min		2 h		4 h	
	% ID	SD	% ID	SD	% ID	SD	% ID	SD	% ID	SD	% ID	SD	% ID	SD
Organs	44.91	5.77	48.56	0.86	56.44	2.81	64.41	1.60	74.07	1.45	57.06	2.31	48.88	3.75
Carcass	39.54	0.70	27.72	2.61	28.44	1.69	26.95	0.86	24.14	0.31	18.09	0.85	18.64	1.49
Urine	0.21	0.30	0.27	0.15	0.76	0.16	2.78	0.71	6.19	0.47	15.60	9.43	25.45	2.80
Faeces	0.00	0.00	0.03	0.03	0.01	0.01	0.10	0.08	0.49	0.37	3.45	1.10	5.48	4.34
Recovery	84.66	5.17	76.58	2.32	85.65	1.13	94.25	1.07	104.88	0.85	94.20	10.99	98.46	2.44

Reviewer's Comment: Agrees with the results obtained from this study indicating that ZK 6013443 is rapidly available in the brain within 2 minutes after injection for imaging to be done and does not accumulate in the brain and other tissues and organs in the body. Thus, no radiation toxicity is expected following administration of this compound at the proposed dose for the planned indication.

Study title: **^{18}F-FAβ NMRI Mouse model data. Dosimetry Report.**

The dosimetry data was originated from the ^{18}F- FAβ NMRI Mouse model data reviewed above following the analysis and extrapolation to human using metabolic and organ mass scaling conducted by (b) (4) The cumulative and residence time obtained from the NMRI mouse data sampled at 2, 5, 15, 30, 60, 120 and 240 mins time points was analyzed using OLINDA to extrapolate the dosimetry data on the tracer. As shown in the dosimetry data (Table 25), based on the extrapolated Mouse model data, an infusion of 200 MBq of ^{18}F- FAβ whole-body effective dose equivalent is 13.6 µSv/MBq to a 70 kg adult patient will give an effective dose of 2.72 mSv.

Table 25: Summary of Organ Dosimetry to an Average Adult Patient (70 kg) from an Intravenous Dose of 18F- FAβ extrapolated from Mouse. Mouse normal data sampled at time points 2, 5, 15, 30, 60, 120 and 240 mins

Organ	Effective Dose (μGy/MBq)	Effective Dose Equivalent (μSv/MBq)
Adrenals	0.0462	0.000
Brain	0.0269	0.000
Breasts	0.402	1.210
Gallbladder Wall	0.0000	0.000
LLI Wall	1.9700	0.986
Small Intestine	0.0676	0.811
Stomach Wall	1.1800	0.000
ULI Wall	0.0717	0.860
Heart Wall	0.0000	0.000
Kidneys	0.0279	0.000
Liver	0.3880	0.000
Lungs	0.8510	0.851
Muscle	0.0305	0.000
Ovaries	2.3000	2.870
Pancreas	0.0314	0.000
Red Marrow	3.3400	3.34
Osteogenic Cells	0.2450	0.735
Skin	0.0685	0.000
Spleen	0.0312	0.000
Testes	0.0000	0.000
Thymus	0.0458	0.000
Thyroid	0.3340	0.201
Urinary Bladder Wall	0.8510	1.020
Uterus	0.0592	0.711
Total Body	0.000	0.000
Total	**12.4**	**13.6**

Table 26: Cumulative estimates for Human provided by the sponsor based on the mouse data and metabolic and organ scaling

Organ	H_1(%ID)	H_2(%ID)	t_1(hr)	t_2(hr)	cumulative activity(hr)
spleen	0.0557	0.0969	1.2128	0.6228	0.0014733
liver	2.7853	0.0096	3.3040	16.5946	0.032046951
kidney	0.0780	0.0001	4.7362	24.9890	0.000718768
lung	0.5554	0.0107	90.8207	0.1446	0.014037314
femur/bone	12.9029	0.0065	43.8768	1.2531	0.018777988
heart	0.1514	0.0003	87.1471	0.1997	0.003818562
brain	0.6970	0.0014	48.0725	0.3073	0.017176688
fat	4.9989	0.0059	1.8940	16.4491	0.075196897
thyroid	0.0077	0.0000	Inf	4.8743	0.000200143
muscle	4.8680	0.0017	Inf	8.9095	0.126449669
skin	1.2745	0.0004	0.7867	10.8256	0.025409415
blood	1.4847	0.0005	9.2916	36.6093	0.008434334
tail	1.1340	0.0008	Inf	28.8616	0.029467937
stomach	0.1112	0.0001	2.4804	13.5559	0.001478975
testicle	0.0136	0.0000	84.2731	83.8596	0.000342228
intestine	2.7525	0.0007	3.5808	21.1018	0.030062339
pancreas	0.0143	0.0000	5.9441	14.7208	0.000112748
adrenals	0.0176	0.0000	7.2631	Inf	0.000337767
carcass*	**20.6700**	**6.7790**	**0.8677**	**10.0966**	**0.542356575**
urine*	**38.6000**	**1.9640**	**55.8983**	**55.9390**	**0.04676279**
faeces*	**0.0095**	**15.3200**	**79.3767**	**94.1791**	**0.010683239**
Total					0.985344629

Reviewer's Comment: The sponsor analyzed and extrapolated the ^{18}F-FAβ NMRI Mouse model data to human using metabolic and organ mass scaling. The effective dose to a 70 kg adult patient will be 0.0136 mSv/MBq and the red marrow sustains the largest effective dose of 3.33 µGy/MBq. Thus, the proposed infusion of 200 MBq of BAY 94-9172 to a 70 kg adult patient would give an effective dose of 2.72 mSv. The potential radiation risks associated with this compound would therefore be comparable to other PET tracers commonly used in nuclear medicine and within general accepted limits.

Study title: **Influence of formulation of BAY 949172 (ZK 6013443) added ZK 6057184 on biodistribution in mice after single intravenous administration**

Key study findings: This study investigated the influence of two different formulations of ZK 6013443 added ZK 6057184 on biodistribution in mice intravenously injected single dose of the formulations. The brain uptake and elimination of the formulations was also compared. The study demonstrated that no significant differences in the biodistribution of Bay 949172 added ZK 6057184 when it was formulated in two different formulations. The uptake and elimination of the radioactivity of the two formulations in the brain and the clearance of radioactivity from blood was also found comparable.

Study No. KM08013

Study Report Location: 4.2.2.2. Pages 1-17.

Conducting laboratory Location:	Bayer Schering Pharma AG, TRG DG, Molecular Imaging Research and New Fields, 13342 Berlin, Germany
Date of study initiation:	February 2008
GLP Compliance:	No
QA Statement:	No
Drug, lot #, and % purity:	ZK 6013443 and ZK 6057184, lot # and purity-Not provided

Study Design:

Doses:	119.6kBq or 158kBq of ZK 6013443 and 0.4 µg ZK 6057184
Frequency of dosing:	Single bolus injection
Route of administration:	Intravenous Injection
Dose volumes:	100 µL
Drug substance per formulation:	Formulation A: 0.119 MBq/ 100µL/ animal Formulation B: 0.158 MBq/ 100µL/ animal
Formulation/Vehicle:	Formulation A: [redacted] (b) (4) Formulation B: [redacted] (b) (4)
Species/Strain:	Mice/NMRI
Number/Sex/Group:	3 males/ time point
Age:	Not provided
Weight:	27.78-30.65 g (males);
Satellite groups:	None
Deviation from study protocol:	No major deviation reported

The NMRI mice (n=3 per time point) were intravenously injected 119kBq or 158MBq of ZK 6013443 and 0.4 µg ZK 6057184 (in 100µL; all time points except 2min) or 102.2kBq (in 100µL; 2 min time point) of per animal via the tail vein at 2, 30, 60, 240 min (time points). ZK 6013443 was co-injected with ZK 6057184 during this study. The compositions of the two formulations employed in the study are stated above. The urine and feces were collected from the mice at the indicated time points after which the animals were sacrificed under anesthesia and spleen, liver, kidney, lung, femur, heart, brain, fat, thyroid, muscle, skin, blood, tail, stomach (without content), testicle, intestine (with content), pancreas, adrenals, and the remaining body (designated as carcass) were removed and measured for radioactivity using the gamma counter. The results of the biodistribution and excretion given as mean value ± standard deviation were reported as % of injected dose per gram of tissue (%ID/g) and % of injected dose per organ (%ID), respectively.

Results: The data on the comparison of biodistribution and excretion of two different formulations of ZK 6013443 added ZK 6057184 in male NMI mice following a single intravenous injection is shown in Table 27, Table 28 and Figure 49. The data demonstrated no significant differences in the biodistribution of Bay 949172 added ZK 6057184 when it was formulated in two different formulations. The graph on the activity-time profile in brain and blood obtained from the treated animals indicates comparable uptake and elimination of the radioactivity in the brain and the clearance of radioactivity from blood in the two formulations.

Table 27: Biodistribution after i.v. injection of BAY 949172 + ZK 6057184 formulation A

	2 min		30 min		60 min		240 min	
Formulation A	% ID/g	SD	% ID/g	SD	% ID/g	SD	% ID/g	SD
Spleen	2,53	0,87	1,23	0,07	1,07	0,21	0,68	0,03
Liver	10,82	1,70	16,95	1,68	12,10	1,46	8,69	0,45
Kidney	8,96	0,85	5,31	0,92	4,81	0,59	3,43	0,61
Lung	24,04	3,92	3,18	0,96	1,68	0,43	1,16	0,07
Femur	1,79	0,30	0,72	0,05	1,20	0,20	3,21	1,29
Heart	7,05	0,62	1,46	0,12	1,54	0,14	1,12	0,04
Brain	4,48	0,19	1,53	0,49	1,17	0,15	0,72	0,11
Fat	0,89	0,18	4,60	1,06	2,57	0,67	1,01	0,16
Thyroid	3,38	0,22	1,22	0,47	1,21	0,08	1,01	0,13
Muscel	2,00	0,41	0,89	0,16	0,75	0,06	0,54	0,09
Skin	0,99	0,06	1,81	0,09	1,55	0,08	0,76	0,04
Blood	2,73	0,12	1,49	0,12	1,60	0,20	1,26	0,13
Tail	7,29	3,02	14,91	10,14	5,68	4,01	8,07	9,07
Stomach	3,99	0,46	6,54	1,01	2,68	0,58	1,80	0,60
Testicle	1,04	0,07	1,08	0,10	0,98	0,07	0,76	0,03
Intestine	1,24	0,88	10,46	1,52	11,32	2,35	12,07	1,06
Pancreas	9,04	12,01	1,02	0,09	1,03	0,03	0,56	0,07
Adrenales	11,62	3,42	5,98	4,40	2,83	0,80	1,34	0,51
	2 min		30 min		60 min		240 min	
Formulation A	% ID	SD	% ID	SD	% ID	SD	% ID	SD
Organs	49,14	3,96	75,95	10,04	67,50	6,54	55,96	3,48
Carcass	41,33	1,37	27,69	2,28	19,09	0,91	18,70	1,65
Urine	0,21	0,05	2,31	0,49	7,09	6,35	21,52	2,93
Faeces	0,00	0,00	0,05	0,03	0,37	0,40	1,34	0,79
Recovery	90,68	3,47	105,99	9,90	94,05	2,15	97,53	8,38

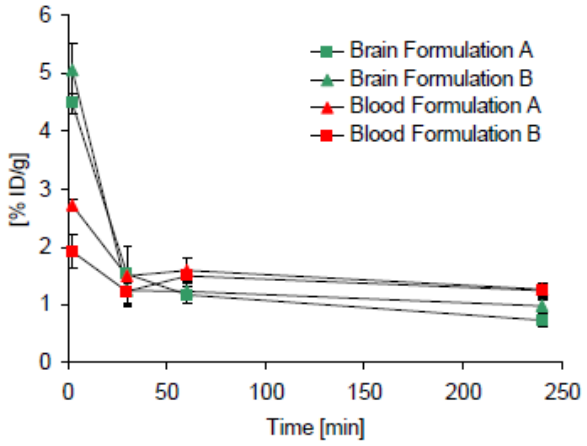

Figure 49: Activity-time profile in brain and blood obtained after i.v. administration of Bay 949172+ZK6057184 formulated in two different formulations (values are given in mean ± S.D.; n=3)

Formulation A: (b) (4) Formulation B: (b) (4)

Table 28: Biodistribution after i.v. injection of BAY 94-9172 and ZK 6057184 formulation B

Formulation B	2 min % ID/g	2 min SD	30 min % ID/g	30 min SD	60 min % ID/g	60 min SD	240 min % ID/g	240 min SD
Spleen	2,22	0,82	1,11	0,19	1,27	0,15	0,85	0,12
Liver	8,33	1,80	10,43	2,53	10,50	0,28	7,28	0,87
Kidney	6,49	0,22	4,19	0,95	4,87	0,61	3,44	0,56
Lung	12,52	4,19	1,82	0,37	1,67	0,10	1,22	0,22
Femur	1,25	0,11	0,79	0,11	1,30	0,34	3,78	0,06
Heart	5,17	0,44	1,43	0,18	1,49	0,11	1,21	0,14
Brain	5,05	0,46	1,25	0,25	1,23	0,15	0,98	0,14
Fat	0,63	0,08	1,57	0,62	3,43	0,77	1,50	0,38
Thyroid	3,65	0,04	1,52	0,20	1,35	0,31	1,22	0,17
Muscel	1,94	0,31	0,75	0,04	0,88	0,11	0,64	0,06
Skin	0,97	0,19	1,78	0,42	1,67	0,27	0,87	0,15
Blood	1,92	0,28	1,22	0,27	1,49	0,12	1,24	0,14
Tail	14,62	7,90	25,48	13,22	6,23	3,50	2,09	0,38
Stomach	4,29	0,83	2,12	0,53	3,42	1,02	1,92	0,48
Testicle	1,00	0,14	0,97	0,22	1,03	0,10	0,84	0,08
Intestine	1,69	0,21	6,49	1,49	10,88	1,61	13,76	1,20
Pancreas	3,51	0,69	1,29	0,30	1,18	0,15	0,82	0,21
Adrenales	8,85	1,82	4,55	1,20	4,35	1,87	1,49	0,35
Formulation B	**2 min % ID**	**2 min SD**	**30 min % ID**	**30 min SD**	**60 min % ID**	**60 min SD**	**240 min % ID**	**240 min SD**
Organs	49,45	0,92	65,97	2,93	64,57	2,46	53,58	2,65
Carcass	39,44	4,16	21,74	2,14	20,57	1,71	18,40	1,17
Urine	0,47	0,65	2,33	1,05	5,25	0,60	19,20	3,61
Faeces	0,00	0,00	0,06	0,03	0,23	0,18	1,61	0,56
Recovery	89,37	4,41	90,09	1,95	90,63	0,62	92,79	2,11

Reviewer's Comment: Agrees with the results obtained from this study which indicates no significant difference in the biodistribution profile in mice of the nonclinical and to be marketed clinical formulations.

Study title: **Metabolic stability of ZK6013443 after incubation with human and mouse liver microsomes**

Key study findings: The metabolic stability of ZK 6013443 after incubation with human and mouse liver microsomes was investigated. Liver microsomes were incubated with of ZK 6013443 (2.92MBq/mL) for 0, 30, and 60 while the control was incubated without microsomes or without cofactor for 60 min. The analysis of the samples by HPLC (gamma-detector) showed that ZK 6013443 was moderately stable in human and mouse liver microsomes. Similar pattern and amount of metabolites was detected with liver mouse and human liver The study also revealed demethylated ZK 6013443, as a probable metabolite of ZK 6013443.

Study No. KM07202

Study Report Location: 4.2.2.2. Pages 1-15.

Conducting laboratory Location: Bayer Schering Pharma AG,

	TRG DG, Molecular Imaging Research,
	13342 Berlin, Germany
Date of study initiation:	January 2007
GLP Compliance:	No
QA Statement:	No
Drug, lot #, and % purity:	ZK 6013443, lot # and purity-Not provided

Study Design:
Liver microsomes and a stock solution of cofactors (Glucose-6-Phosphate, $MgCl_2$, NADP, G-6-P-Dehydrogenase) obtained from the Research Pharmacokinetic department as well as Human liver microsomes [redacted] (b) (4) Mouse liver microsomes [redacted] (b) (4) were employed for this study. The liver microsomes (2µM CYP450) and cofactors were incubated with 2.92 MBq/mL of ZK 6013443 at 37°C for 0, 30, and 60 min (final assay volume 250 µl). The control (2.92 MBq/mL of ZK 6013443) was incubated without microsomes or without cofactor at 37°C for 60 min. Following the incubation period, methanol (1:1) was then added to the samples and they were kept at -80°C for 30min prior centrifugation at 3000 rpm/RT for 15 min. The supernatant was analyzed by HPLC [redacted] (b) (4) The relative amount of ZK 6013443 and of the metabolites (given in %) was calculated from the peak area measured by HPLC. (gamma-detector) and the overall radioactivity measured by HPLC (sum of all peak areas) was used as 100%-value.

Results:
The data from the metabolic detection after incubation of ZK 6013443 with human and mouse liver microsomes indicates that ZK 6013443 was moderately stable in human and mouse liver microsomes. The pattern and amount of metabolites detected on the HPLC (gamma-detector) was also found to be similar in the mouse and human. Up to five radioactive peaks with the retention times of 2.0 min (P1), 10.7 min (P2), 11.7 min (P3), 13.8 min (P5), and 14.6 min (P5) were detected after incubation of ZK 6013443 with mouse and human liver microsomes (Figure 50).

Reference ID: 3361527

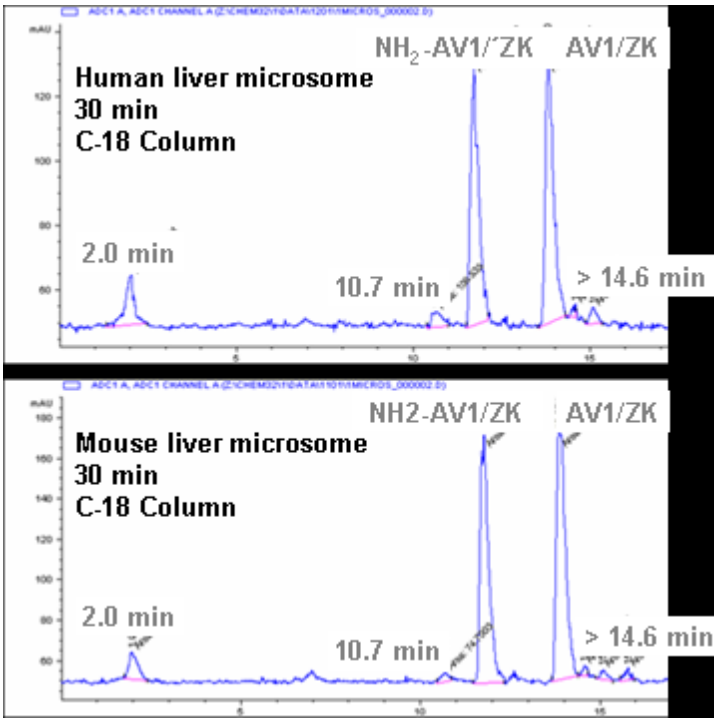

Figure 50: Analytical HPLC-chromatogram (gamma-detector): Liver microsomes and cofactors were incubated with ZK6013443 for 30 min at 37°C and afterwards ZK6013443 and metabolites were extracted and analyzed by HPLC.

The retention time on the HPLC column suggests that P4 is ZK 6013443 and P3 is the demethylated ZK 6013443, predicted as a probable metabolite of ZK 6013443 by the METEOR software.

Reviewer's Comments: Agrees with the result of this study which suggests that demethylated ZK 6013443 could be a metabolite of ZK 6013443 .....

Study title: **Stability of ZK6013443 after incubation in human plasma and detection of metabolites of ZK6013443 in plasma and urine after single intravenous administration in mice**

Key study findings: The stability of ZK 6013443 in human plasma was investigated *in vitro* by incubating human plasma with ZK 6013443 (60 MBq/ mL) for various time intervals (0-120 min) and the control was incubated in PBS (Phosphate-Buffered saline) for 120 min. The samples were extracted with acetonitrile and analyzed with HPLC (gamma-detector). The metabolites of ZK 6013443 in mouse plasma and urine after intravenous injection of ZK 6013443 (7.6 – 11.1 MBq/100 µL per animal) were investigated *in vivo*. Blood and urine were collected at 5, 30, 60 min post injection. Plasma and urine were extracted with acetonitril and analyzed by HPLC (gamma-detector). The HPLC-chromatogram data demonstrates no difference in human plasma and PBS indicating that ZK 6013443 is stable in human plasma over a time period of 120 min

employed in this study. The *in vivo* study suggests two radioactive metabolites (M1- major metabolite rapidly excreted via the kidneys and M2- minor metabolite slowly cleared from kidney.)

Study No.	KM05306
Study Report Location:	4.2.2.2. Pages 1-17.
Conducting laboratory Location:	Bayer Schering Pharma AG, TRG DG, Molecular Imaging Research, 13342 Berlin, Germany
Date of study initiation:	November 2005
GLP Compliance:	No
QA Statement:	No
Drug, lot #, and % purity:	ZK 6013443, lot # and purity-Not provided

Study Design:
In vitro study- Whole fresh heparinized human blood obtained from healthy volunteer was centrifuged for 30 min at 3000 rpm at 4°C. 70µL aliquots of human plasma were incubated with ZK 6013443 (60 MBq/mL) at 37°C for 0, 30, 60, 90, 120 min. The control of ZK6013443 (60 MBq/mL) was incubated in 70 µL PBS (Phosphate-Buffered saline) at 37°C for 120 min. The samples were then extracted with 140 µL acetonitril, centrifuge for 10 min at 13000 rpm at 4°C, and analyzed by HPLC [redacted] (b) (4)

In vivo study- The study was conducted in male NMRI mice intravenous injected per animal ZK 6013443 (7.6 – 11.1 MBq/100µL) in the tail vein and blood and urine samples were collected at 5, 30, 60 min post injection from the animals. The animals were clinically examined to ascertain the absence of abnormal clinical signs. At the indicated time points, animals were sacrificed by decapitation and exsanguinations under isoflurane anesthesia and blood and urine were collected. Heparinized blood sample were centrifuge for 30 min at 3000 rpm at 4°C. 150 µL plasma and 100 µL urine were extracted with acetonitril, centrifuge for 10 min at 13000 rpm at 4°C, and analyzed by HPLC ([redacted] (b) (4) The relative amount of ZK 6013443 and of the metabolites (given in %) was calculated from the peak area measured by HPLC. Overall radioactivity measured by HPLC (sum of all peak areas) was used as 100%-value.

Results:
The results that ZK 6013443 is stable after incubation in human plasma up to 120 min as shown in Table 34 and the HPLC-chromatogram (Figure 50).

Reference ID: 3361527

Table 29: Stability of ZK6013443 after incubation in human plasma detected by HPLC

Medium	**Time (min)**	**MI-8.5 min (%)**	**MII-13.5 min (%)**	**MIII-16.8 min (%)**	**AV1-13.1 min (%)**	**Recovery AV1 (%)**
PBS solution	0 120	2.2 5.1	2.7 4.2	0.7 2.9	94.4 87.7	100.0 92.9
Human plasma	0 30 60 90 120	5.8 5.8 4.8 4.8 5.3	2.0 2.3 1,8 3.3 4.9	3.0 3.0 3.5 3.7 3.3	89.3 88.9 90.0 88.2 86.5	100.0 99.6 100.8 98.8 96.9

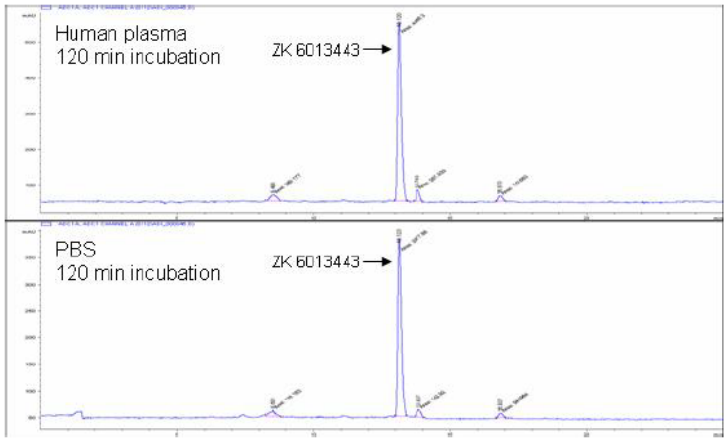

Figure 51: HPLC-chromatogram of ZK 6013443 taken after 120min incubation in human plasma and PBS

The data on metabolite analysis of ZK 6013443 in plasma and urine after administration in male NMRI mice demonstrates that radioactive metabolites were detected in plasma of NMRI mouse 5 min post injection of ZK 6013443. The main metabolite M1 found in plasma is rapidly excreted via the kidneys while metabolite M2 detected in the urine at 60 min post injection was found in small amount indicating a slow clearance via the kidneys (Table 30 and Figure 52).

Table 30: Metabolites of ZK 6013443 in plasma and urine after i.v. administration in male NMRI mice detected by HPLC

Medium	Time (min)	ZK 6013443 (%)	M1-1.4 min (1%)	M2-11.1 min (1%)		
Plasma	5	64.1	23.8	12.1		

Medium	Time (min)	ZK 6013443 (%)	M1-1.4 min (1%)	M2-11.1 min (1%)	M3-2.7 min (1%)	M4-4.2 min (1%)
Urine	5 30 60	0.0 0.0 2.0	0.0 88.0 83.3	0.0 0.0 0.9	0.0 6.3 0.0	0.0 5.7 13.8
Medium	Time (min)	ZK 6013443 (%)	MI-1.7 min (1%)	MII-7.4 min (1%)	MIII-8.6 min (1%)	MIV-13.9 min (1%)
Injection solution	30 180	94.4 73.2	0.0 1.8	0.8 18.9	0.0 2.8	4.7 3.3

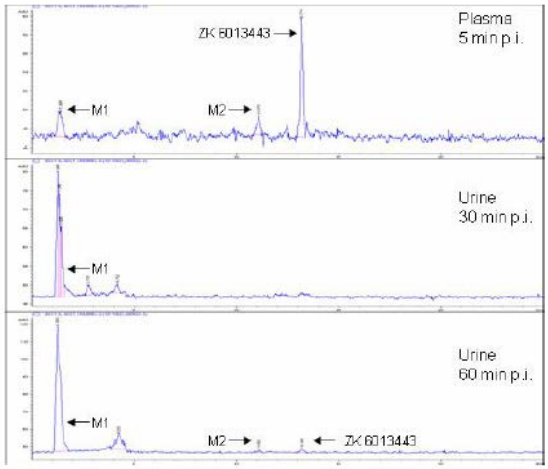

Figure 52: HPLC-chromatogram of ZK 6013443 of plasma and urine

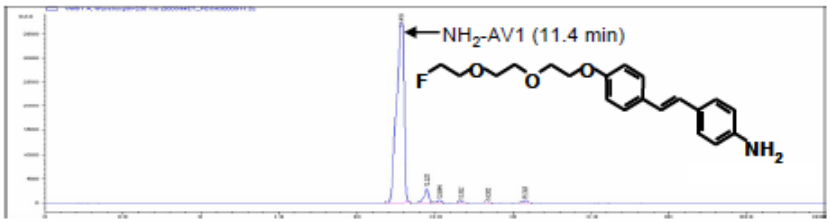

Figure 53: HPLC-chromatogram of NH2-AV-1

M2 has the same retention time on the HPLC as NH_2-AV-1 (11.4 min) indicating that M2 is NH_2-AV-1 and NH_2-AV-1 (Figure 53) was also predicted as a probable metabolite of ZK 6013443 by the METEOR software.

Reviewer's Comments: Agrees with the result of this study

Study title: **Identification of metabolites in plasma after intravenous administration of ZK6013443 in mice**

Key study findings: The identification of ZK 6013443 metabolites in mouse plasma was investigated following an intravenous injection of ZK 6013443 and ZK 6016468 (non-radioactive derivative) to NMRI mice in this study. Plasma extracted from the blood samples collected from the mice 5 min post injection was analyzed using LC-MS/MS. 4 radioactive peaks with the retention times of 1.5 min (P1), 11.5 min (P2), 13.6 min (P3) and 14.3 min (P4) was obtained. PI was not identified, P2 identified as two metabolites composed of a major metabolite (deflourinated ZK 6016468 not detected by the gamma counter since it is non-radioactive) and a minor metabolite (N-demethylated ZK 6016468) while P3 (13.6 min) and P4 (14.3 min) consists of ZK 6016468.

Study No.	KM05306
Study Report Location:	4.2.2.2. Pages 1-17.
Conducting laboratory Location:	Bayer Schering Pharma AG, TRG DG, Molecular Imaging Research, 13342 Berlin, Germany
Date of study initiation:	February 2006
GLP Compliance:	No
QA Statement:	No
Drug, lot #, and % purity:	ZK 6013443 and ZK 6016468, lot # and purity-Not provided

Study Design:
The study was conducted in male NMRI mice intravenous injected ZK 6013443 (83 MBq) mixed with 50 µg ZK 6016468 in 20% HP-ß-CD (in water), 9.5% Ethanol into the tail vein. Heparinized blood sample was collected from sacrificed mouse and centrifuged at 3000 rpm/ 4°C for 20 min. A double volume of acetonitril was added to the plasma and centrifuged at 13000 rpm/4°C for 10 min. Four radioactive peaks were isolated from the supernatant by the use of a preparative HPLC column (gamma-detector) and ZK 6013443 was decayed before LC-MS/MS analysis was performed.

Results:

Reference ID: 3361527

The data on the metabolite analysis of ZK 6013443 in plasma after intravenous injection in male NMRI mice are shown in Table 31, Figure 54 and Figure 55. Four radioactive peaks with the retention times of 1.5 min (P1), 11.5 min (P2), 13.6 min (P3) and 14.3 min (P4) were isolated and analyzed by LC-MS/MS. The 1.5 min peak contained ZK 6016468 suggested to be an unidentified artifact by the sponsor.

Table 31: Metabolites of ZK 6013443 in plasma after i.v. injection in male NMRI mice detected by HPLC (gamma-detector).

Medium	Time (min)	ZK 6013443 (%)	P1-1.5 min (%)	P2-11.5 min (%)	P4-14.3 min (%)
Injection solution	0	97.2	0.0	0.0	2.8
Plasma	5	64.1	18.2	12.6	5.0

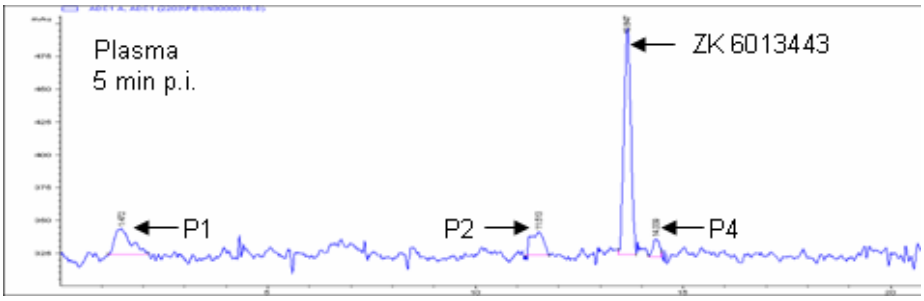

Figure 54: Analytical HPLC-chromatogram (gamma-detector) of extracted plasma 5 min p.i. of ZK6013443/ZK6016468)

Best Available Copy

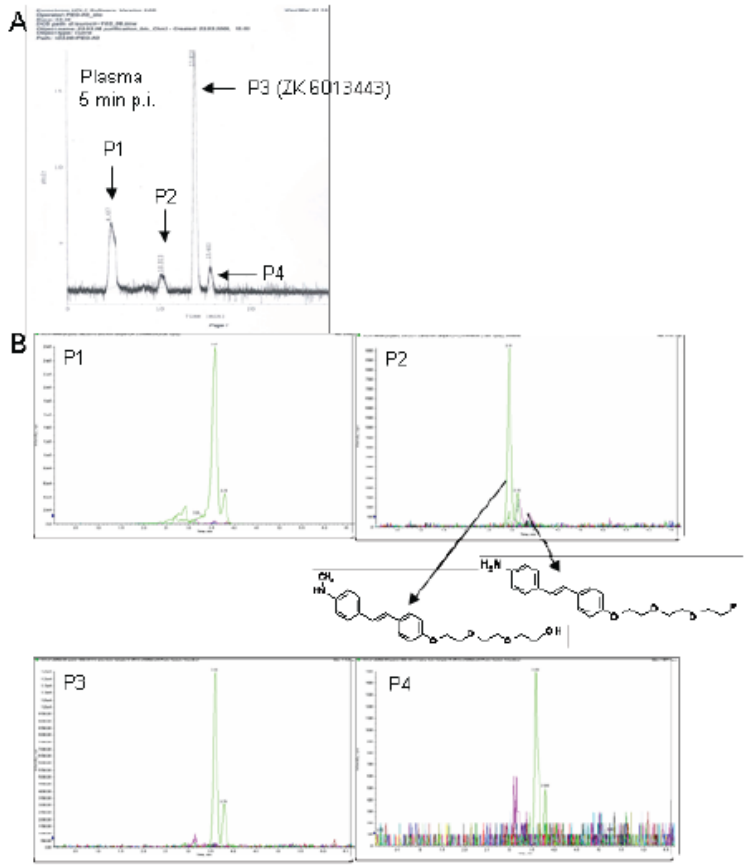

A: Preparative HPLC-chromatogram of extracted plasma 5min p.i. of ZK6013443. 4 peaks with retention times of 4.6min, 10.3min, 13.8min, and 15.6min (differences in retention times between analytical and preparative HPLC are due to inter-systemic variations of the HPLC.
B: Multiple Reaction Monitoring (MRM) chromatogram of isolated radioactive peaks P1 – P4. P1 elutes as two peaks. MS analysis showed that every peak represents ZK6016468. P2 elutes as four peaks. MS analysis showed that the green peaks represent the defluorinated ZK6016468 and the pink peaks represent the N-demethylated ZK6016468. Only ZK6016468 was detected in P3. P4 elutes as two peaks. MS analysis showed that every peak represents ZK6016468.

Figure 55: HPLC chromatogram

Two metabolites identified in the 11.5 min peak (P2) consists of a major metabolite, the defluorinated ZK 6016468, which was not detected with the gamma-detector of the preparative HPLC since it is not radioactive and the minor metabolite identified as N-demethylated ZK 6016478. It was reported that both P3 (13.6 min) and P4 (14.3 min) consists of ZK 6016468.

Reviewer's Comments: Agrees with the result of this study. The study corroborated previous studies reviewed suggesting major and minor metabolites of ZK 6013443 including N-demethylated ZK 6016478. However, metabolite P1 was not identified suggesting that additional studies may be needed to enable full characterization. of the metabolites.

Study title: **Investigation of the polar metabolite fraction of [^{18}F] BAY 94-9172 in mice**

Key study findings: This study was to further characterize the polar metabolite fraction of [^{18}F] BAY 94-9172 in mouse plasma and brain following intravenous injection of the tracer to mice previously investigated using a reversed phase HPLC. Analysis of the plasma and brain samples extracted with acetonitrile/2% TFA obtained from NMRI mice intravenously injected [^{18}F] BAY 94-9172 (82.4-87.2 MBq) led to identification of the metabolites. [^{18}F]fluoroacetic acid was identified as the major constituent of the polar metabolite fraction in plasma and brain of mice while [^{18}F]fluoroacetaldehyde was the second major metabolite and [^{18}F]fluoride was found to be a minor component in plasma and brain along with several other unidentified metabolites in the polar fraction.

Study No.	KM10017
Study Report Location:	4.2.2.2. Pages 1-21
Conducting laboratory Location:	BPH GDD-TRG Diagnostic Imaging, CNS Imaging Research and New Fields BPH GDD-GED Drug Metabolism and Pharmacokinetics Bayer Schering Pharma AG,13342 Berlin, Germany
Date of study initiation:	January 3, 2010
GLP Compliance:	No
QA Statement:	No
Drug, lot #, and % purity:	[^{18}F] BAY 94-9172, lot # and purity-Not provided

Study Design:
The study was conducted in male NMRI mice intravenous injected [^{18}F] BAY 94-9172 (82.4-87.2 MBq) into the tail vein. The mice (n=3) were decapitated 30 min post injection and heparinized blood samples were taken and radioactivity was measured in a gamma counter. Plasma was generated by centrifugation at 3000 rpm, 4°C for 10 min. The plasma was subsequently extracted with 2 volumes of cold acetonitrile/2% TFA and after centrifugation at 13,000 rpm, 4°C for 10 min the supernatants were analyzed by ion exchange HPLC. The brain was dissected, weighed and radioactivity was determined in a gamma counter and the whole brain was then homogenized by the addition of 1.2 mL Tris-HCl buffer (50 mM, pH 7.4) using a glass potter. The homogenized tissue was extracted with 2.4 mL of cold acetonitrile/2% TFA. After centrifugation of brain samples at 3300 rpm, 4°C for 10 min, supernatants were similarly analyzed by ion exchange HPLC. The employed ion exchange chromatography system has been found suitable for the separation of the constituents of the polar metabolite fraction which cannot be separated by conventional C18 columns. (b) (4)

(b) (4) and cannot be analyzed by the ion exchange chromatography. The metabolite pattern of the polar fraction was therefore compared to [^{14}C]-labeled reference compounds, i.e. [1-^{14}C]fluoroacetic acid and [1-^{14}C]fluoroethanol.

Results:
The data on the total radioactivity measured in blood and brain and the percentage of the injected dose per g tissue calculated after [^{18}F] BAY 94-9172 injection into the (Table 32).

Table 32: Total radioactivity expressed as %ID/g (d.c.) in mouse blood and brain at 30 min after injection of [^{18}F]BAY 949172

Animal	**Blood %ID/g d.c.**	**Blood %ID/g d.c.**
mouse 1 mouse 2 mouse 3	2.27 1.67 1.88	1.27 1.51 1.52
mean ± SD	1.94±0.30	1.43±0.14

After the initial extraction of the brain and plasma samples with acetonitrile/2% TFA and further analysis of the samples by HPLC, the data on the extraction efficiency for the samples indicates that plasma supernatant yield of 88% and brain supernatant yield of 66.7% was reported (Table 33).

Table 33: Extraction efficiency for brain and plasma samples at 30 min after extraction with acetonitrile and centrifugation

Sample	**Plasma pellet MBq (Yield %)**	**Plasma pellet MBq (Yield %)**	**Plasma pellet MBq (Yield %)**	**Plasma pellet MBq (Yield %)**
mouse 1 mouse 2 mouse 3	0.100 (13.26%) 0.053 (11.96%) 0.051 (10.22%)	0.654 (86.74%) 0.390 (88.04% 0.448 (89.78%)	0.063 (29.58%) 0.109 (40.07%) 0.081 (30.22%)	0.150 (70.42%) 0.163 (59.93%) 0.187 (69.78%)

<u>Analysis of the plasma samples</u>- Three major peaks were identified in the metabolic pattern of mouse plasma following reverse phase chromatography. Two major metabolite peaks as well as three minor peaks were displayed as shown in Figure 56 and Figure 57 and summarized in Table 34.

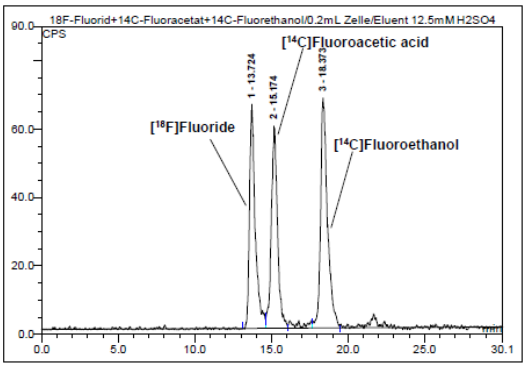

Figure 56: Chromatogram of reference compounds [1-14C]fluoroacetic acid, [1-^{14}C]fluoroethanol, [^{18}F]fluoride with ion exchange chromatography and online radioactivity detection

Best Available Copy

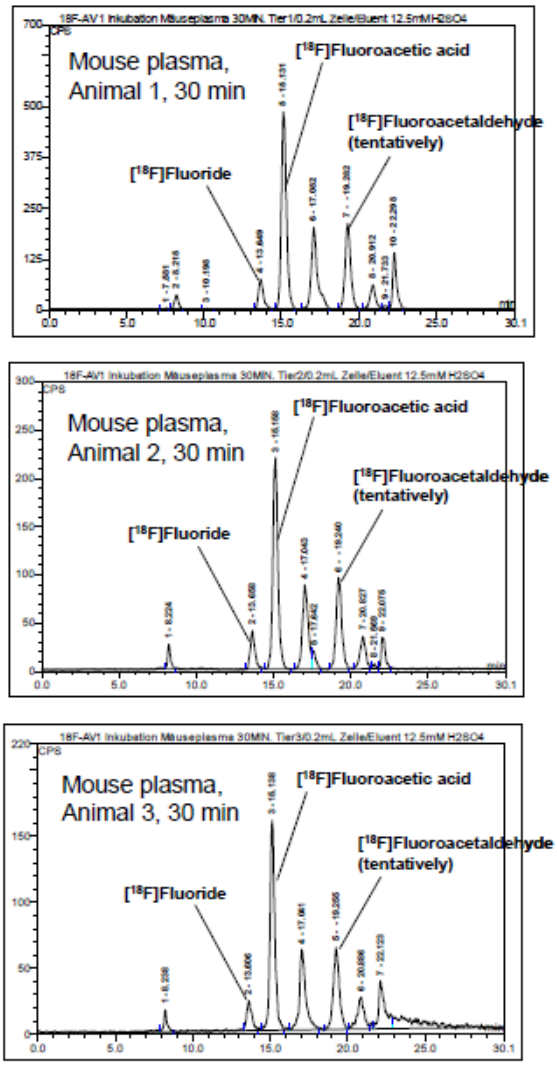

Figure 57: Metabolite pattern in mouse plasma after intravenous administration of [^{18}F]BAY 94-9172 with ion exchange chromatography and online radioactivity detection

Table 34: Results of metabolite analysis in mouse plasma and brain by ion exchange chromatography after intravenous administration of [^{18}F]BAY 94-9172 to mice 30 min post application (mean values of three animals)

Retention time (min)	**Metabolite**	**% of polar fraction in mouse plasma**	**% of polar fraction in mouse plasma**
8.2	Unknown	2.5	<1
13.6	[^{18}F]Fluoride	5.9	4.2
17.0	[^{18}F]Fluoroacetic acid	38	36
15.1	Unknown	19	14

18.4	[^{18}F]Fluoroacethanol	<1	<1
19.2	[^{18}F]Fluoroacetaldehyde (tentatively)	18	31
20.9	Unknown	6.7	9.9
22.2	Unknown	8.4	1-10

The major metabolite eluted at a retention time of 15.1 min and represents approximately 38% of the radioactivity of the polar metabolite fraction, having the same retention time similar to the reference compound [1-^{14}C]fluoroacetic acid eluted at exactly the same retention time indicating fluoroacetic acid to be presumably the major constituent in plasma. This finding was further substantiated by co-eluation of [1-^{14}C]fluoroacetic acid with a plasma sample (Figure 58). At 19.2 min was also a major constituent of the polar metabolite fraction in mouse plasma (18% of radioactivity) and probably corresponds to [^{18}F]fluoroacetaldehyde. Following lack of any available radiolabeled reference compound for fluoroacetaldehyde, its retention time (13.1 min) on an ion exchange was compared to fluoroethanol and fluoroacetic acid and found to co-eluted with [^{18}F]fluoride (F-) indicating, that [^{18}F]fluoride is present as minor constituent in mouse plasma (approx. 6% of radioactivity). In addition other metabolites were detected in mice plasma peaks with retention times of 8.2, 13.7, 17.2, 20.9 and 22.1 min, respectively. However, none of the structures of these components were further investigated in the study.

Analysis of the brain samples-The analysis of the mouse brain homogenate samples separated by ion exchange chromatography also demonstrated two major peaks and three minor peaks as shown in Figure 58 and Figure 59. The major metabolite elutes at a retention time of 15.1 min and represents approximately 36% of the radioactivity of the polar metabolite fraction suggesting fluoroacetic acid. The second major component in mouse brain representing 31% of the radioactivity elutes at 19.2 min (similar to mouse plasma) and probably corresponds to fluoroacetaldehyde. It was reported that the peak at the retention time of 13.6 min co-elutes with [^{18}F]fluoride (F-) indicating [^{18}F]fluoride present as minor metabolite in mouse brain. Similar to the plasma sample, fluoroethanol was also not detected in mouse brain. However, similar to plasma, several metabolites were observed with retention times of 17.0, 19.2, 20.8 and 22.2 min, respectively.

Best Available Copy

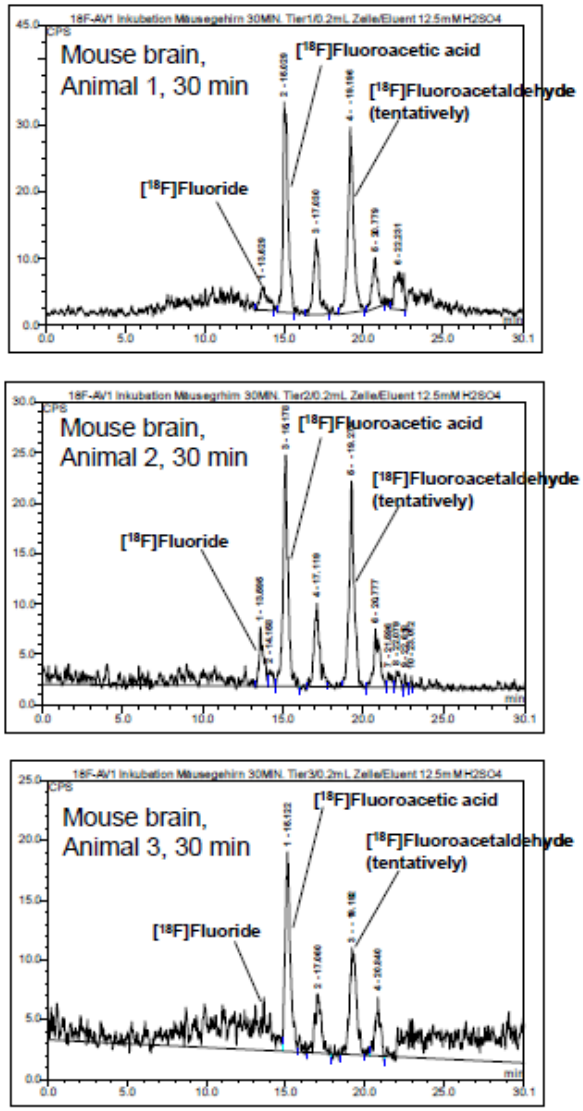

Figure 58: Metabolite pattern in mouse brain after intravenous administration of [^{18}F]BAY 94-9172 with ion exchange chromatography and online radioactivity detection

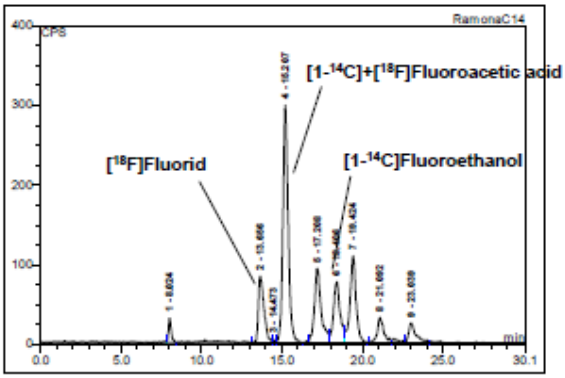

Figure 59: Metabolite pattern in mouse plasma after intravenous administration of [^{18}F]BAY 94-9172 (animal 1, 30 min) spiked with reference compounds [1-14C]fluoroacetic acid, [1-^{14}C]fluoroethanol, [^{18}F]fluoride with ion exchange chromatography and online radioactivity detection

The schematic metabolic pathways of [^{18}F]BAY 94-9172 provided by the sponsor is shown below (Figure 60).

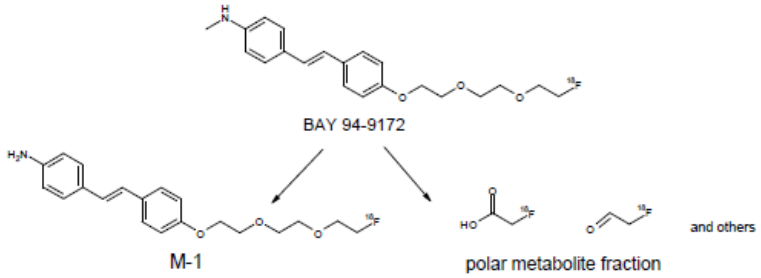

Figure 60: Proposed major metabolic pathways of [^{18}F]BAY 94-9172 in mice

Reviewer's Comments: Agrees with the result of this study indicating similar metabolites in the plasma and brain samples of [^{18}F] BAY 94-9172-treated mice.

Study title: **Detection of metabolites in plasma and brain after intravenous administration of [^{18}F]BAY 94-9172 to mice**

Key study findings: This study investigated the generation and identification of radioactive metabolites in mouse plasma and brain after intravenous injection of BAY 94-9172. Plasma and brain samples extracted from the mice were extracted with acetonitrile and analyzed by HPLC gamma detector. The study showed an uptake of [^{18}F] BAY 94-9172 into the brain within 0-5 mins followed by wash-out of the radioactivity from the brain. Two major metabolites which

cross blood brain barrier; N-demethylated derivative of BAY 94-9172 (unpolar fraction) and [^{18}F]-fluoroacetic acid (polar fraction) were detected.

Study No.	KM09004, KM09065
Study Report Location:	4.2.2.2. Pages 1-24
Conducting laboratory Location:	TRG Diagnostic Imaging, and New Fields Bayer Schering Pharma AG,13342 Berlin, Germany
Date of study initiation:	Not available
GLP Compliance:	No
QA Statement:	No
Drug, lot #, and % purity:	[^{18}F] BAY 94-9172, lot # and purity-Not provided

Study Design:
The study was conducted in male NMRI mice intravenous injected [^{18}F]BAY 94-9172 (42.9-82.9 MBq) dissolved in formulation ((b) (4)) into the tail vein. The mice (n=3) were decapitated at 2, 5, 30, 60 and 90 mins post injection and heparinized blood samples were taken and radioactivity was measured in a gamma counter. Plasma was generated by centrifugation at 3000 rpm, 4°C for 10 min. The plasma was subsequently extracted with 2 volumes of cold acetonitrile and after centrifugation at 13,000 rpm, 4°C for 10 min the supernatants were analyzed by HPLC. The brain was dissected, weighed and radioactivity was determined in a gamma counter and the whole brain was then homogenized by the addition of 1.2 mL Tris-HCl buffer (50 mM, pH 7.4) using a glass potter. The homogenized tissue was extracted with 2.4 mL of cold acetonitrile. After centrifugation of brain samples at 3300 rpm, 4°C for 10 min, supernatants were similarly analyzed by HPLC. The relative amount of BAY 94-9172 and metabolites (given in %) was calculated based on the peak area measured by HPLC. The total radioactivity measured by HPLC (sum of all peak areas) was used as 100%-value. The size and shape of substance peaks are attributed to the analytical system and applied sample volume.

Results:
The data shown below (Table 35) indicates a relatively fast wash out of the radioactivity from the brain, however, only a slow clearance of radioactivity was found in the blood during the observation period. A similar result was reported in earlier studies reviewed above on the distribution and elimination of this tracer.

Table 35: Definition of metabolite fractions by HPLC peak(s) and confirmed co-elution with reference substances

Reference ID: 3361527

HPLC Peak(s)	retention time [min]	co-elution with
PF: polar fraction	2-4.5	
M-1 metabolite	10.5-13.5	ZK6025425 (N-Desmethyl metabolite)
Parent compound	13.5-15.5	BAY 94-9172 (b) (4)
Other	All (minor) peaks not covered by 1.-3.	

The chromatograms obtained for different timepoints post injection revealed four major fractions based on their retention times as shown in Table 40. The parent [^{18}F] BAY 94-9172 was detected as two peaks which co-eluted with a reference (b) (4) A polar metabolite fraction was observed in plasma at 5 mins post injection and in brain at 30 mins post injection and additional non-polar fraction (M1) was also observed in plasma and brain at 2 mins post injection. The sponsor provided the data (Figure 3) showing an agreement in the retention time of M1 and that of N-demethyl metabolite of BAY 94-9172 (ZK 6025425). The study also indicates that different minor metabolites were occasionally detected in plasma.

The percentage of the metabolite fractions in the plasma and brain over the observation time shown in Figure 61 and Figure 62 also demonstrates relatively longer duration of the metabolites in the plasma than in the brain.

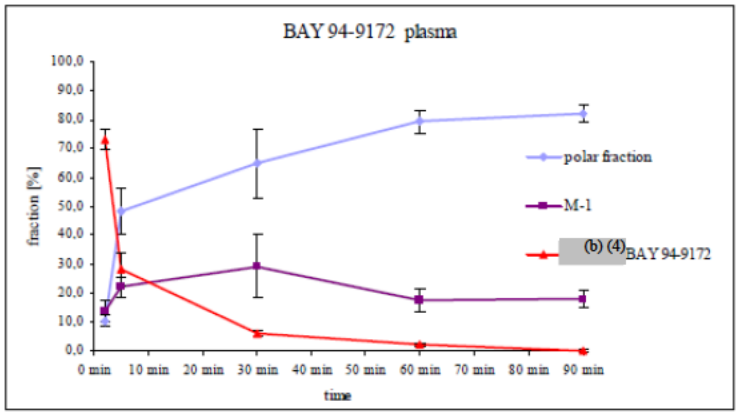

Figure 61: Graphical depiction of percentages of metabolite fractions in plasma over time

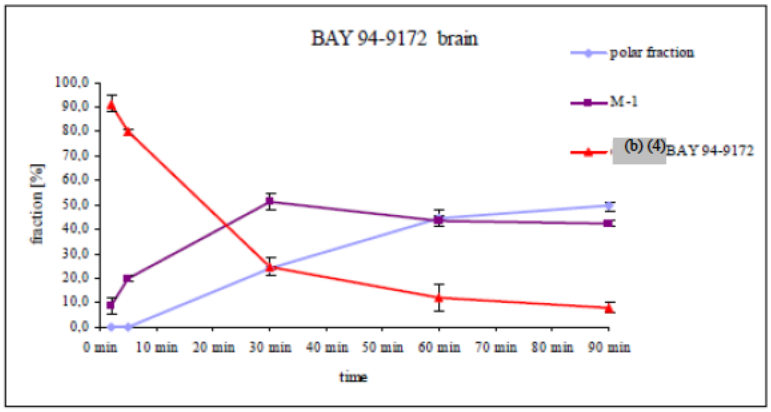

Figure 62: Graphical depiction of percentages of metabolite fractions in brain over time

Reviewer's Comments: Agrees with the result of this study. This study was a follow-up on the previously reviewed study in which the polar metabolite was not fully characterized. The study reaffirmed the rapid uptake of the tracer to the brain and fast clearance from the brain following an intravenous injection. This study also corroborated the previous data on the metabolism of [^{18}F] BAY 94-9172 and identified the polar and non-polar (M1) metabolites of the tracer to be [^{18}F]-fluoroacetic acid and N-demethylated derivative of BAY 94-9172 respectively. The data indicates that [^{18}F] BAY 94-9172 crosses the blood brain barrier and suggests the presence of the [^{18}F] BAY 94-9172 in the brain so that the amyloid beta plaque could be imaged.

Study title: ZK 6016468: *In Vitro* Metabolic Profiling and Species Comparison in Liver Microsomes and Hepatocytes.

Key study findings: This *in vitro* study evaluated the biotransformation of ZK 6016468 in liver microsomes and hepatocytes of rat, dog, mouse and human. Metabolite profiles were generated and metabolite structures elucidated, or already existing structures confirmed using HPLC-UV-MS/MS analysis. The study showed that ZK 6016468 was metabolized *in vitro* in all employed species. Following incubation with human hepatocytes, N-demethylation was the major pathway as well as glucuronidation as the phase II reaction. In rat hepatocytes, N-demethylation was also prominent, however, acetylation was observed as major pathway as phase II reaction. In addition, oxidative cleavage of the fluoro ethyleneglycole side chain was observed as major pathway only in rat hepatocytes.

Study No.	KINE20070117
Study Report Location:	4.2.2.2. Pages 1-53
Conducting laboratory Location:	BSP-GDD-GED-DMPK-Drug Metabolism, Bayer Schering Pharma AG, 13342 Berlin, Germany

Date of study initiation:	Not available
GLP Compliance:	No
QA Statement:	No
Drug, lot #, and % purity:	[^{18}F] BAY 94-9172, lot # and purity-Not provided

Study Design:

Incubation with Liver Microsomes- ZK 6057184 (20 µM) was incubated with liver microsomes (0.5 mg/mL) of human (pool), Wistar rat, Beagle dog, CD-1 mouse and NMRI mouse and in addition with fresh hepatocytes of man and Wistar rat (suspension). Incubations at 0 h were used as negative controls and the incubations were stopped after 1 hour by addition of methanol, stored for approximately 24 h at -18°C and then centrifuged at 13000 rpm for 10 min to pelletize the protein and frozen at -18°C until analysis. The human liver microsomes MP002 (pool) used for the study were purchased from (b) (4) All microsomal preparations were stored at a concentration -of 20 mg/mL in 50 mM potassium phosphate buffer pH 7.4 and 250 mM sucrose at -80 °C.

Incubations with Hepatocytes- Human and rat hepatocytes were incubated in suspension with 5 µM and 20 µM ZK 6057184 for 1h, 2h and 4h. The samples were prepared as described above. The rat liver microsomes were prepared in house according to standard procedures. Enzymatic activities of all microsomal preparations were measured using a variety of standard cytochrome P450 and FMO substrates and all microsomes were found to exhibit good activities. The incubation reaction is started by the addition of 236 µL hepatocyte suspension to 3764 µL medium and 16 µL of a 5 mM stock solution of test compound in acetonitrile. The samples were incubated in a continuously gently shaking water bath at 37°C. The reactions were stopped with 200 µL of acetonitrile, the sample centrifuged for 10 min (13000 rpm) to pelletize the protein and the samples were stored at –18°C for subsequent LC-MS-analysis.

Results:

The metabolite profiles generated following the analysis of the incubation samples of ZK 6057184 using HPLC-UV-MS and HPLCMS/MS was provided in form of chromatograms obtained from the analysis. In addition, the sponsor provided detailed identification of the metabolites based on their chemical and physical properties such as the retention time (t_R) by LC, molecular weight (MW), mass spectrometric fragmentation pattern and elemental composition (determined from the accurate mass measurement). The metabolic pathway identified from all employed species demonstrated that the major pathway is demethylation of the methyl amino moiety leading to M-1 and its isomer M-2 while Formation of N-formyl derivative M-4 is the minor pathway shown in Table 36 (as presented by the sponsor). The study demonstrated that N-demethylation (M-1, M-2) as well as the formation of the N-formyl derivative M-4 observed during microsomal incubations could also be found in the hepatocyte incubations.

Table 36: ZK 6016468: Summary of incubations with liver microsomes of different species with NADPH.

Reference ID: 3361527

Species			Man (m)	Dog (m)	Rat (m)	Mouse NMRI (m)	Mouse CD-1 (m)
Substrate concentration [µM]			20	20	20	20	20
Data path			PHK_STA2_DD-04922_ZK 6057184				
Data files			HM	DM	RM	MM NMRI	MM CD1
Time point [h]			1.0	1.0	1.0	1.0	1.0
t_R #1) [min]	mass $[M+H]^+$	Assignment	[%] #2)	[%] #2)	[%] #2)	[%] #2)	[%] #2)
8.9	346	**M-1**	11.8	12.3	7.1	11.7	12.4
9.6	346	**M-2**	trace #3)	trace #3)	trace #3)	trace #3)	trace #3)
8.5	374	**M-4**	1.9	1.1	2.2	2.0	1.5
10.3	360	**Drug**	86.3	86.6	90.7	86.3	86.1
10.8	360	**VU-1**	< 0.5	< 0.5	< 0.5	n.d.	n.d.

#1) t_R from human hepatocytes, #2) percentage of metabolite calculated from UV detection

#3) minor metabolite, which could not be detected by UV, but only by MS

Furthermore, apart from M-1, M-2 and M-4 formed during incubation with hepatocytes of man, glucuronidation of the demethylated amino group of M-1, M-2 leading to M-8 and its isomer M-9, was also observed as major pathway. As presented by the sponsor (Table 37), few minor metabolites were identified in human hepatocytes only during incubation of ZK 6057184 at 20 µM: glucuronidation of the amino group of the parent compound (M-7), acetylation of the demethylated metabolites M-1 and M-2 (M-5 and its isomer M-6) and glucuronidation at the amino group with oxidation at the stilbene moiety leading to M-10. Furthermore, oxidative cleavage of the fluoro ethylene glycol side chain was observed as minor pathway leading to the carboxylic acid M-13.

Apart from M1, M2 and M4 formed during incubations with rat hepatocytes, N-acetylation of the demethylated metabolites M-1 and M-2 leading to M-5 and M-6 was observed as major phase II reaction. In addition, oxidative cleavage of the fluoro ethylene glycol side chain was also observed leading to the corresponding carboxylic acids M-11, M-12, M-13, M-14, and M-15 (Table 37).

Table 37: ZK 6016468: Summary of incubations with hepatocytes of man and rat (suspension) #4)

Species			Human (f)	Rat (m)
Substrate concentration [µM]			**20**	**20**
Data path			PHK_STA2_DD-04922_ZK	6057184
Data files			HH 18.03.2008	RH 18.03.2008
Time point [h]			4 h	4 h
t_R #1) [min]	mass $[M+H]^+$	Assignment	[%] #2)	[%] #2)
8.9	346	**M-1**	9.2	0.8
9.6	346	**M-2**	trace #3)	trace #3)
8.5	374	**M-4**	trace #3)	1.9
8.6	388	**M-5**	2.2	20
9.3	388	**M-6**	trace #3)	1.7
7.7	536	**M-7**	trace #3)	n.d.
6.7	522	**M-8**	1.6	n.d.
7.3	522	**M-9**	trace #3)	n.d.
7.3	522	**M-10**	trace #3)	n.d.
6.9	400	**M-11**	n.d.	8.7
6.6	356	**M-12**	n.d.	5.8
8.0	328	**M-13**	trace #3)	trace #3)
7.3	356	**M-14**	n.d.	3.8 with M-15
7.6	400	**M-15**	n.d.	3.8 with M-14
10.3	360	**Drug**	83	57
10.8	360	**VU-1**	3.8	3.9

#1) t_R from human hepatocytes or rat hepatocytes

#2) percentage of metabolite calculated from UV detection

#3) minor metabolite, which could not be detected by UV, but only by MS in 20 µM incubation sample

#4) Due to change of chemical structure the UV absorption of the metabolites changes compared to ZK 6057184. Therefore, the percentage of peak area can only be considered as an exploratory result, but cannot be used for quantification.

Reviewer's Comments: The sponsor provided detailed data from the metabolic profiling and species comparison in liver and hepatocytes investigated in this study. The inclusion of the liver and hepatocytes isolated from humans in this study helps to authenticate the relevance of all other pharmacokinetics data obtained from the rodents employed in all previous PK studies conducted on this compound. The data from the *in vitro* study indicates no major species differences in the metabolism of ZK 6016468 in liver microsomes found in all species investigated. This established the relevance of the data from other species. Overall, this reviewer agrees with the result showing that during incubation with human hepatocytes, demethylation was the major pathway as well as glucuronidation as phase II reaction. In rat hepatocytes also demethylation was prominent and acetylation as phase II reaction was observed as major pathway. However, oxidative cleavage of the fluoro ethylene glycol side chain was observed as major pathway only in rat hepatocytes.

Study title: A56320: [^{14}C]BAY 94-9172: Biotransformation in Mice.

Key study findings: This study evaluates the metabolic fate of [^{14}C]BAY 94-9172 and its metabolites in plasma and brain following intravenous injection of [^{14}C]BAY 94-9172 (1 mg/kg). HPLC analysis of plasma and brain extracts was performed with off-line radioactivity detection using a reversed phase HPLC and an ion exchange chromatography to enable separation of a polar fraction of metabolites. The data showed that BAY 94-9172 undergoes two oxidative metabolic pathways; N-demethylation to M-1 and formation of a polar metabolite fraction. Quantitatively, similar metabolite profiles were found in the plasma and brain while the brain radioactivity concentration was approximately 10-40% the plasma concentration.

Study No.	A56320
Study Report Location:	4.2.2.2. Pages 1-40
Conducting laboratory Location:	GDD-GED-DMPK, Bayer Schering Pharma AG, 42096 Wuppertal, Germany
Date of study initiation:	17 March, 2009
GLP Compliance:	No
QA Statement:	Yes
Drug, lot #, and % purity:	[^{14}C]ZK 6057184, lot #-Not provided and purity- 98.7%

Study Design: The metabolite profiles in plasma and brain samples collected from NMRI mice were investigated in 0.083 – 6 hours after intravenous injection of 1 mg/kg [^{14}C]BAY 94-9172.

Incubation with Mouse Liver Microsomes- Liver microsomes (pooled microsomes from male NMRI mice) were prepared in house according to standard procedures and stored at a concentration of 20 mg protein/mL in 50 mM potassium phosphate buffer pH 7.4 and 250 mM sucrose at -80°C. Enzyme activities were measured using a variety of standard cytochrome P450 and FMO substrates. The standard incubation mixtures contained the followings: 1 mM NADP, 1 mM EDTA, 5 mM glucose 6-phosphate, glucose 6-phosphate dehydrogenase (1.5 U/mL), 50 mM phosphate buffer (pH 7.4), 0.5 mg/mL microsomal protein and [^{14}C]BAY 94-9172 (2 and 10 µM) in a total volume of 0.5 mL. After a 5 min preincubation, the reaction was initiated by the addition of NADPH-generating system. The incubation was terminated by adding acetonitrile (200 µL) after 60 min.

Preparation of Plasma and Brain Homogenate- The blood samples were collected into heparinized tubes following exsanguination by a cut through the carotid artery under anesthesia. Separation of the blood cells and plasma was performed by centrifugation and the plasma was prepared for further analysis. The brain was completely removed and the tissue was treated with 1 mL aqua demin. and homogenized. Plasma and brain homogenate were then stored at < -15°C until further analysis.

Results:

Metabolite Profiles in Liver microsomal incubations- Following the incubation of [^{14}C]BAY 94-9172 (final concentrations of 2 and 10 µM) with liver microsomes (0.5 mg protein/mL) for 60 min, metabolite profiles were established with HPLC on RP material and off-line radioactivity detection (Table 38 and Figure 63). During incubation with a substrate concentration of 10 µM [14C]BAY 94-9172, N-demethylation reaction was observed as the primary oxidative reaction

Reference ID: 3361527

yielding M-1 (sponsor's Figure 63). However, when incubated with [^{14}C]BAY 94-9172 at 2 µM, the parent compound was depleted and a major metabolite, M-1 (polar fraction) was observed.

Metabolite Profiles in Plasma-This was investigated in the plasma samples taken after 0.083 to 6 hours after the injection of 1 mg/kg [^{14}C]BAY 94-9172. The plasma samples from the 3 mice at each time point were pooled, treated with acetonitrile and homogenized. There was complete recovery of total radioactivity and after removing the proteins by centrifugation, the supernatants were concentrated and analyzed by HPLC with off-line radioactivity detection.

Table 38: [^{14}C]BAY 94-9172: Formation of metabolites in mouse liver microsomes (NMRI, male)

			HPLC Analysis		
[^{14}C]BAY 94-9172 (µM)	Protein Concentration (mg/mL)	Incubation time (min)	[^{14}C]BAY 94-9172 (%)	M-1 (%)	Polar metabolite fraction (%)
2	0.5	60	5.2	61.1	21.0
10	0.5	60	78.7	16.3	1.1

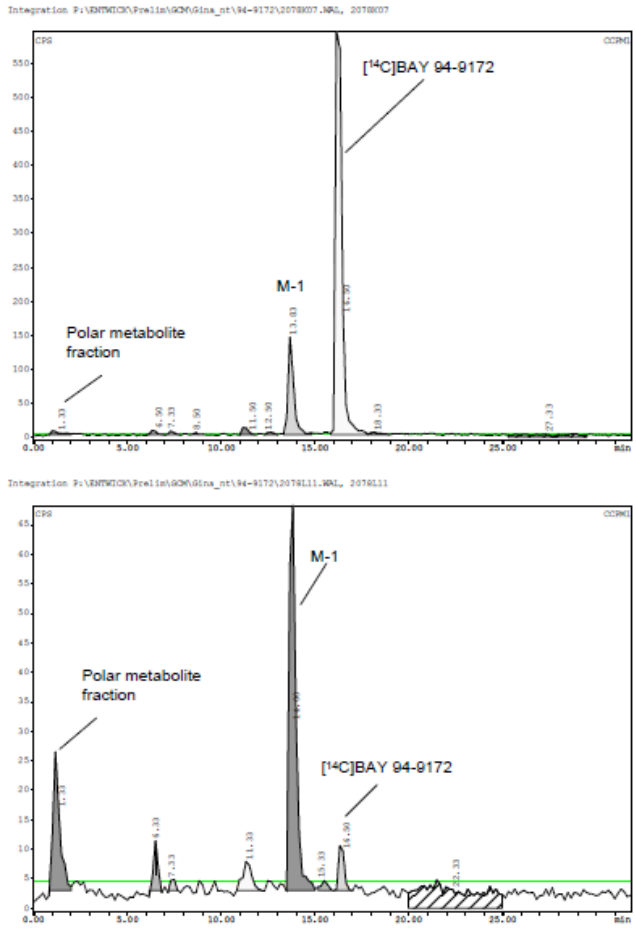

Figure 63: [^{14}C]BAY 94-9172: Metabolite profiles following incubation of [^{14}C]BAY 94-9172 (10 µM, top and 2 µM, bottom) with 0.5 mg liver microsomal protein/mL

The data provided by HPLC retention times of synthetic reference materials identified an unchanged drug and metabolite, M-1. A fraction of polar metabolites later occurred at a later time and it could not be separated by reverse phase HPLC methodology. The sponsor provided the plasma metabolite profiles (Table 39 and Figure 64) indicating that following intravenous administration up to 0.33 hour, parent compound represented the main component in plasma, whereas after 1 hour, BAY 94-9172 and metabolite M-1 were found in similar amounts. Furthermore, a polar metabolite fraction was detected in trace amounts within the first one hour following administration. Elimination of unchanged compound as well as of M-1 caused an increase of the polar fraction over time. However, 6 hours after, unchanged compound completely disappeared from plasma, thus, traces of M-1 was only found while the majority of the radioactivity (67%) was represented by the polar metabolite fraction.

Table 39: [^{14}C]BAY 94-9172: Metabolic pattern in pooled plasma samples 0.083 to 6 h following intravenous administration of 1 mg/kg b.w. [^{14}C]BAY 94-9172 to male mice (NMRI) established with RP chromatography

Animal No. (pool)		671-674	675-678	679-682	683-686	687-690	691-694	695-698
Time point [h]		0.08	0.17	0.33	1	2	4	6
Work up recovery extraction [%]		98.8	94.3	102.0	101.6	105.1	98.1	103.2
Data file [.wal]		2078M26	2078M27	2078M28	2078M29	2078M30	2078M31	2078M32
Total radioactivity conc. [µg-eq/L]		1129	1350	1442	725	576	433	347
Retention time* [min]	Identification	% of radioactivity						
1.3	**Polar metabolite fraction**		1.4	0.8	2.0	16.6	52.5	61.7
1.8	Unknown					3.6		
2.5	Unknown					2.4		
6.8	Unknown		0.4	0.5		2.2		
7.3	Unknown	0.8	0.8	1.5				
9.8	Unknown	2.0	4.6		1.9		1.2	
11.7	Unknown	6.6	12.4		3.1	2.2	8.5	6.4
12.7	Unknown	5.4	3.2	2.5	4.9	5.3	2.7	1.6
13.2	Unknown	1.9	1.5					
14.0	**M-1**	8.4	12.9	22.6	41.3	48.9	27.5	3.2
15.5	Unknown	2.7	1.6		2.0	3.3		
16.7	**[^{14}C]BAY 94-9172**	69.2	59.5	70.7	35.8	16.9	7.7	
17.3	Unknown	1.3						
18.0	Unknown	0.7	0.8					
20.0	Unknown		0.7	1.4				
22.8	Unknown	1.4	0.7					
Metabolites balanced		100.4	100.4	100.0	91.0	101.3	100.0	73.0
Metabolites identified		77.6	73.8	94.1	79.1	82.4	87.7	65.0

The study further investigated the identity of the constituents of the of the polar metabolite fraction [^{14}C]-radiolabeled fluoroacetate and demonstrates that fluoroacetic acid is present in mouse plasma at later time points, and fluoroethanol could be excluded as a potential component of the polar fraction. The amount of fluoroacetate time-dependently increased and accounted for approx. 90% of the radioactivity in the polar fraction after 6 h. The sponsor provided the summary of the pharmacokinetic parameters of [^{14}C]BAY 94-917244) (Table 44) showing that the ($AuC_{0\text{-}6\ h}$) for the parent compound, M-1 and polar fraction accounted for 26.3%, 32.9%, and 25.3% respectively of the radioactivity present in the plasma. The $t_{1/2}$ for BAY 94-9172 was calculated as approximately 1 hour; however, the total radioactivity was significantly longer with approximately 5 hours (Figure 64).

Table 40: [^{14}C]BAY 94-9172: Plasma concentrations [µg-eq/L] and pharmacokinetic parameters of BAY 94-9172 after intravenous administration of 1 mg/kg b.w. [^{14}C]BAY 94-9172 to male mice (NMRI)

Time [h]		Total radioactivity	[^{14}C]BAY 94-9172	Polar metabolite fraction	M-1
0.08		1129	781	-	94.9
0.17		1350	797	18.2	175
0.33		1442	1019	11.4	326
1		725	260	79.5	299
2		576	97.3	95.8	277
4		433	33.1	227	119
6		347	-	214	105
AUC(0-6 h)	[µg-eq·h/L]	3504	939	885	1151
AUC(0-6 h)	[%]		26.8	25.3	32.9
C_{max}	[µg-eq/L]	1442	1019	227	326
t_{max}	[h]	0.333	0.333	4.00	0.333
$t_{1/2}$	[h]	5.47	1.04	n.c.	3.06
Points*		3	3	4	5
Interval*	[h]	2-6	1-4	-	0.33-6

n.c. = not calculated
* = used for regression to determine $t_{1/2}$

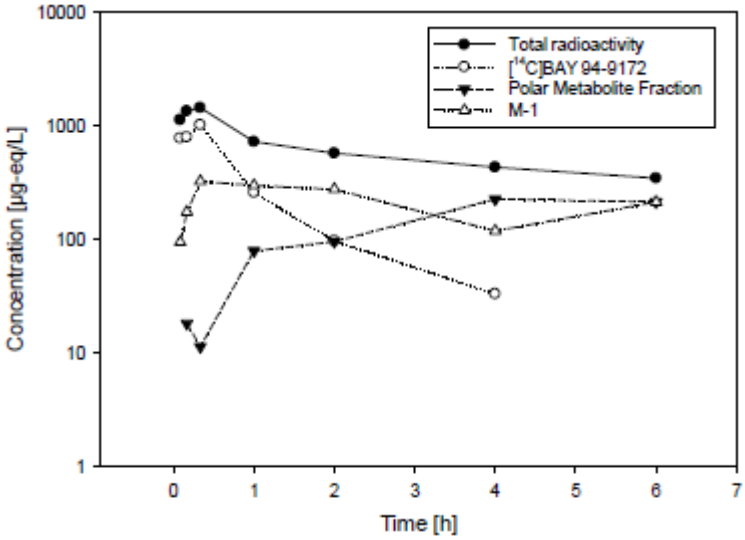

Figure 64: [^{14}C]BAY 94-9172: Plasma concentration *vs*. time curves of total radioactivity, BAY 94-9172 and metabolites after intravenous administration of 1.0 mg/kg b.w. to mice (NMRI) [study No. I 4939-5/A]

Metabolite Profiles in Brain- The metabolite profiles of brain extracts were investigated in samples obtained from the mice after 0.083 up to 6 hour following intravenous administration of [^{14}C]BAY 94-9172 (1 mg/kg). As described with the plasma, the brain specimen were pooled, treated with acetonitrile and homogenized and the recovery of total radioactivity was 88.4%. The extracts were concentrated and analyzed by reversed phase HPLC with off-line radioactivity detection. The summary of the metabolite profiles are shown in Table 41.

Table 41: [^{14}C]BAY 94-9172: Metabolic pattern in pooled brain extracts 0.083 to 6 h following intravenous administration of 1 mg/kg b.w. [^{14}C]BAY 94-9172 to male mice (NMRI) established with RP chromatography

Animal No. (pool)		671-674	675-678	679-682	683-686	687-690	691-694	695-698
Time point [h]		0.08	0.17	0.33	1	2	4	6
Work up recovery extraction [%]		99.2	86.1	89.0	87.7	90.6	80.3	85.9
Data file [.wal]		2078M33	2078M34	2078M35	2078M36	2078M37	2078M38	2078M39
Total radioactivity conc. [µg-eq/L]		461	272	148	73.5	66.5	60.8	59.6
Retention time* [min]	Identification	% of radioactivity						
1.3	**Polar metabolite fraction**			2.8	12.5	29.3	63.2	83.2
6.8	Unknown	1.6						
7.3	Unknown	1.1						
11.7	Unknown	2.6	8.0					
12.7	Unknown	4.6	2.0					
13.7	Unknown		1.4					
14.7	**M-1**	8.7	13.2	21.3	30.0	25.9	18.3	16.8
15.5	Unknown	1.1						
16.7	**[^{14}C]BAY 94-9172**	78.1	74.1	75.8	57.5	44.8	18.5	
17.3	Unknown	2.2	1.2					
Metabolites balanced		100.0	100.0	100.0	100.0	100.0	100.0	100.0
Metabolites identified		86.8	87.4	100.0	100.0	100.0	100.0	100.0

The parent compound represented the main component in brain extracts up to 2 hours and a polar metabolite fraction was detected in trace amounts 0.33 h following administration. Similar to the observation in plasma, elimination of unchanged compound as well as of M-1 resulted in a relative increase of the polar fraction over time. It was found that after 6 hours, unchanged compound completely disappeared from brain, only small amount of M-1 was found and the majority of the radioactivity (83%) was represented by the polar metabolite fraction. Furthermore, the polar metabolite fraction was further separated by the ion exchange chromatography and the data as shown in Table 42.

Table 42: [^{14}C]BAY 94-9172: Metabolic pattern in pooled brain extracts 0.083 to 6 h following intravenous administration of 1 mg/kg b.w. [^{14}C]BAY 94-9172 to male mice (NMRI) established with ion exchange chromatography

Animal No. (pool)		683-686	687-690	691-694
Time point [h]		2	4	6
Work up recovery extraction [%]		90.6	80.3	85.9
Data file [.wal]		2078N05	2078N06	2078N07
Total radioactivity concentration [µg-eq/L]		66.5	60.8	59.6
Retention time* [min]	Identification	% of radioactivity		
8.17	Unknown			6.73
12.0	**Fluoroacetic acid**	48.9	92.4	87.2
15.5	Unknown	7.0	7.6	6.1
19.3	Unknown	33.3		
20.5	Unknown	10.9		
Metabolites balanced		100.0	100.0	100.0
Metabolites identified		48.9	92.4	87.2

Plasma fluoroacetate accounted for 50 - 90% of the radioactivity in the polar metabolite fraction. The pharmacokinetic parameters (Table 43) indicates that AUC_{0-6h} for the parent compound, M-1 and the polar fraction accounted for 43.7%, 35.0%, and 19.8% respectively of the radioactivity present in the brain extracts (Figure 65). The $t_{1/2}$ for BAY 94-9172 was calculated as approximately 2 hours.

Table 43: [^{14}C]BAY 94-9172: Brain concentrations [µg-eq/L] and pharmacokinetic parameters of BAY 94-9172 after intravenous administration of 1 mg/kg b.w. [^{14}C]BAY 94-9172 to male mice (NMRI)

Time [h]		Total radioactivity	[^{14}C]BAY 94-9172	Polar metabolite fraction	M-1
0.08		461	360	-	40.1
0.17		272	202	-	36
0.33		148	112	4.2	32
1		74	42	9.2	22
2		67	29.8	19.5	17
4		61	11.3	38	11
6		60	10.0128	50	-
AUC(0-6h)	[µg-eq·h/L]	472	206	165	93
AUC(0-6h)	[%]		43.7	35.0	19.8
C_{max}	[µg-eq/L]	461	360	50	40
t_{max}	[h]	0.083	0.083	6.00	0.083
t1/2	[h]	n.c.	2.26	n.c.	3.04
Points*		4	4	3	3
Interval*	[h]	-	1-6	-	1-4

n.c. = not calculated
* = used for regression to determine $t_{1/2}$

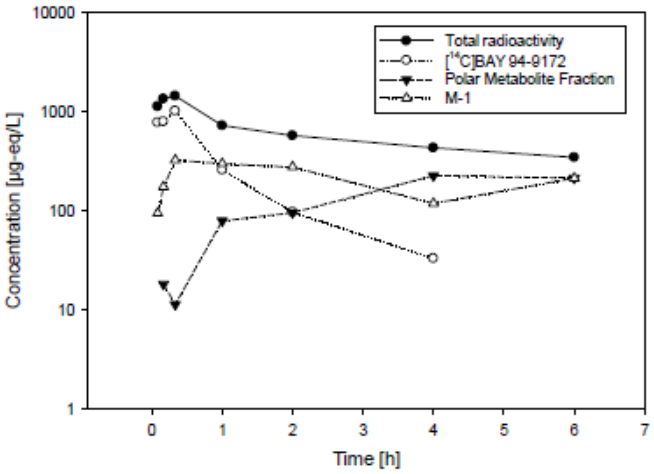

Figure 65: [^{14}C]BAY 94-9172: Plasma concentration *vs*. time curves of total radioactivity, BAY 94-9172 and metabolites after intravenous administration of 1.0 mg/kg b.w. to mice (NMRI) [study No. I 4939-5/A]

The overall data indicates:

1) Incubations of [^{14}C]BAY 94-9172 with liver microsomes of NMRI mouse demonstrates that BAY 94-9172 is subject to two oxidative metabolic pathways: N-demethylation to M-1 and formation of a polar metabolite fraction as shown in Figure 66 and

2) Similar metabolite profiles were demonstrated in plasma and brain radioactivity concentrations reached approximately 10 - 40% of the plasma radioactivity concentrations dependent on the time point investigated.

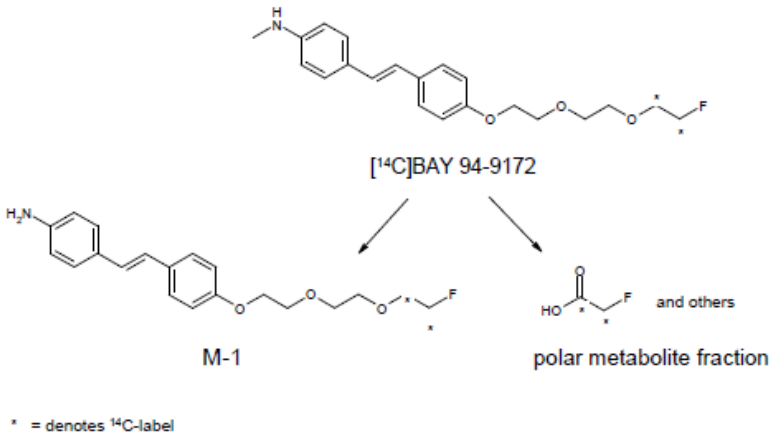

Figure 66: Schematic BAY 94-9172: Metabolic pathways in mouse *in vivo*

Reviewer's Comments: Agrees with the data obtained from this study. The *in vitro* data following incubation of [^{14}C]BAY 94 9172 with liver microsomes gave two oxidative metabolic pathways (N-demethylation to M-1 and formation of a polar metabolite). The data corroborates previous data on the metabolism of the tracer which also suggests the formation of N-demethylation and polar metabolites of the parent compound. The study also demonstrates that metabolite profiles in plasma and the brain were quantitatively similar. The data also indicates that only 10-40% of the plasma radioactivity accounts for the brain radioactivity concentration. This shows that the metabolite concentration in the brain is minimal and the concentration level will probably not complicate the imaging of the brain.

Study title: A56318: Determination of the Inhibitory Potency of BAY 94-9172 Towards Human CYP Isoforms *in Vitro*

Key study findings: This study evaluated the possibility of BAY 94-9172 acting as a direct inhibitor of major human cytochrome P450 isoforms (CYP 1A2, 2C8, 2C9, 2D6, and 3A4). The study was conducted with the [redacted] (b) (4) ZK 6057184 using pooled human liver microsomes *in vitro*. The potential of ZK 6057184 acting as a time-dependent inhibitor of CYP3A4 was also investigated by comparing the inhibitory potential of ZK 6057184 after incubation and after 30 min preincubation with NADPH-supplemented liver microsomes. The result demonstrates no direct-acting inhibitory potency of ZK 6057184 on biotransformation reactions catalyzed by CYP 1A2, 2C8, 2C9, and 2D6 (IC_{50} >2 µM). IC_{50} values of 1.6 µM and 1.4 µM were reported to the inhibition of CYP3A4 activity by midazolam and testosterone respectively. However, 30 min pre incubation of ZK 6057184 with NADPH-supplemented human liver microsomes slightly decreased CYP3A4 activities compared to the co-incubation

experiment as indicated by IC_{50} values of 1.0 µM on midazolam 1'-hydroxylation and 0.7 µM on testosterone 6β-hydroxylation, respectively. It is not expected there would be adverse effects due to any drug-drug interaction of BAY-94-9172 or any of the evaluated CYP isoforms following the administration of BAY-94-9172

Study No.	A56318
Study Report Location:	4.2.2.2. Pages 1-30
Conducting laboratory Location:	GDD-GED-DMPK, Bayer Schering Pharma AG, 42096 Wuppertal, Germany
Date of study initiation:	27 July, 2011
GLP Compliance:	No
QA Statement:	Yes
Drug, lot #, and % purity:	[^{14}C]ZK 6057184, lot #-Not provided and purity- 98.2%

Study Design: The study was designed to determine the inhibitory potency of BAY 94 9172 towards human cytochrome P450 isoforms -CYP 1A2, 2C8, 2C9, 2D6, and 3A4.

CYP Incubation Assay (IC_{50} determination)- The data (Table 44) showing the incubation conditions employed for each assay for the P450 isoforms evaluated is below:

Table 44: Incubation conditions employed by the sponsor for the study

CYP	**Substrate (concentration)**	**Protein (µg/mL)***	**Incubation time (min)**	**ISTD**	**Standard inhibitor (IC50)**
1A2	Phenacetin (45 µM)	600	15	[$^{2}H_3$]Acetaminophen	Furafylline (4.59 µM)
2C8	Amodiaquine (2.0 µM)	14	15	[^{2}H5]Desethylamodiaquine	Montelukast (0.24 µM)
2C9	Diclofenac (4 µM)	14	15	4'-Hydroxy[^{13}C6]diclofenac	Sulfaphenazole (0.2 µM)
2D6	Dextromethorphan (5 µM)	600	10	[$^{2}H_3$]Dextrorphan	Fluoxetine (2.3 µM)
3A4	Midazolam	60		[$^{2}H_3$]Omeprazole	Ketoconazole

Reference ID: 3361527

	(2.5 µM) with preincubation (2.5 µM)	60	30/10	Omeprazole	(0.02 µM) Mibefradil (0.07 µM)
3A4	Testosterone (50 µM) with preincubation (50 µM)	80 80	10 30/10	6µ-Hydroxy[$^2H_3$]testosterone 6µ-Hydroxy[$^2H_3$]testosterone	Ketoconazole (0.01 µM) Mibefradil (0.05 µM)

* human liver microsomes

The co-incubation of CYP 1A2, 2C8, 2C9, 2D6, and 3A4 involved adding ZK 6057184 in acetonitrile (8 µL, 100 µM) to phosphate buffer (192 µL, 50 mM, pH 7.4, containing 1 mM EDTA) and the mixture was sequentially diluted and added 80 µL human liver microsomes preparation in phosphate buffer (50 mM, pH 7.4). The mixture was warmed for 5 min and the reactions were initiated by addition of 20 µL phosphate buffer (50 mM, pH 7.4) containing NADP, glucose 6-phosphate and glucose 6-phosphate dehydrogenase. The reactions were stopped following addition of acetonitrile (100 µL), the precipitated proteins were removed by centrifugation of the well plate (3000 rpm, 10 min, 10°C), supernatants were combined and the analysis performed by LC-MS/MS.

ZK 6057184 (2, 1, 0.5, 0.25, 0.125, 0.063 µM) was pre-incubated with microsomes and NADPH-regenerating system in the absence of the probe substrate (midazolam, testosterone) for 30 min at 37°C. Probe substrates dissolved in water (midazolam) or methanol (testosterone) was then added at the concentrations specified for the co-incubations, and the reactions were allowed to proceed using mibefradil (metabolism-dependent inhibitor) as positive control. The reactions were terminated by the addition of acetonitrile (100 µL) and the samples were prepared for HPLC analysis

Results:
The data on the following standard probes selected as substrates: phenacetin for CYP1A2, amodiaquine for CYP2C8, diclofenac for CYP2C9, dextromethorphan for CYP2D6, and also midazolam and testosterone for CYP3A4 was provided. IC_{50} values were calculated on basis of inhibitory effects at six different concentrations of ZK 6057184. Furthermore, the inhibitory potential of known direct-acting and metabolism-dependent inhibitors of the respective enzymes ("standard inhibitors") as positive controls investigated in parallel (furafylline for CYP1A2, montelukast for CYP2C8, sulfaphenazole for CYP2C9, fluoxetine for CYP2D6, ketoconazole as direct-acting inhibitor for CYP3A4, and mibefradil as metabolism-dependent inhibitor for CYP3A4) is shown in Table 45.

Table 45: BAY 94-9172: Inhibitory effects of ZK 6057184 on formation of metabolites from standard probes mediated by cytochrome P450 isoforms (duplicate incubations, mean value) using pooled human liver microsomes

CYP Isoform	**Probe Reaction**	**IC_{50} for ZK 6057184**	**Positive control Inhibitor IC_{50}**

		(μM)		
CYP1A2	Phenacetin Phenacetin *O*-deethylation	> 2	Furafylline	4.59
CYP2C8	Amodiaquine Amodiaquine *N*-deethylation	> 2	Montelukast	0.24
CYP2C9	Diclofenac Diclofenac 4'-hydroxylation	> 2	Sulfaphenazole	0.2
CYP2D6	Dextromethorphan Dextromethorphan *O*-demethylation	> 2	Fluoxetine	2.3
CYP3A4	Midazolam Midazolam 1'-hydroxylation	1.6	Ketoconazole	0.02
CYP3A4	[^{13}C6]Midazolam [^{13}C 6]Midazolam 1'-hydroxylation (30 min preincubation)	1.0	Mibefradil	0.07
CYP3A4	Testosterone Testosterone 6 -hydroxylation	1.4	Ketoconazole	0.01
CYP3A4	Testosterone Testosterone 6 -hydroxylation (30 min preincubation)	0.7	Mibefradil	0.05

The result indicates no direct-acting inhibitory potency of ZK 6057184 on biotransformation reactions catalyzed by CYP 1A2, 2C8, 2C9, and 2D6 were observed (IC_{50} >2 μM) (Figure 67). The data also showed that CYP3A4 activity was inhibited with IC_{50} values of 1.6 μM and 1.4 μM, respectively when midazolam and testosterone were applied as substrates. Thirty minutes preincubation of ZK 6057184 with NADPH-supplemented human liver microsomes slightly decreased CYP3A4 activities compared to the co-incubation experiment as demonstrated by IC_{50} values of 1.0 μM on midazolam 1'-hydroxylation and 0.7 μM on testosterone 6β-hydroxylation, respectively (sponsor's Figure 68).

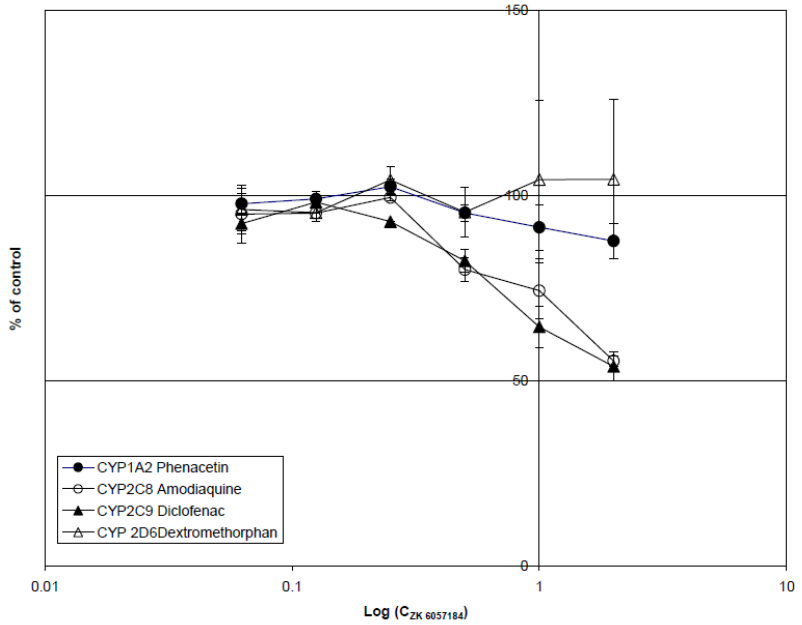

Figure 67: BAY 94-9172: Effect on inhibition on phenacetin *O*-deethylation, amodiaquine *N*-deethylation, diclofenac 4'-hydroxylation and dextromethorphan *O*-demethylation by ZK 6057184 in human liver microsomes *in vitro*

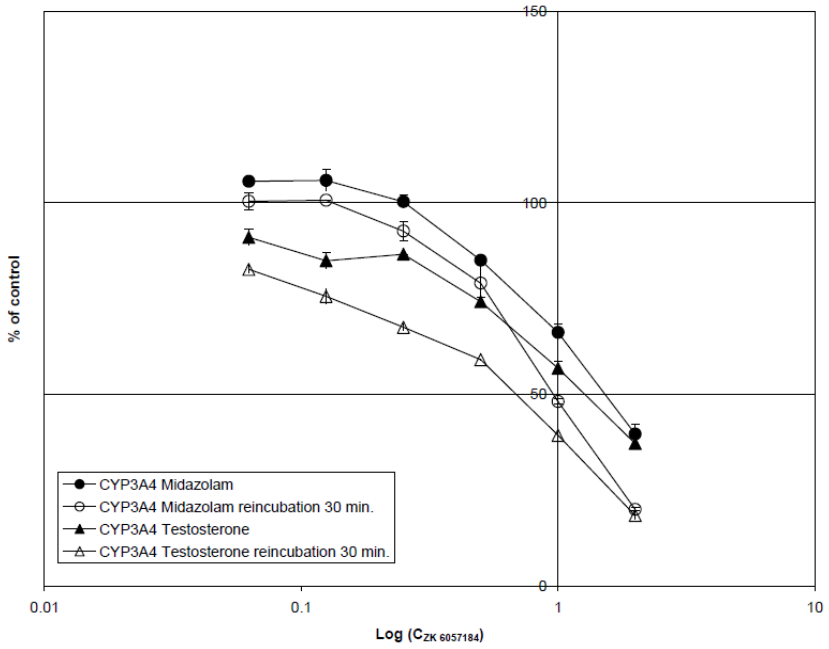

Figure 68: BAY 94-9172: Effect on inhibition on midazolam 1'-hydroxylation and testosterone 6ß-hydroxylation by ZK 6057184 in human liver microsomes *in vitro*

Reviewer's Comments: Agrees with the data obtained from this study which indicates that it is very unlikely any drug-drug interaction by BAY 94-9172 through inhibition of any of the evaluated CYP isoforms (CYP 1A2, 2C8, 2C9, 2D6) and 3A4 would pose risk of clinical significance. This is because the estimated maximum plasma concentration of BAY 94-9172 (C_{max}<0.08 µM) is much lower than the estimated IC_{50} values for the CYP isoforms. This indicates that following the administration of BAY 94-1972 at the proposed dose, the plasma concentration would be too low to induce any interaction with any of the CYP isoforms. Thus, no adverse effects due to any drug-drug interaction of BAY-94-9172 or any of the evaluated CYP isoforms is expected following the administration of this tracer in the clinic.

Study title: A56319: BAY 94-9172: Identification of Human CYP Isoforms Involved in the *In Vitro* Metabolism of [^{14}C]BAY 94-9172

Key study findings: This is an *in vitro* CYP phenotyping study that evaluated the CYP isoforms contributing to the oxidative metabolism of BAY 94-9172. The incubation of [^{14}C]BAY 94-9172 with human liver microsomes (19 isoforms including polymorphic CYPs-2D6, 2C19) in the absence and presence of CYP isoform-selective inhibitors and incubations with recombinant human CYP isoforms were performed during the study. The kinetic parameters for M-1 formation was determined and K_m value of 1.2 µM was obtained indicating that BAY-94-9172 demonstrated affinity for human CYPs employed for the study. Following incubation of [^{14}C]BAY 94-9172 (0.5 µM) with human liver microsomes in the presence of CYP isoform-selective

inhibitors, it was shown that [^{14}C]BAY 94-9172 is a substrate of several CYP isoforms in human. However, no significant involvement of polymorphic enzymes CYP2C19 and 2D6 was observed. It is very unlikely that plasma concentrations of [^{14}C]BAY 94-9172 would reach such a level to be significantly altered when the tracer is administered along with any inhibitors of CYPs in the clinics.

Study No.	A56319
Study Report Location:	4.2.2.2. Pages 1-25
Conducting laboratory Location:	GDD-GED-DMPK, Bayer Schering Pharma AG, 42096 Wuppertal, Germany
Date of study initiation:	22 June, 2009
GLP Compliance:	No
QA Statement:	Yes
Drug, lot #, and % purity:	[^{14}C]ZK 6057184, lot #-Not provided and purity- 98.8%

Study Design: The study was designed to evaluate the CYP isoforms contributing to the oxidative biotransformation of BAY 94-9172. Up to 19 human recombinant CYP isoforms were incubated with 0.5 µM [^{14}C] BAY 94-9172 during this study. They include CYP isoforms that mediated the N-demethylation (CYP1A1, 2J2, 4F2, 4F3b, and 4F12) and CYP2J2 and 3A4 that contributed to formation of polar metabolites as shown in the Table 46.

Incubation of [^{14}C]BAY 94-9172 ([^{14}C]ZK 6057184) with Liver Microsomes: The incubation of [^{14}C]BAY 94-9172 with liver microsomes was performed in the absence and presence of CYP isoform selective inhibitors. The incubation mixtures contained I mM NADP, 1 mM EDTA, 5 mM

Table 46: CYP isoform-selective activities of pooled human liver microsomes MP004

Enzyme measured	**Assay**	**Enzyme activity [pmol/(mg · min)]**
CYP1A2	Phenacetin *O*-deethylation	1186
CYP2A6	Coumarin 7-hydroxylation	948
CYP2B6	(*S*)-mephenytoin *N*-demethylation	41
CYP2B6	Bupropion hydroxylation	612
CYP2C8	Amodiaquine deethylation	1316
CYP2C9	Diclofenac 4'-hydroxylation	2634
CYP2C19	(*S*)-mephenytoin 4'-hydroxylation	92
CYP2D6	Dextromethorphan *O*-demethylation	98
CYP2E1	Chlorzoxazone 6-hydroxylation	858
CYP3A4	Testosterone 6□-hydroxylation	2890

CYP3A4	Midazolam 1'-hydroxylation	1515

glucose 6-phosphate, glucose 6-phosphate dehydrogenase (1.5 U/mL), 50 mM phosphate buffer (pH 7.4), and 0.05 mg/mL or 0.12 mg/mL microsomal protein and [^{14}C]BAY 94-9172 (0.5 µM) in a total volume of 0.5 mL. After 5 min pre-incubation at 37°C, the reaction was initiated by the addition of the NADPH-generating system. The enzyme kinetic parameters were determined by applying [^{14}C] BAY 94-9172 (0.04 – 5 µM) substrate and incubated with 0.05 mg protein/mL for 10 min at 37°C. Mechanism-based inhibitors (1-amino-H-benzotriazole, furaphylline, diethyldithiocarbamate) microsomes were pre-incubated with inhibitors in the presence of NADPH-generating system at 37°C for 20 min before the reaction was initiated by addition of [^{14}C]BAY 94-9172. Fluvoxamine, azamulin, ketoconazole, 4-methylpyrazole, HET0016, quinidine, benzylphenobarbital, sulfaphenazole, quercetin, and montelukast were then incubated with substrate simultaneously. The Incubations were terminated after 20 min by addition of 200 µL acetonitrile. Precipitated proteins were removed by centrifugation (14000 rpm, 3 min) and the supernatant was analyzed by HPLC with off-line radioactivity detection.

Incubation of [^{14}C]BAY 94-9172 ([^{14}C]ZK 6057184) with Human Recombinant CYP Isoforms (b) (4)): Mixtures contained 50 mM phosphate buffer (pH 7.4), 1 mM EDTA, a NADPH-generating system (1 mM NADP, 5 mM glucose 6-phosphate, 1.5 U/mL glucose 6-phosphate dehydrogenase), 0.5 µM [^{14}C]ZK 6057184 and CYP isoforms in a total volume of 0.5 mL was incubated in this study. The reaction was initiated following the addition of NADPH-generating system after 5 min preincubation at 37°C. Final concentration of 50 or 100 pmol CYP/mL of CYP1A2, 2A6, 2B6, 2C8, 2C9, 2C18, 2C19, 3A5, 3A7, 4A11, 4F3A-CYP isoforms and final concentration of 2 pmol/mL of CYP1A1 and 2J2 were used while 10 pmol CYP/mL concentrations of CYP2D6, 2E1, 3A4, 4F2, 4F3B, and 4F12 was applied for this study. The incubations were terminated after 60 min by adding acetonitrile (200 µL), the precipitated proteins were removed by centrifugation (14000 rpm, 3 min) and the supernatant was analyzed by HPLC with off-line radioactivity detection.

Results:
The formation of metabolites following the incubation of [^{14}C]BAY 94-9172 at substrate concentration levels (0.5, 2 and 10 µM) with human liver microsomes demonstrates pronounced degradation of the parent compound at low substrate concentration and high microsomal protein concentration as shown in Table 47.

Table 47: BAY 94-9172: Formation of metabolites in human liver microsomes

			HPLC Analysis		
[^{14}C]BAY 94-9172 (µM)	**Protein Concentration (mg/mL)**	**Incubation time (min)**	**[^{14}C]BAY 94-9172 (%)**	**M-1 (%)**	**Polar metabolite fraction (%)**
10	0.5	60	38.3	27.6	8.7
2	0.5	60	7.0	46.2	18.1

0.5	0.12	20	33.7	47.8	3.3
0.5	0.05	20	78.9	15.6	0.33

The data obtained from incubation of a panel of 19 CYP isoforms with [^{14}C]BAY 94-9172 (0.5 µM) the quantitative investigation of the formation of M-1 and the polar metabolite fraction as presented by the sponsor is shown in Figure 69. The data indicates that the formation rate of metabolite M-1 was most pronounced with CYP1A1, 2J2, 4F2, 4F3B, and 4F12 while most other CYP isoforms such as CYP2C8, 2D6, and 3A4 catalyzed M-1 formation to a small extent. It was found that the formation of the polar metabolite fraction was also catalyzed by several CYP isoforms but less efficiently compared with M-1 formation. The formation rate of the polar metabolite fraction was however most significant with CYP3A4 followed by 2J2, 1A1, 4F3b, and 4F12, respectively. The calculated enzyme kinetic parameters indicate that the formation of M-1 was consistent with Michaelis-Menten kinetics. The substrate inhibition and other kinetic parameters showed that K_m value was 1.2 µM, V_{max} was 912 pmol metabolite M-1/min/mg protein and the K_i value was 1.9 µM as shown in Table 48, Figure 70 and Figure 71. The IC_{50} on CYP3A4 inhibition was 1.7 µM.

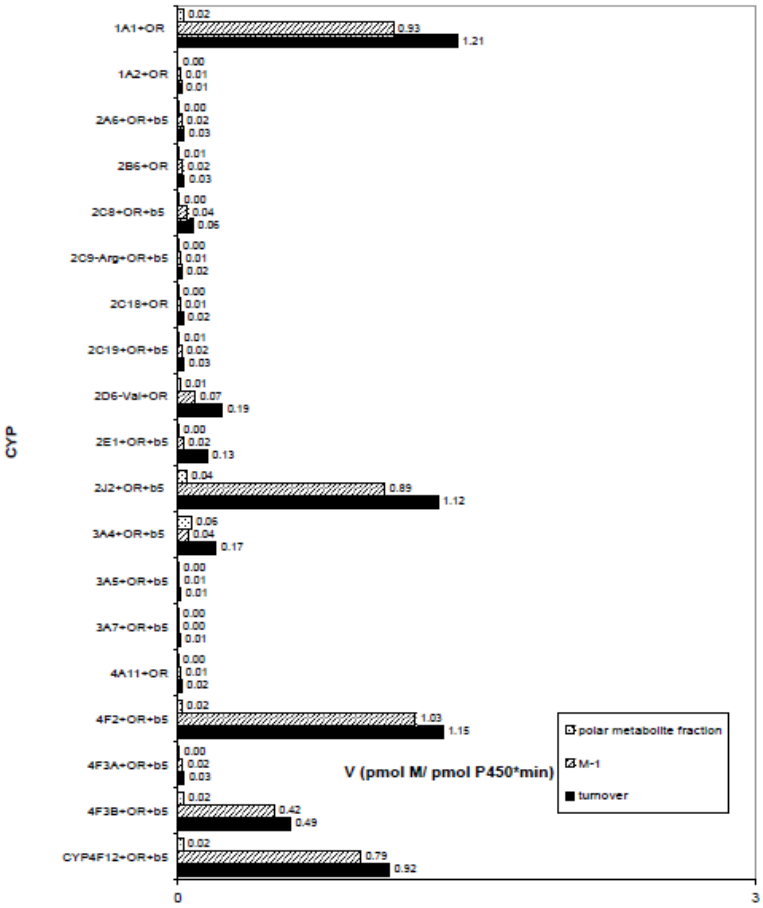

Figure 69: BAY 94-9172: Metabolite formation by screening a panel of human recombinant CYP isoforms (b) (4) at a concentration of 0.5 µM [^{14}C]BAY 94-9172

Table 48: BAY 94-9172: Determination of kinetic parameters of M-1 formation applying human liver microsomes

GCM 2079 G	N	C (µM)	(%)	M-1 formation (nmol/mL)	V/c	[pmol M-1/(mg-min)]
01+02	2	5.0	2.3	0.1153	46.10	230.5
03+04	2	2.0	8.6	0.1711	171.1	342.2
05+06	2	1.0	16.4	0.1638	327.5	327.5
07+08	2	0.5	24.2	0.1211	484.4	242.2
09+10	2	0.17	33.2	0.05539	663.3	110.8
11+12	2	0.08	36.9	0.02948	737.0	58.96
13+14	2	0.04	39.3	0.01403	786.2	28.07
15+16	2	0.008	41.3	0.003308	826.9	6.615

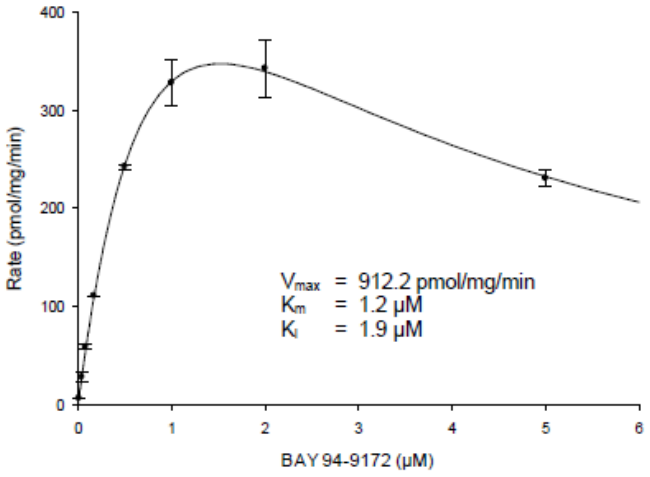

Figure 70: BAY 94-9172: Michaelis Menten plot of incubation of [^{14}C]florbetaben with human liver microsomes (formation of M-1, experiment GCM 2079 G)

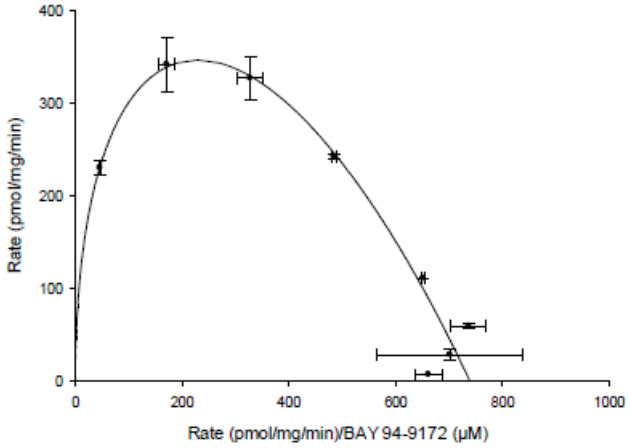

Figure 71: BAY 94-9172: Eadie-Hofstee plot of incubation of [^{14}C]florbetaben with human liver microsomes (formation of M-1, experiment GCM 2079 G)

In a follow-up study to substantiate the contributions of single CYP isoforms present in human liver, the effects of mechanism-based and competitive inhibitors of single CYP isoforms on M-1 formation in pooled human liver microsomes were investigated. Table 49 indicates that preincubation with 1-aminobenzotriazole (1000 µM) almost abolished N-demethylation of [^{14}C]BAY 94-9172, suggesting this pathway to be CYP-mediated. Furafylline (20 µM) and fluvoxamine (3 µM) (selective CYP1A2 inhibitors) failed to considerably affect M-1 formation while CYP isoform-selective inhibitors such as quinidine (5 µM, CYP2D6), montelukast (1 µM, CYP2C8), sulfaphenazole (10 µM, CYP2C9), and benzylphenobarbital (5 µM, CYP2C19) exhibited no considerable inhibitory effects on M-1 formation. However, quercetin (10 µM) another CYP2C8 inhibitor which is less CYP2C8-selective and activities of CYP3A4 as well as

some other CYP isoforms seem to be affected. Thus, the inhibitory effect of quercetin (57% of control) on M-1 formation seems more pronounced than in case of montelukast. The data also demonstrates a moderate decrease of M-1 formation to approx. 60 – 70% of control following an addition of methylpyrazole (200 µM) or diethyldithiocarbamate (50 µM), both CYP2E1 inhibitors.

Table 49: BAY 94-9172: Influence of different CYP isoform-selective inhibitors on M-1 formation from [^{14}C]BAY 94-9172 (1 µM) catalyzed by human liver microsomes (0.05 mg protein/mL)

GCM 2079 O	Inhibitor	c [Inhibitor] [µM]	M-1 % of control
1-4	Control*		
5+6	1-Amino-1H-benzotriazole*	1000	3.4
7+8	Dieethyldithiocarbamate*	50	72.3
11+12	Furaphylline*	20	99.6
15-18	Control		
21+22	Azamulin	1	105.1
23+24	Ketoconazole	10	31.7
25+26	Ketoconazole	1	69.0
27+28	4-Methylpyrazole	200	57.6
29+30	Quinidine	5	101.2
31+32	Benzylphenobarbital	5	104.0
63+64	Sulfaphenazole	10	94.8
67+68	Quercetin	10	57.6
47+48	Montelukast	1	97.0
53+54	HET0016	10	9.2
55+56	HET0016	0.1	19.0
88	Fluvoxamine	3	85.5

* = preincubation 20 min

HET0016 is described as a CYP2J2 inhibitor, however, it is also capable of inhibiting CYP4F enzymes and addition of 10 µM HET0016 to incubations significantly reduced formation of M-1 to 9% of control. The inhibitory effect of HET0016 (0.1 µM) on M-1 formation (19% of control) is primarily due to inhibition of the CYP4F enzyme family. Azamulin and ketoconazole are both CYP3A4/A5 inhibitors; however, azamulin (1 µM) demonstrated no effect on M-1 formation, whereas ketoconazole (1 µM) moderately altered (71% of control) demethylation of Florbetaben. Higher ketoconazole concentration (10 µM) inhibited M-1 formation more pronouncedly (32% of control). Apart from CYP3A4, ketoconazole is also an inhibitor of CYP4F2 and 4F12, thus, the sponsor suggested that a decrease in Florbetaben demethylation could be due mainly to inhibition of these enzymes and not caused by CYP3A4 inhibition. The data from the inhibition studies indicates major contribution of CYP2J2 and CYP4F2, 4F3b, and 4F12 to M-1 formation in human liver. The sponsor expanded the scope of the study by increasing the formation of polar metabolites and incubating [^{14}C]BAY-94-9172 with 0.12 mg protein/mL and 4-methylpyrazole, HET0016, azamulin, and ketoconazole (CYP isoform-selective inhibitors). As shown in Table 50, HET0016 (10 µM), ketoconazole, and azamulin reduced formation of the polar metabolite fraction suggesting that CYP2J2 and 3A4 contribute to this metabolic pathway.

Table 50: BAY 94-9172: Influence of different CYP isoform-selective inhibitors on M-1 and polar metabolite formation from [^{14}C]BAY 94-9172 (0.5 µM) catalyzed by human liver microsomes (0.12 mg protein/mL)

GCM 2079 O	**Inhibitor**	**c[Inhibitor] [µM]**	**M-1 % of control**	**Polar metabolite fraction % of control**
75-77	Control			
78+79	Azamulin	1	106.6	83.6

80+81	Ketaconazole	1	75.6	72.2
82+83	4-Methylpyrazole	200	70.3	97.1
84+85	HET0016	10	18.9	65.9
86+87	HET0016	0.1	36.2	132.8

Reviewer's Comments: Agrees with the result of this study which suggests that BAY 94-9172 is a substrate of several CYP isoforms in human. This study follows up on earlier findings showing that BAY 94-9172 undergoes two oxidative pathways in human liver microsomes involving N-methylation and formation of polar metabolites. During the study, the sponsor adequately consider the low mass dose (<100 µg) of BAY 94-9172 involved in the tracer before selecting the low substrate (0.5 µM) as the preferred concentration for the in vitro assay. A selection of higher substrate concentrations such as 2 µM would have failed to reflect the metabolite's kinetic parameters of the metabolite of the tracer when administered in the clinic. This *in vitro* CYP phenotyping study evaluated the CYP isoforms contributing to the oxidative metabolism of BAY 94-9172. The study demonstrated the affinity of [^{14}C]ZK 6057184 to CYP isoforms in human liver microsomes as indicated by a K_m value of 1.2 µM. The data shows that several CYP isoforms such as CYP1A1, 2J2, 4F2, 4F3b, and 4F12 are involved in the N-demethylation, whereas CYP2J2 and 3A4 contributed to formation of polar metabolites. The data from incubation of [^{14}C]BAY 94-9172 (0.5 µM) with human liver microsomes in the presence of CYP isoform-selective inhibitors confirmed the contribution of several CYP isoforms to the oxidative metabolism and no significant involvement of polymorphic enzymes CYP2C19 and 2D6 was observed. However, despite the data from this study suggesting that the tracer is a substrate of CYP isoforms in human, this reviewer opined that once [^{14}C]BAY 94-9172 is administered at the clinical dose, the plasma levels of the tracer would be too low for any polymorphic CYPs or any significant alterations to occur even when single CYP inhibitors are co-administered to the patients. Thus, the human CYP isoforms is not expected to significantly alter the metabolism of [^{14}C]BAY 94-9172.

Study title: A49560: Positron emission tomographic evaluation of compound [^{18}F]BAY 1008472 and [^{18}F]BAY 949172 in rhesus monkey.

Key study findings: This study examined the PET evaluation of [^{18}F]BAY 949172 and [^{18}F]BAY 1008472 ([^{18}F]BAY 6) in two female rhesus monkeys. Similar brain uptake and metabolic stability were demonstrated by [^{18}F]BAY 949172 and [^{18}F]BAY 1008472. However [^{18}F]BAY 1008472 showed a much faster uptake than [^{18}F]BAY 949172. The *in vitro* quantitative profiles of the two tracers seems to relatively favor [^{18}F]BAY 1008472 better than [^{18}F]BAY 949172 in that [^{18}F]BAY 1008472 demonstrates lower nonspecific binding and faster wash-out than [^{18}F]BAY 949172.

Study No.	A49560
Study Report Location:	4.2.2.2. Pages 1-41
Conducting laboratory Location:	Andrea Varrone, Balázs Gulyás, Christer Halldin Karolinska Institute, The Psychiatry Section, Department of Clinical Neuroscience, Karolinska Hospita,

	SE-17176 Stockholm, Sweden
GLP Compliance:	No
QA Statement:	No
Drug, lot #, and % purity:	[^{18}F]BAY 949172 and [^{18}F]BAY 1008472 lot #- and purity- Not provided.

Study Design: The study was conducted using two female rhesus monkeys (weighing 3.55-4.85 kg) owned by the Psychiatry Section, Department of Clinical Neuroscience, Karolinska Institutet. The animals were anesthetized by an intramuscular injection of ketamine hydrochloride and maintained by administration of a mixture of isoflurane (2-8 %), O_2 and medical air after endotracheal incubation. The head was immobilized with a fixation device and the body temperature, ECG, heart rate, blood pressure, respiratory rate and oxygen saturation were continuously monitored throughout the experiments. HRRT research tomography (CTI) with an in plane spatial resolution of < 1.5 mm was employed as the PET scanner during the study. List mode data were acquired continuously for 123 min immediately after intravenous injection and the image reconstruction was performed using OP-3D-OSEM with PSF modeling with a series of frames of increasing duration (9x20 sec, 3x60 sec, 5x180 sec, 17x360 sec). Data on image quantification, Time Activity Curves (TAC) of standard uptake values (SUV, expressed in %), made for the following regions-of-interest (ROI): Thalamus, Temporal cortex, Frontal cortex, White matter (at the level of the Centrum Semiovale), Cerebellum and Whole Brain were obtained. The sponsor performed two PET measurements with [^{18}F]BAY 949172 and [^{18}F]BAY-6 on each of the rhesus monkeys as shown in Table 51.

Table 51: PET measurements with [^{18}F]BAY 949172 and [^{18}F]BAY 6

Monkey No.	**Compound**	**Injected activity [MBq]**	**Radiochem. Purity %**	**Specific activity [Ci/mmol]**
0408106 (1)	BAY 949172	145	>99%	2954
0707122 (3)	BAY 949172	166	>99%	624
0408106 (1)	BAY-6	167	>97%	491
0707122 (3)	BAY-6	158	>94%	791

Venous blood samples collected at 4, 15, 30, 45, 60 and 90 min after radioligand injection were centrifuged at 2,000 × g for 4 min to obtain plasma (0.5 mL) and the plasma was mixed with acetonitrile (0.7 mL). The supernatant acetonitrile–plasma mixture and the precipitate obtained were counted in a NaI well counter for radioactivity.

Results:

Brain Uptake and Time Activity- The sponsor provided detailed data obtained from brain uptake and time-activity of [^{18}F]BAY 949172 and [^{18}F]BAY 1008472 injected to the monkeys during this study. Sponsor's Figure 1 is a representative PET images of [^{18}F]BAY 949172 and [^{18}F]BAY-6 indicating that [^{18}F]BAY-6 showed similar uptake and lower retention in the brain as

compared with [^{18}F]BAY 949172 (Figure 72 A). Lower retention is shown at the level of the cortex, subcortical regions (e.g. thalamus) and white matter (Figure 72 B and C).

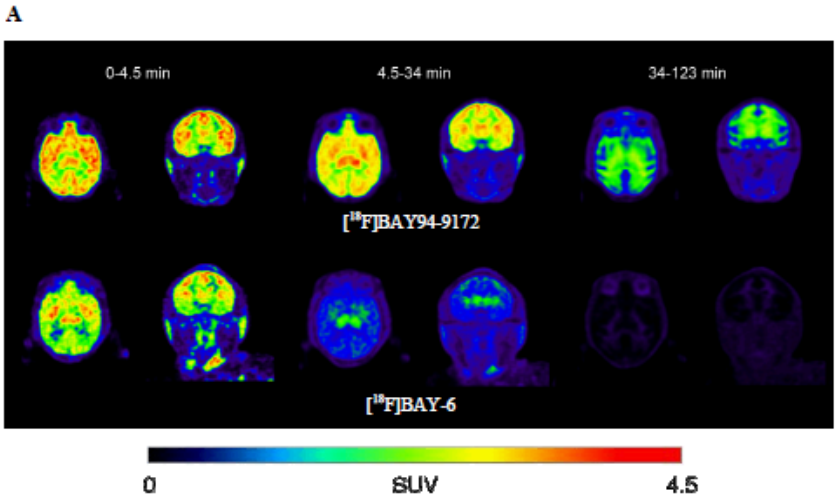

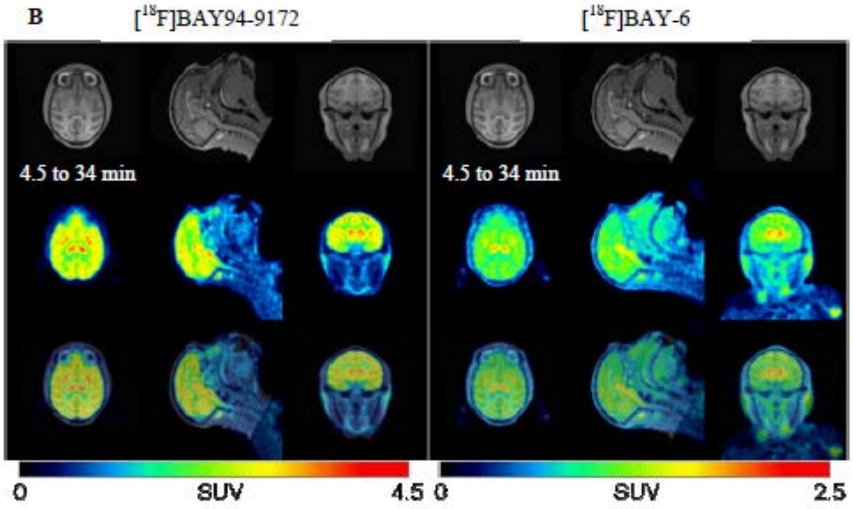

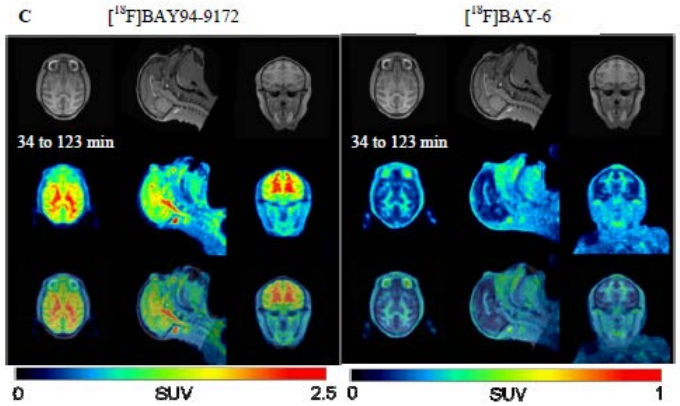

Figure 72: A-C: PET images of [18F]BAY 949172 and [18F]BAY-6 in Monkey 3 at different time intervals after the injection.

(A) PET images of [18F]BAY 949172 and [18F]BAY-6 in Monkey 1 coregistered to the MRI (B and C). Because of the more rapid wash-out from the brain (see A), in B and C the images of [18F]BAY-6 are displayed with a different range of SUV values

The sponsor provided time-activity curves representing whole brain uptake and regional brain uptake of [18F]BAY 949172 and [18F]BAY-6 as shown in Figure 73 A and B. The data showed that the time of peak uptake of [18F]BAY 949172 was between 1.8 and 2.6 min and the peak brain uptake was 239-347% SUV. The peak to 120 min used as an indicator of the wash-out was calculated by dividing the ratio of radioactivity at peak divided by the activity at 120 min and the peak-to-120 min was 2.7-4.5. [18F]BAY-6 showed similar brain uptake and faster wash-out as compared with [18F]BAY 949172 (Figure 73 A and B and (Table 52).

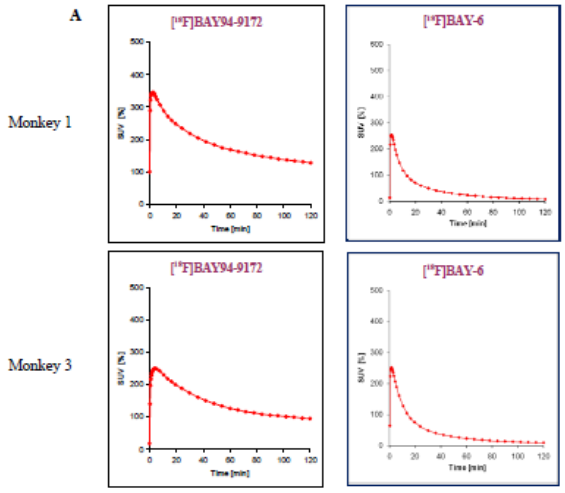

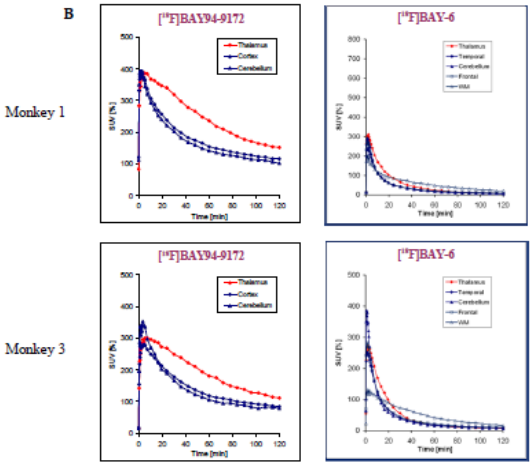

Figure 73: Time activity curves for the whole brain uptake (A) and the regional uptake (B) in thalamus, cortex and cerebellum of [^{18}F]BAY 949172 and [^{18}F]BAY-6 in Monkeys 1 and 3

Table 52: Quantitative parameters evaluated in the comparison between [^{18}F]BAY 949172 and [^{18}F]BAY 6

	Monkey 2		**Monkey 2**	
	[^{18}F]BAY 949172	**[^{18}F]BAY 6**	**[^{18}F]BAY 949172**	**[^{18}F]BAY 6**
Time to peak (min)	2.5	1.5	4.5	1.5
Peak brain uptake (%SUV)	343	253	250	251
Peak-to-120 min	2.7	29.9	2.5	26.1

Metabolism- The analysis of the plasma samples obtained from the monkeys demonstrates that the metabolism of [^{18}F]BAY 949172 was relatively fast with approximately 8-10% of the parent present in the plasma within 30 min and less than 5% after 90 min (Figure 73). Similarly, [^{18}F]BAY-6 showed fast metabolism *in vivo*. As shown in Figure 73, the percent of unchanged radioligand in Monkey 1 and 3 was 48% and 63% at 4 min and 14% and 4% at 30 min, respectively.

Reviewer's Comments: The PET images obtained during this study showed that [^{18}F]BAY 949172 and [^{18}F]BAY 1008472 demonstrated similar brain uptake and metabolism stability in the rhesus monkeys. The PET images indicate that the retention of the tracers were much lower at the level of the cortex, subcortical regions (e.g. thalamus) and white matter. This probably supports the proposed indication of [^{18}F]BAY 949172 which is PET imaging of the amyloid beta plagues that does not concentrate on the white matter but the grey matter. This helps the utility

of [^{18}F]BAY 949172 in the clinic. It is interesting to note that though the PET images of [^{18}F]BAY 949172 and [^{18}F]BAY-6 indicate similar uptake [^{18}F]BAY-6 demonstrates lower retention in the brain than [^{18}F]BAY 949172. This seems to suggest better potential clinical utility for [^{18}F]BAY-6 than [^{18}F]BAY 949172.

6 General Toxicology

6.1 Single-Dose Toxicity

Study title: Study A35105: Acute intravenous toxicity study of polythyleneglycol (PEG)-stilbene in the rat.

Key study findings: The administration of polythyleneglycol (PEG)-stilbene at doses 0, 50, 100 and 400 µg/kg (0, 116X, 233X and 930X MHD) caused no serious treatment-related alterations in the functional and histopathological parameters assessed. The NOAEL as determined in this study was 50 µg/kg (116X MHD).

Study no.: Study A35105

Pages: 1-215

Conducting laboratory and location: (b) (4) (b) (4)

Date of study initiation: February 23, 2006

GLP compliance: Yes

QA report: yes (x) no ()

Reference ID: 3361527

Drug, lot #, and % purity: Polyethyleneglycol (PEG)-stilbene, lot # K05-095;WZ-N99-86-22, and >99.7% purity

Methods

Doses: 0, 50, 100 and 400 µg/kg (116X, 233X and 930X MHD)

Species/strain: Rat/Sprague Dawley

Number/sex/group or time point (main study): A total of 8 animals (male and female) composed of 4 rats/sex/dose for acute toxicity conducted in 2 separate studies as shown below:

Table 53: Animal allocation for the study

Group	Animal No./Sex	Dose	Observation Days
T01	1M-4M 5F-8F	0 (vehicle)	2
T02	9M-12M 13F-16F	50 µg/kg	2
T03	17M-20M 21F-24F	100 µg/kg	14

Group	Animal No./Sex	Dose (mg)	Observation Days
T01	1M-4M 5F-8F	0 (vehicle)	2
T02	9M-12M 13F-16F	0.4	2
T03	17M-20M 21F-24F	0 (vehicle)	14
T04	25M-28M 29F-32F	0.4	14

Route, formulation, volume, and infusion rate: Intravenous administration,

formulated in the vehicle (20% w/v hydropropyl-beta-cyclodextrin).

Satellite groups used for toxicokinetics or recovery: None

Age: Not provided

Reference ID: 3361527

Weight: Not provided

Results:

Mortality: No mortality was reported in any of the animals.

Clinical signs: No serious clinical findings were reported in the animals.

Body weights: No treatment-related effect was reported on the body weight, organ/body weight or organ/organ ratios.

Food consumption: The treatment did not affect food consumption.

Ophthalmoscopy: No treatment-related ophthalmoscopic finding was reported.

Hematology: No treatment related hematological effect was reported in the animals. Furthermore, the sponsor reported no treatment related effects on coagulation parameters.

Clinical chemistry: After administration of 100 µg/kg and 0.4 mg/kg (233X and 930X MHD), there were mild transient alterations in erythrocytic parameters in male rats, serum phosphorus in female rats and troponin I in males and female rats on Day 3.

Gross pathology: No treatment-related histopathology effects were observed in this study.

Organ weight: No treatment-related change in organ weight was reported. However, there was increased liver weight in treated female rats on Day 3.

Histopathology: Adequate Battery: yes (x), no ()—explain

Peer review: yes (x), no ()

Histopathology inventory (optional)

Study	Acute Study			
Species	Dog			
Adrenals	x *			
Aorta	X			
Bone Marrow smear	X			
Bone (femur)	X			
Brain	x *			
Cecum	X			
Cervix	X			
Colon	X			
Duodenum	X			
Epididymis	X			
Esophagus	X			
Eye	X			
Fallopian tube				
Gall bladder	X			
Gross lesions	X			
Harderian gland				
Heart	x *			

Reference ID: 3361527

Ileum	X			
Injection site	X			
Jejunum	X			
Kidneys	x *			
Lachrymal gland				
Larynx	X			
Liver	x *			
Lungs	x			
Lymph nodes, cervical	X			
Lymph nodes mandibular	X			
Lymph nodes, mesenteric	X			
Mammary Gland	X			
Nasal cavity				
Optic nerves	X			
Ovaries	X			
Pancreas	X			
Parathyroid	X			
Peripheral nerve				
Pharynx	X			
Pituitary	x			
Prostate	X			
Rectum	X			
Salivary gland	x			

Reference ID: 3361527

Sciatic nerve	X			
Seminal vesicles				
Skeletal muscle	X			
Skin	X			
Spinal cord	X			
Spleen	x *			
Sternum				
Stomach	X			
Testes	x *			
Thymus	x			
Thyroid	X			
Tongue	X			
Trachea	X			
Urinary bladder	X			
Uterus	x *			
Vagina	X			
Zymbal gland				

x, histopathology performed

*, organ weight obtained

Reviewer's Comment: Agrees with the result of this study which indicates that PEG-stilbene is relatively safe up to a dose of 166X MHD.

Study title: Study A35107: Acute intravenous toxicity study of polythyleneglycol (PEG)-stilbene in the rat.

Key study findings: In this study, the potential toxicity of polythyleneglycol (PEG)-stilbene was investigated at two dose levels (50 and 100 µg/kg -116X and 233X MHD). The animals were observed over a period of 2 days and sacrificed on Day 3 and no mortality and no clinical signs of toxicity, changes in clinical chemistry or any effect on gross necropsy or histopathological parameters was reported in this study. The NOAEL for this compound was determined to be 100 µg/kg (233X MHD).

Study no.: A35107

Page #: 1-174

Conducting laboratory and location: (b) (4)

Date of study initiation: May 31, 2006

GLP compliance: Yes

QA report: yes (x) no ( )

Drug, lot #, and % purity: Polyethyleneglycol (PEG)-stilbene, lot # K05-095;WZ-N99-86-22, and >95.4% purity

Methods

Doses: 0, 50 and 100 µg/kg (0, 116X and 233X MHD)

Species/strain: Rat/Sprague Dawley

Number/sex/group or time point (main study): 4 rats/sex/dose for the acute toxicity study.

The test groups and the control groups were administered single dose of PEG-stilbene and the vehicle and the animals were observed for 2 days for signs of toxicity throughout the experimental period. Full gross necropsy was performed on all surviving animals on Day 3 and histopathology was performed on tissues showing gross necropsy -+abnormalities.

Route, formulation, volume, and infusion rate: Intravenous administration, formulated in the vehicle (20% w/v hydropropyl-beta-cyclodextrin).

Satellite groups used for toxicokinetics or recovery: None

Age: Not provided

Weight: 190 and 210 g

Results:

Mortality: No mortality was reported during this study.

Clinical signs: No serious clinical findings were reported in any of the animals.

Body weights: No treatment-related effect was reported on the body weight, organ/body weight or organ/organ ratios.

Hematology: No treatment-related hematological effect was reported in the animals.

Clinical chemistry: No significant test item related-effects on blood biochemistry parameters were observed during the study period up to 233X MHD.

Gross pathology: No treatment-related histopathology effects were observed in this study.

Organ weight: No treatment-related change in organ weight was reported.

Histopathology: Adequate Battery: yes (x), no ()—explain

Peer review: yes (x), no ()

Histopathology inventory (optional)

Study	Acute			

Reference ID: 3361527

	Study			
Species	Dog			
Adrenals	x *			
Aorta	x			
Bone Marrow smear	x			
Bone (femur)	x			
Brain	x *			
Cecum	x			
Cervix	x			
Colon	x			
Duodenum	x			
Epididymis	x			
Esophagus	x			
Eye	x			
Fallopian tube				
Gall bladder	x			
Gross lesions	x			
Harderian gland				
Heart	x *			
Ileum	x			
Injection site	x			
Jejunum	x			
Kidneys	x *			
Lachrymal gland				

Larynx	x			
Liver	x *			
Lungs	x			
Lymph nodes, cervical	x			
Lymph nodes mandibular	x			
Lymph nodes, mesenteric	x			
Mammary Gland	x			
Nasal cavity				
Optic nerves	x			
Ovaries	x			
Pancreas	x			
Parathyroid	x			
Peripheral nerve				
Pharynx	x			
Pituitary	x			
Prostate	x			
Rectum	x			
Salivary gland	x			
Sciatic nerve	x			
Seminal vesicles				
Skeletal muscle	x			
Skin	x			
Spinal cord	x			

Spleen	x *			
Sternum				
Stomach	x			
Testes	x *			
Thymus	x			
Thyroid	x			
Tongue	x			
Trachea	x			
Urinary bladder	x			
Uterus	x *			
Vagina	x			
Zymbal gland				

x, histopathology performed

*, organ weight obtained

Reviewer's Comment: In this study, the sponsor validates the earlier study (A35105) and also established an acceptable safety margin (233X MHD) for this compound if administered at the proposed 30 µg mass dose. No potential toxicity was demonstrated at the employed doses in this study.

Study title: **A35109: Single intravenous dose toxicity study of PEGN3.HCL in New Zealand White rabbits followed by 14 days recovery**

Key study findings: The sponsor investigated the potential toxicity of administration of single dose PEGN3.HCL at doses 0, 4.9, 24.4 and 48.8 µg/kg (0, 11.4X, 56.7X and 113.5X MHD) followed by 14 days recovery in rabbits. The administration caused no serious treatment-related alterations in the functional and histopathological parameters assessed in this study. The NOAEL for this compound as determined by the endpoint assessed in this study was 48.8 µg/kg (113.5X MHD).

Study no.: (b) (4) M390-05

Page #: Pages 1-320

Conducting laboratory and location: (b) (4)

Date of study initiation: November 21, 2005

GLP compliance: Yes

QA report: yes (x) no ()

Drug, lot #, and % purity: PEGN3.HCL, lot # K05-095;WZ-N99-86-22, and >95.4% purity

Methods

Doses: 0, 4.9, 24.4 and 48.8 µg/kg

Species/strain: Rabbit/New Zealand

Number/sex/group or time point (main study): 3 rabbits/sex/dose as shown below:

Table 54: Animal allocation employed during the study

		Dose Levels			
Group	**Treatment**	**MHD**	**(µg/kg)**	**Dose Volume (mL/kg)**	**Concentration (µg/mL)**
1	Vehicle	0	0	1	0
2	PEGN3.HCl	11.4	4.9	1	4.88
3	PEGN3.HCl	56.7	24.4	1	24.40
4	PEGN3.HCl	113.5	48.8	1	48.80

Three males and females per each group were necropsied on Days 3 and 15.

Route, formulation, volume, and infusion rate: Intravenous administration, formulated in the vehicle (hydropropyl-beta-cyclodextrin).

Satellite groups used for toxicokinetics or recovery: None

Age: 13. 6 weeks (females) 14.6 weeks (males)

Weight: 2.0 – 2.8 kg (females) 2.2 -3.0 kg (males)

Results:

Reference ID: 3361527

Mortality: No mortality was reported.

Clinical signs: No serious clinical findings were reported in these studies.

Body weights: No treatment related effect was reported on the body weight, organ/body weight o organ/organ ratios.

Food consumption: The treatment did not affect food consumption.

Hematology: No treatment related hematological effect was reported in the animals. However, there were sporadic changes in the hematological parameters within baseline values.

Clinical chemistry: There were mild transient alterations in serum liver transaminase enzymes (ALT and AST) at 48.8 µg/kg in one male rabbit on Day 3.

Gross pathology: No treatment-related histopathology effects were observed in this study.

Organ weight: No treatment-related change in organ weight was reported. However, there were sporadic organ weight changes from the control due to inter-animal variations.

Histopathology: Adequate Battery: yes (x), no ()—explain

Peer review: yes (x), no ()

Histopathology inventory (optional)

Study	Acute Study			
Species	Dog			
Adrenals	x *			
Aorta	x			
Bone Marrow smear	x			
Bone (femur)	x			
Brain	x *			

Cecum	x			
Cervix	x			
Colon	x			
Duodenum	x			
Epididymis	x			
Esophagus	x			
Eye	x			
Fallopian tube				
Gall bladder	x			
Gross lesions	x			
Harderian gland				
Heart	x *			
Ileum	x			
Injection site	x			
Jejunum	x			
Kidneys	x *			
Lachrymal gland				
Larynx	x			
Liver	x *			
Lungs	x			
Lymph nodes, cervical	x			
Lymph nodes mandibular	x			
Lymph nodes, mesenteric	x			

Mammary Gland	x			
Nasal cavity				
Optic nerves	x			
Ovaries	x			
Pancreas	x			
Parathyroid	x			
Peripheral nerve				
Pharynx	x			
Pituitary	x			
Prostate	x			
Rectum	x			
Salivary gland	x			
Sciatic nerve	x			
Seminal vesicles				
Skeletal muscle	x			
Skin	x			
Spinal cord	x			
Spleen	x *			
Sternum				
Stomach	x			
Testes	x *			
Thymus	x			
Thyroid	x			
Tongue	x			

Reference ID: 3361527

Trachea	x			
Urinary bladder	x			
Uterus	x *			
Vagina	x			
Zymbal gland				

x, histopathology performed

*, organ weight obtained

Reviewer's Comment: Agrees with the results of this study.

Study title: A35106: Acute intravenous toxicity study of Polyethyleneglycol (PEG)-stilbene in the rabbit.

Key study findings: The sponsor investigated the potential toxicity of intravenous administration of single dose PEGN3.HCL at 25 and 250 µg/kg (58.1X and 581X MHD) followed by 14 days observation period in rabbits. The administration caused no mortality or any serious treatment-related alterations in the functional and histopathological parameters assessed in this study. The NOAEL obtained in the study was 250 µg/kg (581X MHD).

Study no.: (b) (4) M390-05

Page #: 1-186

Conducting laboratory and location: (b) (4)

Date of study initiation: April 12, 2006

GLP compliance: Yes

QA report: yes (x) no ()

Drug, lot #, and % purity: PEGN3.HCL, lot # K05-095;WZ-N99-86-22, and >95.4% purity

Methods

Doses: 0, 25 and 250 µg/kg (0, 58.1X and 581X MHD)

Species/strain: Rabbit/New Zealand

Number/sex/group or time point (main study): 3-4 male rabbits/dose as shown below:

Table 55: Animal allocation for the study

Group	Animal No./(n)	Dose	Observation Days
T01	1M-3M/(3)	0 (vehicle)	14
T02	4M-7M/(4)	250 µg/kg	14
T03	8M-11M/(4)	25 µg/kg	14

Route, formulation, volume, and infusion rate: Intravenous administration, formulated in the vehicle (hydropropyl-beta-cyclodextrin).

Satellite groups used for toxicokinetics or recovery: None

Age: 10 - 14 weeks

Weight: 2.20 – 2.59 kg

Results:

Mortality: No mortality was reported in any of the rabbits.

Clinical signs: No treatment-related clinical findings were reported in the rabbits.

Body weights: No treatment related effect on the body weight, organ/body weight or organ/organ ratios was reported.

Food consumption: The treatment did not affect food consumption.

Ophthalmoscopy: No treatment-related ophthalmoscopic finding was reported.

Hematology: No treatment related hematological effect was reported in the animals.

Clinical chemistry: However, there were elevated troponin levels on Day 15 in both treated groups and the vehicle control. There were also elevated AST and ALT values in one animal administered 581X MHD on Day 3.

Gross pathology: No treatment-related adverse gross effects were observed in this study.

Organ weight: No treatment-related change in organ weight was reported.

Histopathology: Adequate Battery: yes (x), no ()—explain

Peer review: yes (x), no ()

Histopathology inventory (optional)

Study	Acute Study			
Species	Dog			
Adrenals	x *			
Aorta	x			
Bone Marrow smear	x			
Bone (femur)	x			
Brain	x *			
Cecum	x			
Cervix	x			
Colon	x			
Duodenum	x			
Epididymis	x			
Esophagus	x			
Eye	x			
Fallopian tube				
Gall bladder	x			
Gross lesions	x			
Harderian gland				
Heart	x *			
Ileum	x			

Injection site	x			
Jejunum	x			
Kidneys	x *			
Lachrymal gland				
Larynx	x			
Liver	x *			
Lungs	x			
Lymph nodes, cervical	x			
Lymph nodes mandibular	x			
Lymph nodes, mesenteric	x			
Mammary Gland	x			
Nasal cavity				
Optic nerves	x			
Ovaries	x			
Pancreas	x			
Parathyroid	x			
Peripheral nerve				
Pharynx	x			
Pituitary	x			
Prostate	x			
Rectum	x			
Salivary gland	x			
Sciatic nerve	x			

Reference ID: 3361527

Seminal vesicles				
Skeletal muscle	x			
Skin	x			
Spinal cord	x			
Spleen	x *			
Sternum				
Stomach	x			
Testes	x *			
Thymus	x			
Thyroid	x			
Tongue	x			
Trachea	x			
Urinary bladder	x			
Uterus	x *			
Vagina	x			
Zymbal gland				

x, histopathology performed

*, organ weight obtained

The NOAEL obtained from this study was 250 µg/kg (581X MHD).

Reviewer's Comment: Agrees with the results of this study.

6.2 Repeat-Dose Toxicity

Study title: **Study A141484: ZK 6057184- Repeated-dose toxicity study in male and female rats with daily intravenous injection over a period of 4 weeks followed by a recovery period of 4 weeks.**

Key study findings: The administration of polythyleneglycol (PEG)-stilbene at the lowest employed dose of 45 µg/kg (105X MHD) caused no serious treat-related alterations in the functional and histopathological parameters assessed in this study. However, there were reported alteration in respiration in the first two weeks of treatment at 175 and 700 µg/kg (407X and 1628X MHD) treated groups. The NOAEL for this compound as determined by the endpoint assessed in this study was 45 µg/kg (105X MHD).

Study no.: A141484

Page #: Pages 1-1000

Conducting laboratory and location: Bayer Schering Pharma AG,

Nonclinical Drug Safety,

13342 Berlin, Germany

Date of study initiation: February 11, 2008

GLP compliance: Yes

QA report: yes (x) no ()

Drug, lot #, and % purity: ZK 6057184, Batch # CS1036KI, and 97.1% purity

Methods

Doses: 0, 45, 175 and 700 µg/kg (0, 105X, 407X and 1628X MHD)

Reference ID: 3361527

Species/strain: Rat/Wistar (Hsd CpB:WU)

Number/sex/group or time point (main study): 10 rats/sex/dose.

Route, formulation, volume, and infusion rate: Intravenous administration, formulated in the vehicle (20% w/v hydropropyl-beta-cyclodextrin).

Satellite groups used for toxicokinetics or recovery: Yes (6 rats/sex/dose).

Age: males - 8 weeks; females - 8 weeks.

Weight: Males - 217- 273 g

Females – 163 - 202 g

Results:

Mortality: No mortality was reported in any of the animals.

Clinical signs: No clinical findings were reported in animals administered 105X MHD. However, animals administered 407X MHD and higher doses of the test substance demonstrated transient accelerated and irregular respiration in the first 2 weeks of treatment. It was observed that the frequency of the respiratory changes increases with the administered doses.

Body weights: No treatment related effect was reported on the body weight, organ/body weight or organ/organ ratios.

Food consumption: The treatment did not affect food consumption.

Ophthalmoscopy: No treatment-related ophthalmoscopic finding was reported.

Hematology: No treatment related hematological effect was reported in the animals. Furthermore, the sponsor reported no treatment related effects on coagulation parameters.

Clinical chemistry: No treatment-related effect on clinical chemistry was reported. The few changes observed in the animals were regarded as non-treatment related because they were not dose related and/or found also in the controls.

Gross pathology: No treatment-related macroscopic effects were observed in this study. The sponsor also reported no test substance-related microscopic findings in this study. However, a number of microscopic findings were reported in the 175 and 700 µg/kg (407X and 1628X MHD and vehicle-treated groups. This include tubular vacuolation in the kidney, hypertrophy in the urinary bladder with vacuoles in urinary epithelia, presence of foamy macrophages in the lung, small intestine and lymph nodes and chronic inflammation at the injection site. The sponsor

Reference ID: 3361527

attributed these findings to the 20% w/v hydropropyl-beta-cyclodextrin vehicle. Previous findings and literature evidence have shown that cyclodextrin could be renally toxic and disruptive of biological membranes.

Organ weight: No treatment-related change in organ weight was reported.

Histopathology: Adequate Battery: yes (x), no ()—explain

Peer review: yes (x), no ()

Histopathology inventory (optional)

Study	Acute Study			
Species	Dog			
Adrenals	x*			
Aorta	x			
Bone Marrow smear	x			
Bone (femur)	x			
Brain	x*			
Cecum	x			
Cervix	x			
Colon	x			
Duodenum	x			
Epididymis	x*			
Esophagus	x			
Eye	x			
Fallopian tube				
Gall bladder	x			

Gross lesions	x			
Harderian gland				
Heart	x*			
Ileum	x			
Injection site	x			
Jejunum	x			
Kidneys	x*			
Lachrymal gland				
Larynx	x			
Liver	x*			
Lungs	x			
Lymph nodes, cervical	x			
Lymph nodes mandibular	x*			
Lymph nodes, mesenteric	x			
Mammary Gland	x			
Nasal cavity				
Optic nerves	x			
Ovaries	x*			
Pancreas	x*			
Parathyroid	x*			
Peripheral nerve				
Pharynx	x			
Pituitary	x*			

Prostate	x			
Rectum	x			
Salivary gland	x*			
Sciatic nerve	x			
Seminal vesicles				
Skeletal muscle	x			
Skin	x			
Spinal cord	x			
Spleen	x*			
Sternum				
Stomach	x			
Testes	x*			
Thymus	x*			
Thyroid	x			
Tongue	x			
Trachea	x			
Urinary bladder	x			
Uterus	x*			
Vagina	x			
Zymbal gland				

x, histopathology performed

*, organ weight obtained

Reviewer's Comment: The sponsor attributed the reported microscopic findings to the vehicle employed in this study and not the test substance. However, this explanation seems inadequate to this reviewer because no such microscopic findings were reported at a lower dose of 105X

MHD. The microscopic findings in the vehicle controls then complicates this study and it is difficult to ascertain the contributions of the administered test substance to the reported histological alterations in the major organs in rats treated with ≥407X MHD. A NOAEL of 115X MHD was established in this study,

Study title: **Study A42190: ZK 6057184- Repeated-dose toxicity study in male and female dogs with daily intravenous injection over a period of 4 weeks followed by a recovery period of 4 weeks.**

Key study findings: No treatment-related clinical findings or morphological changes were reported in dogs administered 12.5, 50 and 200 µg/kg (29X, 116X and 465X MHD) of ZK 6057184 in this study. NOAEL of 50 µg/kg (116X MHD) was determined in this study.

Study no.: A42190

Page #: 1-896

Conducting laboratory and location: Bayer Schering Pharma AG,

Nonclinical Drug Safety,

13342 Berlin, Germany

Date of study initiation: February 11, 2008

GLP compliance: Yes

QA report: yes (x) no ( )

Drug, lot #, and % purity: ZK 6057184, Batch # CS1036KI, and 97.1% purity

Methods

Doses: 0, 12.5, 50 and 200 µg/kg (0, 29X, 116X and 465X MHD)

Species/strain: dog/Beagle

Reference ID: 3361527

Number/sex/group or time point (main study): 3 dogs/sex/dose.

Route, formulation, volume, and infusion rate: Intravenous administration, formulated in the vehicle (20% w/v hydropropyl-beta-cyclodextrin).

Satellite groups used for toxicokinetics or recovery: Yes (3 dogs/sex/dose).

Age: males- 11-13 months; females – 11-13 months.

Weight: Males - 6.6 – 9.8 kg

Females - 7.2 – 8.9 kg

Results:

Mortality: No mortality was reported.

Clinical signs: No clinical findings were reported in animals administered up to 116X MHD. However, one of the dogs administered 465X MHD demonstrated spontaneous hyperactivity, spasms, coughing on Day 9.

Body weights: No treatment related effect was reported on the body weight, organ/body weight or organ/organ ratios.

Body temperature: No treatment-related effect was reported.

Food consumption: The treatment did not affect food consumption.

Electrocardiography and Heart rate: No treatment-related effect was observed. However, during weeks 1, 3 and 4, partial AV block was observed in one dog and bimodal waves was reported in another dog in the group administered 465X MHD.

Ophthalmoscopy: No treatment-related ophthalmoscopic finding was reported.

Hematology: No treatment related hematological effect was reported in the animals.

Coagulation: No treatment related effects on coagulation parameters.

Clinical chemistry: No treatment-related effect on clinical chemistry was reported. However, there were statistically significant changes in biochemical parameters including magnesium, potassium and total albumin levels of animals administered 465X MHD on Day 22. The magnitude of these changes to the controls is very small and not dose related. Thus, they were not considered dose-related.

Reference ID: 3361527

Gross pathology: No treatment-related microscopic and macroscopic effects were observed in this study and after the additional 4 weeks treatment free recovery period. Lesions reported at the application site in many treated and control animals showed full recovery after a 4-week-treatment recovery period.

Organ weight: No treatment-related change in organ weight was reported.

Histopathology: Adequate Battery: yes (x), no ()—explain

Peer review: yes (x), no ()

Histopathology inventory (optional)

Study	Acute Study			
Species	Dog			
Adrenals	x*			
Aorta	x			
Bone Marrow smear	x			
Bone (femur)	x			
Brain	x*			
Cecum	x			
Cervix	x			
Colon	x			
Duodenum	x			
Epididymis	x*			
Esophagus	x			
Eye	x			
Fallopian tube				

Gall bladder	x			
Gross lesions	x			
Harderian gland				
Heart	x*			
Ileum	x			
Injection site	x			
Jejunum	x			
Kidneys	x*			
Lachrymal gland				
Larynx	x			
Liver	x*			
Lungs	x			
Lymph nodes, cervical	x			
Lymph nodes mandibular	x*			
Lymph nodes, mesenteric	x			
Mammary Gland	x			
Nasal cavity				
Optic nerves	x			
Ovaries	x*			
Pancreas	x*			
Parathyroid	x*			
Peripheral nerve				
Pharynx	x			

Pituitary	x*			
Prostate	x			
Rectum	x			
Salivary gland	x*			
Sciatic nerve	x			
Seminal vesicles				
Skeletal muscle	x			
Skin	x			
Spinal cord	x			
Spleen	x*			
Sternum				
Stomach	x			
Testes	x*			
Thymus	x*			
Thyroid	x			
Tongue	x			
Trachea	x			
Urinary bladder	x			
Uterus	x*			
Vagina	x			
Zymbal gland				

x, histopathology performed

*, organ weight obtained

Reference ID: 3361527

Reviewer's Comment: The data indicates that the sponsor was able to demonstrate adequate safety margin for the proposed 30 µg dose of BAY 94-9172 in the planned study.

7 Genetic Toxicology

Study title: TOXT8078599: Evaluation of ZK 6057184 (ref. BAY 94-9172) in a bacterial reverse mutation study using Salmonella typhimurium (Ames-Test) and Escherichia coli

Key findings: This study was conducted to investigate whether ZK 6057184 (non-radioactive analogue of Florbetaben) up to a maximum recommended dose level of 5.0 mg/plate can induce point mutations in five strains of *Salmonella typhimurium* and in one strain of *Escherichia coli* in the absence and presence of a metabolic activation system (S9 mix). The data indicates that ZK 6057184 does not possess a mutagenic potential in the bacterial reverse mutation test.

Study no.: TOXT8078599

Pages: 1-39

Conducting laboratory and location: Bayer Schering Pharma AG,

Nonclinical Drug Safety

D-13342 Berlin,

Germany

Date of study initiation: January 9, 2008

GLP compliance: Yes

QA reports: yes (X) no ()

Drug, lot #, and % purity: ZK 6057184, lot #: not provided purity was 99.2%

Reference ID: 3361527

Methods:

ZK 6057184 was tested in the absence and presence of an extrinsic metabolizing system (S9 mix) containing Aroclor 1254- induced male rat liver homogenate (S9).

Strains/species/cell line: Four histidine-requiring strains of *Salmonella triphimurium* – TA1535, TA100, TA1537, TA1538 and TA98 and *Escherichia coli* tester strain WP2*uvr*A.

Doses used in definitive study: Doses tested for all tester strains ranges between 100 and 5000 µg/plate content (b) (4) in 0.11 - 5.525 mg/plate ZK 6057184 in the presence and absence of S9 mix.

Basis of dose selection: An initial preincubation testing was performed in all the strains including WP2*uvr*A in the presence and absence of S9 mix. In this study, there was no increased reversion to prototrophy in assays with ZK 6057184 at the doses tested between 0.1 – 5.0 mg/plate, either in the absence or presence of metabolic activation in all the test strains evaluated.

Vehicle controls: Comprised of treatment with dimethyl sulfoxide (DMSO)

Positive controls: The positive control chemicals were 2-nitrofluorene (2NF) for TA98, sodium azide (NaN_3) for TA100 and TA1535, anthracene-2-amine (2-AA) for TA1537, TA1538 and WP2*uvr*A.

Incubation and sampling times: Cultures of all organisms were prepared by overnight incubation (shaking for approximately 8 hours at 37°C) of freshly inoculated nutrient broth. The mutagenicity experiments with preincubation were carried out by adding 0.1 mL of the bacterial suspension, 0.05 mL of the test material, and 0.5 mL of 0.1 mol/L sodium phosphate buffer pH 7.4 or S9 mix to a sterile tube. The content was mixed thoroughly and incubated in a water bath at 37°C.

Results

Study validity: Revertant colonies were counted electronically or manually and the background lawn was inspected for signs of mutagenicity and test article precipitation. The arithmetic means of the number of mutant colonies of the 3 parallel plates in the negative control groups were compared with those of the compound groups. A positive response was considered if the

number of revertants of the compound groups compared to the number of revertants of the negative group was reproducibly higher than 2-fold. A dose-dependent increase in the number of revertants was also considered to indicate a mutagenic effect.

Study outcome: ZK 6057184 did not induce gene mutations by base-pair changes or frame-shifts in the genome of the *S. typhimurium* and *E. coli* strains used, when tested up to 5.0 mg/plate in the absence and presence of S9 mix.

Reviewer's comment: Agrees with the result of this study.

Study title: TOXT7078598: Evaluation of the clastogenic potential of ZK 6057184 (ref. BAY 94-9172) in human peripheral blood lymphocytes.

Key findings: The potential ability of BAY 94-9172 to induce chromosomal aberrations in human peripheral lymphocytes *in vitro* in the presence and absence of metabolic activation system was assessed. ZK 6057184 showed no clastogenic potential in the chromosomal aberration test in vitro with human lymphocytes either in the absence or in the presence of rat liver S9 when investigated up to concentrations of 50 µg/mL (first harvesting time) and 100 µg/mL (second harvesting time) at which precipitation of the test compound could be observed. However, the positive control demonstrated a significant increase in cells with structural chromosome aberrations.

Study no.: TOXT7078598

Volume #, and page #: Volume 1, pages 1-28

Conducting laboratory and location: Bayer Schering Pharma AG,

Nonclinical Drug Safety,

D-13342 Berlin, Germany

Date of study initiation: January 8, 2008

GLP compliance: Yes

Reference ID: 3361527

QA report: yes (x) no ()

Drug, lot #, and % purity: ZK 6057184, Batch # CS1036KI, and 99.2 % purity

Methods

This study involved *in vitro* cytogenetics assay using duplicate lymphocyte cultures from a healthy adult male donor. Concentrations of 1, 2.5, 5, 10, 25, 50 and 100 µg/mL and cyclophosphamide (2.5 µg/mL) was used as a positive control during the assay with S9 mix and triaziquone (0.2 µg/mL) during the assay without S9 activation. Higher concentrations of BAY-94-9172 could not be employed because precipitations were observed at the concentrations. The lymphocyte was prepared by arresting the cells in metaphase by adding colcemide (0.08 µg/mL) about 2-3 hours before the cells were harvested. The cell cycle kinetics was assessed by slides using a modified fluorescence-plus-Giemsa technique (FPG-technique). The analysis of chromosomal aberrations (200 metaphases per concentration, i.e. 100 per duplicate culture) was conducted at:

(a) 4-hour treatment with 5, 25 and 50 µg/mL in the assay without S9 mix and a harvesting time of 19 hours after start of the treatment and
(b) 4-hour treatment with 5, 25 and 50 µg/mL in the assay with S9 mix and a harvesting time of 19 hours after start of the treatment.

The incidence of cells with alterations in chromosome number (excl. aneuploidy) such as endoreduplication and polyploidy was also recorded.

Strains/species/cell line: Cultured human peripheral blood lymphocytes obtained from a healthy male donor.

Doses used in definitive study: The following treatment doses were used in the assay: 1, 2.5, 5, 10, 25, 50 and 100 µg/mL

Basis of dose selection: Scoring of slides obtained from adequate dose levels from each treatment was employed to determine any occurrence of chemically induced mitotic inhibition. This index was used in selection of doses for cytogenic analysis.

Negative controls: Comprised of treatments with DMSO (not more than 1.0% (v/v).

Positive controls: The positive control chemicals were triaziquone and cyclophosphamide.

Incubation and sampling times: The exposure periods were 4 hours with and without S9 mix and harvesting time was 19 hours after start of treatment with the test item. For each experimental group two parallel cultures were analyzed and 100 metaphase plates per culture were scored for structural chromosomal aberrations while 1000 cells were analyzed for mitotic index from

Reference ID: 3361527

each culture and three concentrations per treatment were chosen for chromosomal aberration analysis.

Results

Study outcome: Visible precipitation of the test item in the culture medium was observed at concentrations ≥100 µg/mL in the absence and presence of S9 mix. This limits the concentration employed during the study. No statistically significant increase was reported in the frequency of structural chromosomal aberrations after treatment with concentrations of 5 - 50 µg/mL ZK 6057184. In the assay with S9 mix, there was a statistically significant ($p < 0.05$) increase in the number of aberrant cells to 2.5 % (5 µg/mL) and 3.0 % (25 µg/mL) in comparison to the concurrent solvent control (0 % aberrant cells). The increase in the aberration frequency was however found not dose-dependent and the aberration frequency of 3.0 % did not exceed the spontaneous aberration frequency detected in the control cultures (0-3 %). The positive controls with known mutagens (-S9 mix: triaziquone; +S9 mix: cyclophosphamide) demonstrated clastogenic effects (Table 56).

Table 56: Chromosomal aberrations (% aberrant cells excluding gaps) in cultured human Lymphocytes

				% Aberrant cells	
Test substance	**Concentration (µg/mL)[1]**	**S9 (4 hours)**	**Cells Scored**	**A**	**B**
DMSO	1 % (v/v)	No	200	1.0	0.5
ZK 6057184	5-100	No	200	0.5-2	0.5
Triaziquone	0.02	No	100	23*	-
DMSO	1 % (v/v)	Yes	200	1.5	0.5
ZK 6057184	5-100	Yes	200	0-2.0	0
Cyclophosphamide	3.5	Yes	100	15*	-

1) Test item concentrations correspond to (b) (4) ZK 6057184 ((b) (4)).
* $p < 0.05$, compared to the concurrent solvent control;
A: first harvesting time;
B: second harvesting time

Thus, ZK 6057184 at the employed doses did not induce structural chromosomal aberrations in human lymphocytes *in vitro* in the absence and presence of metabolic activation.

Reviewer's comment: Agrees with the result of this study.

Study title: TOXT6081476: Evaluation of (b) (4) in a bacterial reverse mutation study using Salmonella typhimurium (Ames-Test)

Reference ID: 3361527

Key findings: This study was conducted to investigate whether [redacted] (b) (4) (a potential impurity of BAY 94-9172) can induce point mutations in five strains of *Salmonella typhimurium* in the absence and presence of an extrinsic metabolizing system (S9 mix) containing Aroclor 1254-induced male rat liver homogenate (S9) using a bacterial reverse mutation test. The result showed that [redacted] (b) (4) lacks any mutagenic potential in the bacterial reverse mutation test when tested up to a maximum dose level of 5.0 mg/plate in the absence and presence of a metabolic activation system (S9 mix).

Study no.: TOXT6081476

Page #: Page 37

Conducting laboratory and location: Bayer Schering Pharma AG,

Nonclinical Drug Safety,

13342 Berlin, Germany

Date of study initiation: February 10, 2010.

GLP compliance: No

QA reports: yes () no (x)

Drug, lot #, and % purity: [redacted] (b) (4) Batch # GROS 428-2, and % Purity was >96.2%

Methods

This study evaluated mutagenic activity of [redacted] (b) (4) by examining its ability to revert five histidine-requiring strains of *Salmonella triphimurium* in the absence and presence of S9 fraction (metabolizing system) of the S9 mix isolated from the livers of Aroclor 1254-induced male Sprague-Dawley rats.

Strains/species/cell line: Five histidine-requiring strains of *Salmonella triphimurium* –TA98, TA100, TA1535, TA1537 and TA102.

Doses used in definitive study: The following dose levels were employed for the strains in this study: 0.1, 0.25, 0.5, 1.0, 2.5, and 5 mg/plate.

Basis of dose selection: An initial preincubation study was performed in all employed *Salmonella triphimurium* tester strains TA100 at various doses 0.1- 5 mg/plate in the presence of a solvent and positive control. No toxicity was reported and all the five test strains were evaluated for mutagenicity using the same dose range.

Negative controls: Comprised of treatments with sterile DMSO

Reference ID: 3361527

Positive controls: The positive control chemicals were 2-nitrofluorene (2NF) for TA98, sodium azide (NaN_3) for TA100 and TA1535, 4-Nitro-o-phenylenediamine (4-NPDA) foe TA1537 and mitomycin C (MMC) for TA102.

Incubation and sampling times: In direct plate incorporation study, the quality of mammalian liver post-mitochondrial fraction S9 was ascertained and 0.1 mL of the bacterial suspension, 0.05 mL of the test material, and 0.5 mL of 0.1 mol/L sodium phosphate buffer pH 7.4 or S9 mix was added to a sterile tube containing 2 mL of molten soft agar with minimal amounts of histidine and biotin. The content of the tubes was mixed and poured to histidine-free plates (Vogel-Bonner agar). All plates were prepared in triplicate, allowed to solidify and incubated at 37 °C for approximately 48 hours (TA102) or 72 hours (TA98, TA100, TA1535, TA1537). Negative controls were included in each assay as shown in the table above.

Results

Study validity: The plates were scored for the number of mutant colonies with an automated colony counter (AccuCount 1000, Biologics, BioSys GmbH, Germany). However, manual counting was performed where reliable automatic counting is not possible for instance when there is precipitation of the test compound. The individual plate counts were averaged to give mean values which was compared with the historical ranges. The total colony counts of the 10^{-6} dilution of bacterial culture confirmed the viability and high cell density of the cultures of the individual strains. In this study, the mean solvent control counts were within the normal historical ranges. The colony counts on appropriate negative control plates confirmed the characteristic spontaneous reversion rate. Appropriate positive control chemicals induced marked and reproducible increases in revertant colony numbers with all strains.

Study outcome: None of the five tester strains (*S. typhimurium* TA98, TA100, TA1535, TA1537 and TA102) showed increased reversion to prototrophy in assays with (b) (4) at the doses tested between 0.1-5.0 mg/plate, either in the absence or presence of metabolic activation.

Reviewer's comments: Agrees with the result of this study. The direct plate incorporation procedure and preincubation modification tests both demonstrated that (b) (4) did not induce gene mutations by base-pair changes or frame-shifts in the genome of the *S. typhimurium* strains used, when tested up to a 5.0 mg/plate dose in the absence and presence of S9 mix.

Study title: TOXT0081083: Evaluation of (b) (4) in a bacterial reverse mutation study using *Salmonella typhimurium* (Ames-Test)

Key findings: This study investigated if (b) (4) (an impurity contained in the clinical batch of BAY 94-9172) can induce point mutations in five strains of *Salmonella typhimurium* in the absence and presence of an extrinsic metabolizing system (S9 mix) containing Aroclor 1254-induced male rat liver homogenate (S9) using a bacterial reverse mutation test. The result showed that (b) (4) does not demonstrate any mutagenic potential in the bacterial reverse mutation test when tested up to a maximum dose level of 5.0 mg/plate in the absence and presence of a metabolic activation system (S9 mix).

Reference ID: 3361527

Study no.: TOXT0081083

Page #: Page 37

Conducting laboratory and location: Bayer Schering Pharma AG,

Nonclinical Drug Safety,

13342 Berlin, Germany

Date of study initiation: November 16, 2009.

GLP compliance: No

QA reports: yes () no (x)

Drug, lot #, and % purity: (b) (4) Batch # BRX4GNZ, and % Purity was 100%

Methods

This study evaluated the mutagenic activity of (b) (4) by examining its ability to revert five histidine-requiring strains of *Salmonella triphimurium* in the absence and presence of rat S9 fraction (metabolizing system).

Strains/species/cell line: Five histidine-requiring strains of *Salmonella triphimurium* –TA98, TA100, TA1535, TA1537 and TA102.

Doses used in definitive study: The following dose levels were employed for the strains in this study: 0.1, 0.25, 0.5, 1.0, 2.5, and 5 mg/plate.

Basis of dose selection: An initial preincubation study was performed in all employed *Salmonella triphimurium* tester strains TA100 at various doses 0.1- 5 mg/plate in the presence of a solvent and positive control. No toxicity was reported and all the five test strains were evaluated for mutagenicity using the same dose range.

Negative controls: Comprised of treatments with sterile DMSO

Positive controls: The positive control chemicals were 2-nitrofluorene (2NF) for TA98, sodium azide (NaN_3) for TA100 and TA1535, 4-Nitro-o-phenylenediamine (4-NPDA) for TA1537 and mitomycin C (MMC) for TA102.

Incubation and sampling times: In direct plate incorporation study, the quality of mammalian liver post-mitochondrial fraction S9 was ascertained and 0.1 mL of the bacterial suspension, 0.05 mL of the test material, and 0.5 mL of 0.1 mol/L sodium phosphate buffer pH 7.4 or S9 mix was added to a sterile tube containing 2 mL of molten soft agar with minimal amounts of histidine and biotin. The content of the tubes was mixed and poured to histidine-free plates (Vogel-Bonner agar). All plates were prepared in triplicate, allowed to solidify and incubated at

Reference ID: 3361527

37 °C for approximately 48 hours (TA102) or 72 hours (TA98, TA100, TA1535, TA1537). Negative controls were included in each assay as shown in the table below.

Results

Study validity: The plates were scored for the number of mutant colonies using an automated colony counter while manual counting was employed where reliable automatic counting is not possible. The individual plate counts were averaged to give mean values which was compared with the historical ranges. The mean solvent control counts were within the normal historical ranges. Precipitates in the agar were found from 1 mg/plate onwards; however, growth inhibition of the background lawn was not observed. The colony counts on appropriate negative control plates confirmed the characteristic spontaneous reversion rate. Appropriate positive control chemicals induced marked and reproducible increases in revertant colony numbers with all strains.

Study outcome: None of the five tester strains (*S. typhimurium* TA98, TA100, TA1535, TA1537 and TA102) showed increased reversion to prototrophy in assays with (b) (4) at the doses tested between 0.1-5.0 mg/plate, either in the absence or presence of metabolic activation.

Reviewer's comments: Agrees with the result of this study which indicates that (b) (4) tested up to a maximum dose of 5.0 mg/plate did not induce point mutations on the *S. typhimurium* strains employed in this study in the absence and presence of S9 mix.

Study title: TOXT3081059: Forward cell mutation assay with (b) (4) at the thymidine kinase locus (TK+/-) in mouse lymphoma L5178Y cells

Key findings: This study investigated any potential mutagenic effect of (b) (4) at the thymidine kinase (TK) locus in the mouse lymphoma cell line L5178Y. (b) (4) was tested at concentrations ranging from 2.5-50 µg/mL during assay conducted without and with activation during a treatment time of 3 hours (pulse treatment) and 24 hours (continuous treatment). No cytotoxic effect was demonstrated by (b) (4) at any employed concentrations both in the experiments without and with S9 mix. However, the positive controls NQO (0.025 and 0.1 µg/mL) and 3-MC (2.0 µg/mL) induced significant increases in the mutant frequency indicating the sensitivity of the test system.

Study no.: TOXT3081059

Page #: Page 36

Conducting laboratory and location: Bayer Schering Pharma AG,

Nonclinical Drug Safety,

13342 Berlin, Germany

Date of study initiation: January 7, 2010.

GLP compliance: No

QA reports: yes () no (x)

Drug, lot #, and % purity: (b) (4) Batch # BRX4GNZ, and % Purity was 100%

Methods

This study is based on employing one of the frequently used mutagenicity test with eukaryotic cells which involves the mouse lymphoma assay in L5178Y cells that allows quantification of forward mutations at the autosomal thymidine kinase (TK) locus. The cell culture employed for the assay are mouse lymphoma cells (L5178Y/TK+/-), heterozygous at the autosomal thymidine kinase (TK) locus. The S9 activation system for the assay was isolated from livers of Aroclor 1254 induced male rats. The S9 mix was prepared with 200 mmol/L glucose-6-phosphate, 32 mmol/L NADP and S9 at a ratio of 1:1:2.

Strains/species/cell line: Mouse lymphoma cells (L5178Y/TK+/-), heterozygous at the autosomal thymidine kinase (TK) locus.

Doses used in definitive study: The following dose levels were employed for the strains in this study: 2.5, 5, 10, 25 and 50 µg/mL.

Basis of dose selection: The doses employed for the main experiment were selected based on the findings of the initial experiments for cytotoxicity with pulse (3 hours) and continuous (24 hours) treatment. (b) (4) dissolved in DMSO, was tested up to a maximum concentration of 50 µg/mL. No cytotoxic effect was observed in the experiments with and without metabolic activation after pulse treatment. Similarly, after continuous treatment no cytotoxicity was also observed up to 50 µg/mL. However, distinct precipitation became visible in the test cultures after pulse and continuous treatment at the highest test concentration of 50 µg/mL.

Negative controls: Comprised of treatments with sterile DMSO

Positive controls: The positive control chemicals were 3-methylcholanthrene (3-MC) and 4-nitroquinoline 1-oxide (NQO).

Incubation and sampling times: Cells (1 x 10^7) suspended in 20 mL culture medium (horse serum concentration reduced to 5%) were exposed to concentrations of the test item in the absence or presence of an extrinsic metabolic system (S9 mix) in duplicate. Pulse treatment was performed in 50 mL centrifuge tubes for 3 hours (pulse treatment) at 37 °C with manually mixing every 30 minutes while continuous treatment (24 hours) was performed only in the absence of S9 mix with a reduced cell number (5 x 10^6) in tissue culture flasks. The test item was removed by centrifugation (200 x g, 4 min) after treatment and the cells were washed twice with culture medium. After cell counting approximately 6 x 10^6 cells in 50 mL culture medium (1.2 x 10^5 cells/mL) were sub cultured in tissue culture flasks at 37 °C with 5 % CO_2 for about 2 days. At the end of this growth and expression period the cells were collected by centrifugation and counted. During subsequent mutant selection approximately 2 x 10^3 cells/well were plated in selective medium (culture medium with 3 µg/mL trifluorothymidine) into 96 well microtiter

plates. The plates were incubated for at least 10 days at 37 °C and 5 % CO_2. After the selection period the colonies were manually counted.

Results

Study validity: The colonies were manually counted and a mutant assay is considered acceptable if:

1) At least one negative and/or solvent control and one positive control is completely valuable.
2) The negative and/or solvent controls yield values in the 1st and 2nd plating efficiency (PE) up to a range of 65-130 %.
3) The means of the spontaneous mutant frequency of the negative and/or solvent controls are in a range of 50-170 per 106 cells and in accordance with historical control data and
4) Positive controls induce significant increases (≥ two-folds) in the mutant frequencies compared to the negative controls and yield absolute values above the range of historical control data.

The test item is classified as mutagenic if:

1) It induces at least in one of the concentrations tested a mutant frequency that is two times higher than the mean of the spontaneous mutant frequency of the corresponding control.
2) If there is a reproducible concentration-related increase in the mutant frequency and
3) If the induced mutant frequency exceed a value that based on the global distribution of the background mutant frequency for the mouse lymphoma assay and the spontaneous mutant frequency of the performed assay.

Study outcome:

Solubility- During the main experiments, visible precipitates of the test item were found at the highest test concentration of 50 µg/mL when the stock solutions were added at 1%(v/v) to the incubation mixtures both after pulse and continuous treatment.

Cytotoxicity**-** No cytotoxic effects of (b) (4) were observed both in the experiments without and with metabolic activation at any test concentration. The Plating efficiencies of solvent control cells were in the expected range of 65-130 % (1st PE and 2nd PE); thus meeting the acceptance criteria in both assays.

Mutagenicity- None of the tested concentrations without S9 mix demonstrates an increase in number of mutant colonies that exceeded the threshold of twice the number of mutant colonies of the solvent controls. In addition, no concentration-dependent increase in mutant colonies irrespective of the enhancement factor was observed. The positive control item (NQO) was clearly mutagenic after pulse (0.1 µg/mL) and continuous treatment (0.025 µg/mL) as shown in **Error! Reference source not found.** and **Error! Reference source not found.**. Similarly, in experiments with S9 mix, the induced mutant frequencies did not exceed the threshold of twice the colony counts of the corresponding solvent control at any test concentration and also did not exhibit a concentration-dependent increase. However, the positive control 3-MC (2 µg/mL) showed a clear increase in the mutant frequency.

Table 57: Summary data on assay involving pulse treatment (3 hours) without and with S9 mix (mean values of two independent cultures)

Reference ID: 3361527

	Conc per mL	S9 mix	1.PE relative (%)	SG relative	2.PE absolute (%)	Mutants per 10^6 cells	Mutation index
Solvent control DMSO	1%	-	100	100	104	114	1.0
(b) (4)	2.5 µg	-	106	99	95	108	0.9
	5 µg	-	87	103	93	115	1.0
	10 µg	-	103	100	91	123	1.1
	25 µg	-	89	98	88	105	0.9
	50 µg[p]	-	96	96	93	102	0.9
Positive control NQO	0.1 µg	-	73	92	64	1162	10.2
Solvent control DMSO	1%	+	100	100	97	112	1.0
(b) (4)	2.5 µg	+	108	105	96	114	1.0
	5 µg	+	96	102	88	111	1.0
	10 µg	+	103	101	96	86	0.8
	25 µg	+	99	108	102	81	0.7
	50 µg[p]	+	96	98	97	99	0.9
Positive control 3-MC	2 µg	+	92	100	82	576	5.1

S9: liver homogenate (9000 x g fraction) derived from male rats
PE: plating efficiency
SG: suspension growth
DMSO: dimethyl sulfoxide
NQO: 4-Nitroquinoline 1-oxide
3-MC: 3-Methylcholanthrene
[P]: precipitates

Table 58: Summary data on assay involving continuous treatment (24 hours) without S9 mix; Pulse treatment (3 hours) with S9 mix (mean values of two independent cultures)

	Conc per mL	S9 mix	1.PE relative (%)	SG relative	2.PE absolute (%)	Mutants per 10^6 cells	Mutation index
Solvent control DMSO	1%	-	100	100	101	92	1.0
(b) (4)	2.5 µg	-	90	91	106	82	0.9
	5 µg	-	91	96	94	84	0.9
	10 µg	-	101	93	94	81	0.9
	25 µg	-	79	93	85	85	0.9

	50 µg[p]	-	69	88	83	94	1.0
Positive control NQO	0.1 µg	-	108	123	84	352	3.8
Solvent control DMSO	1%	+	100	100	101	79	1.0
(b) (4)	2.5 µg 5 µg 10 µg 25 µg 50 µg[p]	+ + + + +	98 104 101 84 87	100 106 100 102 95	108 96 92 87 91	68 72 84 85 69	0.9 0.9 1.1 1.1 0.9
Positive control 3-MC	2 µg	+	95	99	87	456	5.8

S9: liver homogenate (9000 x g fraction) derived from male rats
PE: plating efficiency
SG: suspension growth
DMSO: dimethyl sulfoxide
NQO: 4-Nitroquinoline 1-oxide
3-MC: 3-Methylcholanthrene
[P]: precipitates

Reviewer's comments: Agrees with the result of this study which indicates that (b) (4) is not a mutagen in the mouse lymphoma assay, when tested up to precipitating concentrations of the test item in the absence and presence of metabolic activation. However, the positive control items, NQO and 3-MC induced increase in mutant frequency and produced a clear increase in the total number of both types of mutant colonies.

7.2 Other Genetic Toxicity Studies

Study title: **Study No. A141779: Mix of (b) (4) (b) (4) (b) (4) and (b) (4) (Impurities of BAY 94-9172) - Systemic toxicity study in male and female rats with daily intravenous injection over a period of 2 weeks.**

Key study findings: The systemic toxicity study of a mixture of (b) (4) (b) (4) (b) (4) and (b) (4) (Impurities of BAY 94-9172) intravenously injected into rats over a period of 2 weeks was assessed. No adverse effects were reported to a mix of the impurities at 3.3, 10.3 and 37.9 µg/kg. The NOAEL for this mix was 37.9 µg/kg.

Study no.: A141484

Volume #, and page #: Volume 1, pages 1-469

Conducting laboratory and location: Bayer Schering Pharma AG,

Nonclinical Drug Safety,

13342 Berlin, Germany

Date of study initiation: February 11, 2008

GLP compliance: Yes

QA report: yes (x) no ( )

Drug, lot #, and % purity: (b) (4) 99.1% purity; (b) (4) 95.21% purity, (b) (4) 96.93% purity and (b) (4) – 95.26% purity

Methods

Doses: 0, 3.3, 10.3 and 37.9 µg/kg

Species/strain: rat/Wistar (Hsd CpB:WU)

Number/sex/group or time point (main study): 10 rats/sex/dose.

Route, formulation, volume, and infusion rate: Intravenous administration at an infusion rate of 6mL/min,

Satellite groups used for toxicokinetics or recovery: No.

Age: males- 8-9 weeks; females – 8-9 weeks.

Weight: Males – 221-282 g

Females – 161-202 g

Results:

Mortality: No mortality was reported.

Clinical signs: No clinical findings were reported in animals administered up to 37.9 µg/kg dose. However, one female animal administered 37.9 µg/kg dose showed slight apathy between day 11 and day 13 and the vehicle caused signs of local irritation at the injection site at the tail consisting of brownish discolored skin at the tail in both the control and the treated groups.

Body weights: No treatment related effect was reported on the body weight, organ/body weight or organ/organ ratios.

Food consumption: The treatment did not affect food consumption. However, at the high dose of 37.9 µg/kg, mean food consumption was slightly reduced in the second week of treatment in the female animals ($p < 0.05$), which did not reflect in total food consumption.

Ophthalmoscopy: No treatment-related ophthalmoscopic finding was reported.

Hematology: No treatment related hematological effect was reported in the animals.

Coagulation: No compound-related effect was observed up to the high dose of 37.9 µg/kg.

Clinical chemistry: No treatment-related effect on clinical chemistry was reported. There was a statistical significant higher triglyceride level (+39 %) in male animals and higher inorganic phosphate level in female animals (+24 %) dosed at 9.9 µg/kg of the impurity mix compared to control animals ($p < 0.05$). This is considered incidental because of lack of dose-dependence.

Urinalysis: No treatment-related effect was reported.

Gross pathology: No treatment-related macroscopic effects were observed in this study.

The only observed treatment-related findings - vascultis/perivasculitis at the injection site in all treated animals - reflect the mechanical stimulus of the injection procedure. No compounds-related histological findings were reported in this study.

Organ weight: No treatment-related change in organ weight was reported.

Histopathology: Adequate Battery: yes (x), no ( )—explain

Peer review: yes (x), no ( )

Histopathology inventory (optional)

Study	Acute Study			
Species	Dog			
Adrenals	x*			
Aorta	x			
Bone Marrow smear	x			
Bone (femur)	x			

Brain	x*			
Cecum	x			
Cervix	x			
Colon	x			
Duodenum	x			
Epididymis	x			
Esophagus	x			
Eye	x			
Fallopian tube				
Gall bladder	x			
Gross lesions	x			
Harderian gland				
Heart	x*			
Ileum	x			
Injection site	x			
Jejunum	x			
Kidneys	x*			
Lachrymal gland				
Larynx	x			
Liver	x*			
Lungs	x			
Lymph nodes, cervical	x			
Lymph nodes mandibular	x*			

Lymph nodes, mesenteric	x			
Mammary Gland	x			
Nasal cavity				
Optic nerves	x			
Ovaries	x*			
Pancreas	x*			
Parathyroid	x*			
Peripheral nerve				
Pharynx	x			
Pituitary	x*			
Prostate	x			
Rectum	x			
Salivary gland	x*			
Sciatic nerve	x			
Seminal vesicles	x*			
Skeletal muscle	x			
Skin	x			
Spinal cord	x			
Spleen	x*			
Sternum				
Stomach	x			
Testes	x*			
Thymus	x*			
Thyroid	x			

Tongue	x			
Trachea	x			
Urinary bladder	x			
Uterus	x*			
Vagina	x			
Zymbal gland				

x, histopathology performed

*, organ weight obtained

Reviewer's Comment: Agrees with the result of this study.

Study title: TOXT2078629: Mix of (b) (4) (b) (4) (b) (4) and (b) (4) (Impurities of BAY 94-9172) - Systemic toxicity study in male and female rats with daily intravenous injection over a period of 2 weeks.

Key study findings: The systemic toxicity study of a mixture of (b) (4) (b) (4) (b) (4) and (b) (4) (Impurities of BAY 94-9172) intravenously injected into rats over a period of 2 weeks was assessed. No adverse effects were reported to a mix of the impurities at 3.3, 10.3 and 37.9 µg/kg. However, there were slight reductions in food intake in females administered 37.9 µg/kg. The NOAEL for this mix was 37.9 µg/kg.

Study no.: TOXT2078629

Page #: Pages 1-469

Conducting laboratory and location: Bayer Schering Pharma AG,

Nonclinical Drug Safety,

13342 Berlin, Germany

Date of study initiation: February 19, 2008

GLP compliance: Yes

QA report: yes (x) no ()

Drug, lot #, and % purity: (b) (4) 99.1% purity; (b) (4) - 95.21% purity, (b) (4) - 96.93% purity and (b) (4) - 95.26% purity

Methods

Doses: 0, 3.3, 10.3 and 37.9 µg/kg

Species/strain: Rat/Wistar (Hsd CpB:WU)

Number/sex/group or time point (main study): 10 rats/sex/dose.

Route, formulation, volume, and infusion rate: Intravenous administration at an infusion rate of 6mL/min,

Satellite groups used for toxicokinetics or recovery: No.

Age: males- 8-9 weeks; females – 8-9 weeks.

Weight: Males – 221-282 g

Females – 161-202 g

Results:

Mortality: No mortality was reported.

Clinical signs: No clinical findings were reported in animals administered up to 37.9 µg/kg dose. However, one female animal administered 37.9 µg/kg dose showed slight apathy between day 11 and day 13 and the vehicle caused signs of local irritation at the injection site at the tail consisting of brownish discolored skin at the tail in both the control and the treated groups.

Body weights: No treatment related effect was reported on the body weight, organ/body weight or organ/organ ratios in the animals.

Reference ID: 3361527

Food consumption: The treatment did not affect food consumption. However, at the high dose of 37.9 µg/kg, mean food consumption was slightly reduced in the second week of treatment in the female animals ($p < 0.05$), which did not reflect in total food consumption.

Ophthalmoscopy: No treatment-related ophthalmoscopic finding was reported.

Hematology: No treatment related hematological effect was reported in the animals.

Coagulation: No compound-related effect was observed up to the high dose of 37.9 µg/kg.

Clinical chemistry: No treatment-related effect on clinical chemistry was reported. There was a statistical significant higher triglyceride level (+39 %) in male animals and higher inorganic phosphate level in female animals (+24 %) dosed at 37.9 µg/kg of the impurity mix compared to control animals ($p < 0.05$). This is however considered incidental because of lack of dose-dependence.

Urinalysis: No treatment-related effect was reported.

Gross pathology: No treatment-related macroscopic effects were observed in this study. The only observed treatment-related findings - vascultis/perivasculitis at the injection site in all treated animals. No compounds-related histological findings were reported in this study.

Organ weight: No treatment-related change in organ weight was reported.

Histopathology: Adequate Battery: yes (x), no ()—explain

Peer review: yes (x), no ()

Histopathology inventory (optional)

Study	Acute Study			
Species	Rat			
Adrenals	x*			
Aorta	x			
Bone Marrow smear	x			
Bone (femur)	x			

Brain	x*			
Cecum	x			
Cervix	x			
Colon	x			
Duodenum	x			
Epididymis	x			
Esophagus	x			
Eye	x			
Fallopian tube				
Gall bladder	x			
Gross lesions	x			
Harderian gland				
Heart	x*			
Ileum	x			
Injection site	x			
Jejunum	x			
Kidneys	x*			
Lachrymal gland				
Larynx	x			
Liver	x*			
Lungs	x			
Lymph nodes, cervical	x			
Lymph nodes mandibular	x*			

Lymph nodes, mesenteric	x			
Mammary Gland	x			
Nasal cavity				
Optic nerves	x			
Ovaries	x*			
Pancreas	x*			
Parathyroid	x*			
Peripheral nerve				
Pharynx	x			
Pituitary	x*			
Prostate	x			
Rectum	x			
Salivary gland	x*			
Sciatic nerve	x			
Seminal vesicles	x*			
Skeletal muscle	x			
Skin	x			
Spinal cord	x			
Spleen	x*			
Sternum				
Stomach	x			
Testes	x*			
Thymus	x*			
Thyroid	x			

Tongue	x			
Trachea	x			
Urinary bladder	x			
Uterus	x*			
Vagina	x			
Zymbal gland				

x, histopathology performed

*, organ weight obtained

Reviewer's Comment: Agrees with the result of this study.

Study title: EXTT9078888: Chromosome aberration test in human lymphocytes in vitro with (b) (4) (b) (4) (b) (4) (b) (4) – Impurities of ZK 6013443 (ref. BAY 94-9172)

Key findings: The potential ability of (b) (4) (b) (4) (b) (4) (b) (4) to induce chromosomal aberrations in human peripheral lymphocytes *in vitro* in the presence and absence of an exogenous metabolic activation system was assessed. In the study, equal portions of (b) (4) (b) (4) (b) (4) (b) (4) was dissolved in dimethyl sulfoxide (DMSO) in two independent experiments. No biologically relevant increase in the number of cells carrying structural chromosomal aberrations was observed after treatment with the test item in these experiments. No relevant increase in the frequencies of polyploid metaphases was found after treatment with the test item as compared to the frequencies of the controls. However, the positive control demonstrated a significant increase in cells with structural chromosome aberrations.

Study no.: EXTT9078888

Pages: 1-41

Conducting laboratory and location: (b) (4)

[redacted] (b) (4)

Date of study initiation: February 4, 2008

GLP compliance: Yes

QA reports: yes (X) no ()

Drug, lot #, and % purity: [redacted] (b) (4) (94.75% purity), [redacted] (b) (4) (98.84% purity), [redacted] (b) (4) (94.66% purity), [redacted] (b) (4) 95.51% purity), lot #s were not provided

Methods

This study involved *in vitro* cytogenetics assay using duplicate lymphocyte cultures from a 31 years old female donor who was not receiving medication in the two independent experiments. The highest concentration level used, 5000 µg/mL, was chosen with reference to the current OECD Guideline for *in vitro* mammalian cytogenetic tests requesting for the top concentration clear toxicity with reduced mitotic indices below 50 % of control, and/or the occurrence of precipitation. Up to 200 µg/mL of the test item (mixture of [redacted] (b) (4) [redacted] (b) (4) [redacted] (b) (4) and [redacted] (b) (4) was applied as top concentration for treatment of the cultures in the pre-test. Test item concentrations between 1.3 and 200 µg/mL (with and without S9 mix) were chosen for the evaluation of cytotoxicity. Precipitates were observed at 37.3 µg/mL and above concentrations, in the absence and presence of S9 mix. Concentration of 200 µg/mL was employed as the highest concentration for the definitive study. The treatment conditions used in this assay involved 4 and 22 hours exposures without metabolic activation and at approximately 4 hours with metabolic activation. After appropriate incubation period with test article or control article, the cultures were washed with RPMI-complete medium and returned to the incubator until harvest at 22 hours. All the cultures were examined for signs of cytotoxicity and precipitates after addition of test complete battery of genetic toxicology tests and both the *in vitro* and *in vivo* tests substance to the cultures, after the 4- and 22-hour incubation period, and prior to harvest. The sponsor analyzed the percent polyploidy and endoreduplication by evaluating 250 metaphase cells.

<u>Strains/species/cell line:</u> Cultured human peripheral blood lymphocytes obtained from a 31 years old female donor who was not receiving medication.

Doses used in definitive study: The following treatment doses were used in the assay: 1.3, 2.3, 4.0, 7.0, 12.2, 21.3, 37.3, 65.3, 114.3, and 200 µg/mL.

Basis of dose selection: Scoring of slides obtained from adequate dose levels from each treatment was employed to determine any occurrence of chemically induced mitotic inhibition. This index was used in selection of doses for cytogenic analysis.

Negative controls: Comprised of treatments with DMSO (not more than 1.0% (v/v).

Positive controls: The positive control chemicals were ethylmethane sulfonate (EMS) for without S9 mix and cyclophosphamide (CPA) for S9 mix experiments.

Incubation and sampling times: In Experiment I (Exp.I), the exposure periods were 4 hours with and without S9 mix. In Experiment II (Exp.II), the exposure periods were 4 hours with S9 mix, 22 and 46 hours without S9 mix as shown in the Table below. The chromosomes were prepared 22 hours (Exp. I) and also 22 and 46 hours (Exp. II) after start of treatment with the test item. In each experimental group, two parallel cultures were analyzed. 100 metaphase plates per culture were scored for structural chromosomal aberrations while 1000 cells were analyzed for mitotic index from each culture and three concentrations per treatment were chosen for chromosomal aberration analysis.

Results

Study validity: The assay is considered acceptable if it meets the following criteria:

a) The number of aberrations found in the solvent controls falls within the range of historical laboratory control data range: 0.0 - 4.0 % aberrant cells, excluding gaps.

b) The positive control substances should produce significant increases in the number of cells with structural chromosome aberrations, which are within the range of the laboratory's historical control data.

The results are evaluated and the test item is classified as non-mutagenic if:

a) The number of induced structural chromosome aberrations in all evaluated dose groups is in the range of historical control data (0.0 - 4.0 % aberrant cells, excluding gaps).

b) No significant increase of the number of structural chromosome aberrations is observed.

The test item is classified as mutagenic if:

a) The number of induced structural chromosome aberrations is not in the range of historical control data (0.0 - 4.0 % aberrant cells, excluding gaps) and

b) Either a concentration-related or a significant increase of the number of structural chromosome aberrations is observed.

The test item can be classified as aneugenic if:

Reference ID: 3361527

a) The number of induced numerical aberrations is not in the range of historical control data (0.0 – 0.8 % polyploid cells).

Study outcome: In Experiment I, visible precipitation of the test item in the culture medium was observed at 37.3 µg/mL and above in the absence and presence of S9 mix. In Experiment II, precipitation occurred at 65.3 µg/mL and above in the presence and absence of S9 mix (22 hrs) and at 37.3 µg/mL and above (46 hrs) in the absence of S9 mix. In both experiments, in the absence and presence of S9 mix, no biologically relevant increase in the number of cells carrying structural chromosome aberrations was observed as shown in the figure below.

Table 59: Summary data of the chromosomal aberration study with (b) (4) (b) (4) (b) (4) (b) (4)

					Aberrant cells in %		
Expt	**Preparation interval**	**Test item concentration in µg/mL**	**Polypoid cells in %**	**Mitotic indices in % of control**	**including gaps**	**excluding gaps**	**With exchange**
1	22 hrs	Solvent control[1]	0.0	100	1.5	1.0	0.0
		Positive control[2]	0.2	59.9	15	15.0[s]	4.5
		12.2	0.2	91.6	2.0	1.5	0.0
		21.3	0.0	68.8	1.0	0.5	0.0
		37.3[p]	0.0	76.9	2.0	1.0	0.0
2	22 hrs	Solvent control[1]	0.2	100	0.0	1.0	0.0
		Positive control[3]	0.0	33.8	9.0	9.0[s]	3.0
		7.0	0.2	91.6	2.0	2.0	0.0
		21.3	0.4	88.6	0.0	0.0	0.0
		65.3[p]	0.2	88.6	0.0	0.0	0.0
3	46 hrs	Solvent control[1]	0.4	100	0.5	0.5	0.0
		Positive control[4]	0.0	72.4	8.5	8.5[s]	4.0
		4.0	0.2	96.3	2.0	2.0	0.0
		12.2	0.0	83.7	2.0	2.0	0.0
		37.3[p]	0.2	85.4	2.5	2.5	0.0
4	22 hrs	Solvent control[1]	0.2	100	0.0	0.0	0.0
		Positive control[4]	0.4	52.9	14.0	13.5[s]	2.5
		12.2	0.2	96.0	2.5	2.0[s]	0.0
		21.3	0.2	93.6	2.0	2.0[s]	0.0
		37.3[p]	0.2	110.1	1.5	1.0	0.0
5	46 hrs	Solvent control[1]	0.2	100.0	1.5	1.5	0.0

		Positive control[5] 21.32 37.3 65.3[p]	0.0 0.2 0.4 0.0	37.3 107.8 96.0 84.2	8.5 2.5 1.0 3.0	8.5[s] 2.0 1.0 2.0	1.0 0.0 0.0 0.5

Experiment (Expt) 1=Exposure period 4 hrs without S9 mix
Expt 2=Exposure period 22 hrs without S9 mix
Expt 3=Exposure period 46 hrs without S9 mix
Expt 4=Exposure period 4 hrs with S9 mix
Expt 5=Exposure period 4 hrs with S9 mix
* Inclusive cells carrying exchanges
P Precipitation occurred
S Aberration frequency statistically significant higher than corresponding control values
1 DMSO 1.0 % (v/v)
2 EMS 825.0 µg/mL
3 EMS 770.0 µg/mL
4 EMS 330.0 µg/mL
5CPA 37.5 µg/mL
6CPA 30.0 µg/mL

However, EMS (330, 770 and 825 µg/mL, respectively) and CPA (30 and 37.5 µg/mL, respectively) were used as positive controls and showed distinct increases in cells with structural chromosome aberrations.

Reviewer's comment: The data presented by the sponsor indicating that under the experimental conditions reported, the test item (b) (4) (b) (4) (b) (4) (b) (4) did not induce structural chromosomal aberrations in human lymphocytes *in vitro* when tested up to precipitating concentrations in the absence and presence of metabolic activation.

Study title: TOXT3078620: Evaluation of (b) (4) (b) (4) (b) (4) and (b) (4) potential impurities of ZK 6013443 (ref. BAY 94-9172) in a bacterial reverse mutation study using *Salmonella typhimurium* (Ames-Test) and *Escherichia coli*

Key findings: This study was conducted to investigate whether (b) (4) (b) (4) (b) (4) and (b) (4) potential impurities of the PET tracer ZK 6013443, can induce point mutations in five strains of *Salmonella typhimurium* and in one strain of *Escherichia coli*. The tested mixture of the four possible impurities of ZK 6013443 demonstrated a weak mutagenic potential in the bacterial reverse mutation test with *Salmonella typhimurium* strains TA100, TA1535 and TA1538.

Study no.: TOXT3078620

Pages: 1-50

Conducting laboratory and location: Bayer Schering Pharma AG,

Nonclinical Drug Safety

D-13342 Berlin,

Germany

Date of study initiation: January 25, 2008

GLP compliance: Yes

QA reports: yes (X) no ()

Drug, lot #, and % purity: (b) (4) (98.84% purity), (b) (4) (94.75% purity), (b) (4) (95.51% purity) (b) (4) (94.66% purity), lot #s were not provided

Methods:

The test item was tested as a mixture of equal parts [25 % (w/w)] of the four impurities in the absence and presence of an extrinsic metabolizing system (S9 mix) containing Aroclor 1254-induced male rat liver homogenate (S9).

Strains/species/cell line: Four histidine-requiring strains of *Salmonella triphimurium* – TA1535, TA100, TA1537, TA1538 and TA98 and *Escherichia coli* tester strain WP2*uvr*A.

Doses used in definitive study: Doses tested for all tester strains ranges between 100 and 5000 µg/plate in the presence and absence of S9 mix.

Basis of dose selection: An initial toxicity range-finder study (Trial 25450-A1) was performed in Strain TA100 and WP2*uvr*A in the presence and absence of S9 mix. In this study, there was no dose-related decrease in the number of revertants per place and normal bacterial background lawns, thus, no toxicity was reported and all the five test strains evaluated.

Vehicle controls: Comprised of treatment with dimethyl sulfoxide (DMSO)

Positive controls: The positive control chemicals were 2-nitrofluorene (2NF) for TA98, sodium azide (NaN_3) for TA100 and TA1535, 9-aminoacridine (AAC) for TA1537 and N-Methyl-N'-nitro-N-nitrosoguanidine and ethyl methansulfonate for WP2*uvr*A.

Incubation and sampling times: Cultures of all organisms were prepared by overnight incubation (shaking for approximately 8 hours at 37°C) of freshly inoculated nutrient broth. The mutagenicity experiments with preincubation were carried out by adding 0.1 mL of the bacterial

Reference ID: 3361527

suspension, 0.05 mL of the test material, and 0.5 mL of 0.1 mol/L sodium phosphate buffer pH 7.4 or S9 mix to a sterile tube. The content was mixed thoroughly and incubated in a water bath at 37°C.

Results

Study validity: Revertant colonies were counted electronically or manually and the background lawn was inspected for signs of mutagenicity and test article precipitation. The arithmetic means of the number of mutant colonies of the 3 parallel plates in the negative control groups were compared with those of the compound groups. A positive response was considered if the number of revertants of the compound groups compared to the number of revertants of the negative group was reproducibly higher than 2-fold. A dose-dependent increase in the number of revertants was also considered to indicate a mutagenic effect.

Study outcome: The mixture of the four possible impurities of ZK 6013443 ((b) (4) (b) (4) (b) (4) and (b) (4) employed in this study demonstrates a weak mutagenic potential in the bacterial reverse mutation test with *Salmonella typhimurium* strains TA100, TA1535 and TA1538. However, no increased reversion to prototrophy was reported in *Salmonella typhimurium* tester strains TA1537 and TA98 and the *E. coli* strain WP2*uvr*A at doses between 0.1 – 5.0 mg/plate in assays with or without metabolic activation.

Reviewer's comment: Agrees with the result of this study.

8 Carcinogenicity

The sponsor requested for a waiver from conducting carcinogenicity studies on Florbetaben. The waiver was granted.

9 Reproductive and Developmental Toxicology

The sponsor also requested for a waiver from conducting reproductive and developmental toxicity study on Florbetaben on October 2, 2012. The request was justified as follows:

1) Duration of Use- Florbetaben is intended for short term use in that the product will be administered as a single injection.

2) Low Mass Dose- Microdose of Florbetaben will be injected to the subjects. Moreover, in a sub-acute repeated dose toxicity studies, no effects on male or female reproductive

tract were observed after daily intravenous injection of up to 200X MHD based on body surface area over a period of 4 weeks in rats and dogs.

3) Intended Target Population- The target population consists of men and mostly postmenopausal women. The radioacive risk will be mentioned in the label tracer

The above justifications support the sponsor's request for waiver of reproductive and developmental toxicology studies.

Nonclinical Recommendation: Nonclinical recommended the approval of the sponsor's request for a waiver from conducting reproductive and developmental toxicity studies with Florbetaben based on the above justifications. Furthermore, the labeling will adequately address the potential risk on reproductive toxicity of the Florbetaben. There is no safe radiation dose for a radiopharmaceutical. Therefore, a statement that any radiopharmaceutical has a potential to cause fetal harm will be included in the labeling. Thus, the labeling will suggest that the use of Florbetaben is associated with a precaution in patients who are pregnant (Pregnancy Category C).

10 Special Toxicology Studies

Study TOXT9082216: Local tolerance test in rabbits after single intravenous administration in the uncongested ear vein and after single paravenous administration at the hind leg.

Key study findings: The local tolerance of ZK 6057184 was tested in rabbits after a single application into the uncongested marginal vein of the ear and a single paravenous application into the hind leg of rabbits. Mild to moderate injection site reactions were reported in treated and control animals. The study suggests no severe or irreversible effects were demonstrated following a single injection of the test article and the vehicle into the uncongested marginal vein of the ear or after a single paravenous application.

Study no.: TOXT9082216

Section #, and page #: 4.2.2, pages 1-32

Conducting laboratory and location: Bayer Schering Pharma AG,

Nonclinical Drug Safety,

13342 Berlin, Germany

Reference ID: 3361527

Date of study initiation: February 3, 2011

GLP compliance: No

QA report: yes (x) no ()

Drug, lot #, and % purity: ZK 6057184, Batch # GROS 430-02C, and 98.2% purity

Methods

Doses: 0, 0.5 mL (intravenous) and 0, 1 mL (paravenous)

Species/strain: Rabbit/New Zealand White (SPF)

Number/sex/group or time point (main study): 2 rabbits/group.

Route, formulation and volume: Intravenous into the uncongested marginal vein of the ear; paravenous into the surrounding tissue of the saphena vein of the hind leg. The product was formulated in the vehicle (0.9% (w/v) NaCl-solution) and 0.5 mL (intravenous injection) and 0, 1 mL (paravenous injection).

Age: Not provided

Weight: Males – 3.8-4.9 kg

Females – 4.1-6.3 kg

A total of 8 rabbits were employed for this study. Each of the four male and four female rabbits were injected with 0.5 mL of a solution containing 3 µg/mL ZK 6057184 into the uncongested marginal vein of the right ear. Similarly, 0.5 mL of a 0.9% (w/v) NaCl-solution was injected into the marginal vein of the left ear and served as a control. The rabbits were observed for 3 to 8 days. These animals were then injected perivenously with 1.0 mL of the test formulation containing 3 µg/mL ZK 6057184 into the surrounding tissue of the saphena vein of the right hind leg. Under the same conditions, 1.0 mL of a 0.9% (w/v) NaCl-solution was injected into the surrounding tissue of the saphena vein of the left hind leg and served as a control. The clinical signs were monitored immediately, 2 and 4 hours post injection then once daily until day 3 and 8. The body weight was also recorded on the day of treatment and daily until the end of observation period on days 3 and 8. Tissue samples taken from each sites of injection for intravenous and paravenous administration were subjected to microscopic and histological examination.

Reference ID: 3361527

Results:

Clinical Signs: Slight to moderate reddening and vessel injection was found in the injection sites 3 days after a single dose administration of the test compound (0.5 mL) into the uncongested marginal vein of the ear. Hematoma was also reported in an animal for a day while after 8 days post administration, slight reddening, vessel injection and hematoma were reported. These reactions were associated with the injection procedure as the findings were localized along the puncture tract, indicating the traumatic etiology of the lesions. The sponsor provided the detailed information on the findings from the local tolerance test after an injection in the uncongested vein before sacrificed on 3rd or 8th day in Table 60 and Table 61 respectively as provided by the sponsor.

Table 60: Summary data on local findings of a local tolerance test in rabbits after a single intravenous application-Day 3 Necropsy

Findings	left ear 0.5 mL 0.9%(w/v) NaCl-solution				right ear 0.5 mL **ZK 6057184**			
	male		female		male		female	
	A/B	**x-y**	**A/B**	**x-y**	A/B	x-y	A/B	x-y
Reddening, slight								
- area of the puncture tract (injection point)	1/1	2						
- area of the puncture tract					1/1	1		
- tissue around the puncture tract							6/2	1-3
- proximal of the puncture tract					2/1	2-3		
Reddening, moderate								
- tissue around the puncture tract					4/1	1-3		
Vessel injection (red discolouration)								
- area of the puncture tract			1/1	2	2/1	1		
Vessel injection (blue discolouration)								
- area of the puncture tract	1/1	2			4/1	1-3	3/2	1-3
- proximal of the puncture tract	1/1	2			4/1	1-3	3/2	1-3
Hematoma								
- area of the puncture tract					1/1	2		

A/B = summation of positive findings/number of animals concerned
x-y = first - last day of occurrence of a finding

Table 61: Summary data on local findings of a local tolerance test in rabbits after a single intravenous application-Day 8 Necropsy

Findings	left ear 0.5 mL 0.9%(w/v) **NaCl**-solution				right ear 0.5 mL **ZK 6057184**			
	male		female		male		female	
	A/B	**x-y**	**A/B**	**x-y**	A/B	x-y	A/B	x-y
Reddening, slight								
-area of the puncture tract			8/1	1-7				
-tissue around the puncture tract	12/2	1-5	4/1	2-5	10/2	1-7	1/1	7
-proximal of the puncture tract					1/1	2		
Vessel injection (blue discolouration)								
-area of the puncture tract	10/2	1-7	7/1	1-7	8/1	1-8	3/1	3-5
-proximal of the puncture tract	3/1	1-4	6/1	2-7	2/1	1-8	3/1	3-5
- distal of the puncture tract					1/1	2		
Hematoma								
-area of the puncture tract							6/1	1-7
-tissue around the puncture tract							1/1	3

A/B = summation of positive findings/number of animals concerned
x-y = first - last day of occurrence of a finding

Findings from the single paravenous injection into the surrounding tissue of the vein of the hind leg caused slight to moderate reddening and swelling, single hematomas and discharge of blood after 3 and 8 days, as shown in Table 62 and Table 63 respectively as provided by the sponsor. The findings were attributed to the injection procedure because the reactions were localized along the puncture tract, indicating the traumatic etiology of the lesions.

Table 62: Summary data on local findings of a local tolerance test in rabbits after a single paravenous application-Day 3 Necropsy

Findings	left leg 1.0 mL 0.9%(w/v) **NaCl**-solution				right leg 1.0 mL **ZK 6057184**			
	male		female		male		female	
	A/B	x-y	A/B	x-y	A/B	x-y	A/B	x-y
Reddening, slight								
- tissue around injection point					1/1	1	1/1	1
- area of administration					3/1	1-2	1/1	1
Reddening, moderate								
- tissue around injection point	2/1	1			3/1	1-2		
- area of administration					1/1	3		
Swelling, slight								
- tissue around injection point	1/1	1			2/1	1	2/2	1
- area of administration	2/2	1	1/1	1	4/1	1-3	2/2	1
Swelling, moderate								
- tissue around injection point					2/1	1	2/2	1
- area of administration					1/1	1	1/1	1
Hematoma								
- injection point					1/1	1		
- tissue around injection point	4/1	1-3	4/1	1-3				
- area of administration			1/1	3				
Movements of defense during administration					1/1	1		
Discharge of blood	1/1	1			1/1	1		

A/B = summation of positive findings/number of animals concerned
x-y = first - last day of occurrence of a finding

Table 63: Summary data on local findings of a local tolerance test in rabbits after a single paravenous application-Day 8 Necropsy

Findings	left leg 1.0 mL 0.9%(w/v) **NaCl**-solution				right leg 1.0 mL **ZK 6057184**			
	male		female		male		female	
	A/B	x-y	A/B	x-y	A/B	x-y	A/B	x-y
Reddening, slight								
- injection point			1/1	1				
- tissue around injection point	1/1	1	3/1	3-5				
Reddening, moderate								
- tissue around injection point	1/1	1	2/1	1-2	1/1	1		
- area of administration			2/1	1				
Swelling, slight								
- tissue around injection point	1/1	1	1/1	8			1/1	1
- area of administration	3/2	1	3/2	1-8	2/2	1	4/2	1
Swelling, moderate								
- area of administration			2/1	1	1/1	1		
Hematoma								
- tissue around injection point	8/1	1-7	4/1	1-5				
- area of administration	6/1	1-5	5/1	1-5				
- distal of injection point	1/1	8						
Movements of defense during administration			1/1	1				
Discharge of blood			1/1	1				

A/B = summation of positive findings/number of animals concerned
x-y = first - last day of occurrence of a finding

Body weight: No treatment related effect was reported on the body weight.

Post mortem examination: The result of the macroscopic and histologic assessment of the injection sites at the uncongested marginal ear indicates a hematoma at the injection site of a test article treated rabbit and this correlates to congestion histology. A slight congestion was observed in ¾ rats after 3 days. A minimal to slight congestion was observed in one test article – treated and two control rabbits after 8 days.

The findings on day 3 after paravenous injection to the rabbits demonstrated test article-treated reactions such as swelling and reddening in one male animal and a hematoma was noted in one control female animal. The histological examination of the test article-treated injection sites showed circumscript inflammatory responses in dermis and/or subcutis in 3/4 animals on day 3. In addition, hemorrhage, focal ulceration of the epidermis, inflammatory reaction in subcutis and adjacent perimysium were also reported in a male test article-treated animal. At the paravenous injection sites of the control article, focal hemorrhages (3/4 animals), dermal and/or subcutaneous inflammatory infiltrates were observed in 4/4 animals. On day 8, no gross findings were noted. Dermal repair response (granulation tissue consisting of fibroblasts, capillaries, leukocytes and provisional matrix) was observed in 2/4 control rabbits. In 3/4 treated animals, a similar repair response was noted in adjacent muscle (2/4 animals) and in dermis (1/4 animals).

Reviewer's Comment: This reviewer agrees with the result of this study which indicates that no severe or irreversible local injection site reactions are expected during intravenous or paravenous administration of Florbetaben in the clinic.

Study TOXT4078630: ZK 6057184 (ref.: (b) (4) Local tolerance test in the dog (M+F) after single infusion into the uncongested vena cephalica antebrachii.

Key study findings: The local tolerance of ZK 6057184 was evaluated in dogs administered a single intravenous infusion of ZK 6057184 (5 µg/mL) in the uncongested vena cephalica antebrachii in the left fore leg and 0.9 % (w/v) NaCl-solution in the right foreleg (control). The result demonstrates no compound-related effects at the injections sites in the clinical observations as well as in the macroscopical and histological examinations of the test article- or vehicle control-treated injection sites.

Study no.: TOXT4078630

Section #, and page #: 4.2.2, pages 1-26

Conducting laboratory and location: Bayer Schering Pharma AG,

Nonclinical Drug Safety,

13342 Berlin, Germany

Date of study initiation: February 6, 2008

GLP compliance: No

QA report: yes (x) no ()

Drug, lot #, and % purity: ZK 6057184, Batch # CS1036K1, and 97.1% purity

Methods

Doses: 0, 5 µg/mL

Species/strain: Dog/Beagle

Number/sex/group or time point (main study): 2 dogs/group.

Route, formulation, volume and infusion rate: Intravenous into the into the uncongested *Vena cephalica antebrachii*. The product was formulated in the vehicle (0.9% (w/v) NaCl-solution), 10 mL and 10 mL/min infusion rate.

Age: Male – 31 months

Female – 15 months

Weight: Male – 10.6 kg

Female – 6.2 kg

A total of 2 dogs (a male and a female) were employed for this study. Each dog received one injection of 10 mL of ZK 6057184 (5.0 µg/mL) or control formulation [0.9 % (w/v) NaCl- solution into the uncongested *Vena cephalica antebrachii* of the foreleg (10 mL/min). The animals were observed for 4 days. The injection sites of the animals were evaluated clinically before, during, immediately after and approximately 30 minutes on administration day and thereafter once daily until the animals were sacrificed on day 4. The body weight was also recorded on the day of treatment and at the end of the study on day 4. Tissue samples taken from each sites of injection for intravenous and paravenous administration were then subjected to microscopic and histological examination.

Results:

Clinical Signs: No treatment-related clinical findings were reported at the injection sites.

Body weight: No treatment related effect was reported on the body weight.

Macroscopic and histological examination: No serious macroscopic findings were reported at the injections sites after the injection of ZK 6057184 or the control article. However, injection of the control article microscopically caused thrombus in the male and with minimal subcutaneous hemorrhage in the female. Histological evaluation revealed minimal subcutaneous hemorrhage in both animals administered the test article while the female dog administered the control article has a minimal focal lymphoid cell infiltration in the wall of veins. The sponsor attributed the focal lymphoid infiltration in one animal to a non-specific background lesion while the cellular composition (lymphocytes) probably indicates a process which was lasting longer than four days, and has nothing to do with the treatment.

Reviewer's Comment: This reviewer agrees with the result of this study which indicates no treatment-related injection sites reaction or macroscopic and histological effects after a single injection of ZK 6057184 to the dogs.

Study title: TXST20070304: Local tolerance test of ZK 6057184 (ref.: (b) (4) in the rabbit (M+F) after single intravenous administration into the uncongested vein of the ear and with single paravenous administration.

Reference ID: 3361527

Key study findings: The local tolerance effect of ZK 6057184 was assessed following a single intravenous injection or a single paravenous application in rabbits. No treatment-related changes in body weight or clinical signs were reported during the study. Following intravenous injection of ZK 6057184 (2.5 µg/mL), no treatment-related effects were reported while reddening and swelling were observed at higher dose of 5.0 µg/mL. No macroscopic or histological findings were also reported in these animals. However, Reddening and swelling with granulation tissue and inflammatory infiltrates on day 8 were observed in rabbits perivenously injected ZK 6057184 (2.5 – 5.0 µg/mL). There was a time-dependent decrease in the severity of the redness and swelling indicating reversibility of the clinical findings.

Study no.: TXST20070304

Page #: Pages 1-29

Conducting laboratory and location: Bayer Schering Pharma AG,

Nonclinical Drug Safety,

13342 Berlin, Germany

Date of study initiation: January 10, 2008

GLP compliance: Yes

QA report: yes (x) no ()

Drug, lot #, and % purity: ZK 6057184, Batch # CS1036KI, and 97.1 % purity

Methods

Doses: 0, 2.5 and 5.0 µg/mL

Species/strain: Rabbit/New Zealand White (SPF)

Number/sex/group or time point (main study): 8 rabbits/sex for step I

: 2 rabbits/sex for step II

Route, formulation and volume: Intravenous-5.0 mL; paravenous-1.0 mL

Injection speed: Intravenous- 5.0 mL/min; paravenous: bolus

Step I and II: intravenous into the uncongested marginal vein of the ear

Step I: paravenous into the surrounding tissue of the vein of the hind leg

Age: males- Not provided

Reference ID: 3361527

Weight: Males – 3.2 -3.5 kg

Females – 2.5 – 3.0 kg

Effects of treatment of body weight and clinical signs were monitored during the study.

STEP I: Intravenous Injection- Four male and female New Zealand White rabbits each were administered in the step I with 5.0 mL of a solution containing 5.0 or 2.5 µg/mL ZK 6057184 into the uncongested marginal vein of the right ear (5.0 mL in 60 seconds). Using the same condition, 5.0 mL of a 0.9 % (w/v) NaCl-solution was injected into the marginal vein of the left ear.

Perivenous Injection- These animals were also injected perivenously with 1.0 mL of 5.0 or 2.5 µg/mL ZK 6057184 into the surrounding tissue of the congested vein of the right hind leg. 1.0 mL of a 0.9 % (w/v) NaCl-solution was injected into the surrounding tissue of the congested vein of the left hind leg. Two rabbits/sex were necropsied on days 3 and 8.

STEP II: An additional 2 males and 2 females were injected intravenously with the formulation containing 5.0 µg/mL ZK 6057184 followed by an administration of 5.0 mL 0.9 % (w/v) NaCl-solution to simulate the wash out procedure in humans as shown in sponsor's Table TT2. This step was performed with regard to the observed local findings at the uncongested marginal vein after administration of the solution containing 5.0 µg/mL ZK 6057184 in the first step. The rabbits were then necropsied on day 3.

Results:

Body weight: No treatment related changes in body weight were reported in the animals.

Clinical signs: Following intravenous administration, no treatment-related findings were noted on day 3 and on day 8 after single administration of 5.0 mL of a formulation containing 2.5 µg/mL ZK 6057184 into the uncongested marginal vein of the ear of the rabbit. Similarly, following the paravenous injection, there were no serious reactions reported. However, slight to moderate swelling was found at the administration area in 3 out of 8 animals on day 1 to day 4.

Macroscopic and Histologic Assessment: No treatment-related effects was induced by ZK 6057184 (2.5 µg/mL) in macroscopic and histological examinations on day 3 and on day 8. Higher dose of 5.0 µg/mL caused slight to moderate reddening proximal of the puncture tract and at the half of the ear (lateral of the central artery) up to day 5 and slight swelling at the tissue around. However, no macroscopic or histological findings were also reported in these animals. Reddening and swelling with slight to marked granulation tissue and inflammatory infiltrates on day 8 were observed in rabbits perivenously injected ZK 6057184 (2.5 – 5.0 µg/mL). No serious or irreversible clinical signs were demonstrated by ZK 6057184 during this study.

Reference ID: 3361527

Reviewer's Comment: Agrees with the result of this study. The result of this study corroborated the previous studies indicating that that no serious reaction is expected from an intravenous injection of ZK 6057184 in the clinic.

11 Integrated Summary and Safety Evaluation

Florbetaben (4-[(E)-2-(4-{2-[2-(2-[18F]fluoroethoxy)ethoxy]ethoxy}phenyl)vinyl]-N-methylaniline) is a derivative of polyethyleneglycol stilbene labeled with fluoride-18 (18F) for Positron Emission Tomography (PET) imaging proposed for detection of Aβ plaques in brains, thereby assisting in the differential or confirmatory diagnosis in adult patients who are being evaluated for Alzheimer's disease (AD) or other causes of cognitive decline. Florbetaben is intended for intravenous administration to adult patients who are being evaluated for Alzheimer's disease (AD) and other cognitive decline at a recommended dose of 300 MBq (8.1 mCi).

Safety pharmacology

CNS safety: Neurological safety profile of Florbetaben was evaluated in conscious Sprague Dawley rats intravenously administered with Florbetaben. The animals were observed for behavioral changes up to 14 days post-treatment. No mortality or treatment-related changes in clinical observations was reported during the study. However, there were reports of increased serum phosphorus in Day 3 females administered 100 µg/kg (233X MHD) which was not accompanied with any histological findings, as a result the cause of this effect could not be determined. The NOAEL obtained in females is 50 µg/kg (117X MHD) while NOAEL from male rats is 100 µg/kg (233X MHD). Thus, no evidence of CNS effect is demonstrated in this study. In another study, the neurotropic effects on behavior and body temperature in rats intravenously administered Florbetaben (140X - 1395X MHD) was investigated. Florbetaben effect was evaluated in 62 behavioral and neurological symptoms and the rectal temperature was assessed. No change in the behavior or the body temperature was reported in the animals. Effect of Florbetaben on motor coordination was also evaluated in conscious rats and no impairment of motor coordination in rats after single intravenous administration of doses up to 1395X MHD.

CVS safety: In an *in vitro* study, the intrinsic effect of Florbetaben on the HERG K^+ current was investigated in stably transfected CHO cells. Florbetaben demonstrated no affect the HERG K^+ current at the employed concentrations of 0.01, 0.1 and 1 µmol/L (12.5X, 125X and 1250X expected human unbound plasma level of estimated human dose of this product). In a pivotal cardiovascular study in conscious telemetered beagle dogs, Florbetaben (0, 6.7X 34.2X and 68.4X MHD) was intravenously administered and the animals demonstrated no treatment-related effects were reported on the ECG parameters, rhythm, or blood pressure. In another study, effect of consecutive administration of Florbetaben (34.9X, 93X and 349X MHD) on

Reference ID: 3361527

cardiohemodynamics and ECG parameters in anesthetized. No treatment-related effect was reported in the study.

Renal system: The effect of Florbetaben on renal function was evaluated in conscious rats following a single intravenous injection. No change in the renal excretion rates of fluid and sodium and potassium as well as creatinine and osmolar clearances of treated- (0, 140X 349X and 1395X MHD) and control rats were demonstrated in this study.

Respiratory system: Florbetaben (140X - 1395X MHD) effect on respiratory function was investigated in conscious rats using whole body plethysmography system. Florbetaben did not cause any change in respiratory frequency, tidal volume or minute volume in the animals at any time point during the investigation. The NOAEL was determined as 1395X MHD.

Pharmacokinetics

In vitro and in vivo (rodents, dog and monkeys) studies were conducted to characterize the pharmacokinetics profile of Florbetaben. HPLC/UV or LC/MS/MS analysis indicates that Florbetaben is bound to human plasma proteins (blood/plasma ratio of 0.44 in human) and stable in serum and moderately stable in liver microsomes. Rat data showed that Florbetaben is characterized by blood clearance of 6.7 L/h/kg, volume of distribution of 2.8 L/kg and distribution $t_{1/2}$ of 0.15 h. Rat blood kinetics data showed that Florbetaben remained in the blood longer than 3 hours post injection. Blood radioactivity time profile of Florbetaben following a single intravenous injection in rats demonstrates an initial rapid distribution followed by a slight but constant increase in distribution over the 3 hours observation period and a distribution $t_{1/2}$ of 2.7±1.0 min. Toxicokinetics study conducted in dogs indicates no sex-related differences in exposure in the treated animals and no accumulation or induction in terms of $AUC_{(0-6)}$ or C_{max} following repeated dosing.

The biodistribution data on Florbetaben obtained from NMRI mice demonstrates an initial brain uptake of radioactivity (4.77 ± 0.15%ID/g at 2 min), initial wash out of radioactivity from the brain (1.59 ± 0.13%ID/g at 30 min) and slow clearance was observed in the brain. Florbetaben was mostly excreted in the kidney and the feces and a total recovery of 98.46% was reported at 4 hour post injection. No potential radiation toxicity of radioactivity was demonstrated by the dosimetry data. Stability and metabolite identification studies were conducted in mice. It was found that following an intravenous injection of [^{18}F]Florbetaben using HPLC and LC-MS/MS showed that Florbetaben is metabolized to [^{18}F]fluoroacetaldehyde (non-polar fraction) and [^{18}F]-fluoroacetic acid (polar fraction). Additional studies conducted to characterize the polar metabolites showed that similar metabolites were found in the plasma and brain samples of [^{18}F]Florbetaben. *In vitro* data on biotransformation of Florbetaben in liver microsomes and hepatocytes of rat, dog, mouse and human demonstrates that demethylation was the major pathway in human and rat hepatocytes while glucuronidation and acetylation as phase II reaction was observed as major pathway respectively in human and rat hepatocytes. However, oxidative cleavage of the fluoro ethylene glycol side chain was observed as major pathway only in rat hepatocytes.

An *in vitro* study conducted to assess if Florbetaben acts as a direct inhibitor of major human cytochrome P450 isoforms demonstrates no direct-acting inhibitory potency of Florbetaben on biotransformation reactions catalyzed by CYP 1A2, 2C8, 2C9, and 2D6 (IC_{50} >2 μM). The study demonstrates IC_{50} values of 1.6 μM and 1.4 μM to the inhibition of CYP3A4 activity by midazolam and testosterone respectively. No evidence of any clinically relevant drug-drug

interactions to Florbetaben via inhibition of the employed major human cytochrome P450 isoforms was demonstrated in the study. In another *in vitro* study, CYP phenotyping study was conducted to evaluate the CYP isoforms contributing to the oxidative metabolism of Florbetaben in the absence and presence of CYP isoform-selective inhibitors and incubations with recombinant human CYP. The data shows that the plasma level of Florbetaben would be too low for any polymorphic CYPs or any significant alterations to occur even when single CYP inhibitors are co-administered to the patients. Therefore, the human CYP isoforms is not expected to significantly alter the metabolism of [^{14}C]Florbetaben. The PET evaluation of [^{18}F]Florbetaben and a closely related PET tracer, [^{18}F]BAY 1008472 was conducted in rhesus monkey. [^{18}F]BAY 1008472 demonstrates faster uptake, a lower nonspecific binding and faster wash-out than [^{18}F]Florbetaben in rhesus monkey.

Toxicology

Single-dose toxicity: Acute and expanded single-dose toxicity studies were conducted in rats and rabbits. In rats, no mortalities were reported in any control or in rats intravenously administered Florbetaben (116X, 233X and 930X MHD). No serious treatment-related alterations in the evaluated functional and histopathological parameters were also found in the animals. However, 233X and 930X MHD caused mild transient alterations in erythrocytic parameters in male rats, serum phosphorus in female rats and troponin I in males and female rats on Day 3. Thus, a NOAEL of 116X MHD was established in the study. In a repeat of this study at two dose levels (116X and 233X MHD), no mortality, clinical signs of toxicity, changes in clinical chemistry or any effect on gross necropsy or histopathological parameters was reported in the study. A NOAEL of 233X MHD was determined in the study.

An expanded single-dose toxicity study with 14 days recovery period conducted in the rabbits (0, 11.4X, 56.7X and 113.5X MHD) demonstrates no serious treatment-related alterations in the functional and histopathological parameters assessed during the study. There were however mild transient alterations in serum liver transaminase enzymes (ALT and AST) at 113.5X MHD in one male rabbit on Day 3. The NOAEL (determined by the endpoint assessed) was 48.8 µg/kg (113.5X MHD). In another expanded single-dose toxicity study, higher doses (25 and 250 µg/kg (58.1X and 581X MHD) of Florbetaben were administered to the rabbits and the animals were also observed for 14 days. No mortality or any serious treatment-related alterations in the functional and histopathological parameters was reported in the study. There was elevated troponin levels on Day 15 in the treated and control groups as well as elevated AST and ALT values in one animal administered 581X MHD on Day 3. NOAEL obtained from the study was 250 µg/kg (581X MHD).

Repeat-dose toxicity: Repeat-dose toxicity studies were conducted in rats and dogs.

No serious treatment-related alterations in the evaluated functional and histopathological parameters were reported following a repeated administration of Florbetaben (105X, 407X and 1628X MHD) to rats over a period of 4 weeks followed by a recovery period of 4 weeks. However, there was alteration in respiratory parameters in the first two weeks of treatment in the 407X and 1628X MHD treated groups. NOAEL of 45 µg/kg (105X MHD) was determined in this study. Microscopic findings in the 407X and 1628X MHD and vehicle-treated groups include

Reference ID: 3361527

tubular vacuolation in the kidney, hypertrophy in the urinary bladder with vacuoles in urinary epithelia, presence of foamy macrophages in the lung, small intestine and lymph nodes and chronic inflammation at the injection site. Following repeated administration of Florbetaben (29X, 116X and 465X MHD) to dogs over 4 weeks followed by a recovery period of 4 weeks, no mortality or serious clinical signs were reported in the animals. One of the dogs administered 465X MHD demonstrated spontaneous hyperactivity, spasms and coughing on Day 9. Partial AV block was observed during weeks 1, 3 and 4, in one dog and bimodal waves was reported in another dog in the group administered 465X MHD. No microscopic or macroscopic effects were reported in this study except lesions found at the injection site in the treated and control animals. However, the animals fully recovered by the 4-week-treatment recovery period and NOAEL of 50 µg/kg (116X MHD) was determined in this study.

Genetic toxicity: No evidence of mutagenic effect (with or without metabolic activation) in the Ames test, Chromosomal aberration test on human peripheral lymphocytes was demonstrated up to 5.0 mg/plate concentration.

Carcinogenicity: No studies were conducted.

Reproductive and developmental toxicity studies: No studies were conducted.

Special Toxicology

Genetic Toxicity of Impurities: Chromosomal aberration tests in human peripheral lymphocytes conducted on the mix of Florbetaben impurities ((b) (4) (b) (4) (b) (4) (b) (4) was negative. However, the mix demonstrates a weak mutagenic potential in the bacterial reverse mutation test with *Salmonella typhimurium* strains TA100, TA1535 and TA1538. An impurity ((b) (4) present in the clinical batch of Florbetaben, was also evaluated for mutagenic potential and found negative in the bacterial reverse mutation test when tested up to (5.0 mg/plate), in the absence and presence of metabolic activation. The impurity, (b) (4) (2.5-50 µg/mL), was also negative in forward cell mutation assay at the thymidine kinase locus (TK +/-) in mouse lymphoma L1517Y cells with and without activation during a treatment time of 3 hours (pulse treatment) and 24 hours (continuous treatment).

Local Tolerance

Florbetaben was tested for injection site reaction effect in rabbits and dogs. In the rabbits, following a single injection (0.5 mL) into the uncongested marginal vein of the ear and a single paravenous application (1 mL) into the hind leg of rabbits, no severe or irreversible effects of the test article and the vehicle was reported. In dogs, intravenously infused a single dose (5 µg/mL) in the uncongested vena cephalica antebrachii in the left fore leg and 0.9 % (w/v) NaCl-solution in the right foreleg (control), similarly, no compound-related effect at the injections sites was demonstrated.

Reference ID: 3361527

Table 64: Summary of toxicity studies conducted on Florbetaben

Toxicity	**Species**	**NOAEL** (mg/kg) M/F	**Safety Margin** Based on AUC*	**Prominent findings** (if any)
Single-dose toxicity study	Rat	50 µg/kg	116	mild transient alterations in erythrocytic parameters in male, serum phosphorus in females and troponin I in box sexes on Day 3 at 233X and 930X MHD.
	Rat	100 µg/kg	233	
	Rabbit	48.8 µg/kg	113.5	mild transient alterations in serum liver transaminase enzymes (ALT and AST) at 113.5X MHD in one male rabbit on Day 3.
	Rabbit	250 µg/kg	581	elevated troponin levels on Day 15 in the treated and control groups and elevated AST and ALT values in one animal administered 581X MHD on Day 3.

Reference ID: 3361527

Repeat-dose toxicity study	Rat	175 µg/kg	407	tubular vacuolation in the kidney, hypertrophy in the urinary bladder, foamy macrophages in the lung, small intestine and lymph nodes and chronic inflammation at the injection site in 1628X MHD- and vehicle-treated animals.
	Dog	50 µg/kg	116	at 465X-MHD spontaneous hyperactivity, spasms and coughing on Day 9 in a dog; AV block during weeks 1, 3 and 4 in a different dog and bimodal waves in another dog.
Systemic toxicity study Local tolerance study Local tolerance study	Rat	37.9 µg/kg	-	-
	Rabbit	0.5 mL-intravenous 1 mL-paravenous	-	-
	Dog	5 µg/mL	-	-

*AUC in human: xxx ng.hr/ml at xx mg/day.

12 Appendix/Attachments

REFERENCES

Reference ID: 3361527

A.H. Tammer, G.Coja, et al. (2002) “Genetation of a recombinant Fab antibody reactive with Alzheimer’s disease-related Aß peptide”. Clin Exp Immunol 129: 453-463.

Rowe, C. C. *et al*. (2008) "Imaging of amyloid beta in Alzheimer's disease with [^{18}F]-BAY 94-9172, a novel PET tracer: proof of mechanism." Lancet Neurol 7(2):129-35

This is a representation of an electronic record that was signed electronically and this page is the manifestation of the electronic signature.

/s/

SUNNY O AWE
08/22/2013

ADEBAYO A LANIYONU
08/22/2013
I concur

PHARMACOLOGY/TOXICOLOGY FILING CHECKLIST FOR NDA/BLA or Supplement

NDA/BLA Number: 204-677 **Applicant:** Piramal Imaging **Stamp Date:** December 21, 2012

Drug Name: Florbetaben **NDA/BLA Type:** Original

On **initial** overview of the NDA/BLA application for filing:

	Content Parameter	Yes	No	Comment
1	Is the pharmacology/toxicology section organized in accord with current regulations and guidelines for format and content in a manner to allow substantive review to begin?	X		
2	Is the pharmacology/toxicology section indexed and paginated in a manner allowing substantive review to begin?	X		
3	Is the pharmacology/toxicology section legible so that substantive review can begin?	X		
4	Are all required (*) and requested IND studies (in accord with 505 b1 and b2 including referenced literature) completed and submitted (carcinogenicity, mutagenicity, teratogenicity, effects on fertility, juvenile studies, acute and repeat dose adult animal studies, animal ADME studies, safety pharmacology, etc)?	X		
5	If the formulation to be marketed is different from the formulation used in the toxicology studies, have studies by the appropriate route been conducted with appropriate formulations? (For other than the oral route, some studies may be by routes different from the clinical route intentionally and by desire of the FDA).	X		
6	Does the route of administration used in the animal studies appear to be the same as the intended human exposure route? If not, has the applicant submitted a rationale to justify the alternative route?	X		
7	Has the applicant submitted a statement(s) that all of the pivotal pharm/tox studies have been performed in accordance with the GLP regulations (21 CFR 58) or an explanation for any significant deviations?	X		
8	Has the applicant submitted all special studies/data requested by the Division during pre-submission discussions?	X		

File name: 5_Pharmacology_Toxicology Filing Checklist for NDA_BLA or Supplement 010908

PHARMACOLOGY/TOXICOLOGY FILING CHECKLIST FOR NDA/BLA or Supplement

	Content Parameter	Yes	No	Comment
9	Are the proposed labeling sections relative to pharmacology/toxicology appropriate (including human dose multiples expressed in either mg/m2 or comparative serum/plasma levels) and in accordance with 201.57?	X		
10	Have any impurity – etc. issues been addressed? (New toxicity studies may not be needed.)	X		
11	Has the applicant addressed any abuse potential issues in the submission?		X	Not Applicable
12	If this NDA/BLA is to support a Rx to OTC switch, have all relevant studies been submitted?			Not Applicable

IS THE PHARMACOLOGY/TOXICOLOGY SECTION OF THE APPLICATION FILEABLE? ___ Yes**_____**

If the NDA/BLA is not fileable from the pharmacology/toxicology perspective, state the reasons and provide comments to be sent to the Applicant.

Please identify and list any potential review issues to be forwarded to the Applicant for the 74-day letter.

Sunny Awe 01/28/2013
Reviewing Pharmacologist Date

Adebayo Laniyonu 01/29/2013
Team Leader/Supervisor Date

File name: 5_Pharmacology_Toxicology Filing Checklist for NDA_BLA or Supplement 010908

This is a representation of an electronic record that was signed electronically and this page is the manifestation of the electronic signature.

/s/

SUNNY O AWE
01/29/2013

ADEBAYO A LANIYONU
01/29/2013